Next generation CAR T cells targeting HER2-positive tumors

Macarena Román Alonso

Universitat Autònoma de Barcelona

Facultat de Medicina

Departament de Bioquímica i Biologia Molecular

Programa de Doctorat en Bioquímica, Biologia Molecular i Biomedicina

Next generation CAR T cells targeting HER2-positive tumors

Thesis presented by Macarena Román Alonso for the degree of Doctor of Philosophy (PhD) in Biochemistry, Molecular Biology and Biomedicine by Universitat Autònoma de Barcelona

Barcelona, 2024

Author:

Macarena Román Alonso

Director:

Dr. Joaquín Arribas López

Academic Tutor:

Dr. Laura Soucek

INDEX

LIST OF FIGURES

SUMMARY

Despite significant advancements in anti-HER2 therapies over the last few decades, primary or acquired resistances persist, along with associated adverse effects due to widespread HER2 expression in normal tissues, such as the heart or the lungs. Therefore, the development of more effective and safer treatments for HER2-positive tumors, particularly in the advanced and metastatic setting, remains a major unmet clinical need.

While redirecting T lymphocytes with bispecific antibodies (TCBs) or chimeric antigen receptors (CARs) has shown success in certain hematological malignancies, its efficacy against solid tumors remains limited, partly due to the scarcity of tumor-specific antigens (TSAs). p95HER2, a truncated form of HER2 frequently expressed in HER2-overexpressing tumors, has emerged as a promising TSA for targeted immunotherapies.

This thesis presents the development of CAR T cells targeting p95HER2, which displayed robust activity against p95HER2-expressing cell lines both *in vitro* and *in vivo*. However, efficacy against patient-derived xenografts (PDXs) was limited. To improve their efficacy, we equipped these CAR T cells with bispecific T cell engagers targeting CD3 and HER2 (TECH2s), whose affinity was modulated in order to bind cells that overexpress HER2 but not those expressing normal levels of the protein. This dual targeting strategy, called p95HER2.CAR-TECH2Me, exhibited a very potent antitumor activity on p95HER2-/HER2-positive PDXs with no effect on cells expressing physiological levels of HER2, demonstrating its potential as a safe and effective immunotherapeutic strategy against a subset of patients with HER2-positive tumors.

RESUMEN

A pesar de los avances de las últimas décadas en el desarrollo de terapias dirigidas contra HER2, la persistencia de resistencias primarias o adquiridas, además de los efectos adversos asociados a la expresión de HER2 en tejidos normales, como el corazón o los pulmones, limitan su potencial. Por tanto, existe la necesidad de desarrollar terapias más efectivas y seguras contra tumores HER2-positivos, especialmente para pacientes en estados avanzados o metastásicos.

Aunque la redirección de linfocitos T con anticuerpos bispecíficos (TCBs) o receptores de antígeno quiméricos (CARs) ha mostrado éxito en ciertos tumores hematológicos, su eficacia contra tumores sólidos sigue siendo limitada, en parte debido a la escasez de antígenos específicos de tumor (TSAs). p95HER2, una forma truncada de HER2 frecuentemente expresada en tumores HER2.positivos, se posiciona como un TSA prometedor para el desarrollo de inmunoterapias dirigidas.

Esta tesis presenta el desarrollo de células CAR T dirigidas contra p95HER2, con una actividad robusta contra líneas celulares p95HER2-positivas tanto *in vitro* como *in vivo*. Sin embargo, la eficacia contra xenoinjertos derivados de pacientes (PDXs) es limitada. Para mejorar su potencial, equipamos estas células CAR con anticuerpos biespecíficos de células T con unión a CD3 y HER2, (TECH2s), cuya afinidad se modificó para unirse exclusivamente a células que sobreexpresan HER2, pero no a aquellas que expresan niveles normales. Esta estrategia de doble diana, llamada p95HER2.CAR-TECH2Me, muestra una actividad antitumoral muy elevada en PDXs p95HER2-/HER2-positivos sin efecto en células que expresan niveles fisiológicos de HER2, demostrando su potencial como una estrategia inmunoterapéutica segura y efectiva contra un subconjunto de pacientes con tumores HER2-positivos.

INTRODUCTION

1. HER2 and cancer

1.1. HER receptors

Human epidermal growth factor receptor-2 (HER2), also known as ERBB2 or Neu, is a membrane tyrosine kinase receptor that belongs to the human epidermal growth factor receptors (HER) family, along with HER1 (EGFR, ERBB1), HER3 (ERBB3) and HER4 (ERBB4). All family members share three main structural components: an extracellular ligand-binding domain, a transmembrane region and a cytoplasmic tyrosine kinase domain. These receptors are expressed in various epithelial, mesenchymal and neuronal tissues, and play fundamental roles in development, proliferation, differentiation and survival [1].

In the absence of ligand binding, these receptors exist as resting monomers embedded in the plasma membrane. Upon ligand binding, receptor-ligand complexes will move around the plasma membrane until they encounter other receptor complexes, forming both homo- and heterodimers. Receptor dimerization stimulates their intrinsic tyrosine kinase activity, triggering autophosphorylation and ultimately initiation of cell signaling pathways [2], primarily mediated through the mitogen-activated protein kinase (MAPK), phosphatidylinositol-4,5-bisphosphate 3-kinase (PI3K) and protein kinase C (PKC) signaling pathways [3]. Ligands such as epidermal growth factor (EGF), amphiregulin (AR) and transforming growth factor-α (TGFα), bind specifically to HER1, whereas betacellulin (BTC), heparin-binding EGF (HB-EGF) and epiregulin (EPR), bind to both HER1 and HER4. Among the neuregulin (NRG) ligands, NRG-1 and NRG-2 bind to HER3 and HER4, while NRG-3 and NRG-4 bind selectively to HER4. In contrast, no direct ligand for HER2 has yet been discovered [4].

Nevertheless, ample evidence shows that even in the absence of direct ligand binding, HER2 exists in a constitutively “open” conformation that resembles a ligand-activated state and serves as the preferred heterodimerization partner for all other HER family members [5] **(Fig.1).** In addition, heterodimers containing HER2 exhibit prolonged activation of downstream signaling pathways, with HER2-HER3 heterodimer being the

most active [1, 6]

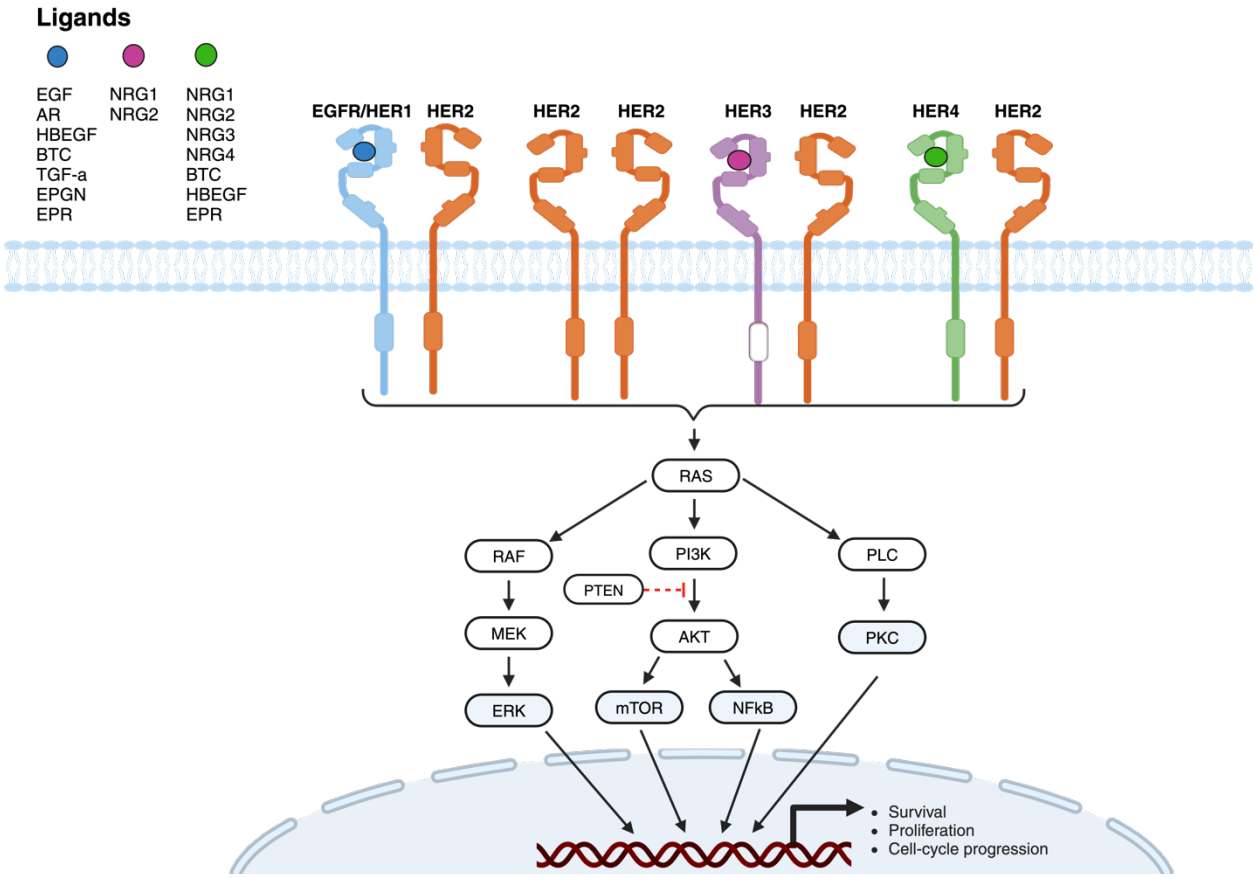

Figure 1: HER family members, ligands and main signaling pathways

The four family members, EGFR, HER2, HER3, and HER4, dimerize preferentially with HER2. Different ligands have been identified for all of them, except for HER2. Upon ligand binding and homo/heterodimer formation, receptor phosphorylation results in activation of the indicated downstream signaling pathways. Consequently, different nuclear factors are recruited and modulate the transcription of different genes involved in cell-cycle progression, proliferation and survival. PTEN is a negative regulator of the PI3K pathway. EGFR: epidermal growth factor receptor; HER: human epidermal growth factor receptor; RAF: rapidly accelerated fibrosarcoma; MEK: mitogen-activated protein kinase kinase; ERK: extracellular signal-regulated kinase; PI3K: phosphatidylinositol 3-kinase; PTEN: phosphatase and tensin homolog; AKT: protein kinase B; mTOR: mammalian target of rapamycin; NFκB, nuclear factor κB; PLC: phospholipase C; PKC: protein kinase C. Image adapted from [7] and [8]

1.2. HER2 alterations in cancer

Nearly four decades ago, HER2 was functionally implicated in the pathogenesis of human breast cancer (BC) [9], sustaining proliferative signaling, one of the Hallmarks of Cancer [10]. HER2 overexpression has been correlated with a poorer outcome in BC [7] and associated with the development and severity of various other cancers [11]. HER2 overexpression is primarily caused by gene amplification, which is located in chromosome 17 (17q12q21). Alternative mechanisms for protein overexpression include the increase in transcriptional levels and defects in the endocytosis pathway, and receptor mutations can also over activate HER2 signaling pathway [12].

HER2 overexpression is predominantly observed in malignancies of epithelial origin, contrasting with its infrequency or absence in mesenchymal, neuroendocrine and central nervous system cancers [13]. Accordingly, HER2 is widely known to be overexpressed in BC (15-20%), gastric (GC) and gastroesophageal (GEC) (10-30%), ovarian (20-30%) and non-small cell lung cancer (NSCLC) (<5%). Additionally, HER2 overexpression can be found in many other cancers with different incidence rates, including bladder, uterus, cervix, endometrium, testicular, prostate, head and neck, salivary duct, colorectum, liver, pancreas and biliary tract cancers [14–16].

Based on data from the PanCancer Atlas Studies, which analyzed tumor samples across diverse origins from 10953 patients, 6% of all patients exhibited tumors with ERBB2 genomic alterations, with 3.5% being HER2 amplification, highlighting the clinical relevance of this molecular aberration **(Fig.2)** (cBioPortal, February 2024). Because of the highest prevalence in BC and GC, these HER2-overexpressing tumors will constitute the focus of this thesis.

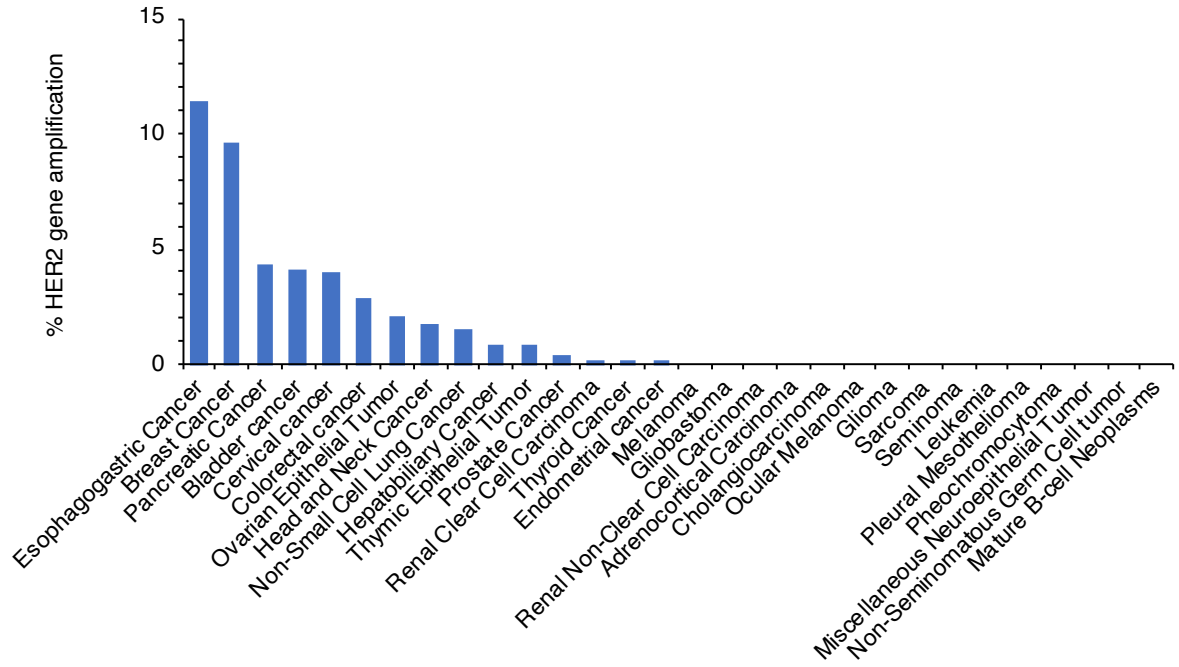

Figure 2: HER2 gene amplification in cancer

Data from the TCGA Research Network PanCancer Atlas studies (10967 samples / 10953 patients). This graph has been adapted from cBioportal database (February 2024) to show only the frequency of HER2 gene amplifications, by cancer type, in descending order of frequency. TCGA: The Cancer Genome Atlas

1.2.1. Breast cancer

According to recently updated data from the World Health Organization (WHO), BC is the second most frequently diagnosed cancer worldwide, the first in women, with 2.3 million new cases (11.6%) and an estimated 669,846 deaths annually (GLOBOCAN, 2022). Hormone and growth factor receptor research in BC have shaped targeted therapy developments, significantly improving survival rates. Early diagnosis is crucial for the outcome of the patients. Non-invasive BC has a 99% 5-year survival rate, while invasive BC with regional lymph node involvement maintains an 85% rate. However, when distant metastases occur, the survival rate drops to less than 30% [17].

Subtypes

Gene expression profiling studies identified six main intrinsic subtypes of BC based on the PAM50 gene expression signature [18]. Treatment decisions, however, are commonly based on conventional histology and immunohistochemistry (IHC) expression of key proteins: the hormone receptors (HR) estrogen receptor (ER) and progesterone receptor (PR), HER2 and the proliferation marker Ki67. This classification recognizes five clinical subtypes of BC: triple negative, luminal A-like, luminal B-like HER2-negative, Luminal B-like HER2-positive and HER2-enriched (non-luminal) BC **(Fig.3)** [19].

Triple negative breast cancer (TNBC), the most aggressive and heterogeneous subtype, lacks ER, PR and HER2, comprising 10-15% of BCs. It is enriched in BRCA-1 mutated patients and associated with a high rate of metastasis [20]. Treatment traditionally involved surgery, chemotherapy and radiation, despite limited benefits. More recently, oral poly (ADP-ribose) polymerase inhibitors (PARPi) [21], immune checkpoint inhibitor (ICI) immunotherapy (pembrolizumab) [22] and topoisomerase inhibitors [23] have increased the therapeutical options for these patients [24].

Luminal A tumors, constituting 60-70% of BCs, are characterized by high ER and/or PR levels, low Ki67, and generally have a favorable prognosis with lower relapse rates. Treatment primarily involves hormonal therapy. Conversely, **Luminal B-like HER2-negative** tumors, representing 10-20% of BCs, are more proliferative and aggressive, with a worse prognosis. These tumors are ER-positive, albeit at lower levels than luminal A, and Ki67 high. Standard treatment involves hormonal therapy and chemotherapy. **Luminal B-like HER2-positive** present otherwise similar characteristics and treatment, but with an additional option for anti-HER2 targeted therapy, which will be explained in the next section, due to HER2 overexpression [19].

HER2-enriched (non-luminal) tumors are characterized by high expression of HER2, an ER-negative profile, and high Ki67 index. Despite their aggressiveness, the introduction of anti-HER2 therapies, such as the monoclonal antibody (mAb) trastuzumab, has notably improved the prognosis of this patients in the last decades [25]. **HER2-positive tumors**, including luminal B and non-luminal, account for around

15% of all BC tumors [19].

The concept of **HER2-low** BC has gained relevance in recent years after the clinical success of novel HER2-targeting antibody drug conjugates (ADCs) in this group of patients. Therefore, the number of patients who could potentially be treated with some anti-HER2 therapies may increase, since HER2-low tumors make up more than half of total BCs (55-60%) [26, 27], most of which were previously classified as HER2-negative [28]. However, toxicities associated to HER2-targeted therapies and the emergence of resistances remain a challenge that leads to frequent relapses and metastases [20, 29].

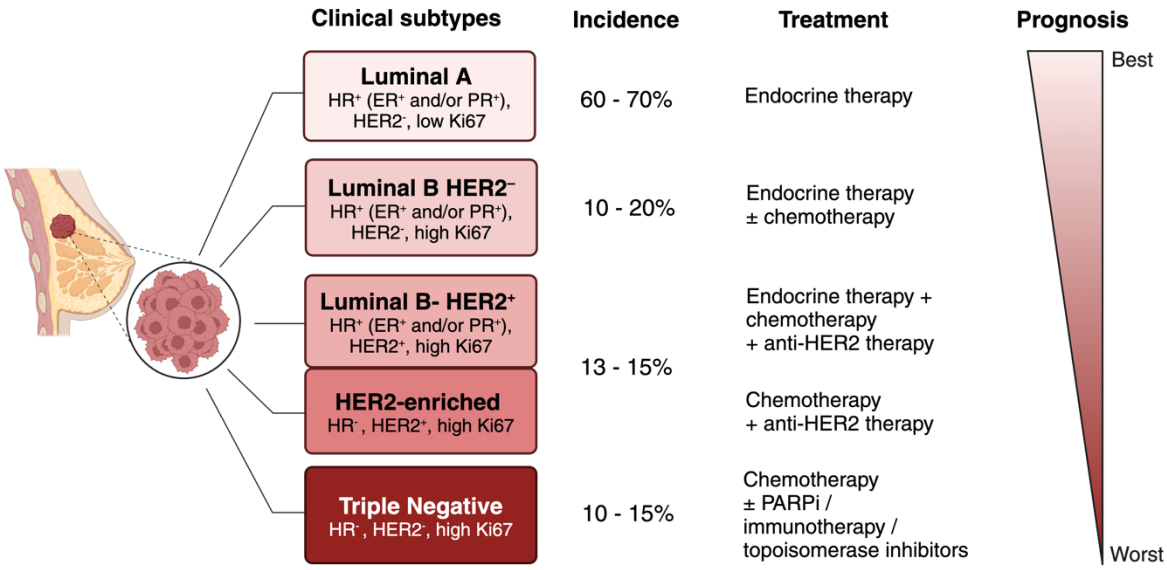

Figure 3: Clinical subtypes of BC based on histopathological factors

BC classification currently used in clinical practice identifies 5 subtypes: luminal A, luminal B HER2-negative, luminal B HER2-positive, HER2-enriched, and TNBC. This classification is based on 4 biomarkers: ER, PR, HER2 and Ki67. Incidence, treatment options and prognosis of each subtype are indicated in the figure. ER: progesterone receptor; PR: progesterone receptor, TNBC: triple negative BC; PARPi: PARP inhibitors. Adapted from [19].

Metastatic profiles

Advanced BC is currently treatable but virtually incurable and metastases serve as the primary cause of death in nearly all patients, with a median overall survival in this stage of 2-3 years [30]. In addition, around 20% of patients are de novo diagnosed at an already advanced metastatic stage [31, 32]. Metastatic patterns vary among subtypes: both luminal types show the highest risk for bone metastasis, along with frequent occurrences of liver, brain, and lung metastases. In contrast, triple-negative BC (TNBC) and HER2-positive subtypes exhibit a lower incidence of bone metastasis but a higher rate of brain, liver, and lung metastases. Notably, HER2-positive tumors pose the highest risk for brain metastases [33].

1.2.2. Gastric and esophageal cancer

GC stands as the fifth most frequently diagnosed cancer and remains the fourth leading cause of cancer-related mortality (GLOBOCAN, 2022). Characterized by high molecular and phenotypic heterogeneity, efforts to delineate GC subtypes through various platforms have not yet yielded a clinically relevant consensus [34]. Diagnosis is typically confirmed histologically through endoscopic biopsy [35, 36]. The highest rate of HER2 positivity has been reported in gastroesophageal junction cancers (GEJC) [36] with intestinal type histology (31.8%) [14]. Consequently, HER2-targeted therapies have been explored and approved for the treatment of this subset of HER2-positive patients.

2. HER2-targeted therapies

HER2-targeted therapies have markedly improved the prognosis for women harboring breast tumors with HER2 overexpression. These therapies have also been explored, and in some cases approved, for the treatment of other HER2-positive or mutated solid tumors, such as gastric, biliary tract, colorectal, non-small-cell lung and bladder cancers [14]

Approved HER2-targeted therapies bind and act at different levels and can be grouped into three main categories: monoclonal antibodies (mAbs), antibody-drug conjugates (ADCs) and Tyrosine kinase inhibitors (TKIs). mAbs and ADCs are antibodies that bind to the extracellular domain of HER2, interfering with its membrane expression, dimerization and eliciting antibody mediated immune responses. ADCs further deliver cytotoxic agents. TKIs bind to the intracellular kinase domain with different affinities and specificities, impairing the catalytic activity of HER2 **(Fig.4).**

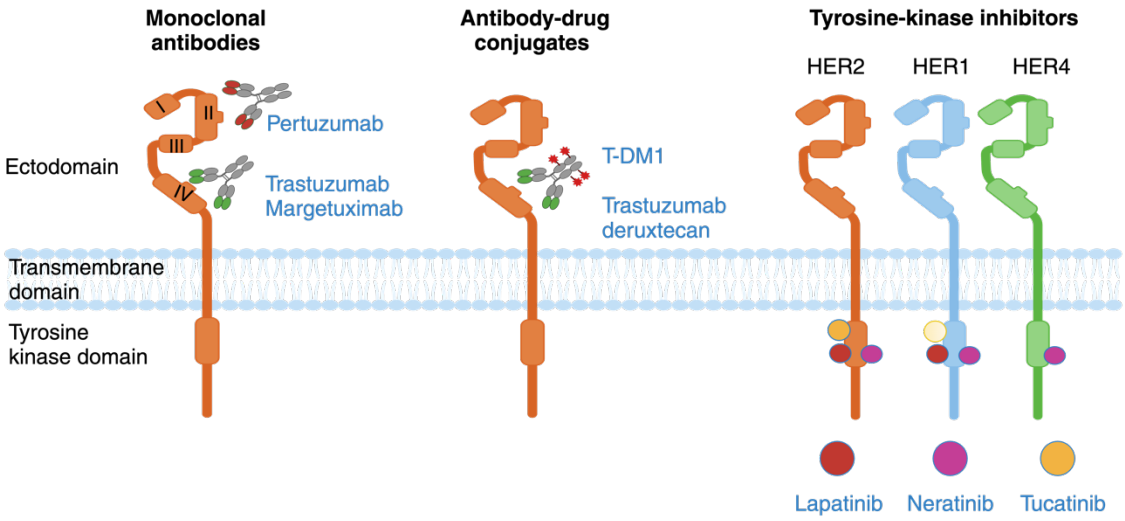

Figure 4: Approved HER2-targeted therapies

The mAb pertuzumab binds to domain II, whereas trastuzumab and margetuximab binds to domain IV of HER2. The two approved ADCs (T-DM1 and trastuzumab deruxtecan) are based on trastuzumab and are further loaded with anti-cancer drugs, aimed to be specifically delivered. The tyrosine kinase inhibitors, lapatinib, neratinib and tucatinib, impair the intracellular kinase domains of different HER receptors and with different affinities (i.e. tucatinib to HER2 and HER1)

2.1. Classification of approved HER2-targeted therapies

2.1.1. Monoclonal antibodies

mAbs have significantly advanced the treatment of HER2-positive BC over the last two decades [37]. Three anti-HER2 mAbs have been approved to date by the American and European regulatory agencies, with two of them constituting the frontline treatment in HER2-positive BC.

Trastuzumab (Herceptin® and other biosimilar drugs), a recombinant antibody targeting the juxtamembrane region of HER2 (domain IV), was the first biological drug approved in 1998, marking a transformative milestone in HER2-positive BC treatment [5]. Trastuzumab stands as a first-line treatment option for both early and advanced HER2-positive BC, either as a monotherapy or combined therapy [38], and for metastatic GC or GEJC, in combination with chemotherapy [14]. Trastuzumab acts through two main mechanisms: (I) interfering with HER2 signaling, inhibiting dimerization and promoting receptor internalization and/or degradation [39]; and (II), most relevantly, inducing antibody Fc-mediated immune responses [4]. These responses include antibody-dependent cellular cytotoxicity (ADCC) and antibody-dependent cellular phagocytosis (ADCP), which are mediated by innate immune cells such as NK cells and macrophages, containing Fc receptors that bind the Fc antibody portion [40], and complement dependent cytotoxicity (CCC) [41, 42].

Pertuzumab (Perjeta®) is a mAb that inhibits ligand induced HER2 heterodimerization by binding to the extracellular dimerization domain (domain II) [43]. Synergizing with trastuzumab, it forms a dual blockade strategy and constitutes the frontline treatment for metastatic BC patients and in the early-stage adjuvant setting [44, 45]**.** However, trials in GC have not shown the benefit of dual blockade observed in BC [14].

Margetuximab (Margenza®), a second-generation monoclonal antibody that binds the same epitope as trastuzumab, has an engineered Fc that enhances ADCC and ADCP. Approved in 2020 by the FDA (Food and Drug Administration), but not yet the EMA (European Medicines Agency), for advanced HER2-positive metastatic BC in combination with chemotherapy. Recent suggestions propose combining

Margetuximab with TKIs to further enhance efficacy in this advanced setting [46].

Due to the expression of HER2 in normal tissues, HER2 is considered a tumor associated antigen (TAA), and toxicities due to on-target off-tumor effects have been reported for trastuzumab and other anti-HER2 therapies. Cardiotoxicity, which manifests as clinical heart failure or left ventricular ejection fraction (LVEF) decline, is one of the main concerns, since HER2 is also expressed in cardiomyocytes [47]. Other frequent side effects are related to treatment infusion, diarrhea and pneumonitis. However, the main challenge of trastuzumab-based treatment is represented by the onset of resistance phenomena.

2.1.2. Antibody-drug conjugates

Despite the effectiveness of anti-HER2 monoclonal antibodies, their combination with chemotherapy remains crucial for optimal response. Antibody-drug conjugates (ADCs) aim to enhance specificity and reduce side effects by delivering potent cytotoxic agents selectively to tumor sites [48, 49].

Ado-Trastuzumab Emtansine or T-DM1 (Kadcyla®) was the first-in-class ADC, approved for HER2-positive BC. T-DM1 Integrates a trastuzumab backbone bound to the cytotoxic agent emtansine (DM1), a tubulin polymerization inhibitor [48]. It is approved for the second-line treatment of HER2-positive BC in both the metastatic and adjuvant settings if residual invasive disease is observed after neoadjuvant treatment [50, 51].

More recently, the field of anti-HER2 therapies has experienced a new revolution with the appearance of **Fam-Trastuzumab deruxtecan, T-DXd or DS-8201** (Enhertu®). This ADC, also based on trastuzumab, differs from T-DM1 in payload, drug-to-antibody ratio, and the linker. T-DXd's topoisomerase I inhibitor payload and unique properties allow it to effectively target bystander tumor cells. Clinical trials termed as DESTINY (DESTINY trials) validated its efficacy, leading to accelerated FDA approval in 2019 for unresectable or metastatic HER2-positive BC [52]. Subsequent approvals include HER2-low BC [53], HER2-mutant NSCLC [54], and advanced HER2-positive gastric

or gastroesophageal junction adenocarcinoma. Notably, T-DXd has shown promising results in treating brain metastases in HER2-POSITIVE BC patients in the TUXEDO-1 trial (NCT04752059) [55].

While the approval of these therapies highlights their risk-benefit balance, the concern over serious toxicities remains prominent. Many ADCs exhibit off-target toxicities resembling those observed with systemically administered payloads, in addition to on-target off-tumor toxicities and other poorly understood adverse effects, potentially life-threatening [56]. One major concern is the potential lung toxicity associated with anti-HER2 ADCs. Trials evaluating these drugs have reported variable incidences of deaths related to interstitial lung disease (ILD). Furthermore, the emergence of patients resistant even to the most novel ADCs is becoming evident, emphasizing the need for continued research and innovation in the field of anti-HER2 treatments, such as immunotherapeutic approaches [57].

2.1.3. Tyrosine Kinase inhibitors (TKIs)

An alternative approach for targeting HER2 involves the use of tyrosine kinase inhibitors (TKIs), which directly inhibit the downstream catalytic domain by acting as ATP competitors. These small molecules possess a crucial advantage in their ability to traverse the blood-brain barrier, making them effective against brain tumors [58]. Currently, three orally administered TKIs are approved by the FDA and EMA for HER2-positive tumors, mainly as the third line of treatment.

Lapatinib (Tykerb®) a dual inhibitor targeting HER1 and HER2 receptors, competitively and reversibly binds to their intracellular ATP-binding domains, effectively slowing tumor growth. Most trials assessing the combination of trastuzumab and lapatinib versus trastuzumab alone, alongside chemotherapy in the neoadjuvant treatment, consistently demonstrated a significant increase in pathological complete response (CR) rates when compared to a single HER2-blockade [25, 59]. However, cardiac toxicities are also increased in the dual blockade strategy compared to trastuzumab alone [60]. Therefore, its use is reserved for the later lines of treatment or for brain metastasis [61, 62].

Neratinib (Nerlynx®) is an irreversible inhibitor of HER1, HER2, and HER4 receptors. In 2017, it received its first approval for HER2-positive early-stage BC [63], and due to its ability for preventing recurrence, it was later approved for extended adjuvant therapy for patients with HER2-positive BC with high risk of relapse [64, 65]. A recent clinical trial comparing Neratinib and Lapatinib in combination with Capecitabine in previously treated HER2-positive metastatic BC (NCT01808573), concluded that Neratinib plus chemotherapy was superior to the Lapatinib combination in terms of progression free survival (PFS) and other secondary outcomes [66].

Tucatinib (Tukysa®) is the more recently approved TKI (2020) to treat HER2-POSITIVE MBC. It is reversible and highly selective for the kinase domain of HER2, with minimal inhibition of EGFR (1000-fold lower affinity) [67], resulting in a reduction in toxicity when compared to other TKI counterparts. Tucatinib is indicated in combination with trastuzumab and capecitabine for the treatment of HER2-positive locally advanced or metastatic BC who have received at least 2 prior anti-HER2 treatment regimens [68].

Each TKI targets different HER-receptors and therefore are associated with unique toxicity profiles. The most reported adverse events in all of them is diarrhea. Other gastrointestinal disorders (i.e., nausea and emesis) are also frequent, as well as skin rash, headache, anemia and pyrexia [69]. Less frequent but more severe are the cardiovascular toxicities, particularly a decline in left ventricular ejection fraction (LVEF) and congestive heart failure [70]. It is possible that tucatinib or other highly selective HER2 TKI will be used more broadly in the near future, as they appear to be better tolerated.

2.2. Toxicities associated to HER2-targeted therapies

The diverse array of HER2-targeted therapies underscores the dynamic landscape of precision medicine in HER2-positive cancer treatment. Despite the improvement of outcomes and survival of HER2-positive patients, these therapies are associated with many serious adverse events, being the most worrying are cardiac toxicity (trastuzumab), gastrointestinal toxicity (mainly TKIs), liver toxicity (T-DM1 and tucatinib), thrombocytopenia (T-DM1) and interstitial lung disease (T-DXd) and can be further exacerbated in combination with chemotherapy. **Table 1** provides a summary of the current EMA approved agents, their indication and important identified risks.

Drug	Type	EMA Approved indications	Most relevant toxicities *
Trastuzumab	mAb	○ Early HER2+ BC (1st line) ○ Metastatic HER2+ BC (1st line +) ○ Metastatic HER2+ GC/GEJC (1st line)	Cardiotoxicity, infections, lung toxicity and hematotoxcity
Pertuzumab	mAb	○ Early HER2+ (1st line + trastuzumab, if high risk of recurrence) ○ Metastatic HER2+ BC (1st line + trastuzumab)	Neutropenia, gastrointestinal disorders, fatigue
T-DM1	ADC	○ Early HER2+ BC (with residual invasive disease) ○ Metastatic HER2+ BC (2nd line)	Hematotoxicity, fatigue, hepatotoxicity and hypokalemia
T-D**Xd**	ADC	○ Metastatic HER2+BC (2nd/3rd line) ○ Metastatic HER2-low BC (1st/2nd line) ○ HER2+ metastatic GC/GEJC (2nd line) ○ HER2-mutant NSCLC	Hematotoxicity, fatigue, hepatotoxicity, hypokalemia, gastrointestinal disorders, interstitial lung disease, pneumonitis and cardiotoxicity
Lapatinib	TKI	○ Metastatic HER2+BC (3rd line + trastuzumab/ chemotherapy)	Diarrhea and skin toxicity
Neratinib	TKI	○ Early HER2+BC/HR+ (extended adjuvant)	Gastrointestinal disorders (diarrhea and vomiting)
Tucatinib	TKI	○ Metastatic HER2+BC (3rd line)	Gastrointestinal disorders (diarrhea) and hepatotoxicity

Table 1: Indications and main toxicities of EMA approved anti-HER2 targeted drugs

List of EMA approved anti-HER2 therapies as of February 2024. Type of drug, indications and main severe toxicities are indicated, with data obtained from the European public assessment report product information from the EMA website. mAb: monoclonal antibody; ADC: antibody-drug conjugate; TKI: tyrosine kinase inhibitor; BC: Breast Cancer; GC: gastric cancer; GECJ: gastroesophageal junction cancer NSCLC: Non-small cell lung cancer; HR: hormone receptor. *Administration-related and immunogenic reactions not included.

2.3. Mechanisms of resistance to HER2-targeted therapies

While the use of these targeted agents has greatly improved outcomes for patients with HER2-positive tumors, many patients still do not respond to therapy or relapse after initial response to treatment, ultimately leading to metastasis [71].

Clinical resistance to HER2-targeted therapies can be attributed to several mechanisms, including diminished binding of agents to the HER2 receptor, hyperactivation of downstream signaling molecules, signaling through alternative pathways, and inadequate triggering of antitumor immune responses [72]. Additionally, truncated forms of HER2, resulting in the shedding of HER2 ectodomain, have been proposed as resistance mechanisms, as they can evade monoclonal antibody targeting due to the lack of a targeting epitope [73]. In the case of antibody–drug conjugates, additional mechanisms of resistance may include defects in internalization, in the endosome–lysosome pathway, the drug efflux, or in drug cytotoxic action [74].

Overcoming these therapeutic challenges and improving survival rates, especially for advanced/metastatic HER2-positive cancer patients, requires the development of new treatment approaches. Cancer immunotherapy has emerged as a promising alternative, and this thesis focuses on the development of novel effective immunotherapeutic approaches for this subset of patients.

3. p95HER2: a truncated form of HER2

Besides the full-length HER2 protein (1.255 amino acids and 185 kDa), there exists a spectrum of truncated forms in the context of HER2-positive tumors, generally referred to as p95HER2 forms. These forms have gained attention due to their potential implications in cancer progression, as they can exhibit altered signaling properties, affecting cellular functions and contributing to oncogenic processes [75]

Truncated variants are generated through, at least, two mechanisms: proteolytic cleavage and alternative initiation of mRNA translation. The first case involves the metalloprotease ADAM10, which cleaves the extracellular domain of HER2 producing two separate fragments: a detectable HER2 extracellular domain in serum (sHER2) and a membrane-anchored carboxyl terminal fragment (CTF), with a molecular weight of 95-100 kDa **(648-CTF p95HER2)** [76]. Secondly, the translation of the mRNA encoding HER2 can initiate from two internal codons located at positions 611 and 678, before and after the transmembrane domain [77]. This alternative initiation leads to the production of two p95HER2 fragments: one weighing 100 to 115 kDa **(611-CTF p95HER2)** that, despite lacking a signal peptide, can be effectively transported and located to the plasma membrane, and the other ranging from 90 to 95 kDa **(678-CTF p95HER2),** that could be found both in the cytoplasm and the nucleus [77].

The intracellular variant is an inactive form and the 648-CTF had an activity comparable to that of full-length HER2. In contrast, the 611-CTF is a hyperactive form, since it induces a stronger activation of HER2 signaling pathways [78]. To date, the specific mechanism underlying the alternative initiation of translation remains unclear. This thesis will focus on the 611-CTF fragment, which will be referred to solely as p95HER2 throughout the text **(Fig.5).**

3.1. Implications of p95HER2 in tumor aggressiveness and therapeutic resistance

p95HER2 possesses a constitutively active kinase domain capable of autonomous signaling due to its ability to form homodimers maintained by intermolecular disulfide bonds. This leads to a much faster and more acute activation of different signaling cascades, promoting uncontrolled cell proliferation and migration and making tumors expressing p95HER2 more aggressive [79]. In addition, this fragment induces cell migration much more efficiently than full-length HER2 through the phosphorylation of cortactin, a cytoskeleton-binding protein [78]. Therefore, several studies have proposed p95HER2 as a biomarker of an aggressive subtype of HER2-positive BC [80].

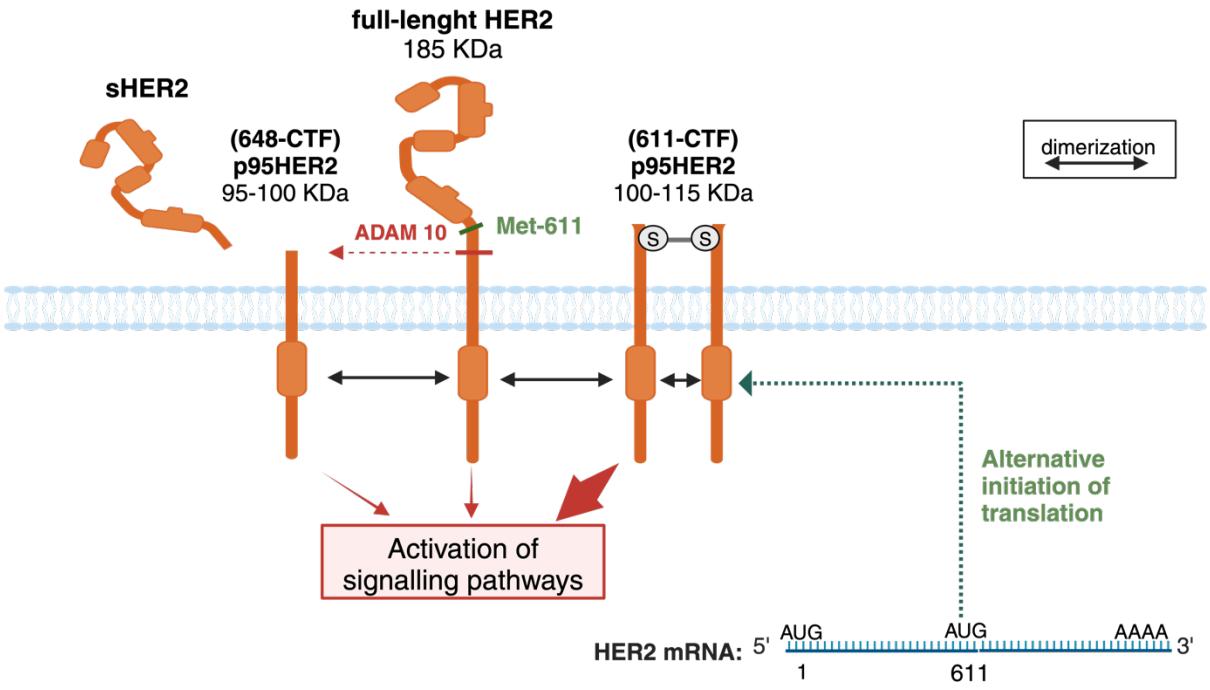

Figure 5: Truncated forms of HER2: p95HER2 carboxyl terminal fragments

Proteolytic cleavage in a site proximal to the transmembrane region gives rise to the 95-100 kDa variant (648-CTF) and an extracellular form that can be found in serum (sHER2). Alternative initiation of translation from methionine 611 (Met-611) produces a 100-115 kDa protein (611-CTF), a hyperactive form due to its ability to form dimers maintained by strong intermolecular disulfide bonds. Monoclonal antibodies targeting the 611-CTF are not able to recognize the full length HER2. Image adapted from [73]

An additional concern associated with p95HER2 is its role in therapy resistance. HER2-overexpression may lead to downregulation of ER receptors, reducing the effectiveness of endocrine therapy, and p95HER2 has been shown to exacerbate this downregulation [81]. Moreover, tumors expressing p95HER2 displayed reduced responsiveness to trastuzumab when used in monotherapy due to the absence of the trastuzumab-binding epitope [82]. However, contradictory findings have arisen regarding the correlation between p95HER2 expression levels and the clinical outcomes of HER2-positive BC patients undergoing treatment with trastuzumab-based therapy. One study showed the combination of chemotherapy with trastuzumab was associated with a more favorable pathological complete response in the presence of p95HER2 expression [83], explained by a HER2 stabilization induced by chemotherapy and higher sensitivity to chemotherapy in p95HER2 positive cells. [84]. Later, the identification of a high p95HER2/HER2 ratio in patients with metastatic BC has been associated with unfavorable outcomes during treatment with trastuzumab-based therapies, underscoring the need for additional research into the potential of the p95HER2/HER2 ratio as a prognostic or predictive biomarker for HER2-targeted therapy [80, 85]. What seems clear is that TKIs, since they act at the intracellular protein level, are able to block the activity of the p95HER2 fragments, making them a good therapeutic alternative in these p95HER2-positive resistant tumors [86].

3.2. p95HER2 is a Tumor Specific Antigen (TSA)

p95HER2 is a tumor-specific antigen (TSA), unlike HER2, which is expressed in normal tissues of epithelial and mesenchymal origin [87]. This discovery was enabled by the generation of mAbs that selectively target p95HER2 without binding to the full-length HER2 molecule [81, 88] by recognizing epitopes located in the N-terminus of p95HER2 that are inaccessible in the full-length HER2. These mAbs have also paved the way for the development of diagnostic and therapeutic tools.

About 30% HER2-positive breast tumors also express p95HER2, with the majority being HER2-amplified (80%). This finding was the initial indication pointing to p95HER2 as a potential TSA [81]. Notably, the presence of p95HER2 has also been

identified in lung [89] and endometrial cancers [90].

Our group has preclinically demonstrated that redirection of T cells via p95HER2 TCB is effective against HER2-positive tumors expressing p95HER2 and lacks on-target off-tumor toxicity. This p95HER2 TCB has activity, albeit limited, against p95HER2-positive BC tumors, while it has no effect on a variety of normal cells expressing physiological levels of HER2 [87]. These results confirm p95HER2 as a potentially safer clinical target and make it an attractive TSA to redirect other immunotherapies, such as CAR T cells, the focus of this thesis.

4. The immune system and cancer

Over the last decades, research exploring the intricate interplay between cancer and the immune system has uncovered profound insights into the mechanisms underlying tumor development and progression. The immune system, traditionally recognized for its role in defending the body against infections, also plays a critical role in surveilling and controlling cancerous cells through a complex network of immune cells, signaling molecules and regulatory checkpoints. However, cancer cells may evolve strategies to evade immune detection and destruction, constituting one of the Hallmarks of cancer [10], ultimately leading to tumor growth and metastasis. This section aims to underscore the intricate mechanisms governing the interplay between cancer and the immune system. Such comprehension is pivotal for developing novel therapeutic strategies to harness the body's immune defenses against cancer, known as immunotherapy.

4.1. Cancer-immunity cycle

The cancer immunity cycle delineates the interactions between the immune system and cancer across a series of well-defined stages. Cancer is characterized by the accumulation of genetic alterations and the breakdown of DNA repair systems. These genomic changes lead to the expression of cancer antigens, offering the immune system an opportunity to recognize cancer cells as foreign entities. TAAs are derived from normal cellular proteins, whereas TSAs result from mutations or abnormal protein expression [91–93]. Targeting TAAs, like HER2, carries the risk of side effects due to their expression in normal tissues. In contrast, TSAs, like p95HER2, offer more favorable targets for therapy as they are uniquely expressed in tumor cells and have not induced immune tolerance during development, facilitating the appearance of tumor-reactive immune cells. However, targeting TSAs derived from DNA mutations (neo-antigens) faces limitations, as mutations are often not shared between patients, necessitating complex sequencing technologies for personalized approaches [94].

Following tumor cell death, antigens are released into the TME, initiating the first phase

of the cancer-immunity cycle. The second phase involves **antigen presenting cells** (APCs), primarily dendritic cells (DCs), which capture and present these antigens using major histocompatibility complex (MHC) molecules, MHC-I and MHC-II. Antigen-loaded DCs travel to the lymph nodes, where they present these antigens to cognate T cells (third phase), which recognize them through their T cell receptor (TCR) molecules when presented by matching MHC molecules [95]. Of note, antigen presentation and T cell priming occur both in the lymph nodes or at the tumor site in tertiary lymphoid structures [93].

CD8 cytotoxic T lymphocytes (CTLs) recognize MHC-I presented antigens and are considered the most potent mediators in the antitumor response, directly attacking and killing cancer cells. **CD4 T cells** specifically identify antigens displayed by MHC-II molecules and cooperate in the activation and proliferation of CD8 T cells through the secretion of numerous activating cytokines, such as interleukin (IL)-2 (IL-2) and interferon-γ (IFN-γ) [96]. Upon activation, T cells clonally expand and differentiate into effector T cells, expressing chemokine receptors that allow exiting the lymph nodes and trafficking to the tumor (fourth phase). If they successfully infiltrate the tumor (fifth phase), bypassing the complex tumor microenvironment (TME), CD8 T cells specifically interact for the second time with the cognate antigen-MHC-I complex on the surface of malignant cells (sixth phase), culminating in the last step (seventh phase) of the cancer-immunity cycle: tumor cell elimination [93] **(Fig.6)**. The precise mechanisms for killing malignant cells will be addressed in the following section.

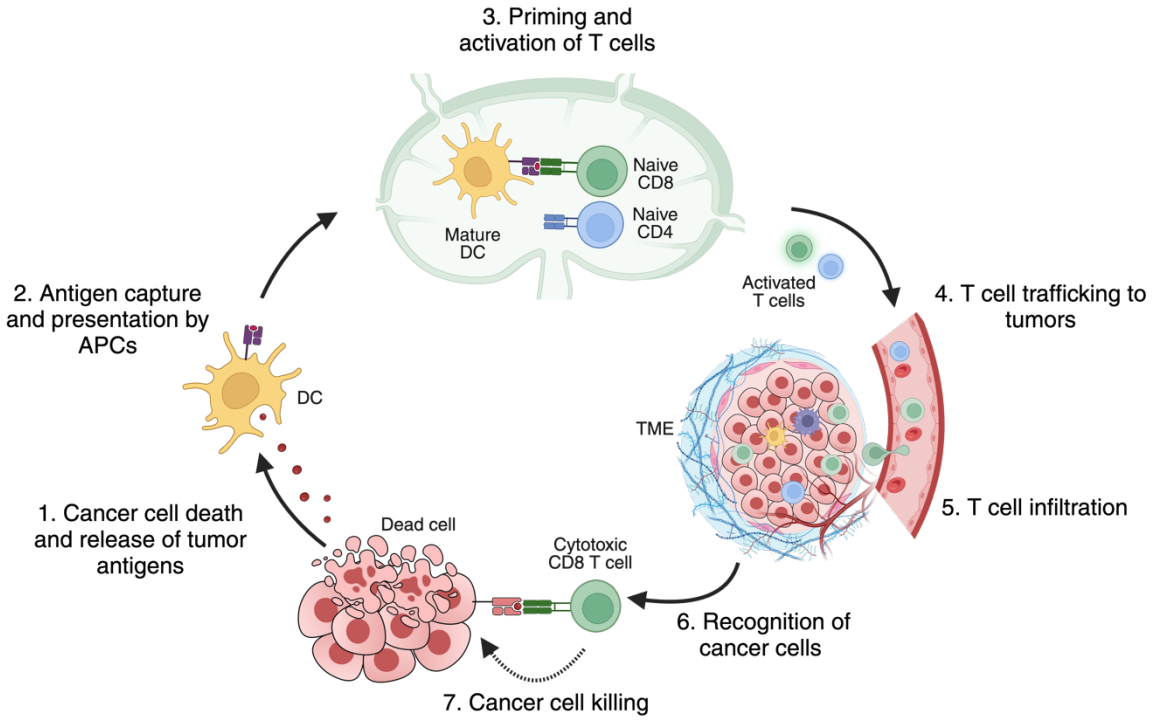

Figure 6: The cancer immunity cycle

The cancer immunity cycle is a self-propagating cyclic process, constituted by various phases or stages. Upon tumor cell death, antigens are released (1), which are then captured and presented by APCs (2). Naive T cells in the lymph nodes are activated upon encountering these antigens presented by APCs (3). Activated T cells migrate (4) and infiltrate the TME (5), where they recognize tumor cells through the interaction between the TCR and MHC molecules presenting tumor antigens (6). This recognition triggers the cytotoxic effects of T cells, ultimately leading to killing of tumor cells (7). Subsequent apoptosis of tumor cells releases additional tumor antigens, perpetuating the cycle of immune-mediated tumor cell destruction. Figure adapted from [97]. APC: Antigen presenting cell; DC: dendritic cell; TME: tumor microenvironment; MHC: major histocompatibility complex.

Understanding the cancer immunity cycle provides a pivotal foundation for comprehending mechanisms of T cell mediated killing, cancer-immunoediting and deciphering the mechanisms behind immunological resistance, which will ultimately lead to the development and application of successful immunotherapies for the treatment of cancer patients [98].

4.2. T cell activation, immune synapse and killing mechanisms

Successful activation of T cells, including both CD8 CTLs and CD4 helper T cells, relies on the integration of three key signals [99].

The **first signal** crucial for T cell activation is initiated by the binding of the T cell receptor (TCR) to antigenic peptides presented by major histocompatibility complex (MHC) molecules on antigen-presenting cells (APCs). This interaction triggers the recruitment or activation of key signaling molecules such as the lymphocyte-specific protein tyrosine kinase (Lck) and the ζ-chain-associated protein kinase 70 (ZAP-70), initiating a complex signaling network that leads to the reorganization of the T cell cytoskeleton and the polarization of signaling molecules towards the site of TCR engagement. This process ultimately results in the formation of a highly specialized and organized structure known as the immunological synapse (IS) between the T cell and the APC. Apart from the TCR interaction, other co-stimulatory receptors (e.g., CD28) and adhesion molecules (e.g., LFA-1) are also important contributors to the proper formation of the IS [100, 101]. Additionally, activated T lymphocytes can also directly recognize antigens presented on the MHC-I of malignant cells and eliminate them [94]. In addition, it has been recently discovered that CD8 T cell activation induces the expression of the innate receptor NKG2 for the elimination of MHC class-I deficient tumors, a feature previously thought exclusive to NK cells [102].

Co-stimulatory receptors present at the interface between APC and T cell during TCR antigen recognition provide the **second signal** required for successful T cell activation. The interaction of these co-stimulatory receptors, which include CD27, 4-1BB, OX40, CD30 and CD28, with their ligands amplify T cell activation, proliferation and survival. In contrast, there are also co-inhibitory receptors that diminish T cell activation, like CTLA-4, PD-1, TIM3, LAG3 and TIGIT [103, 104].

The **third signal** for complete T cell activation comes from cytokine stimulation, which is mainly provided by activated APCs, CD4 helper T cells and other cells present in the lymph node or tumor. IL-12, IFNα and IL-1 are the predominant sources of this third signal, providing survival, activation strength and differentiation [105].

Upon successful activation, T cells release or display various effector molecules, including cytolytic proteins, cytotoxic cytokines, and surface-bound ligands, collectively contributing to target cell killing.

Cytolytic proteins, such as perforin and granzymes, are central to CTL-mediated killing. Perforin forms pores in the target cell membrane, facilitating the entry of granzymes into the cytoplasm, where they activate caspases and induce apoptosis. Cytotoxic cytokines include the tumor necrosis factor (TNF) family ligands, like TNF- α, and IFN-γ, which play multifaceted roles in T cell-mediated cytotoxicity. IFN-γ can directly induce apoptosis and cell cycle arrest in tumor cells, while also modulating the TME by enhancing antigen presentation and promoting immune cell activation and recruitment [106]. The group of surface-bound ligands, include TNF-related apoptosis-inducing ligand (TRAIL) and Fas ligand (FasL), which can also trigger apoptosis in target cells upon binding to their receptors [107]**(Fig.7).**

In summary, the coordinated action of these signals and effector molecules orchestrates the potent cytotoxic response of T cells. T cell redirection immunotherapies, like the chimeric antigen receptor (CAR) T cells developed in this thesis, artificially induce these killing mechanisms, generating a potent antitumor response.

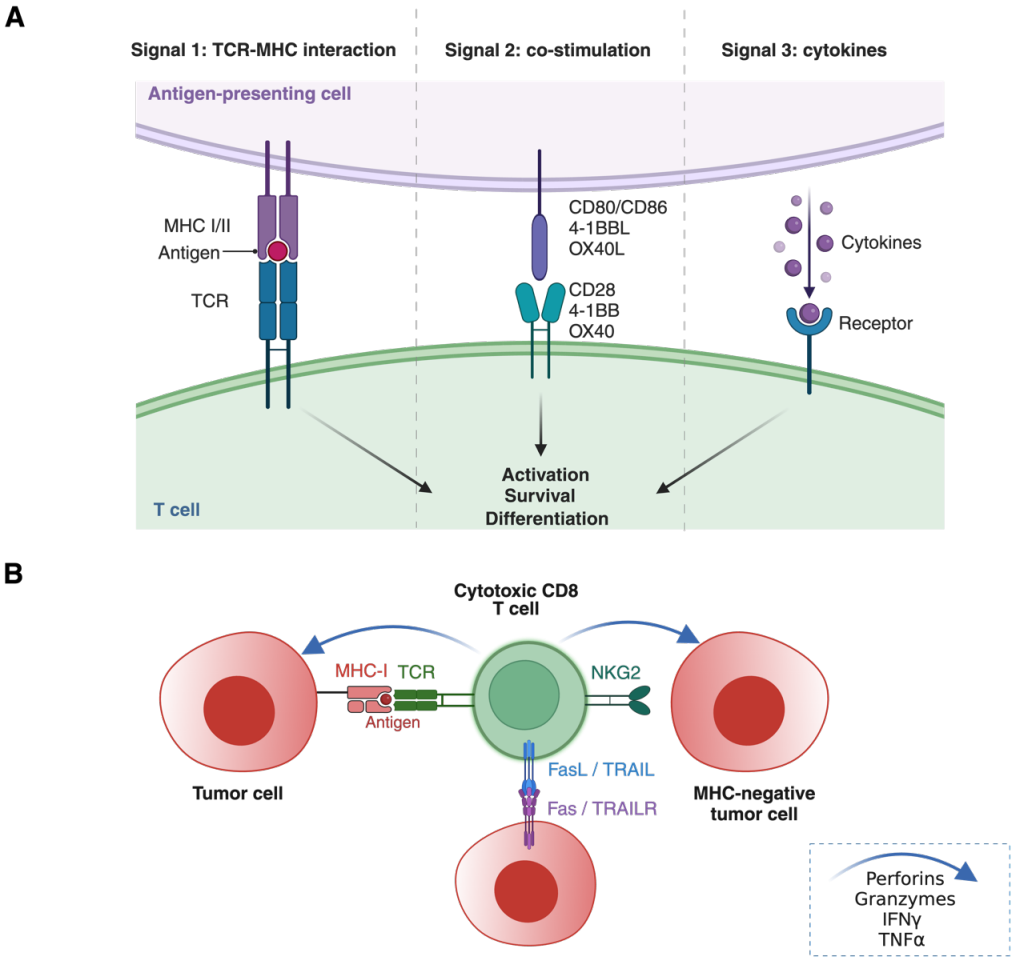

Figure 7: Signals for T cell activation and mechanisms of killing cancer cells

(A) Complete T cell activation relies on three key signals: 1) TCR recognition of antigen-MHC complexes; 2) Co-stimulation via receptors like CD28, 4-1BB and OX40 that bind to their corresponding ligands, CD80/86, 4-1BBL and OX40L respectively; and 3) Cytokine stimulation such as IL-12 and IFNα. **(B)** Upon successful activation, T cells elicits recognition of tumor cells through direct recognition of antigens presented by MHC via the TCR receptor or through recognition of MHC deficient tumors through the expression of NKG2 receptor. This recognition elicits killing of T cells through the secretion of several cytolytic molecules and cytokines, such as perforins, granzymes, TNF-a and IFN-γ. Additionally direct Induction of apoptosis can occur through FAS/TRAIL ligands. MHC, major histocompatibility complex; TCR, T cell receptor; IFN-γ: interferon gamma; TNF-a: tumor necrosis factor-alpha; FasL: Fas ligand; TRAIL: TNF-related apoptosis-inducing ligand; TRAILR: TRAIL receptors.

4.3. Cancer immunoediting

Despite their crucial role in eliminating cancer cells, T cells are not the only players in this complex succession of events aimed to eradicate malignant cells and prevent tumor progression. The immune system continuously seeks abnormal cells, engaging both innate and adaptive immune responses, even at the pre-cancerous stages. This phenomenon is commonly referred to as "immunosurveillance" and is now recognized as the initial step in the broader and intricate process known as "cancer immunoediting". "**Cancer immunoediting** unfolds in three distinct phases, often termed "the three Es": elimination, equilibrium and escape, characterizing the dynamic interplay between tumor cells and the immune system [108] **(Fig.8)**. Cancer immunoediting is not confined to natural tumor progression but it is also observed in patients undergoing anticancer immunotherapies [108].

During the **elimination** or **immunosurveillance phase**, the immune system actively eliminates emerging tumor cells before they progress to clinically detectable stages. This phase involves the coordinated efforts of both innate and adaptive immune cells. Natural killer (NK) and Natural Killer T cells (NKT) are pivotal components of the antitumor innate immunity, engaging in direct recognition and elimination of cancer cell, as well as secreting proinflammatory cytokines such as IFN-γ and TNFα, further enhancing the immune recruitment. Additionally, γδ T cells, a hybrid between adaptive and innate immune cells, recognize cancer cells through their TCR and other ligands, and directly target them by secreting cytolytic molecules (granzymes and perforin) and proinflammatory cytokines. Macrophages and DCs also play crucial roles by presenting tumor antigens to CD8 and CD4 T cells, thereby initiating the adaptive antitumor immune response. Successful elimination of cancer cells during this phase concludes the immunoediting process, while failure to completely eradicate malignant cells or the emergence of immune-resistant variants facilitates tumor progression to the next phase [109, 110].

The **equilibrium phase** represents a delicate balance between the immune effector system and residual cancer cells, that can last for years, known as tumor dormancy. These remaining cancer cells are held in check by continuous immune pressure,

preventing their proliferation and expansion, mainly though the action of cytotoxic CD8 T cells, IL-12 and IFN-γ, secreted mainly by CD4 T cells and macrophages respectively. During this phase, a process known as “immune-editing” occurs, allowing the selection of less immunogenic cancer cell variants and other immunosuppressive mechanisms that enable disease progression [108–110]

The **escape phase** encompasses the outgrowth of immune-edited tumor cells, culminating in the development of clinically detectable tumor. In addition to intrinsic immunogenic alterations within tumor cells, the establishment of an immunosuppressive TME, characterized by the presence of immunosuppressive molecules, like TGF-β, IL-10 and cells, most notably regulatory T cells (Tregs) and myeloid derived suppressor cells (MDSC), also plays a significant role in facilitating tumor escape [109, 110]. These mechanisms will be further discussed in the next section.

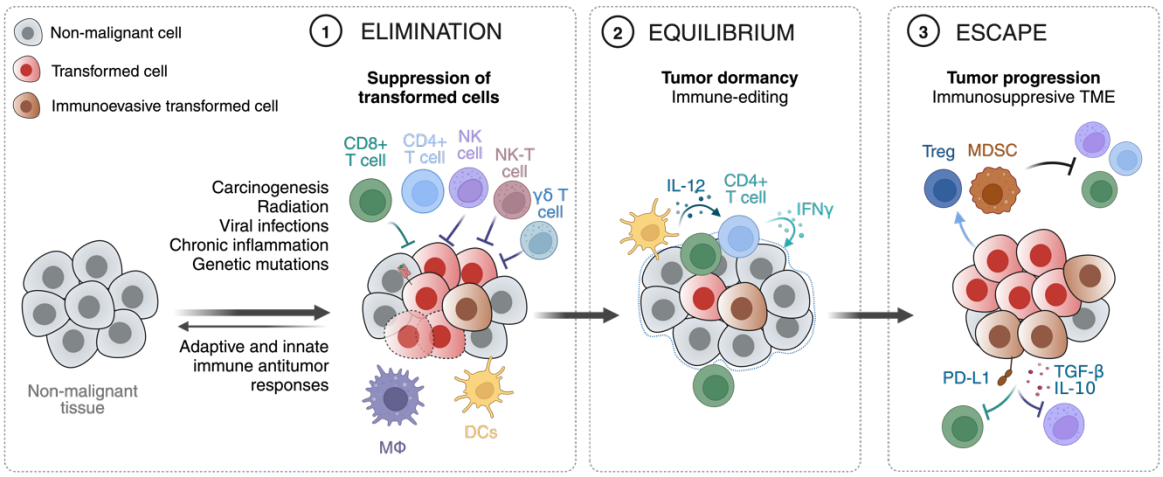

Figure 8: Cancer immunoediting: “the three Es”

Normal cells can become malignant under different stimuli initiating the cancer immunoediting process, which encompasses three sequential stages: elimination, equilibrium, and escape. (1) The elimination phase entails a collaborative effort between the innate and adaptive immunity to recognize and eliminate cancer cells. (2) The equilibrium phase is characterized by limited net growth and immune-editing of cellular immunogenicity. (3) The escape phase is marked by unrestrained growth driven by immunosuppressive molecules and cells and tumor intrinsic resistance mechanisms. NK: natural killer: DC, dendritic cell; MΦ: Macrophage; MDSC, myeloid-derived suppressor cell; Treg: regulatory T cell. Adapted from [108]

4.4. Immune escape mechanisms

Given the complex and coordinated nature of immune explained above for the successful tumor control, it becomes evident that diverse mechanisms of resistance may arise, as has been described preclinically and observed in patients [111]. Immune cells represent just one component of the TME, alongside endothelial cells and fibroblasts [112]. The TME profoundly influences tumor cell behavior, exerting significant impacts on disease onset, progression, and response to therapy. Resistance mechanisms can be broadly classified into two categories: tumor-intrinsic and tumor-extrinsic. Tumor-intrinsic mechanisms encompass strategies employed by cancer cells to evade immune surveillance, while tumor-extrinsic resistance mechanisms are mediated by other cellular populations present within the TME [113]. These mechanisms may manifest during various stages of tumor progression and are also observed during immunotherapy treatment.

Tumor-intrinsic resistance mechanisms

Tumor-intrinsic mechanisms of resistance include the downregulation or loss of tumor antigens, the release of immunosuppressive molecules, and upregulation of immune checkpoint molecules, among others [114].

Cancer cells release **immunosuppressive factors** like IL-10, transforming growth factor-beta (TGF-β), IL-4 and indoleamine 2,3-dioxygenase (IDO) [115]. Simultaneously, tumors may overexpress ligands that bind to co-inhibitory immune receptors on the surface of T cells, including **immune checkpoint molecules** like programmed cell death-ligand 1 and 2 (PD-L1 and PD-L2), leading to the induction of tumor tolerance and T cell exhaustion [116].

Furthermore, tumor cells can evade immune detection by downregulating or completely shutting down the **antigen-presenting machinery**, such as the loss of beta-2-microglobulin (B2M), which is essential for MHC-I surface expression, thereby rendering cells invisible to the immune system [117, 118]. However, this evasion mechanism may be mitigated when tumor antigens support the proliferation of tumor

cells, known as “oncogenic drivers” [119]. Complete loss of MHC-I is infrequent because NK cells identify these cells as defective and eliminate them efficiently [120]. Additionally, defects in immune synapse formation, [121] and in the IFNγ and TNF signaling pathways constitute additional tumor-intrinsic mechanisms of resistance to immune mediated killing, also in the context of immunotherapies [122–124]

Tumor-extrinsic resistance mechanisms

Tumor-extrinsic mechanisms encompass a complex interplay involving diverse cell types and are profoundly influenced by the unique anatomical and physical characteristics of the TME, particularly evident in solid tumors like pancreatic cancers compared to hematological malignancies [125, 126].

Physical conditions inherent to solid tumors, such as a dense extracellular matrix (ECM), hypoxia, acidification, and poor nutrient supply, pose significant barriers to immune cell infiltration, function and survival. Additionally, immunoevasive tumor cells have the capacity to induce or attract **immune cells with immunosuppressive functions**, including regulatory T cells (Tregs), myeloid-derived suppressor cells (MDSCs) and tumor associated macrophages (TAMs), as well as immunosuppressive stromal cells like cancer-associated fibroblasts (CAFs). These populations collectively contribute to the establishment of a protumorigenic ecosystem [111].

The understanding of these immune escape mechanisms provides critical insights for the development of novel cancer immunotherapies aimed at overcoming these barriers and restoring effective antitumor immune responses.

5. Cancer immunotherapy

Cancer immunotherapy aims to stimulate and enhance the immune system's natural mechanisms, enabling it to recognize and eliminate cancer cells. Immunotherapy has demonstrated its potential to induce durable responses and, in some cases, long-term remission in multiple cancer types. Unlike traditional therapies like chemotherapy and radiation, that may harm healthy cells, immunotherapy aims to enhance the body's natural defenses selectively, reducing side effects. This innovative therapeutic strategy offers new hope and avenues for the treatment of early and advanced-stage cancers, particularly in the context of solid tumors.

Immunotherapy can work in several ways. One approach consists of therapies aimed at boosting a pre-existing response, which depend on classical recognition of the tumor cells by the T cells through the MHC-TCR interaction. The second strategy is by redirecting T cells towards a tumor antigen, independent of antigen recognition by the TCR. The first group includes therapeutic vaccines, oncolytic viruses, stimulatory cytokines, immune checkpoint inhibitors (ICIs), co-stimulatory agonists and the MHC-dependent adoptive cell therapies (ACTs): tumor infiltrating lymphocytes (TILs) and engineered-TCR T cell therapy. The second group includes the T cell redirection strategies, such as engineered TCBs or T cell engagers (TCE), and CAR T cell therapy, another ACT [127] **(Fig.9)**

ACTs, including TIL, TCR and CAR T cell therapies, involve harvesting, genetically modifying and/or expanding a patient's own immune cells (such as T cells) to enhance their antitumor capabilities before reinfusion. To date, only autologous ACTs have been approved [128]. This thesis will focus on the subset of T cell redirection therapies, characterized by their ability to bypass classic MHC-TCR recognition to kill cancer cell, and other approaches will be described briefly.

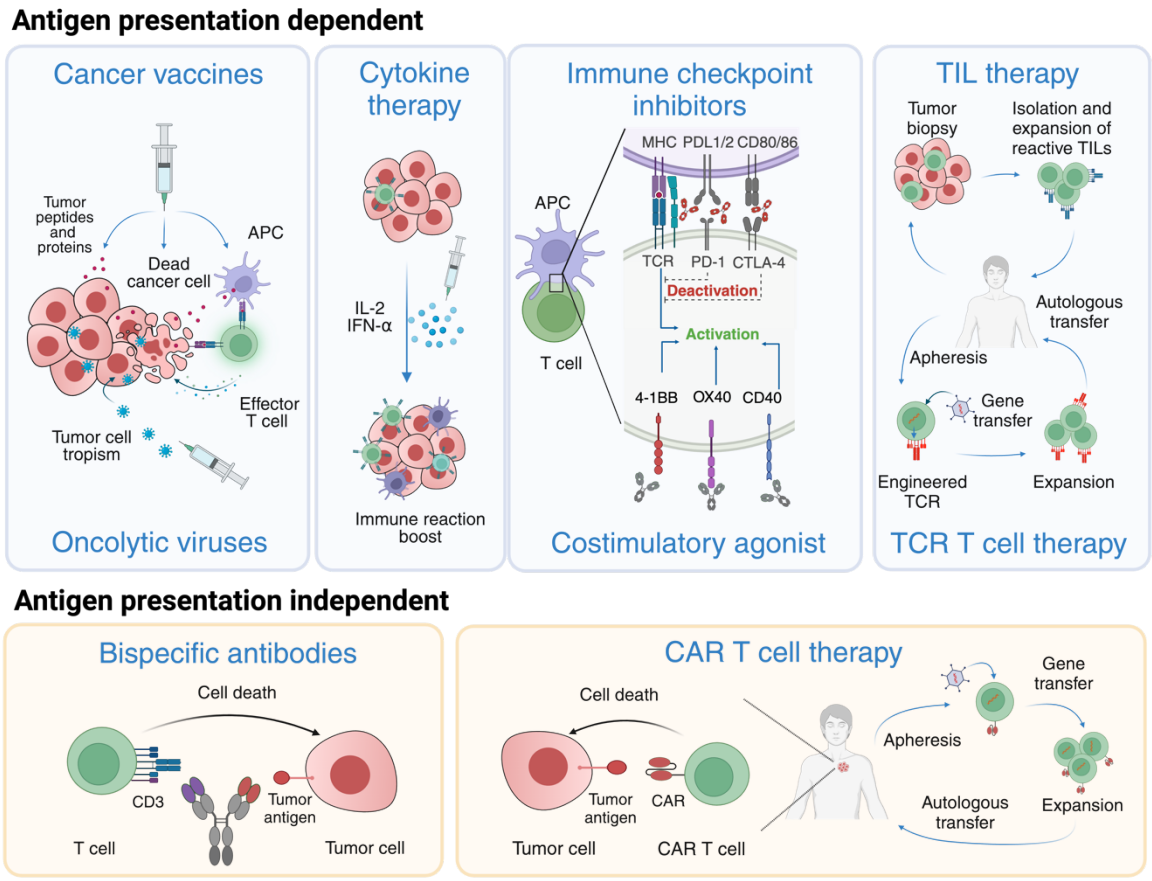

Figure 9: Main types of cancer immunotherapies

Immunotherapeutic strategies can be categorized into antigen presentation-dependent (blue) or -independent (yellow). Cancer vaccines and oncolytic viruses deliver antigens to improve the recognition of tumor cells by T cells, with oncolytic virus exerting a direct cytolytic effect. Cytokine therapy provides activating stimuli to boost the antitumor immune response. Immune checkpoint inhibitors (anti-PD-L1/PD-1/CTLA-4) block inhibitory signals that inhibit T cell functionality and agonists targeting costimulatory receptors like 4-1BB, OX40 or CD40 enhance T cell activation. In TIL therapy, tumor reactive T cells are isolated from tumor biopsies, expanded and reinfused back to the patient, with the possibility of purifying the tumor-reactive clones. TCR T cell therapy transduces patients' T cells with an exogenous TCR to guarantee a specific recognition against a certain antigen, followed by reinfusion after expansion. CAR T cells and bispecific antibody-driven T cells recognize the tumor cell independently of the antigen presentation through the peptide-MHC-TCR, and bind to a particular tumor surface antigen, causing T cell activation and direct killing of tumor cells. CAR, TIL and TCR T cell therapy, are considered cellular or adoptive cell therapies.

5.1. MHC-TCR interaction dependent strategies

Vaccines

Cancer vaccines aim to expose the immune system to specific antigens to generate active immunity against the tumor. They can be preventive (e.g., vaccine for human papillomavirus) or therapeutic, using technologies such as short antigen peptides, whole protein vaccines, autologous cancer cell vaccines (weakened or inactivated), autologous DCs, bacterial-based vaccines, and nucleic acid-based vaccines [129]. Sipuleucel-T (Provenge®), a personalized dendritic cell vaccine used to treat advanced prostate cancer, and Bacillus Calmette-Guerin (BCG) for early-stage bladder cancer are the only two approved ones.

Oncolytic virus therapies

Oncolytic viruses selectively target and destroy malignant cells. Engineered or naturally occurring viruses, such as adenoviruses or herpes simplex viruses, specifically replicate within cancer cells, leading to a specific type of programmed cell death that releases signals and molecules that attract immune cells, known as immunogenic cell death. With advances in genetic engineering, oncolytic virus therapies have made much progress in recent years. In particular, talimogene laherparepvec (T-Vec), also known as Imlygic®, a genetically attenuated herpes simplex virus administered locally, has been approved for the treatment of unresectable metastatic melanoma [130]

Cytokine therapies

Cytokines act as vital messengers in the immune system. IL-2, which stimulates T-cell proliferation, and IFN-alpha (IFN-α), which can induce tumor cell senescence and apoptosis, exemplify cytokines used for CIT [131]. Clinical studies have proven the therapeutic effect of IFN-α at high dosages for chronic myeloid leukemia [132] and melanoma [133]. However, their clinical use is limited due to severe toxicities [134, 135].

Co-stimulatory agonists

The immune system relies on a balance between co-stimulatory and inhibitory signals to regulate the activation and function of T cells. By activating these co-stimulatory receptors, such as 4-1BB, OX40, and CD40, co-stimulatory agonists can enhance the immune response against cancer cells. However, as monotherapies, co-stimulatory agents have demonstrated limited clinical antitumor activity, so combination with other immune therapies seems to be a better approach [136–138]

Immune check-point inhibitors (ICIs)

Immune checkpoint blockade (ICB) is a strategy that involves blocking the binding of immune checkpoints, PD-1 and CTLA-4, to their cognate antigens, PD-L1 and B7/CD80, respectively. The aim is to inactivate the “brakes” and enhance T cell immune responses. ICIs constitute the most widely use immunotherapy in the last decade, particularly for the treatment of melanoma and non-small cell lung cancer (NSCLC), but also for renal cancer, head and neck carcinoma, Hodgkin lymphoma and TNBC, among others [139–141]. These agents include anti-CTLA-4 (ipilimumab, tremelimumab), anti-PD-1 (pembrolizumab, nivolumab, cemiplimab, toripalimab, tislezizumab) and anti-PD-L1 (atezolimumab, durvalumab, avelumab) antibodies. Recent studies have identified several new immune checkpoint targets, including lymphocyte activation gene-3 (LAG-3), T cell immunoglobulin and mucin-domain containing-3 (TIM-3), T cell immunoglobulin and ITIM domain (TIGIT), V-domain Ig suppressor of T cell activation (VISTA), and other [116]. However, a considerable portion of patients remains unresponsive to immune checkpoint inhibitors, and the identification of better predictive biomarkers, which to date is limited to tumor mutation burden (TMB) and PD-L1 expression, should guide treatment strategies. [142, 143].

TIL therapy

TIL therapy, pioneered over 40 years ago by Dr. Steven Rosenberg at the National

Cancer Institute [144], involves harvesting, culturing, and expanding lymphocytes that have infiltrated tumors. The process includes infusing these cells back into the patient, sometimes incorporating the selection and enrichment of neoantigen-specific reactive TILs.

This therapeutic approach has the potential to target a diverse range of antigens and effectively infiltrate tumors. However, it requires the presence of effector T cells with antitumor activity, which is not the case for many cancer types. Overcoming limitations, such as insufficient *in vivo* persistence and immune suppression in the harsh TME, often involves prior lymphodepletion and co-administration of IL-2. This helps activate, support expansion, and prolong the survival of infused T cell [145]. The successful application of TIL therapy is currently limited to some tumor types such as melanoma [146] and advanced cervical cancer [147]**.** Preliminary efficacy has also been demonstrated in non-small cell lung cancer [148]**,** colorectal cancer [149] and BC [150].

TCR engineered T cell therapy

Engineered TCR-T cell immunotherapy involves infusing T cells that have been genetically modified *ex vivo* to express specific TCRαβ genes capable of recognizing peptides presented on the tumor cell surface by MHC molecules. This approach allows for targeting not only surface antigens but also intracellular antigens. While TCR-T therapy has demonstrated success in treating solid tumors, especially melanoma [151], challenges include identifying specific tumor antigens for TCR targeting. Even when using highly specific antigens, some TCR T cell clinical trials have resulted in severe and even fatal toxicities [153, 154]. Another challenge involves ensuring that the T cells have optimal avidity and fitness to effectively target and survive in the TME. Improving TCR affinity, providing additional T cell co-stimulation, or utilizing antibodies to block immunosuppressive signals can enhance therapeutic outcomes [155, 156].

5.2. MHC-TCR independent T cell redirection strategies

Due to their remarkable potency and specificity, and their success in the treatment of hematological malignancies, T cell redirection strategies stand out as a particularly

promising avenue within the realm of immunotherapy for targeting surface antigens, since they bypass MHC restriction and cause T cell activation independent of the TCR specificity [157]. In the context of HER2-positive BC, HER2 contributes to the downregulation of MHC class I expression through a pathway dependent on RAS/mitogen-activated protein kinase [158], thus MHC-TCR independent strategies will bypass this possible mechanism of resistance.

In contrast to TCRs, CAR T cells and TCBs engage with these antigens forming a non-classical immune synapse (IS), eliciting T cell activation [159]. Then, activated T cells mediate their killing effects through the secretion of cytotoxic molecules (perforin and granzyme), the Fas-FasL axis, as well as the release of cytokines (IFNγ), utilizing, at least in part, the conventional TCR signaling machinery [160].

Both strategies face common challenges, including lack of tumor antigen specificity, antigen heterogeneity and local immune suppression. The success of CAR T cell therapy and BiTEs® in treating B cell malignancies can be attributed to the lack of an immunosuppressive TME and to the effective targeting of the CD19 antigen, which is highly expressed, despite cases of antigen downmodulation, and highly specific for the B cell lineage. Notably, targeting normal CD19-positive B cells does not cause severe side effects. However, this suitability is not replicable for most targetable antigens, particularly those present in solid tumors [157]. The most frequently targeted antigens both preclinically and clinically, with CAR T cells and BiTEs® in solid tumors are HER2, EGFRvIII (glioblastoma), mesothelin (mesothelioma), GD2 (neuroblastoma), Glypican-3 (hepatocellular carcinoma), CEA (multiple solid tumors), PSMA (prostate), Claudin 18.2 (some solid tumors), EpCAM (multiple solid tumors) and AFP (hepatocellular carcinoma and some others) [157, 161]. Except EGFRvIII, the rest are TAAs, and thereby are also expressed in healthy tissues at low levels, posing toxicity risk [154, 162, 163]. Therefore, targeting alternative TSAs like p95HER2, as proposed in this thesis, as well as discovering novel ones or modifying targeting affinities to discriminate between malignant and healthy tissues [164–166], as have been tested with HER2, are crucial for developing safer T cell redirection strategies. In addition, cytokine

release syndrome (CRS) and neurotoxicity, known as immune effector cell–associate neurotoxicity syndrome (ICANS), are frequent and severe toxicities following both T cell redirection therapies, independently of the target antigen [167, 168].

T cell bispecific antibodies

Bispecific antibodies (bsAbs) constitute a diverse group of engineered antibodies designed to bind two different epitopes or antigens simultaneously. These antibodies can act in multiple ways: (I) by redirecting specific immune effector cells to selectively kill cancer cells; (II) by targeting more than one cell surface antigen, increasing target specificity or blocking to different biological pathways; and (III) by delivering drugs to tumors [169]. TCBs and other TCEs, first described by Staerz and colleagues [170] consist of two antigen- binding domains of different specificities, one binding to a tumor antigen and the other binding to the TCR, typically by targeting CD3ε, inducing TCR-mediated T cell activation and eventually killing of target cell [171].

These molecules can present various formats, broadly categorized into two groups: IgG-like, which retains an Fc region, and non-IgG-like, lacking an Fc region. Full-length TCBs with an Fc region exhibit prolonged half-lives in circulation compared to those without along with enhanced solubility, stability, and the potential to retain Fc-mediated effector functions such as ADCC, ADCP and CDC. In the latter case, these molecules are considered T cell trispecific antibodies [172]. However, in many cases, the Fc domain is engineered to abolish immune effector functions, thereby preventing unwanted inflammatory responses [173].

In contrast, the shorter-length non-IgG-like format displays relatively shorter circulation kinetics but offers improved tissue-penetrating capacity, lower immunogenicity and reduced nonspecific activation of the innate immune system, reducing toxicities. This format is particularly preferred for in situ antibody secretion, exemplified by bispecific T cell engagers or BiTEs®, which consist of two single-chain variable fragment (scFv) molecules targeting CD3 and the desired tumor antigen, joined by simple linkers [174]. Improvements of this non-Fc format can be achieved by increasing the stability by fusing a scFv to the C terminus of the light or heavy chain of an IgG [161]. Other formats

such as TandAbs®, constructed by linking two diabodies (two covalently linked polypeptide chains, where one chain contains parts from one antibody and the other chain contains parts from another antibody) with peptide linkers, and DARTs, designed with a disulfide bond between two peptide chains, offer further options for versatile bispecific antibody design [175].

While the recruitment of T cells remains the preferred strategy due to their high cytotoxic potential and abundance, alternative immune cells can be engaged by substituting the CD3 arm, for example, NK cells using CD56 targeting, known as Bispecific NK engagers (BIKES) or trispecific T cell engagers (TRIKES), provided they retain Fc immune functions [176].

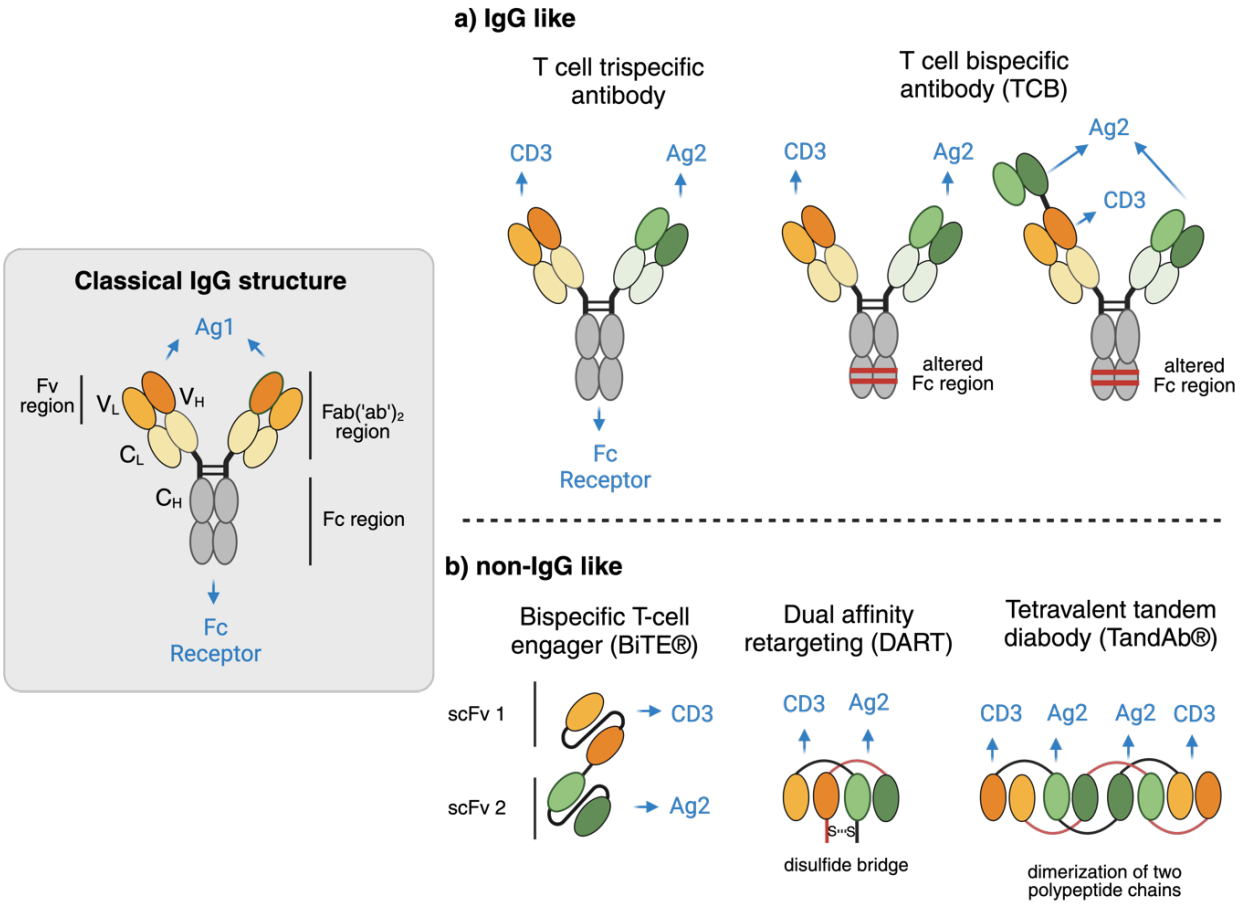

Figure 10: Examples of designs and formats of tri- and bi-specific antibodies

Engineered bi-specific antibodies can be broadly classified according to the (a) presence (IgG like) or (b) absence of an Fc domain (non-IgG like), and presenting a wide variety of structural formats within each group. All bi-specific antibodies contain two single chain variable fragments (scFv) derived from the variable antigen binding region of classical IgG molecules that target two different targets or epitopes. In the IgG like group, antibodies that preserve FC domain intact are considered T cell trispecific antibodies, since they can also bin to FC ligands present in some immune cells. To avoid exacerbated immune reactions, this FC domain can be truncate, and thereby are considered bispecific. Examples of three different bispecific engagers lacking FC molecules are represented, such as BiTEs®, DARTs® and TandAbs®. Ag2: Antigen 2; Fv: variable fragment; Fc: constant fragment; Fab: antigen binding fragment; IgG: Immunoglobulin G; scFv: single chain variable fragment.; V_H: variable heavy chain; V_L: variable light chain; C_H: constant heavy chain; C_L: constant light chain.

There are five T cell redirecting bispecific antibodies approved for the treatment of hematological tumors, which target different B cell antigens: CD19, BCMA and CD20.

Blinatumomab (Blicynto®), the first BiTE® (bispecific T-cell engager) approved, targets CD3 and CD19 for relapsed or refractory B precursor acute lymphoblastic leukemia (ALL) [177]. Teclistamab (Tecvayli®), a CD3 and BCMA targeting antibody, is approved for multiple myeloma (MM) [178]. Additionally, three bispecific antibodies targeting CD3 and CD20 have been approved for the treatment of relapsed or refractory tumors: mosunetuzumab (Lunsumio®) for follicular lymphoma, epcoritamab (Tepkinly®) for diffuse large B-cell lymphoma, and glofitamab (Columvi®) for diffuse or not large B-cell lymphoma. In contrast, only one T cell engager has been approved for treating solid tumors: tebentafusp (Kimmtrak®). It is a first-in-class agent that redirects T cells via CD3 scFv to target a specific gp100 peptide presented by HLA-A*02:01 molecules, through a soluble engineered-TCR, which makes it different to the previously described BiTEs®, which engage antigens through antibody-derived scFvs. This innovative treatment has recently gained approval for uveal melanoma, a rare and aggressive form of melanoma affecting the eye, providing a targeted therapeutic option where none previously existed [179].

Limitations of TCBs and BiTEs®

While TCBs and BiTEs® hold immense therapeutic potential, several limitations must be addressed to maximize their efficacy and applicability in clinical settings, in addition to the general limitations of T cell redirecting therapies regarding the antigen and the TME. Firstly, the manufacturing process for bispecific antibodies is intricate and resource-intensive, requiring specialized cell line production procedures, and rigorous analytical and purification methods [180]. Overcoming these challenges demands significant investments in time, expertise, and resources to ensure the production of high-quality therapeutic products, usually not affordable for academic institutions. Moreover, post-production issues such as degradation, aggregation, denaturation, fragmentation, and oxidation of antibodies pose additional hurdles that need to be mitigated to ensure the stability and efficacy of the final product [180].

Another consideration is the short serum half-life of BiTE®s, which typically lasts for several hours. While this short half-life offers precise control over drug levels in

patients, it necessitates continuous intravenous infusion for sustained therapeutic effect. Portable minipumps have emerged as a practical solution for administering BiTE® antibodies over extended periods, as demonstrated with agents like blinatumomab [181][181][181] continues to evolve, offering new avenues for improving cancer treatment outcomes.

In situ production of BsAbs

In situ production of bispecific antibodies represents a promising solution to manufacturing challenges and aims to optimize therapeutic outcomes by increasing circulation kinetics and overcoming the immunosuppressive TME. Platforms to deliver bsAbs in tumor tissues include engineered oncolytic viruses [182, 183].

T lymphocytes were first recognized as bsAb vehicles nearly a decade ago, when primary human peripheral blood lymphocytes were modified ex vivo with a vector encoding an anti-CEA × CD3 diabody [184]. Other examples include T cells secreting bispecific engagers targeting CD3 and CD123, EphA2 and CD19 respectively, known as ENG-T cells [185]. Additionally, the so-called STAb-T cells developed by the group of Dr. Álvarez-Vallina, are also autologous engineered T cells secreting, for example, anti-BCMA T cell engagers for treating multiple myeloma [186].

Antibodies secreted by CAR T cells are currently of particular interest [187]. This approach presents a substantial advantage because not only transduced T cells recognize and kill antigen-positive tumor cells but also unmodified bystander T cells can be activated and redirected against tumor cells through bsAbs, synergistically leading to potent antitumor immune responses [188]. This combination can be applied for the targeting of different antigens to address heterogeneity, but also the same antigen, like CD19 CAR T cells secreting CD19 BiTEs STAb-T19. The latter strategy showed that combination of the two molecules, even when targeting the same antigen, overcome CAR-mediated CD19 downmodulation and was superior in long-term *in vivo* assays, demonstrating lower relapse rates [189]. All this previous research has been key in the development of the next generation CAR T presented in this thesis.

TCBs, BiTEs® and other immune cell redirection antibodies for the treatment of HER2-positive tumors

The concept of TCBs targeting HER2 emerged in 2001 [190], marking the beginning of extensive exploration and development in this field. Several HER2 TCBs and BITEs have entered early phase clinical trials, underscoring the growing interest and investment in these therapies for the treatment of HER2-positive tumors [57, 191]. Among these, Genentech's humanized HER2 TCB, Runimotamab, has advanced into phase I trials (NCT03448042), demonstrating activity against several locally advanced or metastatic HER2-expressing cancers [192].

Another interesting approach is the infusion of autologous ex vivo activated T cells loaded with HER2/CD3 BiTEs, known as HER2Bi–aATCs or HER2BATs, combined also with low-dose IL-2 and granulocyte-macrophage colony-stimulating factor (GM-CSF). This therapy has been developed at the University of Virginia and results from a phase I/II (NCT03272334) trial demonstrated preliminary efficacy, and no dose-limiting toxicities [188, 192].

A trispecific T cell engager (SAR-443216) targeting HER2/CD3/CD28 with potent T cell-dependent cytotoxicity for HER2-low tumors is currently under evaluation in a phase I trial (NCT05013554) [193]. Similarly, TAC01-HER2 targets HER2 /CD3/CD4 co-receptor, and is undergoing evaluation in phase I/II trial (NCT04727151). In addition, an NK cell engager (NKCE) targeting HER2 is also under clinical investigation. DF1001 (Dragonfly Therapeutics) is a tri-specific NKCE therapy (TriNKET) being investigated in patients with various advanced-stage HER2-positive solid tumors, including in combination with the anti-PD-1 antibody nivolumab (NCT04143711, NCT05597839), with appealing safety and notable efficacy results, including in HER2-low tumors [194].

However virtually every HER2-targeting therapy presents concerns regarding the risk of on-target off-tumor toxicities due to the expression of HER2 in healthy tissues. To address this issue, researchers have developed TCBs with both CD3 and HER2 arms masked by unstructured polypeptides (XTEN), which are only exposed upon protease

cleavage [192]. TCBs with reduced affinity for HER2 to allow recognition of HER2-overexpression in tumors have also been described [165, 166]. Alternatively, targeting a TSA expressed in a subset of HER2-positive tumors, like p95HER2 could also provide enhanced safety to this promising therapeutic strategy. Our group has demonstrated the feasibility of this approach through the development of a TCB targeting p95HER2 in preclinical models. Compared to a HER2 TCB, the p95HER2 TCB did not affect HER2-expressing non-transformed cells, making it a potentially safer treatment for a subgroup of HER2-positive tumors [87].

CAR T cell therapy

CARs are synthetic receptors engineered to redirect effector immune cells, typically T cells, towards cells expressing a specific target antigen on their cell surface [195]. The CAR structure generally consists of an antigen binding domain, a transmembrane domain, and intracellular signaling motifs capable of T cell activation. The extracellular domain is composed of single-chain variable fragment (scFv) derived from an antibody which recognizes the tumor antigen independently of MHC presentation [195].

Classical production of CAR T cells involves genetic modification of primary lymphocytes using viral vectors like g-retroviral vectors or lentiviral vectors, which integrate semi-randomly into the human genome, with the latter considered to subtly involve lesser genotoxicity in hematopoietic progenitors [196]. More sophisticated and precise gene editing methods are being increasingly studied and applied [197–199].

The success of CAR T cell therapy in certain subsets of B cell leukemia or lymphoma, with remarkable efficacy and enduring clinical responses, is evident through the approval of six CAR T cell therapies—four targeting CD19 and two targeting BCMA. These results have encouraged scientists, including our group, to develop CAR T cell therapies for the treatment of a wide diversity of cancers with limited treatment options, including solid tumors. However, effectiveness of CAR T in solid tumors to date has been generally limited. Promising recently published results from a phase I/II clinical trial led by Drs. Quintarelli and Locatelli, testing disialoganglioside GD2-targeted CAR T cells containing two co-stimulatory domains demonstrated unprecedented results in

treating relapsed or refractory high-risk neuroblastoma, a pediatric cancer responsible for 11% of all cancer-related deaths in children. Among the 27 enrolled patients, the overall response rate was 63%, including 9 patients with a complete response and 8 with a partial response. The 3-year overall survival reached 60%. Although efforts are still required for extending these results to other therapies and malignancies, this groundbreaking clinical trial instills hope to the scientific community and our group, for the development of successful CAR T cell treatments for solid tumors [200], in our case, the development of p95HER2 CAR T cells for the treatment of a subset of unresponsive HER2-positive tumors.

CAR T cells structure and evolution

In 1993, Eshhar and colleagues developed the first chimeric single-chain fragment variable (scFv) receptor [201]. Named T-bodies at that time, these early CARs combined antibody binding domains with the CD3-zeta (CD3ζ) signaling domain of a TCR/CD3 complex, which contain 3 immunoreceptor tyrosine-based activation motifs (ITAMs), able to elicit TCR mediated signaling pathways [202]. However, they exhibited limited cytotoxicity and proliferation due to the absence of co-stimulatory and cytokine signaling.

Over the past two decades, CAR design improvements have given rise to second-generation CARs, featuring additional co-stimulatory domains like CD28 or 4-1BB, and third-generation CARs with two extra co-stimulatory domains [203]. These modifications impact T cell functional and metabolic profiles, with CD28-based CARs promoting potency but limited persistence, and 4-1BB-based CARs providing prolonged persistence with a less potent effect [204, 205]. However, other variables, such as binding affinity and target antigen, profoundly influence CAR T cell features. The fourth-generation of CARs introduces an additional protein, such as cytokines (TRUCKS) or co-stimulatory ligands, which is expressed either constitutively or inducibly upon CAR activation [206] **(Fig.10).** Of note, all the approved CAR T cell therapies for hematological tumors are of second-generation, and the GD2-targeted CAR T cells which have shown remarkable result in glioblastoma are third generation

[200], proving hope that evolution and improvement of CAR T cells may finally make them work in solid tumors.

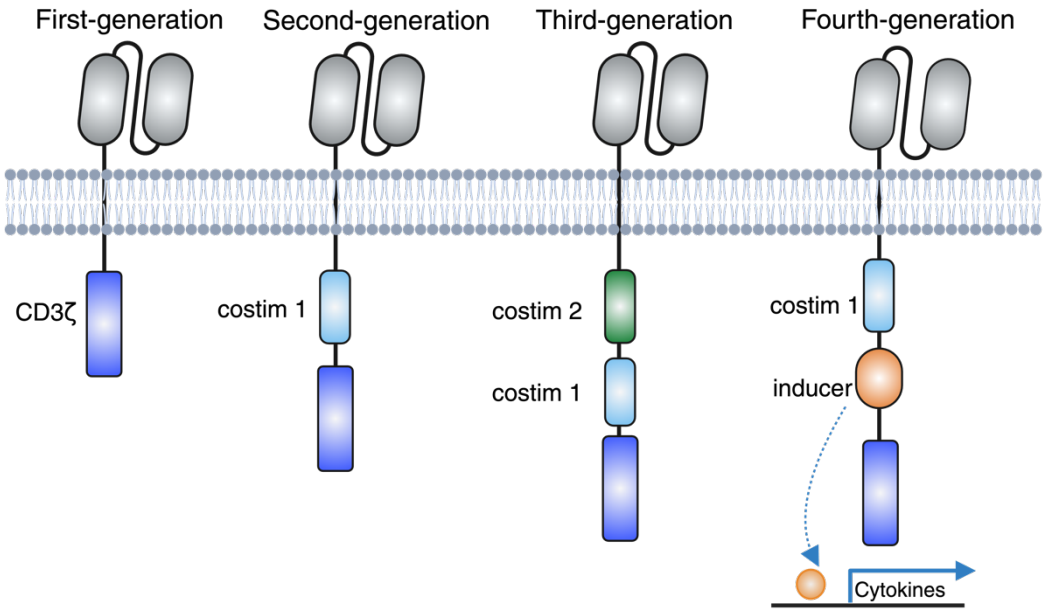

Figure 11: The evolution of the CAR T cell construct designs

Schematic representation of the evolution of CAR molecules, from the first-generation to the fourth-generation, incorporating additional co-stimulatory domains (costim) and the induction of additional molecules, like cytokines.

Limitations of CAR -T cell therapies

While CAR T cell therapy has demonstrated remarkable clinical responses, numerous obstacles hinder its therapeutic efficacy in both solid tumors and hematological malignancies. General challenges of CAR T cell therapy include severe life-threatening toxicities, antigen escape and heterogeneity, limited T-cell persistence and exhaustion. In the case of solid tumors restricted trafficking, limited tumor infiltration and an immunosuppressive TME are additional obstacles. Also, as described in previous sections, apart from the antigen-independent frequent adverse effects of T-cell redirection therapies, toxicities frequently arise from targeting solid tumor TAAs, also expressed in healthy tissues. To surmount these significant challenges, innovative strategies and approaches are necessary to engineer more potent CAR Tcells with enhanced anti-tumor activity and reduced toxicity [207, 208], as well as to develop

better and more suitable models to predict safety and efficacy [209].

The *ex vivo* engineering of CAR T cells presents logistical challenges due to the complexity of the manufacturing process. It involves the use of viral vectors, which is time-consuming and necessitates specialized facilities and trained personnel [22]. γ-Retroviral and lentiviral vectors require costly manufacturing, biosafety testing and storage. Non-viral approaches would be advantageous if they prove to be as effective, such as DNA transposons, RNA transfection and the use of targeted nucleases, including meganucleases, zinc-finger nucleases (ZFNs), transcription activator-like effector nucleases (TALENs), and CRISPR/Cas9. Among these tools, ZFNs and CRISPR/Cas9 are presently the most advanced [196]. These viral manufacturing constraints, together with the GMP requirement for manufacturing of clinal grade CAR T cell products, limit their availability for routine clinical use, particularly for autologous CAR T cells [209]. Moreover, defining specific regulatory requirements for CAR T cells facilitating translation to the clinic, especially for academically developed products, is still a pending issue.

In addition, there have been instances of production failures observed in a small percentage of patients with hematologic malignancies. The feasibility of generating and expanding CAR Tcells from patients with solid tumors who have undergone prior chemotherapy remains uncertain, and the incidence of production failures in these patients is yet to be determined due to limited clinical experience [210].

Lastly, although still seems quite far today because of the difficulty to selectively and efficiently deliver genes to specific cells, such as T cells, the future of CAR T field will tend to a gene therapy modality, in which CAR generation is produced in the patients *in vivo,* using several gene delivery systems to avoid ex vivo manufacturing and allow off-the shelf therapies [211].

Next generation or multifunctional CAR T cells

Second-generation CAR T cells seem to be sufficient in the treatment of hematological malignancies but not in solid tumors, which face additional challenges negatively

affecting the potential of this therapy. To overcome the challenges associated with CAR T cell therapy for solid tumors, researchers have developed several strategies to enhance their effectiveness. These approaches include modifying the CAR T cells to improve their trafficking and persistence, targeting multiple antigens to overcome antigen heterogeneity and/or downmodulation, and incorporating co-stimulatory molecules or ICIs to enhance T cell activation and persistence in the TME [212]. A term commonly used to describe new CAR T cell designs and combinatorial strategies beyond fourth generation CAR T cells is "next-generation CAR T cells" [206, 208, 213], which constitutes the focus and gives title to this thesis. Although promising preclinical results and some preliminary clinal data, clinical evidence is still missing to determine if these more sophisticated configurations finally solve or mitigate the above-mentioned limitations of CAR T cell therapy.

Some next-generation strategies focus on **optimizing CAR design** to improve T cell fitness, potency, metabolism, proliferative capacity, persistence and antitumor responses [214, 215]. While robust T cell activation is crucial for efficacy, it can lead to detrimental tonic signaling, defined as a sustained activation of the T cells in either a ligand-independent or dependent fashion [216–218]. Preclinical testing has explored various strategies and combinations to strike a balance between potent T cell activation and preventing exhaustion, awaiting further clinical evidence to validate the most effective approaches [208]. The co-stimulatory and signaling domains provide a customizable structure in CAR design based on tumor type, burden, target antigen and concerns of toxicity [218, 219]. For example, a preclinical study by Judit Feucht and colleagues showed that by modifying and calibrating specific immunoreceptor tyrosine-based activation motifs (iTAMs) of CD3Z signaling domain of CD28-based CAR T cells, mitigated T cell exhaustion and enhanced their activity, compared to conventional CARs [215].

Another trend in the field focuses in CAR T cells generated through **targeted integration** using diverse gene editing techniques, as opposed to random integration viral methods, potentially offers superior control of CAR expression. Targeting the CAR to the T Cell Receptor alpha constant (TRAC) locus, under the control of the

endogenous TCR promoter, enhances CAR T phenotype, reducing tonic signaling, and increasing antitumor effects and persistence *in vivo* [198]. Additionally, targeted integration allows for the elimination of the endogenous TCR, one of the steps for the development of **universal or allogeneic CAR-Ts** [220], which require many other additional genetic modifications. Clinical trials (NCT04557436, NCT05377827) are already underway to evaluate the feasibility of employing this strategy which has already shown some clinical benefit in a few children with B-cell acute lymphoblastic leukemia [199]

Like fourth generation CAR T cells secreting cytokines, another particularly promising avenue involves **armoring CAR-Ts** to secrete chemokines, ICIs or other immunomodulatory agents in the TME, or other BiTEs® for enhancing the immune response. For example, CAR T cells secreting CCL19 can improve immune cell infiltration and CAR T survival in the TME [221] [222]. Incorporating immune checkpoint inhibitors prevents CAR T cell exhaustion and inactivation, showing positive outcomes in a phase I study using mesothelin-targeted CAR T cells armored with the secretion of anti-PD-1 antibodies for the treatment of malignant pleural diseases [223]. CAR T cells designed to **target a combination of antigens**, either through BiTE® secretion or dual CAR specificities, offer the advantages of increasing specificity for malignant cells, mitigating of antigen escape and targeting the tumor and its microenvironment. Tandem CAR-Ts, characterized by two interconnected scFv domains, allow a single CAR T cell to recognize multiple tumor antigens. Alternatively, as explained in the previous sections, in situ production of TCBs and BITES through CAR T cells appears to be a very attractive strategy. Marcela Maus' group has developed a promising strategy which involves the combined expression of a CAR specific for EGFRvIII, a glioblastoma-specific tumor antigen, and a BiTE® against EGFR, an antigen frequently overexpressed in glioblastoma but also expressed in normal tissues. This combination allowed the elimination of heterogenous tumors and the recruitment of bystander T cells within the tumor in mouse models [188] and has now progressed to a phase I clinical trial (NCT05660369). After demonstrating limited efficacy of second-generation p95HER2 CAR T cells in this thesis, we followed a very similar strategy to improve the potential of our therapy.

Alternative cell types

Researchers are exploring the modification of non-T-cell leukocytes, specifically NK cells and macrophages, to express CARs [224].

While **CAR NK** cells offer advantages such as allogeneic use and potential lower toxicity, challenges of CAR T therapy, including issues related to tumor antigen, CAR design, the immunosuppressive TME, and manufacturing, still apply. The short half-life of NK cells may be beneficial in mitigating severe toxicity but could pose challenges for repeated administrations [225].

On the other hand, **CAR macrophages**, despite their ability to infiltrate solid tumors and interact with almost all cellular components [226], have limited clinical experience. Currently, only one active interventional trial is using autologous anti-HER2 CAR macrophages for advanced HER2-positive solid tumors unresponsive to prior therapies (NCT04660929).

HER2 targeting CAR T cells

As previously highlighted in this introduction, HER2, being a widely expressed oncogene in various cancers, has been the focus of numerous targeted therapies as well as immunotherapies, including TCBs and BiTEs. Consistent with this extensive therapeutic arsenal, HER2-targeting CAR T cells have also been extensively explored. CAR T cell therapy offers several potential advantages over current HER2 treatments, including a distinct mechanism of action, the capability to penetrate and eliminate tumors inaccessible to antibodies [227], and the potential for combinatorial targeting [228][229].

However, since HER2 is a TAA expressed in normal tissues, toxicities are a major concern. In fact, the first clinical trial testing a third-generation HER2 CAR T cells in combination with iL-2 for the treatment of metastatic HER2-positive cancer ended tragically with the death of the first treated woman (NCT00924287). Recognition of HER2 in normal lung cells led to severe lung toxicity and multiple organ failure [154].

Despite this setback, subsequent trials involving HER2 CAR T cells have been initiated across a diverse range of cancers employing considerable dose reduction from the 10^{10} lethal CAR T cell infusion, with doses ranging from 10^4 to 10^8 CAR T cells in early phase clinical trials [230–232] or incorporating safety switches (BPX-603), although this trial (NCT04650451) has been terminated due to a dose limiting toxicity observed in another trial with same technology targeting prostate stem cell antigen (PSCA). So far, clinical results have shown varying degrees of success, generally modest although safe, across different cancer types including breast, brain malignancies, sarcomas, pleural and peritoneal metastasis, ependymoma and biliary tract and pancreatic tumors [57]. For instance, anti-HER2 CAR T cells tested in the treatment of sarcomas showed poor persistence levels (Ahmed 2015). Therefore, since dose reductions for targeting a TAA like HER2 compromise effectivity, targeting a TSA like p95HER2 through CAR T cells, apart from conferring higher safety, will potentially allow to increase these doses and increasing the chance of clinical therapeutic responses. This thesis is based on this hypothesis to develop p95HER2 CAR T cells with potential safe and effective clinical application.

In addition, our group has preclinically demonstrated that disruption of IFN-γ signaling pathway is a mechanism of acquired resistance against second-generation HER2 CAR T cell redirection therapies [233, 234], in contrast to other CAR T cells targeting liquid tumors which do not rely on this pathway for CAR T cell killing [222]. Strategies to overcoming or reverting this acquired resistance are under investigation, and further investigation is needed to determine if these mechanisms could also affect p95HER2 targeting CAR T cells.

In conclusion, despite facing several limitations, CAR T cell therapies can be improved in various ways and provide significant promise for patients with advanced and metastatic HER2-positive tumors unresponsive to current treatments. Targeting the TSA p95HER2 may be a safer alternative than HER2-directed CAR T cells, and armoring strategies may increase their therapeutic potential.

HYPOTHESIS

Despite the success of current anti-HER2 therapies, their efficacy is hindered by severe toxicities derived from targeting HER2 in healthy tissues, and the development of resistances. Given the unmet clinical needs in advanced and metastatic HER2-positive cancer patients, we hypothesize that CAR T cells targeting p95HER2, a TSA expressed in a relevant proportion of HER2-positive cancers, will constitute a safe, effective and expandable immunotherapeutic strategy against a subset of HER2-positive tumors.

OBJECTIVES

Main objective: develop safe and efficacious p95HER2 CAR T cells with potential for clinical translation.

1. Generate and characterize p95HER2 CAR T cells *in vitro*.
2. Evaluate the antitumor efficacy of p95HER2 CAR T cells against tumor cell lines *in vivo.*
3. Assess safety by evaluating the impact of p95HER2 CAR T cells on cells expressing normal levels of HER2.
4. Evaluate the antitumor effect of p95HER2 CAR T cells against PDXs *in vivo.*
5. Validate the feasibility of GMP-manufacturing for the final product, enabling the initiation of a phase I clinical trial.

MATERIALS & METHODS

Cell lines and primary cultures

BC **MCF7** cells (#HTB-22); normal breast **MCF10A** cells (#CRL-10317); human embryo kidney tissue highly transfectable derivative cell line **HEK293T** cells (#CRL-11268); two lung cancer cells **H1781** (#CRL-5894) and **H2170** (#CRL-5928); two ovarian cancer cells **COV434** (#CVCL_2010) and **SKOV3** (#HTB-77); and two GC cell lines **MKN45** (#CRL-1739) and **NCI-N87** (#CRL-5822) cell lines were purchased from American Type Culture Collection (ATCC) (Manassas, VA, USA). **OE19** (#96071721) were obtained from Sigma-Aldrich. **GP2-293** cells (#631458) were obtained from ClonTech/Takara Bio. **MCF7 p95HER2**, **MCF10A p95HER2** and **MCF10A HER2** cells were generated as described previously [87].

MCF7, COV434 and SKOV3 cell lines were cultured in Dulbeccos's minimal essential medium:F12 (DMEM:F12) (#21331-046, Gibco-LifeTechnologies). OE19, NCIN87, H1781 and H2170 were maintained in RPMI 1640 (#61870-044, Gibco-LifeTechnologies). All media was supplemented with 10% fetal bovine serum (FBS) (#10270-106, Gibco-LifeTechnologies) and 1% L-Glutamine (#X0550-100, Biowest). MCF10A cells were further supplemented with 1% HEPES (#H0887), 0.5 ug/ml hydrocortisone (#H0888), 20 ng/ml hEGF (#E9644), 100 ng/ml cholera toxin (#C8052), 1ug/µl puromycin (#P7255), all from Sigma-Aldrich, 100µg/µl hygromycin (#10687010, Gibco) and 10 µg/ml Insulin (#11376497001, Roche). MCF7p95HER2 shp21 (MCF7p95HER2) cells were maintained in DMEM:F12 supplemented with 10% FBS, 1% L-Glutamine, 1µg/µl puromycin (#P7255, Sigma-Aldrich) and 200 µg/ml G418 geneticin (#11811-031, Gibco-LifeTechnologies), and doxycycline hyclate (#D9891, Sigma-Aldric) was used at a concentration of 1ug/ml for induction of p95 HER2 and shP21.

Induced pluripotent stem cells (iPSCs) derived cardiomyocytes (**iCell Cardiomyocytes**) (#R1105) were purchased from Cellular Dynamics, were thawed, plated and maintained according to the instructions and using the special media provided by the supplier. **Human small airway epithelial primary cells** (#C-12642O, PromoCell) were cultured in a commercial serum-free cell culture medium for epithelial

cells from the distal respiratory tract from the same provider (#C-21070, PromoCell).

All cells were cultured at 37°C and 5% CO2 in a humidified cell culture incubator.

PBMCs isolation

PBMCs were isolated from fresh buffy coats from healthy donors, obtained through the Blood and Tissue Bank of Catalonia (BST), by density gradient centrifugation Blood was diluted 1:3 with 1X phosphate-buffered saline (PBS) and transferred to a 50 ml falcon tube with Ficoll-Paque PLUS (#17-5446-02, GE Healthcare) at a 1:2 ratio. Tubes were centrifuged for 30 minutes at 400xg and 21ºC without brakes. After centrifugation, the upper yellow layer was aspirated and the white layer, corresponding to mononuclear cells, was harvested, transferred to a clean 50ml-Falcon tube, and diluted at least 4 times with PBS1X. After obtaining the buffy coat, red blood cells (RBC) were lysed with pre-warmed 1X RBC lysis buffer (#00-4333-57, Invitrogen) for 5 min at room temperature. PBMCs were washed with PBS 1X, centrifuged for 10 minutes at 400g, counted, frozen at –80 °C in Crystor® CS10 media (#07959, STEMCELL Technologies), and moved to liquid nitrogen storage after 48h until use for transduction.

For obtaining PBMCs from a cancer patient, 20 ml of peripheral blood were obtained at Vall d'Hebron University Hospital (Barcelona) after informed consent (IC) obtention under protocols approved by the Ethical Committee of Vall d'Hebron Hospital in accordance with the Declaration of Helsinki. Processing to obtain PBMCs was performed as explained above for fresh buffy coats.

Tumor samples and patient-derived tumor xenografts

All tumor samples from patients were collected at Vall d'Hebron University Hospital (Barcelona) under protocols approved by the Ethical Committee of Vall d'Hebron Hospital in accordance with the Declaration of Helsinki. Written informed consent was obtained from all patients who provided tissue samples.

PDX667 (ER-/PR-/HER2^{+}) was extirpated by core needle biopsy (CNB) from a BC patient's metastasis in the skin. PDX67 (ER-/PR-/HER2^{+}) was extirpated by CNB from a primary BC tumor. PDX433 (ER^{+}/PR^{-}/HER2^{+}) was extracted by CNB from a BC patient's metastasis in the liver and was set up in culture in complete DMEM:F12 media after tumor growth in NSG mice. For *in vivo* experiments for testing CAR T cells, PDX67 and PDX667 were implanted from tumor fragments, whereas for PDX433 experiments, tumors were generated from established cell cultures.

Fragments of patient samples were implanted into the fat pad of NOD.Cg-*Prkdc*^{scid} *Il2rg*^{tm1Wjl}/SzJ (NSG®) mice (#614, Charles River), and 17ß-estradiol (1 mM) (#E8875-1G, Sigma- Aldrich) was added to drinking water. Tumor xenografts were measured with calipers three times per week, and tumor volume was determined using the following formula: (length × width2) × (p/6).

p95HER2 mAbs and humanized scFvs

Murine monoclonal antibodies targeting human p95HER2 were generated previously using hybridoma technology [235]. Humanization of the heavy (V_H) and light (V_L) chains of the two best candidates, 14D and 15C, was performed at Roche Innovation Center Zurich (Roche, Switzerland) using proprietary technology. Three humanized versions of each murine antibody were produced, sequenced and tested.

Dot blot analysis

Dot blot assay to determine the epitope of the p95HER2 antibodies 32H, 14D and 15C was performed as follows. Overlapping 8-mer peptides from the extracellular region of human HER2 were chemically synthesized by custom order at Instituto de Química Avanzada de Cataluña from Centro Superior de Investigaciones Científicas (IQAC-CSIC), shipped as solid powder, solubilized according to provider instructions and adjusted to a concentration of 1mg/ml. Using a narrow-mouth pipette tip, 2 µl of each peptide were immobilized to a nitrocellulose membrane (#10600002, GE Healthcare Biosciences), with a previously drawn grid using a pencil, and allowed to dry. Blocking

with 5% TBS-tween (1× tris-buffered saline with 0.1% tween 20 (#P7949, Sigma-Aldrich)) with 5% bovine serum albumin (BSA) (#9647, Sigma-Aldrich), for 30 minutes at room temperature using a petri dish as reaction chamber Then, the tested antibodies were diluted in 5% bovine serum albumin (BSA) to a concentration of 20 µg/ml and incubated with the membrane for 30 minutes at room temperature. After washing with, membranes were incubated with horseradish peroxidase- linked secondary antibody (GE Healthcare) for 1 h and developed using Immobilon Western Chemiluminescent HRP Substrate (#WBKLS0500, Millipore). Chemiluminescence visualization of antibody binding was performed using an Amersham TM Imager 600 (GE Life Sciences). The same assay was performed to determine the binding to human (MPIWKFPDEEG) and mouse (MPIWKYPDEEG) sequences containing the epitope, by generating the corresponding customized peptides (IQAC-CSIC).

Design and generation of retroviral vectors containing CAR and/or TECH2 constructs

All p95HER2 CAR, TECH2 and p95HER2.CAR-TECH2 constructs were synthetized and cloned into the retroviral vector pMSGV1, which includes the murine stem cell virus (MSCV) long-terminal repeat (LTR) promoter (GenScript, Netherlands). The p95HER2CAR constructs contain a CD8 hinge domain, CD28 transmembrane an intracellular co-stimulatory domain and a CD3ζ signaling domain.

Nine anti-p95HER2 CAR T were generated with different scFvs derived from anti-p95HER2 mAbs. Empty pMSGV1 construct was used for control (UTD). TECH2 constructs are composed by two scFvs against HER2 and CD3 linked by a (G4S)3 linker. The two scFvs are preceded by an IgK leader sequence and followed by a T2A and a transgene coding for eGFP to evaluate transduction efficiency of the constructs. The high affinity anti-HER2 scFv is based on 4D5-8 scFv, the medium affinity on 4D5-5 scFv and the low affinity on 4D5-3 scFv as previously described in [164, 236]. The anti-CD3 scFv and linkers were derived from a publicly available sequence for blinatumomab. The p95HER2.CAR-TECH2 constructs have the p95HER2 CAR under the LTR promoter followed by a T2A and the TECH2 sequences without the eGFP.

The complete sequences of the constructs are described in patent EP20382457.8 and EP22382294.

Retrovirus production

CAR retroviruses were produced as follows. GP2-293 cells were seeded in plates coated with Poly-L-Lysine 0.001% w/v (#P8920, Sigma-Aldrich). The day after, cells were transfected with 4 µg of envelope plasmid RD-114 (a gift from Alena Gros' Lab, VHIO) and 9 µg of transfer plasmid (encoding the different CAR constructs), with 60 µL of Lipofectamine 2000 (#11668019, Invitrogen). Media was changed after 6-8 hours. Cell supernatants containing retrovirus particles were collected 48 h later, centrifuges twice at 500g for 10 minutes to remove any residual packaging cell, and used freshly for T cell transduction or frozen at -80ºC.

Retroviral transduction of human T cells for CAR T cell production

Frozen PBMCs previously isolated were thawed and activated by adding 300 IU/ml IL-2 (Proleukin®) (#703892-4, Novartis) and anti-CD3/anti-CD28 Dynabeads (#11131D, Gibco) in PBMC media (RPMI 1640 (#61870, Gibco), 10% heat-inactivated FBS, 1% L-glutamine, 1% HEPES (#H0887, Sigma-Aldrich) and 1% penicillin–streptomycin (#P4333, Merck Life Science) and cultured for 2 days. Retroviruses corresponding to different CAR constructs were transduced into activated T cells in 10ug/ml retronectin-coated plates (#T100A, Takara). Cultures were allowed to expand, with continuous fresh media addition to maintain a concentration of approximately $1x10^6$ cells 7 ml, for 10 days in their media supplemented with 300 IU ml^{-1} IL-2, at which point they were cryopreserved in Cryostor® CS10 (#7930, StemCell Tecnologies) and stored in liquid nitrogen.

Transduction efficiency analysis by FACS

After 3 days in culture, $0.1x\ 10^6$ transduced T cells were washed twice with 1xPBS and

re-suspended in home-made FACS buffer (1xPBS, 2.5 mM EDTA, 1% BSA, and 5% horse serum (#26050088, Life Technologies)) for 20 minutes at 4ºC. Then, cells were stained for 30 minutes with 1/20 dilution of biotinylated anti-mouse F(ab')2 antibody (#115-065-072, Jackson ImmunoResearch), wash twice with PBS and stained with 1/150 dilution of streptavidin-APC (#405207, Biolegend) or 1/100 streptavidin-FITC (#SA1001, Invitrogen) and 1/300 anti-CD3-PE (#300408, Biolegend) for other 30 minutes. For TECH2-eGFP constructs, transduction efficiency was assessed though endogenous eGFP expression. Zombie Aqua (#423101, Biolegend) was used as a viability marker at 1:1000 dilution. Stained samples were analyzed by flow cytometry on BD FACS Canto II or BD FACS Celesta (BD Bioscience) and analyzed using FlowJo software. See **Fig.56** for gating strategy analysis

In vitro cytotoxicity, T cell activation and T cell proliferation co-culture assays

10,000 target cells were seeded in 96-well flat bottom plates and incubated at 37ºC, 5% CO_2 overnight. Then, CAR T cells, that were normalized to transduction efficiency, were added at different ratios of target cell : CAR-positive T cells. Plates were incubated for 48 additional hours. Co-cultures were then harvested with trypsin (#25300096, Life Technologies), and resuspended in previously described home-made FACS buffer for flow cytometric analysis. Death percentage of target cells was determined by counting the alive cells on each well and normalized to wells containing T cells transduced with an empty vector. The viability marker Zombie Aqua (#423102, Biolegend) was used at 1/1000 to discriminate alive and dead cells. Tumor cells were identified by staining with 1/100 anti-EpCAM-AF647 (#324212, Biolegend) or by negative selection of T cells using 1/100 anti-hCD3-PE (#300408, Biolegend). To identify transduced cells or bystander activation of T cells, anti-mouse F(ab')2 antibody followed by 1/10 streptavidin-FITC (#SA1001, Invitrogen), and 1/300 anti-CD25 BV421 (#302630, Biolegend) and 1/300 CD8-PE/Cyanine7 (#344712, Biolegend) were also added to the wells. Samples were assayed in the LSR Fortessa cytometer (BD Biosciences) and analyzed using FlowJo software. See **Fig.56** for gating strategy analysis

For antigen stimulation proliferation assays, CAR T cells were co-cultured with adherent MCF10A or MCF10A overexpressing p95HER2 cells at 1:1 effector: target ratio in RPMI-based PMBC media supplemented with 50 IU/ml IL-2, using 12-well plates. At days 0, 7 and 14, an exact volume from total cell culture was analyzed in FACS Canto cytometer (BD Biosciences) using the HTS system that enables acquiring an exact volume, and thereby allowing extrapolating detected counts of CAR T cells to the total number of cells present in the co-culture. Samples were stained with 1/100 anti-hCD3-PE (#300408, Biolegend) and 1/1000 viability marker Zombie Aqua (#423102, Biolegend). Every 24-48 hours, cell suspensions were transferred to a new well with freshly seeded MCF10A or MCF10Ap95HER2 to replenish dead cells or avoid target cell overgrowth, and controlled volumes of fresh media were added, trying to maintain a cell density of $1x10^6$ T cells/ml. Population doublings relative to day 0 were calculated.

Exhaustion and phenotype characterization

To evaluate exhaustion and phenotype of CAR T cells, 0.2 x 10^6 CART cells at day 10 post-transduction were isolated, washed with PBS1X and incubated for 30 minutes at 4ºC in FACS buffer. For exhaustion staining, cells were labelled with 1/300 anti-hCD4-BV421 (#317434, BioLegend), 1/100 anti-hCD8-PE/Cy7 (#344712, BioLegend), 1/300 anti-hLag3-PE-(#12-2239-42, Invitrogen), 1/300 anti-hPD1-BV650 (#564104, BD Biosciences) and anti-hTIM3-APC (#345012, BioLegend), and incubated for 30 minutes at 4ºC. For phenotype characterization, understood as the differentiation state of CAR T cells, we stained samples with 1/300 anti-hCD4-BV421 (#317434, BioLegend), 1/300 anti-hCD8-APC/Cy7 (#344714, BioLegend), 1/100 anti-hCCR7-BV650 (#353234, BioLegend) and 1/1000 anti-hCD45RO-PE (#304205, BioLegend).

In addition, to study the positively transduced fraction in both stainings, 1/20 biotinylated anti-mouse F(ab')2 antibody (#115-065-072, Jackson ImmunoResearch) followed by 1/100 streptavidin-FITC (#SA1001, Invitrogen) were added to the samples. Fluorescence minus one (FMO) control were included to define the negative gates for selected populations. Dead cells were excluded from analysis using Zombie Aqua at

1/1000 dilution. Data was acquired using LSR Fortessa cytometer (BD Biosciences) and analyzed using FlowJo software. See **Fig.56** for gating strategy analysis

Membrane proteome array

The Membrane Proteome Array (MPA) screening was conducted at Integral Molecular, Inc. (Philadelphia, PA). The MPA is a protein library composed of ~6,000 human membrane protein, each overexpressed in HEK293T cells by individual transfection in separate wells of a 384-well plate. Transfected cells were pooled by columns and rows, so that each protein was represented in two unique wells of a matrix and incubated with an scFV-hIgG1 fusion containing the H1-14D scFv of the CAR T(Creative Biolabs). H1-14D scFv binding to specific targets was identified by detecting fluorescence of a secondary labelled antibody on Intellicyte iQue (Sartorius). Each individual membrane protein target was assigned values corresponding to the binding values of their unique row and column pools, allowing for specific deconvolution, and targets displaying binding of greater than 3 standard deviations above background in both wells were selected for downstream validation experiments.

To validate the hits, MCF10A cells were infected with lentivirus to overexpress IL2RB (#HsCD00437471, DNAsu) and UBXN8 (#HsCD00954617, DNAsu), and cells were under 20 µg/ml blasticidin (#ant-bl-1, InvivoGen) selection for a week to ensure survival of transduced cells. For detection of the overexpressed proteins, the following antibodies were used at a concentration of 2ug/ml, coupled to the appropriate labeled secondary antibody (all at 1/500 dilution): anti-V5 tag (#R961-25, Invitrogen) and anti-IL2RB (#MAB224, R&D Systems) were coupled with AF488 conjugated with anti-mouse IgG (#A11001, Invitrogen) and anti-UBXN8 (#HPA077538, Sigma-Aldrich) was coupled with AF488 conjugated to anti-rabbit IgG (#A11008, Invitrogen). H1-14 scFv-Fc was used at the same concentration (2ug/ml), followed by AF488 conjugated anti-human IgG (#A11013, Invitrogen)

HER2, p95HER2 and CD3 expression by IHC

Tumor samples were fixed in 4% formaldehyde buffered to pH 7 (stabilized with methanol) for 24 hours and were then formalin-fixed and paraffin-embedded (FFPE). Fixed tissue samples were sectioned at 4 µm thickness, heated at 60 °C, deparaffinized with xylene and hydrated with two steps of incubation with different dilutions of ethanol. Then, antigen was exposed using commercial DAKO retrieval solutions, Ph6 for p95HER2 and HER2 (#S236984-2, Agilent Dako) and Ph9 for CD3 (S236784-2, Agilent Dako). Next, the following primary antibodies were used and diluted in in Envision Flex antibody diluent Dako (#K800621-2, Agilent Dako): in-house anti-p95HER2 (32H2) antibody at 0.5 µg/ml, 1/2000 commercial anti-HER2 (#A0485, Agilent Technologies) and 1/100 anti-CD3 (# ab16669, abcam), incubated for 1 hour at room temperature. Next, the slides were washed with PBS1X and incubated 20 minutes at room temperature with EnVision System-HRP labeled polymer secondary anti-mouse antibody (#K4000, Agilent Dako) for 32H2 and anti-HER2, and anti-rabbit secondary antibody (#K4002, Agilent Dako) for CD3. Samples were then wash with PBS and DAB substrate chromogen (#K3468, Agilent) added for 1 to 4 minutes, and counterstained with harris hematoxylin and eosin (H&E) (#H3404, Vector Laboratories) for 2 min, followed by dehydration with ethanol and xylene, and finally mounted in DPX (Dibutylphthalate Polystyrene Xylene) (#06522, Sigma Aldrich). Evaluation of positivity was not performed by a certified pathologist.

HER2 and p95HER2 expression by FACS

Human cancer cell lines were harvested with Accutase (#L0950-100, Biowest) and 0.2 x 106 cells per staining were isolated, washed with PBS1X (#L0615-100, Biowest) and resuspended in FACS buffer containing 2.5 mM EDTA, 1% BSA, and 5% horse serum in PBS1X for 30 minutes at 4ºC. Cells were stained with α-p95HER2 (32H2, in house α-HER2 (trastuzumab, Herceptin, #8470009036744, Roche), normal mouse IgG control (#sc-2025, Santa Cruz Biotechnology) or normal human IgG control (#ABIN491543, Antibodies-Online) for 30 minutes at 4ºC. All primary antibodies were used at 2 µg/ml. After this incubation, cells were washed twice with PBS1X and labelled

with Alexa Fluor® 647-conjugated anti-mouse IgG (#A-21236, Invitrogen) or anti-human IgG (#A-21445, Invitrogen) secondary antibodies both at 1/500 dilution for 30 minutes at 4ºC. Viable cells were determined by using Zombie Aqua (#423101, BioLegend) at 1/1000 dilution. Analysis of p95HER2 and HER2 expression in human cell lines was done in either LSR Fortessa or FACS Canto and evaluated with FlowJo software.

HER2 and p95HER2 expression by WB

One 100mm dish per cell line (at 70% confluence) was frozen the day before performing protein extraction. Protein extracts were isolated by lysing the cells in homemade lysis buffer (130 mM NaCl, 0.01% NP-40, 1% glycerol, 2 mM EDTA pH 8 and 20 mM Tris-HCl pH 7.4), supplemented with phosphatase inhibitors 5 µM b-Glycerolphosphate, 5 mM sodium fluoride, 1 mM sodium orthovanadate and cOmplete TM, EDTA-free Protease Inhibitor Cocktail (#COEDTAF-RO, Sigma-Aldrich, 1 tablet per 10 mL lysis buffer). After this incubation, cells were scraped and transferred to Eppendorf's tubes. To normalize protein concentrations, we performed a quantitative BCA protein assay. Samples were diluted 1:5 with Laemmli SDS sample buffer and incubated for 5 minutes at 96ºC. After typical protein separation by gel electrophoresis (SDS PAGE) and transfer to a 0.45µm nitrocellulose membrane (#10600002, GE Healthcare Biociences) in Transfer Buffer 1X at a constant voltage of 100V, membranes were blocked in 5% milk in home-made TBS-Tween for 45 minutes at RT. Then, membranes were incubated with primary antibodies recognizing HER2 (α-C-terminalHER2) (CB11, #MU134-UCE, BioGenex), human p95HER2 (32H2, in-house) and human GAPDH (#Ab128915, Abcam) overnight at 4ºC. Both primary antibodies were used at 1:1000 dilution in 5% milk in TBS-Tween. Membranes were washed and incubated with anti-mouse (#GENA931-1ML, Amersham Biosciences) or anti-rabbit (#GENA934-1ML, Amersham Biosciences) horseradish peroxidase-labelled (HRP) secondary antibodies both used at 1:5000 dilution in 5% milk in TBS-T. Blots were finally developed using Immobilon Western Chemiluminescent HRP Substrate (#WBKLS0500, Milipore) and chemiluminescence imaging analysis was done in

Amersham Imager 600. Western blots were quantified with Fiji.

TECH2 purification, quantification WB and binding assays

HEK293T cells were infected with the same retrovirus used to transduce T cells expressing the different TECH2 constructs separated by a T2A with eGFP fluorescent protein. After confirming a transduction efficiency higher than 90% by eGFP detection flow cytometry, HEK293T cells expressing the different TECH2s were expanded. Supernatants containing TECH2Hi and TECH2Me, or control supernatants from untransduced HEK293T cells, were collected and TECH2 proteins were purified using affinity chromatography through a commercial HisPur Ni-NTA His-Tag binding kit (#88229, Thermo Fisher Scientific). Then, purified supernatants were diafiltered using Amicon Ultra-15 3 kDa Centrifugal filters (#UFC900324, Milipore) for PBS1X buffer exchange and further concentration.

Protein size was checked by western blot analysis, directly loading purified supernatants extracts for proteins in an SDS-PAGE, transferred to a nitrocellulose membrane, blocked with 5% non-fat dry milk in TBS-Tween, as previously explained, and stained overnight with anti-6x-His Tag monoclonal antibody conjugated with HRP (#MA1-135-HRP, Thermo Fisher Scientific). The membrane was washed three times and developed as explained in previous section.

TECH2 proteins, which include a 6xHistidine-tag within the TECH2 construct, were quantified using a competitive enzyme-linked immunosorbent assay (ELISA) kit (#L00436, GenScript) according to the manufacturer's instructions. Absorbance readings were measured at 450 nm using a SPARK® multimode microplate reader (TECAN), and concentrations were determined by interpolating values from the standard curve. For analysis of TECH2Me levels secreted by p95HER2.CAR-TECH2Me in culture during expansion, T cells expressing p95HER2.CAR-TECH2Me or untransduced vector were counted and placed at 0.2 x 10^6 CAR-positive T cells/ml and allowed to expand for 12 days in the presence of 300 IU/ml IL-s, without media replacements but adding controlled volumes for proper nutrient support . At days 0, 4

and 12, supernatant was collected, centrifuged to eliminated cell remanent, and TECH2 levels secreted into the media were measured by competitive his-tag ELISA (#L00436, GenScript).

Concentrations of TECH2Hi and Me produced by HEK293T were normalized according to the results from the ELISA assay for binding assays using different target cells. Target cells were harvested using accutase (#L0950-100, Biowest) and 0.2 x 106 cells per staining were isolated, washed with PBS1X (#L0615-100, Biowest) and resuspended in home-made FACS buffer containing 2.5 mM EDTA, 1% BSA, and 5% horse serum in PBS1X for 30 minutes at 4ºC. Purified and quantified TECH2s were used as primary antibodies and anti-6x-His Tag Monoclonal Antibody conjugated with Alexa Fluor 488 (#MA1-135-A488, Thermo Fisher Scientific) was used for detection. BD FACS Canto II or BD FACS Celesta (BD Bioscience) and analyzed using FlowJo software. For *in vitro* co-culture assays, production of highly purified TECH2Me was externalized to GeneScript using CHO cells.

Mice

For *in vivo* experiments, 4-6-week-old female and male NSG (NOD.Cg-Prkdcscid Il2rgtm1Wjl/SzJ) (#614, Charles River) were purchased. Mice were randomized by tumor size. Because of ethical reasons, we ended the experiments before the full development of graft-versus-host disease or when tumor volume surpassed 1500 mm3. Experiments were not performed in a blind fashion. Animal work was performed according to protocols approved by the Ethical Committee for the Use of Experimental Animals at the Vall d'Hebron Institute of Oncology.

In vivo tumor growth assays

Different cell lines and PDXs were used to generate xenografts in 6–8-week-old NSG mice. MCF7-p95HER2 cells ($3x10^6$), MCF7 cells ($3x10^6$) and the PDX established cell line from PDX433 ($1x10^6$) were implanted into the fourth mammary fat pad, while OE19 cells ($5x10^5$) and NCI-N87 cells ($1x10^6$) were implanted subcutaneously. In all cases, cells were injected using a 1:1 suspension of Matrigel (#356234, Cultek): cells in PBS.

In the case of PDX67 or PDX667, tumor fragments of approximately 3x3 mm were implanted orthotopically into the fourth pad of NSG mice. All experiments were performed in a single flank fashion.

Beta estradiol (#E8875, Sigma-Aldrich) was added to drinking water. p95HER2 expression of MCF7p95HER2 cells was induced with doxycycline (1 g/L) (#D9891, Sigma-Aldric) in drinking water. Tumor volume was measured using calipers twice a week using the formula (length x width2) x (π/6) and mouse body weight was monitored once a week. Once tumors reached 200-300 mm3, mice were randomized into treatment groups with similar tumor volumes and treated intravenously with the indicated doses of CAR T cells. In all experiments, UTD T cells were normalized to total cells of the treatment with lowest transduction, to ensure that the maximum allogenic effect is also observed in the control group. The same is performed in all *in vitro* cytotoxicity assays.

Lung and intracranial and tumor assays

For lung metastases, MCF7-p95HER2 ($1x10^6$) or PDX433 cells ($1x10^6$) transduced with lentiviral vector pLENTI-CMV-V5-Luc Blast (#21474, Addgene) to express firefly luciferase were injected in the tail vein of 6–8-week-old NSG mice. To generate brain tumors MCF7-p95HER2.luciferase cells ($5x10^5$) were stereotactically inoculated in the brains of 4–5-week-old NSG mice. MCF7p95HER2 cells were induced with doxycycline treatment (1g/liter). Mice were monitored through bioluminescence imaging with the IVIS-200 Imaging System from Xenogen (PerkinElmer) by injecting D-luciferin intraperitoneally and were randomized to different treatment groups when tumors were established.

Ex vivo analysis of blood, tumors and other organs for biodistribution evaluation

Mice blood and tumors were collected and analyzed at the indicated timepoints in each experiment. The mouse blood was obtained from the facial vein and 30-50 µl were processed. Blood was lysed twice with pre-warmed 1X RBC lysis buffer (#00-4333-57, Invitrogen) for 5 minutes at room temperature. Final pellet was resuspended in FACS

buffer, blocked for 20 minutes and stained for flow cytometry analysis.

For obtaining serum samples, 50-100 µl of blood were added to tubes containing a clotting-gel (Micro sample tube Serum Z-Gel) (#41.1378.005, Sarstedt) and spined at 10000 x g for 5 minutes. The supernatant above the gel contains the purified serum, which was then used for quantifying TECH2Me using competitive his-tag ELISA (#L00436, GenScript), as described previously.

Mice were euthanized by cervical dislocation and necropsies performed. Tumors were cut into small pieces and divided into samples for IHC or flow cytometry. Samples for IHC were fixed and embedded in paraffin.

Determination CAR T cell infiltration in tumors and organs (spleen, lung, liver, kidney, brain) for the biodistribution analysis was performed with fresh tissues by flow cytometry. Tumors and organs were kept in ice and humidified with PBS 1X until processing. First, samples were weighted for enabling calculation of infiltration by sample mass (mg). Then, mechanical disaggregation was performed using blades to cut the tumors and tissues into small pieces, followed by enzymatic digestion in 300 U/ml collagenase IA (#C2674, Sigma-Aldrich) and 100 U/ml hyaluronidase IS (#H3506, Sigma-Aldrich) DMEM F-12 medium. After 1 hour of incubation at 37ºC with shaking at 10 x g, the tissue mixture was filtered through 100 um strainers (#732-2759, VWR), and further disaggregated by pressing it against the rough surface of a syringe plunger base to ensure complete dissociation. After washing with 1XPBS to ensure maximum cell recovery, strainers are discarded and cell suspension spined. Cell pellet is further subjected to red blood cells lysis once and washed with 1XPBS. The final pellet is resuspended in FACS buffer according to initial sample weight, so all cell suspensions are at the same concentration for proper back-calculation of infiltration/mg organ or tumor. The following antibodies were used to stain the samples for flow cytometry analysis of CAR T cell infiltration in blood, tumors and organs: 1/300 anti-mCD45-AF488 (#103122), 1/100 anti-hCD3-PE(#300408), 1/300 anti-hCD4-BV421 (#317434), 1/300 anti-hCD8-PECy7 (#344712), 1/20 biotinylated anti-mouse F(ab')2 (#115-065-072, Jackson ImmunoResearch) coupled to 1/150 APC-streptavidin (#405207, Biolegend), all from Biolegend). An exact volume was acquired on LSR Fortessa and

data was analyzed with FlowJo software (BD Life Sciences). Cell infiltration data is represented as number of CD3-positive cells or CD3-positive-CAR-positive T cells per milligram of tumor, organ or per microliter of blood

Clinical grade manufacturing of p95HER2.CAR-TECH2ME

To produce the retroviral particles, the commercial packaging cell line 293Vec RD114 (BioVec Pharma), which contains the packaging plasmids Rev, Gag/pol and RD114 envelope integrated in its genome, is expanded and transfected with the therapeutic plasmid of interest, the pMSGV1–p95HER2.CAR-TECH2Me (produced by GenScript). The viral supernatant is harvested and clarified by centrifugation 48h after transfection, and it is finally concentrated by diafiltration using the KrosFlo® KR2i TFF System (Repligen). Lastly, the concentrated viral particles are cryopreserved in CryoMACS® freezing bags (#200-074-400, Miltenyi) in TexMACS™ medium (#170-076-306, Miltenyi) at a concentration of ≥ $1x10^6$ viral particles/ml.

To produce the CAR T cells, the automated closed system CliniMacs® Prodigy (Miltenyi) is used. Briefly, T cells from healthy donors' leukapheresis are isolated by CD4+ /CD8+ magnetic cell separation and activated using the T Cell TransAct (#200-076-204, Miltenyi). Two days after, retroviral transduction is performed by spinoculation at 32ºC and using Vectofusin-1 (#170-076-165, Miltenyi) as a transduction enhancer. T cells are cultured in serum-free TexMACS™ medium supplemented with IL-2 for 10 days (Proleukin®) (#703892-4, Novartis). The finished product (FP) is cryopreserved in CryoMACS® freezing bags (#200-074-400, Miltenyi) in Plasmalyte (Baxter) supplemented at 5% w/v with HSA and at 10% Dimethyl sulfoxide (DMSO) at the adjusted cell dose to ensure the specific cell range determined in the clinical trial.

Statistics

Data are represented as average ± standard deviation (SD) and were analyzed using the two-sided Student's t-test using Excel. Statistical significance was considered with

p-value less than 0.05. For *in vivo* experiments, mice were allocated randomly in treatment groups and growth curves were compared using two-sided Student's t-test at each time point. Data was considered statistically significative when p value < 0.05. Statistical details can be found in the figure legends. Efforts were made to reduce the number of animals used in the experiments.

RESULTS

1. Development of second-generation p95HER2 CAR T cells

CARs are artificial receptors that merge an antigen-binding domain, typically a single-chain variable fragment (scFv) from a monoclonal antibody, with intracellular signaling motifs capable of triggering T cell activation. This thesis is focused on the generation of CAR T cells, a tumor specific antigen expressed in a subset of HER2-positive tumors.

1.1. Screening of p95HER2 antibodies for CAR generation

Previously, our group developed several anti-p95HER2 monoclonal antibodies that do not bind to full length HER2 **(Fig 12A)** [81]. To select the more suitable scFv for the generation of p95HER2 CAR T cells, we performed binding assays using MCF10A cells overexpressing p95HER2 **(Fig 12B)**.

Out of eight monoclonal antibodies, we selected the three, termed as 14D, 15C y 32H, that bound to p95HER2 with highest intensity by means of flow cytometry analysis. Then we performed a dot-blot assay to identify their epitope, using 8-mer peptides surrounding the methionine in position 611 where alternative initiation of translation of this truncated form starts, covering the sequence employed for the humanization of mice for mAb generation. The epitopes recognized by these anti-p95HER2 antibodies were similar, but not identical; while the optimal epitope recognized by 14D and 15C antibodies was PIWKFPDE, the epitope optimally recognized by 32H2 was one amino acid shorter: PIWKFPD **(Fig12C).** The corresponding mouse sequence (PIWK**Y**PDE), differing only in one amino acid, was not recognized by any of the anti-p95HER2 antibodies **(Fig12D).** This finding will constitute a limitation throughout this work, since mouse models will not be a suitable species for systemically testing on-target off-tumor toxicities.

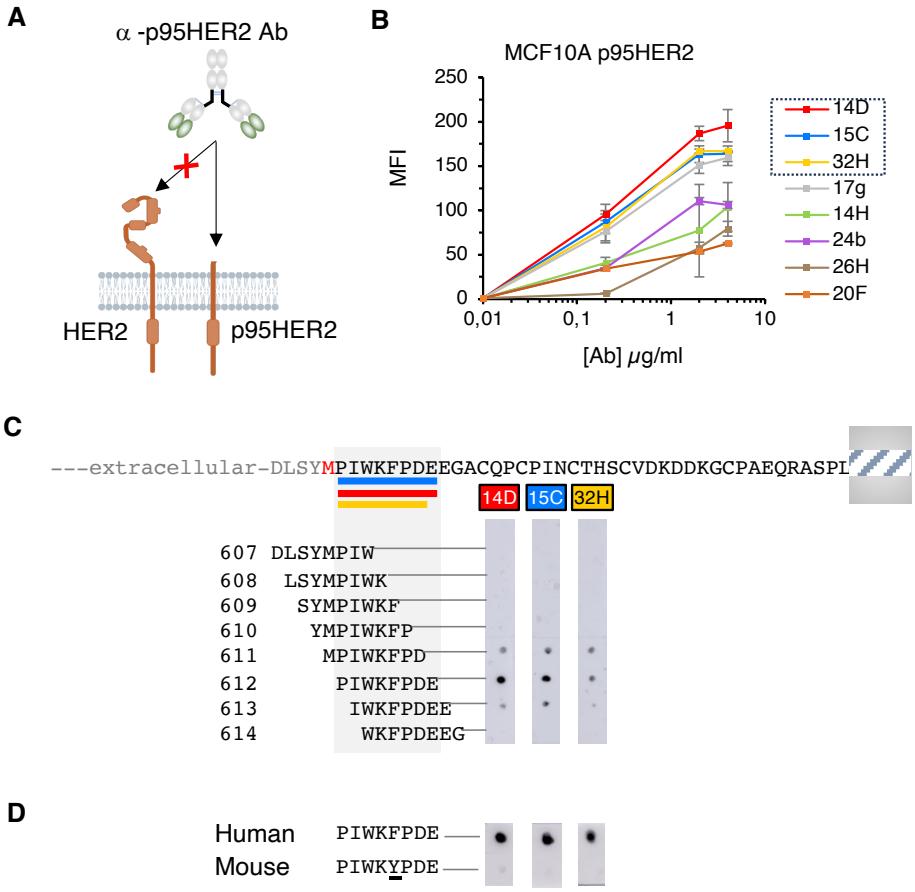

Figure 12: Selection of p95HER2 antibodies for CAR scFv generation

(A) Anti-p95HER2 monoclonal antibodies of mouse origin developed previously our group are specific for p95HER2, not recognizing full-length HER2 protein. **(B)** MCF10A cells transduced with p95HER2 were stained with different concentrations of the indicated antibodies and analyzed by flow cytometry. Mean fluorescence intensities (MFI) are expressed as averages of four determinations ± SD. **(C)** Schematic showing the amino acid sequence of the extracellular juxtamembrane region of HER2. p95HER2 starts at methionine 611 (highlighted in red). Overlapping 8-mer peptides were synthesized, immobilized, and incubated with the indicated antibodies, an anti-mouse secondary antibody coupled to peroxidase and developed. **(D)** PIWKFPD and PIWKYPD peptides, corresponding to the human and mouse sequences, respectively, were synthesized, immobilized, and incubated with anti-p95HER2s. Then, blots were processed as described in (C).

1.2. Generation and characterization of p95HER2 CAR T cells

We sequenced the cDNA encoding the variable light (V_L) and heavy (V_H) domains of the hybridomas that generate the selected anti-p95HER2 antibodies using high-throughput sequencing technologies. Subsequently, these sequences were used to construct the single-chain variable fragment (scFv) for second-generation CARs, incorporating CD28 co-stimulatory and CD3ζ signaling domains **(Fig. 13A).** The three murine CAR constructs, derived from the three selected monoclonal antibodies, were cloned into a gamma-retroviral vector based on Murine Stem Cell Virus (MSCV), designated pMSGV1, and placed under the regulation of the internal 5' LTR promoter **(Fig. 13B)**. An empty pMSGV1 vector served as a control to produce untransduced CAR T cells (UTD).

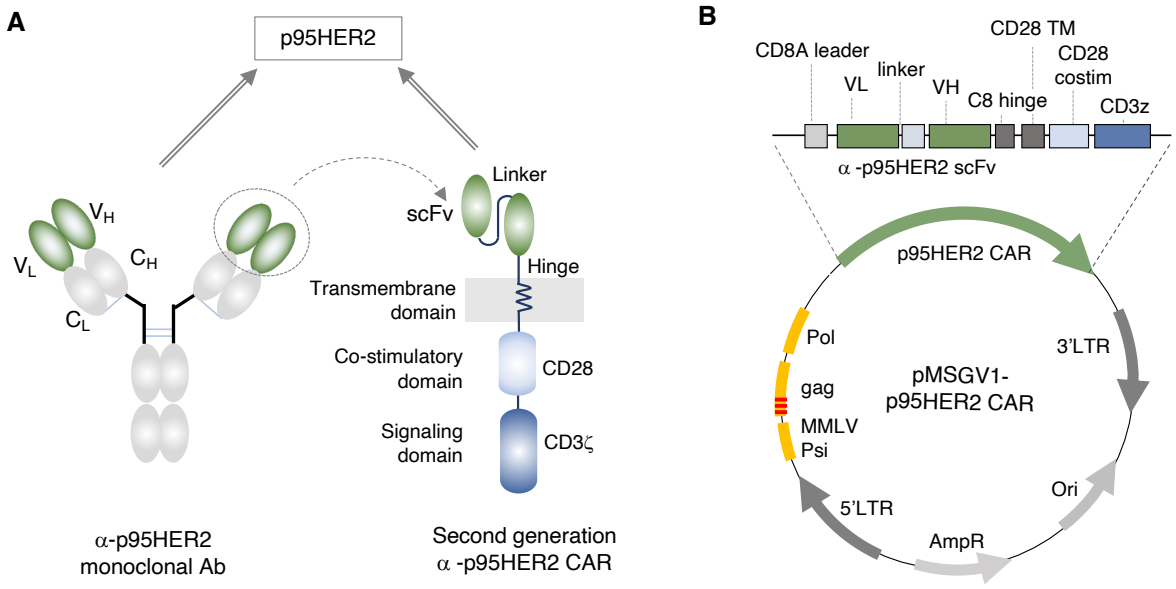

Figure 13: Structure of the p95HER2.CAR and gamma-retroviral vector scheme

(A) The single chain variable fragment (scFv) of p95HER2 antibodies were used to construct a CAR containing the signaling domains of the CD28 and CD3e receptor. **(B)** DNA was inserted into the gamma-retroviral vector pMSGV1, under the regulatory control of the 5'LTR (long terminal repeat) promoter. The plasmid encompasses an ampicillin resistance gene (AmpR), an origin of replication (Ori) and the accessory genes: Moloney Murine Leukemia Virus packaging signal (MMLV Psi), a truncated gag (Group-Specific Antigen) and Pol (Polymerase), located between the 5'LTR and the CAR gene, which contribute to vector functionality.

To generate CAR T cells, activated peripheral blood mononuclear cells (PBMCs) from healthy donors were transduced with p95HER2 CAR retroviral vectors **(Fig.14A).** The T cell surface expression of CAR molecules was analyzed by flow cytometry and stained using an anti-mouse Fab2'-IgG antibody. Only two CARs, 14D and 15C, were detected on the T cell surface **(Fig.14B)** and were able to kill MCF7 cells (derived from a non-HER2-amplified breast tumor) overexpressing p95HER2, co-cultured at different ratios **(Fig.14C)**. This lack of killing discards a detection problem of the 32H variant.

Interestingly, the 32H antibody was the one utilized in our laboratory to develop the p95HER2-TCB [87]. For unknown reasons, the 32H scFv failed to be expressed in the membrane in the T cells with this particular CAR design, and therefore was excluded for further development.

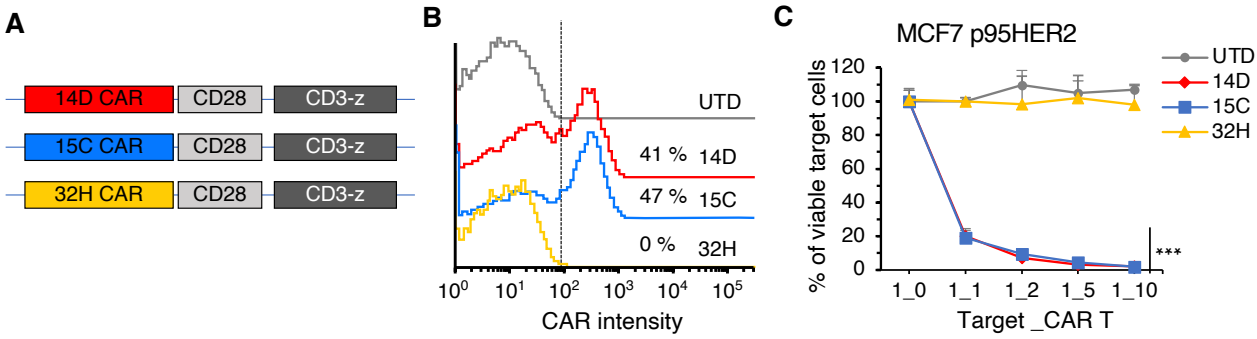

Figure 14: Expression and cytotoxicity of different p95HER2 CAR T cells on MCF7 cells expressing p95HER2.

(A) Simplified schematic representation of the three CAR constructs targeting p95HER2. **(B)** Surface expression of the indicated CARs in A on T cells at day 4 post-transduction; Representative analyses from one PBMCs healthy donor. Percentages of CAR-positive cells from total T cells are indicated. **(C)** MCF7 p95HER2 cells were co-cultured with CAR T cells at the indicated ratios. After 48h, the percentage of viable target cells were assessed by flow cytometry using EpCAM as a marker. N=3 expressed as means ± SD. Statistics compare UTD with the indicated CAR T cells. *P<0.05, **P<0.01, ***P<0.001 two-tailed t test. UTD: untransduced T cells.

1.3. Humanization of p95HER2 CAR T cells

It is known that, when administered to patients, antibodies or even CARs from non-

human origin, and from mouse origin in particular, may induce undesired human anti-mouse antibody (HAMA) responses [237]. In our effort to enhance the clinical application of our CAR T cells, we aimed to humanize the scFv targeting p95HER2, since it is the extracellular part that can be potentially targeted by human antibodies. In collaboration with Roche, the sequences of the murine scFv regions of these CARs were humanized to various degrees, using sequence of the humanized antibody trastuzumab (Roche) as a reference, since it is known to produce little HAMA responses [238]. All the humanized versions of the 14D CAR have the same variable light chain. With the resulting sequences, we generated six humanized p95HER2 CAR T cells, three derived from the 14D and 3 from the 15C antibodies, named H1, H2 and H3 in ascending degree of humanization **(Fig.15A)**, measured as the percentage of aminoacidic changes compared to the murine version **(Fig.15B)**.

A

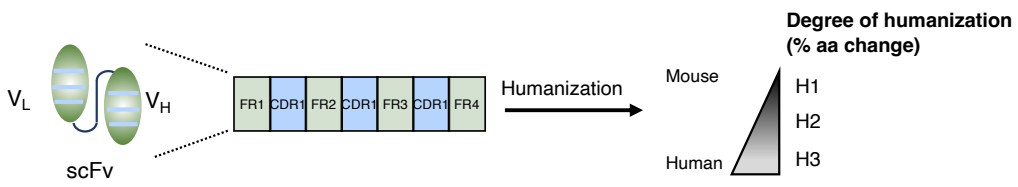

B

14D variants	% V_H aa change	% V_L aa change
H1-14D	6.7% (8 aa)	19.6% (21 aa)
H2-14D	11.7% (14 aa)	19.6% (21 aa)
H3-14D	19% (23 aa)	19.6% (21 aa)

15C variants	% V_H aa change	% V_L aa change
H1-15C	8.3% (10 aa)	20.5% (22 aa)
H2-15C	10% (12 aa)	22.4% (24 aa)
H3-15C	23.3% (28 aa)	24.3% (26 aa)

Figure 15: Humanization of p95HER2 CAR scFv sequence

(A) The humanization of the variable light (V_L) and heavy (V_H) chains of the 14D and 15C anti-p95HER2 antibodies was performed by the pharmaceutical company Roche, resulting in three versions of each of the two selected murine antibodies: H1, H2, and H3, in ascending order of humanization. Changes were mainly, but not exclusively, performed in the FRs, to decrease the probability of affecting antigen binding affinity by modifying CDRs. **(B)** Tables showing the percentages of aminoacidic change of each version. CDR: complementarity determining region; FR: framework region; aa: amino acid.

1.4. *In vitro* characterization of humanized p95HER2 CAR T cells

The six humanized p95HER2 CAR constructs were cloned into the same retroviral

vector **(Fig. 16A)** and PBMCs were transduced following the same strategy. Again, there was a version, H3-15C, that was absent from the cell surface **(Fig.16B).** Transduction efficiency exhibited a slight decline with an increasing degree of humanization but was higher than 30% in all versions.

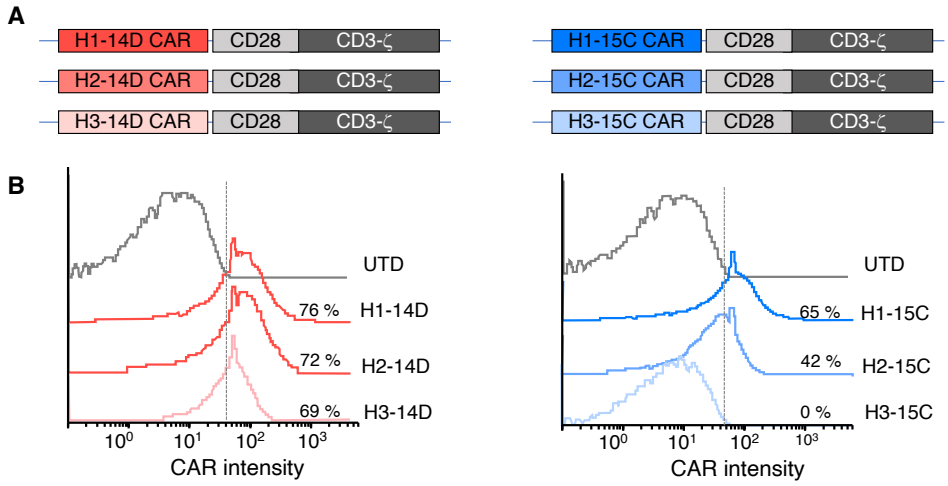

Figure 16: Transduction efficiencies of humanized 14D and 15C p95HER2 CAR T cells

(A) Simplified schematic representation of the chimeric receptors containing the humanized scFv described in figure 15. **(B)** Surface expression of the indicated CARs on T cells at day 4 post-transduction; Percentages of CAR-positive cells from total T cells are indicated. Representative analyses from one PBMCs healthy donor. UTD: untransduced T cells.

Then, to identify the most promising versions, we subjected the six humanized CAR T cells to *in vitro* characterization through co-culture experiments with target cells expressing either an empty vector or p95HER2. First, we assessed the specific killing capacity of these CAR T cells on MCF7 cells expressing p95HER2 and parental MCF7 cells, expressing basal levels of HER2, at different Target: CAR T ratios. Among the 14D derived CAR T cells**,** H1-14D showed a robust specific killing only of p95HER2-expressing target cells **(Fig.17A)**. The cytotoxicity induced by H2-14D, a slightly more humanized version, was lower but still significant. H3-14D CAR was not expressed and therefore no target cell-death was observed with this variant. H1-15D was the only 15C-derived CAR that showed efficient killing of p95HER2-positive target cells, although certain non-specific killing was also observed on antigen-negative cells **(Fig.17B).**

In addition to cytotoxic effect, we assessed the late activation marker CD25 on CD8 T cells at 1:1 ratio by flow cytometry analysis at 48h of the co-culture experiment. The three CARs tested that showed killing capacities (H1-14D, H2-14D and H1-15C) presented a statistically significant increase in the expression of the activation marker CD25 **(Fig.17C)** when co-cultured with target cells expressing the p95HER2 antigen over vector cells. Of note, H1-15C CD8 T cells showed the highest activation in the absence of antigen that could explain the unspecific killing of vector target cells observed in **Fig.17B.**

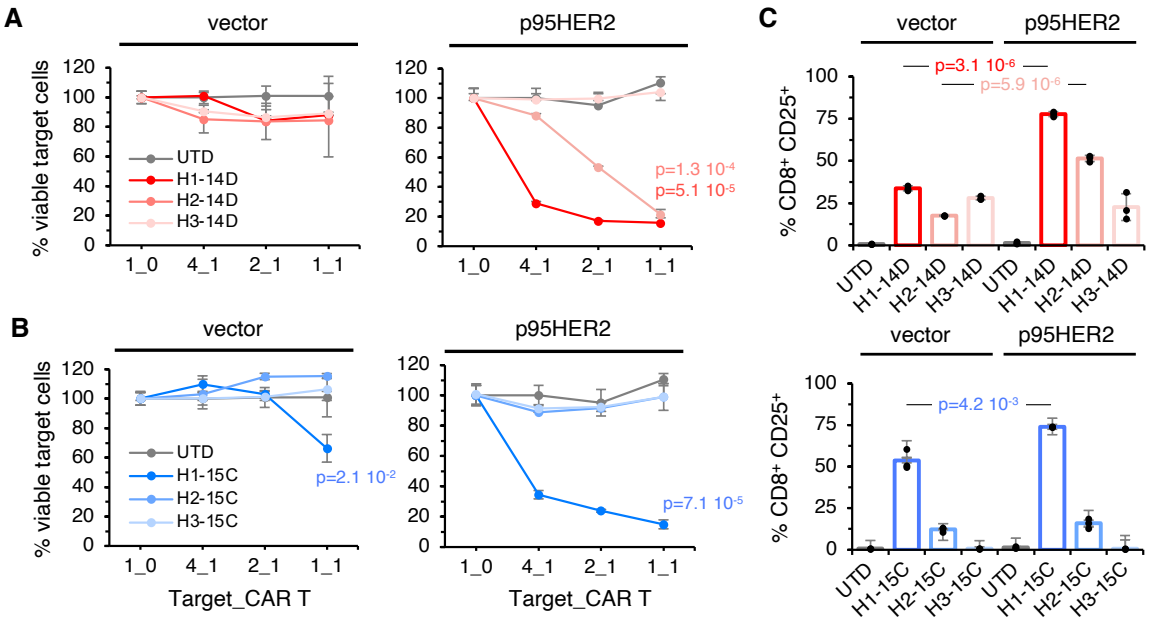

Figure 17: Cytotoxicity and activation of indicated humanized p95HER2 CAR T cells on MCF7 cells expressing or not p95HER2.

(A, B) MCF7p95HER2 or MCF7 cells were co-cultured with CAR T cells at the indicated ratios. At 48h, viable target cells were assessed by flow cytometry. Statistics compare UTD with hp95HER2 CAR T cells. **(C)** CAR T cells from A and B at 1:1 Target : CAR T ratio was stained with CD8 and CD25 at endpoint of the experiment and analyzed by flow cytometry. Statistics compare each CAR T cells co-culture with p95HER2-positive cells with vector cells. Representative analyses from one PBMCs healthy donor. N=3 expressed as means ± SD. Two-tailed *t* test was performed, and *p* values are shown in the graphs when differences are statistically significant. UTD: untransduced T cells.

Once we confirmed that these three candidates were able to activate and kill target cells in a short-term *in vitro* setting, we studied their ability to proliferate upon

continuous antigen stimulation. Two of these CARs (H1-14D and H1-15C) exhibited a prolonged antigen specific proliferation by measuring the number of CAR T cells **(Fig.18).** Despite its ability to kill p95HER2-positive cells and activate specifically, the H2-14D CAR did not promote T cell proliferation, indicating that the extent of antigen specific activation induced by this CAR is comparatively lower.

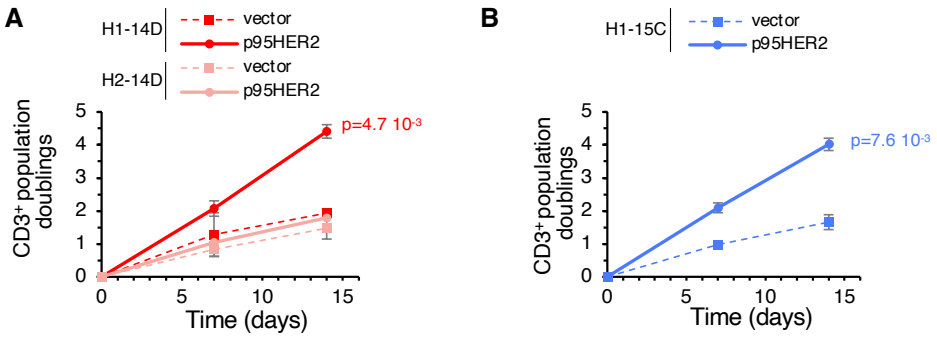

Figure 18: Long term proliferation capacity of humanized p95HER2 CAR T cells.

(A) H1- and H2-14D and **(B)** H1-15C CAR T variants were co-cultured with MCF10A parental or MCF10A p95HER2 overexpressing cells and allowed to proliferate for 14 days. Every 2-3 days, T cells were transferred to a new plate with freshly plated target cells, and fresh media was periodically added to maintain a T cell confluency of $1x10^6$ cells/ml. At the indicated days, CD3+ T cells were count and population doubling related to day 0 are represented. Results are expressed as averages of two independent experiments ± SD. Statistics compare co-culture with p95HRE2 or vector target cells for each CAR T. Two-tailed t test was performed, and *p* values are shown in the graphs when differences are statistically significant. UTD: untransduced T cells.

In summary, *in vitro* data show that H1-14D CAR T is the best candidate in terms of specificity and antitumoral efficacy. Next, we aimed to corroborate these results *in vivo*, testing the three candidates that showed at least T cell activation and cytotoxic effect. A summary of the workflow followed from the first step of antibody screening until the selection of these potential humanized CAR candidates is summarized in **Fig.19**.

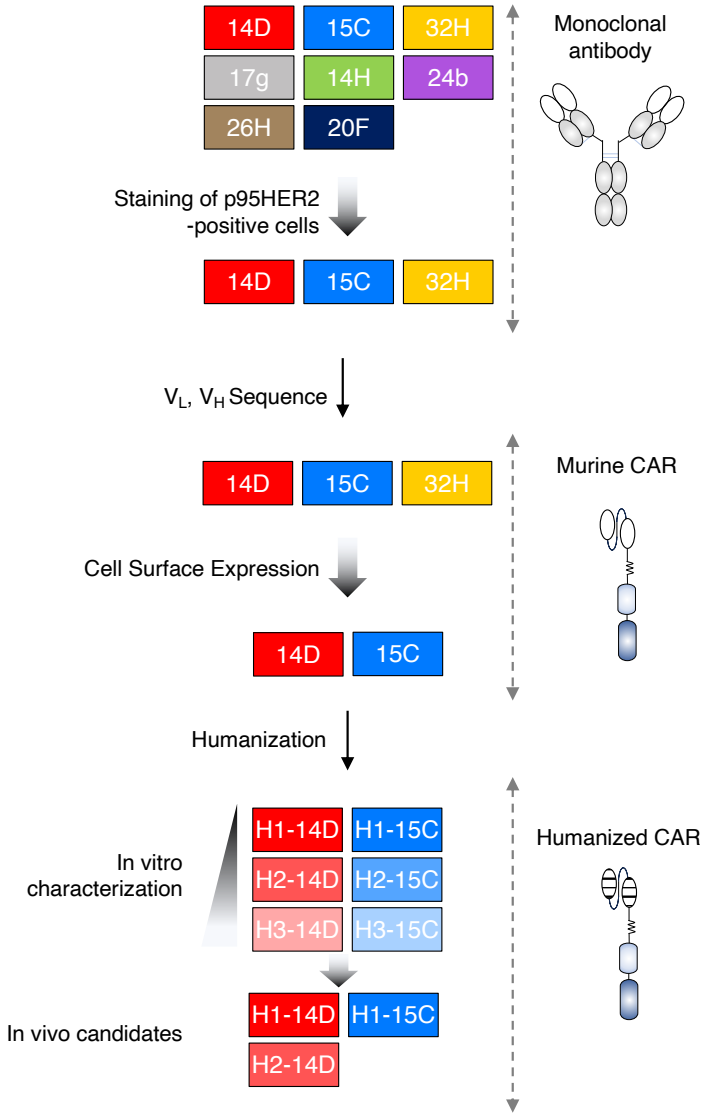

Figure 19: Workflow illustration for the generation and selection of p95HER2 CAR T cell candidates.

Starting from various p95HER2 specific monoclonal antibodies, we selected those with the highest affinity for p95HER2 to create CARs. We proceeded with the two unique versions that expressed correctly when transduced in T cells at the cell surface: 14D and 15C. From these, we generated six humanized versions, three of each and selected the three best candidates based on their *in vitro* performance for further *in vivo* testing.

2. Antitumor effectivity assessment of humanized p95HER2-CAR T cell candidates *in vivo*

2.1. Antitumor effect of humanized p95HER2 CAR T cells in *in vivo*

To assess the *in vivo* efficacy of p95HER2 CAR T cells, first we conducted an experiment to optimize the dose of CAR T cells, which ae injected intravenously into the lateral vein, using the H1-14D version. For this purpose, we established an orthotopic BC model, engrafting MCF7 cells overexpressing p95HER2 into immunocompromised NSG (NOD *scid* gamma) mice **(Fig.20A).** UTD T cells normalized to the same number of total cells of each dosing protocol were used as a control, and no differences between treatments were observed. Among the tested dosing regimens, administering two doses of 3 million CAR-positive T cells separated by ten days proved to be optimal. Moreover, this double dose outperformed even a higher single dose of 10 million CAR-positive T cells **(Fig.20B).** Therefore, we identified the regimen of 2 doses of 3 million CAR-positive cells as the preferred approach for subsequent exploratory and comparative *in vivo* experiments.

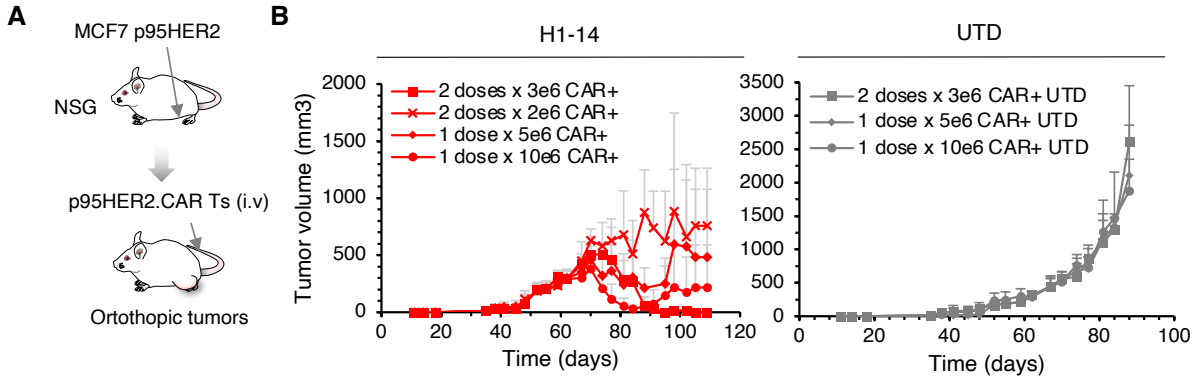

Figure 20: Selection of the optimal administration regimen for p95HER2 CAR T cells

(A) Schematic drawing illustrating the orthotopic implantation of MCF7 cells expressing p95HER2 were injected into the mammary fat pads of NSG mice **(B).** When tumors reached 200 mm3 animals were randomized into different doses groups using H1-14D CAR T cells (left). UTD cells (right) were used as controls of allogenic effect, normalized to the number of total T cells taking into account transduction efficiency. The first dose was given at day 62, and second doses were administered after 10 days. Tumor volumes are depicted in mm3. N=5 expressed as means + SD. UTD: untransduced T cells; i.v.: intravenous administration Is in the lateral tail vein.

Once we validated the feasibility of this orthotopic BC *in vivo* model to evaluate the antitumor activity and the optimal dosing schedule of p95HER2 CAR T cells, we proceeded to compare H1-14D with the other candidates, H1-15C and H2-14C, in two separate *in vivo* experiments. In the first experiment, using the previously explained setting, the efficacy of the H1-14D CAR T cells on MCF7 cells expressing p95HER2 outperformed that of H1-15D **(Fig. 21A)**. On day 84, one or two mice of each group were sacrificed, and their tumors processed to analyze the presence of infiltrating human T lymphocytes. As expected, human CD3⁺ cells were detected in tumors from mice treated with H1-14D or H1-15D CAR T cells. CAR-positive cells showed a similar distribution, arguing that hCD3⁺, which are more easily detected, are a good indicator of the infiltration of CAR-positive T cells **(Fig.21B).**

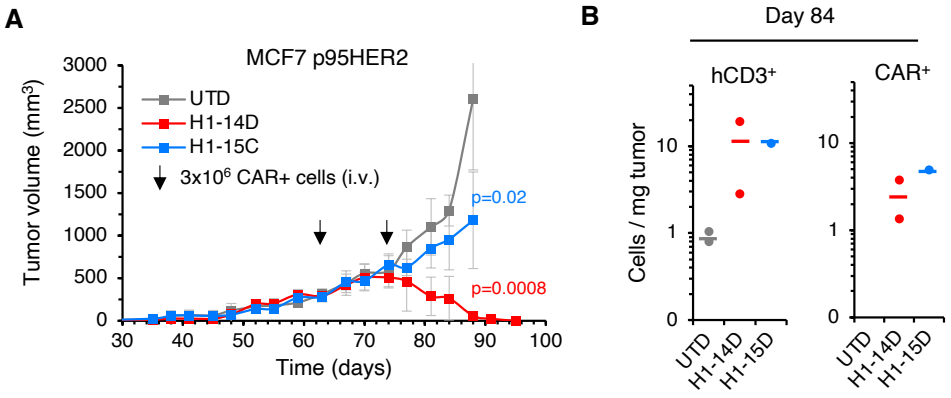

Figure 21: Antitumor efficacy comparison between the H1-14D and H1-15C p95HER2 CAR T cells

(A) At the time points indicated by the black arrows, 3x10⁶ CAR+ T cells transduced with different p95HER2 CARs (H1-14D or H1-15C) or equivalent total T cells transduced with empty vector (UTD) were injected into the tail vein of NSG mice bearing MCF7p95HER2 tumors. Tumor volumes are represented as averages ± SD (n=5 per group). Statistics compare UTD with p95HER2 CAR T cells. Two-tailed t test was performed, and p values are shown in the graphs when differences are statistically significant. **(B)** At day 84, one or two mice from each group were euthanized. Tumors were excised and processed, and the numbers of infiltrating human CD3⁺ lymphocytes (hCD3⁺) and CD3⁺ cells expressing CARs (CAR⁺) were quantified and presented as counts per milligram of tumor tissue. The averages of the measurements are shown with horizontal lines. UTD: untransduced T cells; i.v.: intravenous administration Is in the lateral tail vein.

A comparable conclusion was drawn when comparing the *in vivo* antitumor efficacy of H1-14D and greater humanized version H2-14D in the same experimental model. H1-14D CAR T cells demonstrated a robust and consistent antitumor effect leading to tumor suppression across all treated mice **(Fig. 22A)**. In contrast, H2-14 CAR T cells initially diminished tumor growth but eventually resulted in relapse, despite exhibiting similar levels of tumor infiltrating and circulating human CD3⁺ cells prior to this tumor escape **(Fig. 22B).** Therefore, *in vivo* antitumor assessment showed that the best candidate is the H1-14D and we chose this candidate for further preclinical and clinical evaluation

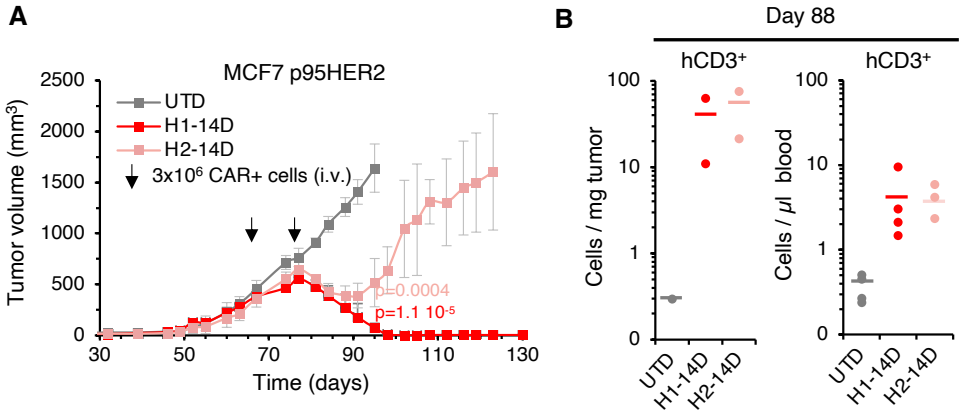

Figure 22: Antitumor efficacy comparison between the H1-14D and H2-14D p95HER2 CAR T cells

(A) A similar approach as in Figure 10 was used to compare the effects of the p95HER2 CARs H1-14D and H2-14D. Tumor volumes are represented as averages ± SD (n=5 per group) Statistics compare UTD with hp95HER2 CAR T cells. Two-tailed t test was performed and p values are shown in the graphs. **(B)** Levels of human CD3 infiltrating the tumor (left) and in blood circulation (right) were quantified and presented as counts per milligram of tumor tissue or µl of blood. The averages of the measurements are shown with horizontal lines. . UTD: untransduced T cells; i.v.: intravenous administration Is in the lateral tail vein.

2.2. Long term antitumor efficacy evaluation of H1-14D CAR T cells

Long-term monitoring of two mice treated with H1-14D exhibited sustained responses over an extended period **(Fig. 23A)**. These mice were also used to investigate whether long-lived p95HER2 CAR T cells protected against re-engrafting MCF7 p95HER2 cells

into these previously treated mice, in parallel to age-matched untreated controls, after almost 300 days from last dose. Remarkably, tumors developed in these control mice but not in the mice previously treated with p95HER2 CAR T cells. 24 days after re-engraftment of tumors, blood samples were analyzed, confirming the presence of circulating human CD3+ T cells in both animals treated with H1-14D CAR T **(Fig.23B)**. These findings provide compelling evidence that mice treated with this p95HER2 CAR T cells retain long-term protection against tumors expressing p95HER2.

In summary, H1-14D CAR T cells displayed a potent antitumor effect, both *in vitro* and *in vivo*, surpassing that of other CAR T constructs. Therefore, due to its effectiveness profile, H1-14D was selected as the lead CAR construct for further development and extensive safety assessment.

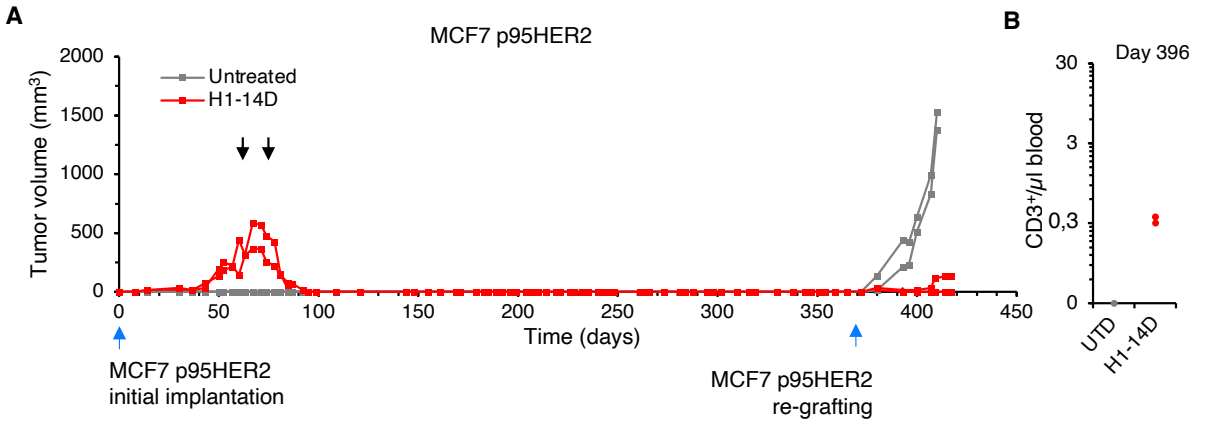

Figure 23: Tumor rechallenge experiment revealed prolonged protection against tumor relapse by persistent CAR T cells

(A) Two mice treated as in previous figures with H1-14D underwent extended monitoring (depicted by red lines) after complete remission of their tumors. As indicated by the blue arrow, MCF7 cells expressing p95HER2 were implanted orthotopically in the mammary glands at day 0 and re-grafted in these mice in the opposite mammary gland at day 365, while an equivalent re-grafting was performed in age-matched untreated mice for control purposes, which were not implanted with tumors initially. **(B)** At day 396, the numbers of circulating human lymphocytes were analyzed and expressed as number of human $CD3^+$ cells per μl of blood.

3. H1-14D CAR T: safety assessment

3.1. Identification of potential "off targets" using a Membrane Proteome Array (MPA) screening

To assess the specificity of the selected CAR, H1-14D, we used the membrane proteome array (MPA) platform, an assay performed by the company Integral Molecular, widely used for profiling the specificity of antibodies and other ligands that target human membrane proteins. It involved analyzing the binding of H1-14D scFv, fused to a human IgG1 for detection purposes, to a protein array containing ~6000 native human membrane proteins by flow cytometry**.** Protein A, which binds to human antibodies' Fc, was used as positive binding control. As anticipated, HER2 did not exhibit significant cross-reactivity with the H1-14D scFv, but two potential cross-reacting proteins were identified **(Fig. 24):** the cell surface receptor IL2RB and the transmembrane protein UBXN8, known to be located primarily at the endoplasmic reticulum [239].

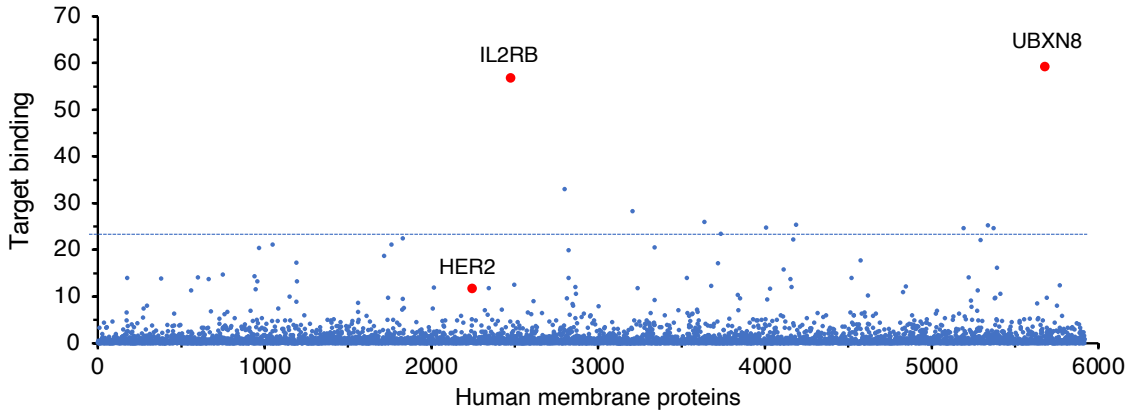

Figure 24: Specificity of the H1-14D p95HER2 scFv

Membrane Proteome Array result revealed two positive hits, marked in red. The blue line indicates the binding value above which hits are considered positive, but only two passed the validation process. HER2, as expected, is not recognized by H1-14D scFv.

Adhering to the provider's recommendations, we chose to internally perform a preclinical safety evaluation to confirm this finding and to determine whether these two potential off targets pose a genuine risk to our therapy.

First, we sought to validate the binding of H1-14D scFv to potential hits in our experimental setting. We transduced MCF10 cells with lentiviral vectors encoding IL2RB and UBXN8 tagged at the cytoplasmic domains with the V5 epitope. Flow cytometry analysis of permeabilized cells demonstrated efficient expression of V5-tagged IL2RB and UBXN8 **(Fig. 25A)**. Similar analysis of non-permeabilized transfected cells with antibodies against a luminal domain of UBXN8 and against the extracellular domain of IL2RB confirmed that, in contrast to IL2RB, UBXN8 is not exposed at the cells surface **(Fig. 25B).**

Importantly, staining with H1-14D scFv revealed no specific cell surface signal in cells overexpressing IL2RB or UBXN8 **(Fig. 25C)**, contradicting the findings of the MPA company. Parental MCF10A cells and MCF10A overexpressing p95HER2 served as a control to demonstrate proper binding of H1-14D to p95HER2. This finding suggests that, in our hands, H1-14D scFv does not recognize the proposed off-targets; thus, the two potential off-targets were false positives.

In addition, to conclusively rule out these hits, we decided to perform functional CAR T killing assays against the generated MCF10A cell lines expressing UBXN8 and IL2RB. Accordingly, p95HER2 CAR T cells did not have any effect on cells expressing these transmembrane proteins **(Fig. 25D)**. We concluded that the two only candidate cross-reacting proteins identified in the transmembrane protein array were false positives and that the p95HER2 antibody chosen to construct the p95HER2 CAR does not likely cross-react with any human transmembrane protein other than p95HER2.

From this point forward, we will simply refer to H1-14D p95HER2 CAR T cells as p95HER2 CAR T cells

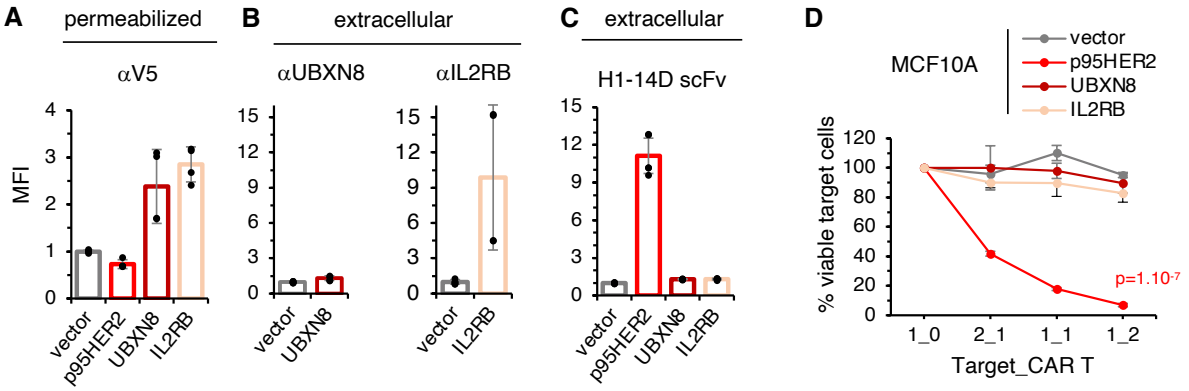

Figure 25: Validation of MPA results

(A, B, C) MCF10A cells were transduced with empty vector or the vectors encoding p95HER2, UBXNB8 or IL2RB tagged, the latter two tagged with the V5 epitope, were stained with anti-V5 antibodies (A), antibodies against UBXNB8 or IL2RB (B) or the scFv of H1-14D (C). **(D)** The same cells as in B were co-cultured with p95HER2 CAR (H1-14D) T cells for 48 h. Then, viable target cells were quantified by flow cytometry using EpCAM as a marker. N=3 expressed as means ± SD. Statistical two-tailed *t* test was performed; *p* values are shown when significant.

3.2. Effect of H1-14D p95HER2 CAR T cells on cells expressing normal levels of HER2

Despite we have previously demonstrated that p95HER2, unlike HER2, is not expressed in healthy tissues [87], we still wanted to address potential side effects on normal tissues induced by p95HER2 CAR T cells. Subsequently, we evaluated its killing effect on MCF7 cells, which express HER2 levels comparable to those found in normal epithelial tissues, in comparison to a trastuzumab-based HER2 CAR T **(Fig.26A).** The HER2 CAR T cell has the same structure as the p95HER2 CAR T cell construct, differing only in the scFv component.

While the HER2.CAR T efficiently targeted and killed MCF7 cells, the p95HER2 CAR T exhibited no effect **(Fig.26B),** even though considerable levels of circulating CAR T cells were detected for both CAR T treatments **(Fig. 26C).**

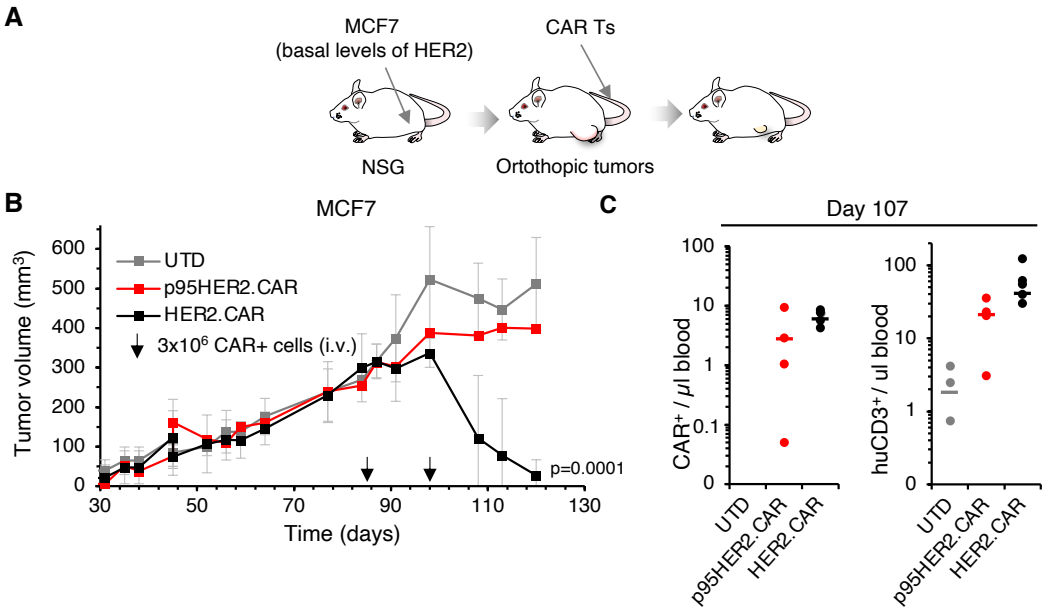

Figure 26: Effect of p95HER2 and HER2 CAR T cells on MCF7 cells

(A) Unmodified MCF7 cells were implanted into the mammary fat pads of NSG mice. **(B)** $3x10^6$ T cells transduced with empty vector (UTD), p95HER2 CAR (H1-14D) or a trastuzumab-based HER2 CAR were injected intravenously (arrows). Tumor volumes are represented as averages ± SD (n=5 per arm). Statistical two-tailed *t* test was performed, statistically significant *p* values are shown. **(C)** At the end of the experiment, the numbers of circulating CAR-positive cells (left) and human CD3+ lymphocytes (right) were analyzed and expressed as counts per µl of blood. UTD: untransduced T cells; i.v.: intravenous administration Is in the lateral tail vein.

In conclusion, our findings suggest that the p95HER2 CAR T does not target cells expressing physiological levels of HER2, indicating a potential reduction in off-target effects on normal tissues, at least compared to HER2 targeted therapies.

4. Effect of humanized p95HER2 CAR T cells against lung and brain tumors

Metastatic BC remains a largely incurable disease [46]. Thus, there is a need to search for innovative therapies targeting lung and brain metastases, common sites for the migration of BC cells migrate.

To model metastasis in the lungs, we injected luciferase-expressing MCF7 p95HER2 cells (MCF7p95HER2.Luc^{+}) into the tail vein of immunosuppressed NSG mice **(Fig.27A)**. Within one month, evident cell growth in both lungs was observed, indicated by the increase in bioluminescence signal. Treatment with p95HER2 CAR T cells effectively suppressed lung tumor growth, as revealed by bioluminescence lung signal measurements and images **(Fig.27B, C)** and maintenance of bodyweight, in contrast to the weight loss seen in the control group due to lung cancer progression **(Fig.27D).**

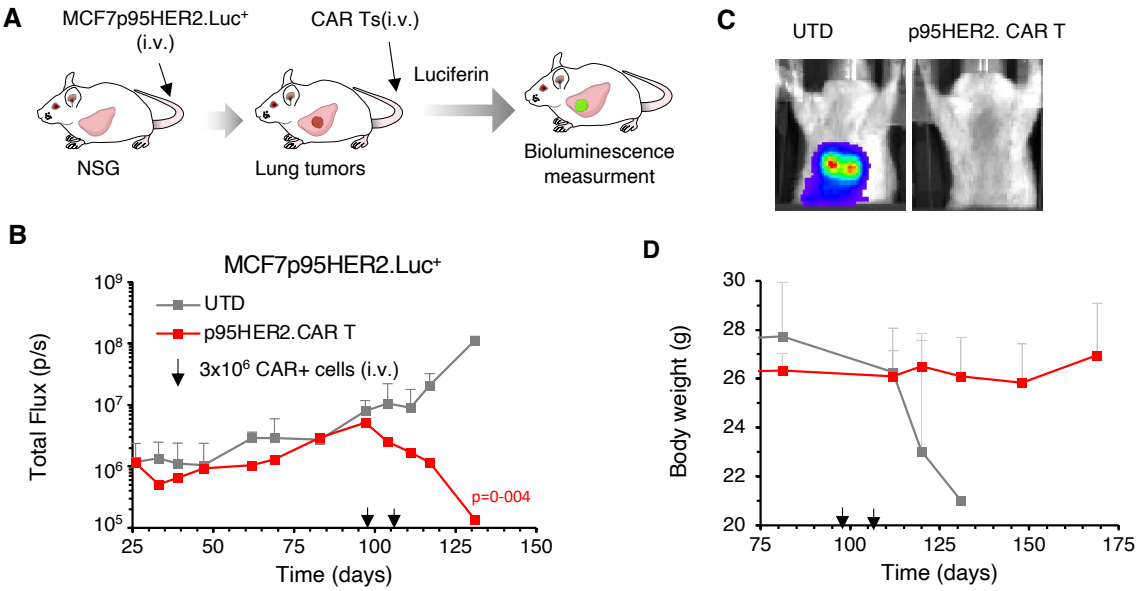

Figure 27: Effectivity of p95HER2 CAR T against lung tumors

(A) MCF7 p95HER2 cells expressing luciferase (MCF7p95HER2.Luc+) were injected into the tail vein of NSG mice to induce lung cancer **(B)**. At the time points indicated by the arrows, mice were treated with 3X10^6 p95HER2 CAR T cells or UTD T cells. Tumor growth was monitored by bioluminescence measurement after luciferin administration (n=3 per group) represented as averages ± SD. Statistical two-tailed *t* test was performed, *p* value at last timepoint is shown **(C)** Representative bioluminescence images at endpoint. **(D)** Mouse weight evolution expressed in grams (g) and represented as averages ± SD. UTD: untransduced T cells; i.v.: intravenous administration Is in the lateral tail vein.

Next, to model brain metastasis, we injected intracranially luciferase expressing MCF7p95HER2. One day after the injection, cells were detectable in the brain and we treated the mice with p95HER2 CAR T cells or UTD T cells following the established dosing protocol **(Fig. 28A)**. Average of bioluminescent signal and images reveal that p95HER2 CAR T cells significantly reduced these brain tumors **(Fig. 28B,C).** Therefore, we concluded that the p95HER2 CAR T cells could cross the blood brain barrier and kill p95HER2 expressing tumor cells growing in the brain. Again, control groups suffered a dramatic loss of weight, whereas the p95HER2 CAR T treated group maintained a constant body weight, an indicative of healthy status **(Fig. 28D).**

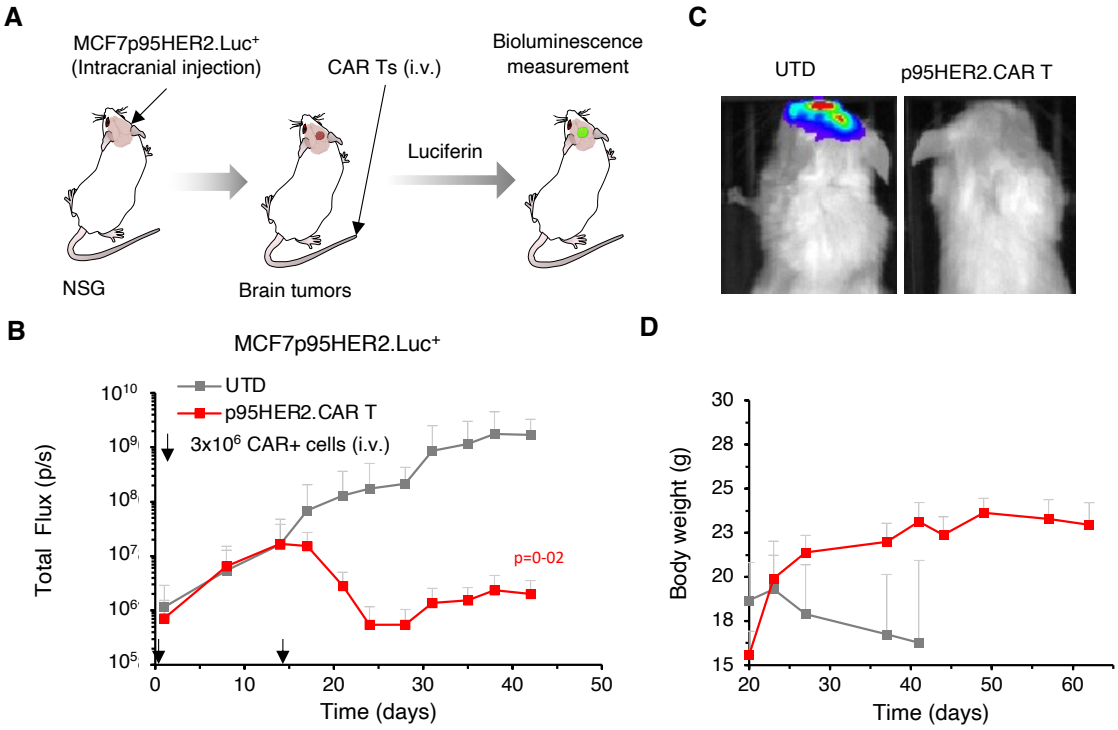

Figure 28: Effect of p95HER2-CAR T cells on intracranial MCF7.p95HER2.luciferase tumors

(A) Schematic drawing illustrating intracranial injection of MCF7 p95HER2/luciferase cells in NSG mice. **(B)** Intracranial tumor growth monitored by assessing bioluminescence, expressed as means ± SD; n≥ 4 per group. **(C)** Representative images of the brain tumor growth monitored by assessing the bioluminescence represented as averages ± SD. Statistical two-tailed *t* test was performed, *p* value at last timepoint is shown. **(D)** Evolution of mice body weight, expressed in grams (g) and represented as averages ± SD. UTD: untransduced T cells; i.v.: intravenous administration Is in the lateral tail vein.

Collectively, the results presented here show that second-generation CAR T cells targeting p95HER2 are effective against cancer cells expressing p95HER2 in different tissues, such as the lungs and the brain.

5. Antitumor effect of humanized p95HER2 CAR T cells on p95HER2-positive BC PDXs

5.1. Antitumor effect and correlation with T cell infiltration

Patient-derived xenografts (PDXs), although still imperfect experimental models, are considered to recapitulate human tumors better than cell lines [240]. For this reason, we then challenged our candidate against two HER2-positive BC PDXs *in vivo*, one negative (PDX510) and one positive (PDX67) for p95HER2 expression, that were orthotopically grafted in NSG mice **(Fig.29A).** p95HER2 CAR T cells had no effect on a HER2-positive, p95HER2 negative PDXs **(Fig.29B).** In contrast, they had a significant effect on p95HER2-positive PDXs **(Fig.29C).** This antitumor effect was comparable to that previously observed with anti-p95HER2 TCB antibodies [87], but far more limited than that observed with cell lines.

Immunohistochemical staining of tumors in the p95HER2 CAR T treated group at endpoint revealed that many positive cells persisted (data not shown), ruling out the possibility of antigen loss as the cause of partial resistance in this model. However, a correlation between T cell infiltration and response was observed, showed by anti-human CD3 staining analyzed by flow cytometry **(Fig 30A),** and immunohistochemistry **(Fig. 30B).**

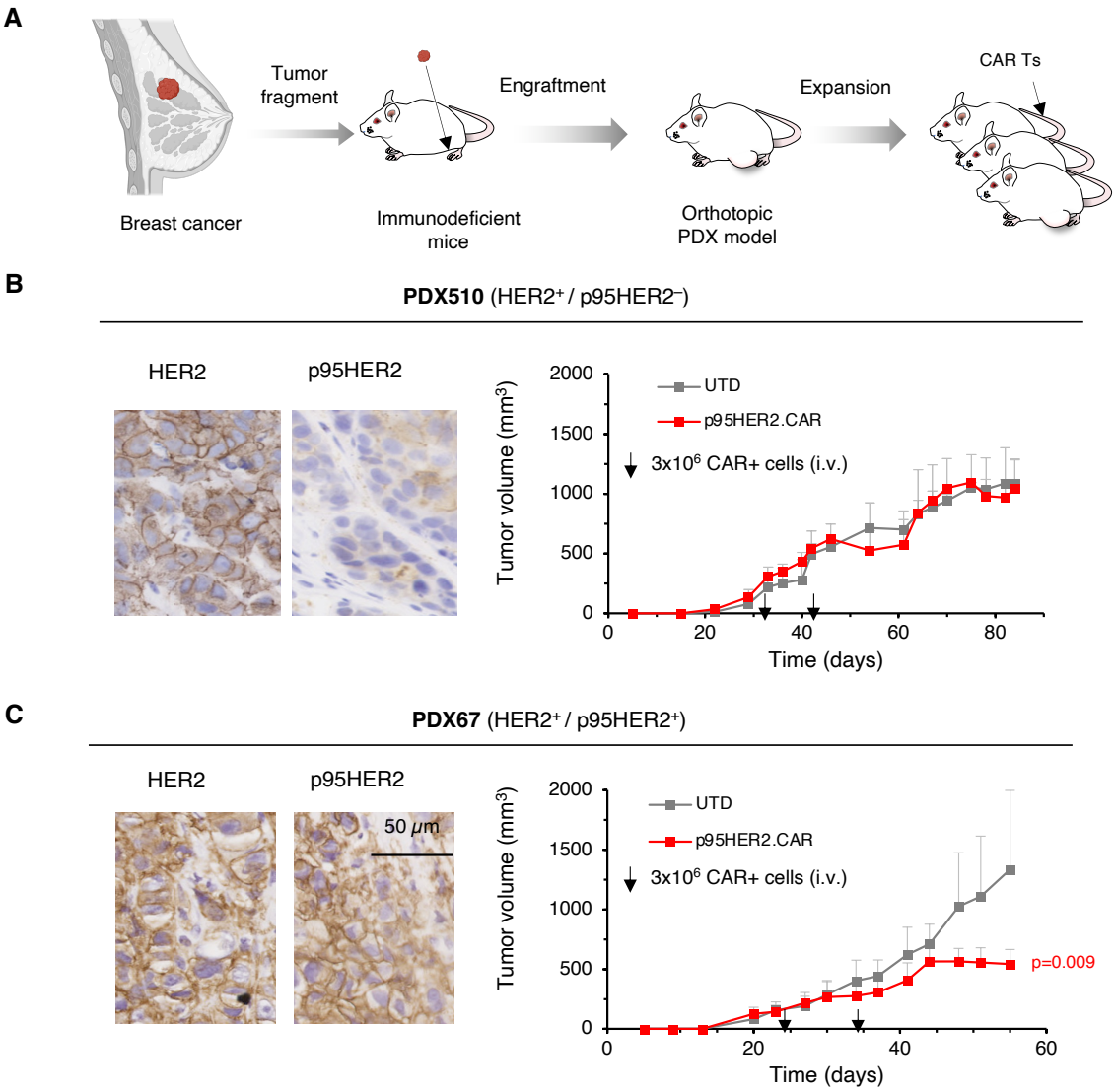

Figure 29: Antitumor effect on PDX models

(A) Schematic showing the establishment of PDX models starting from tumors samples from patients. **(B,C)** The indicated PDXs were grown in NSG mice. At the time points indicated by the arrows, 3x106 T cells transduced with empty vector (UTD) or p95HER2 CARs were injected i.v. Tumor volumes are represented as averages ± SD (n=6 per arm). Statistical two-tailed *t* test was performed, *p* value at last timepoint is shown. Left, Immunohistochemical analysis of HER2 and p95HER2 expression on samples from the same PDXs.

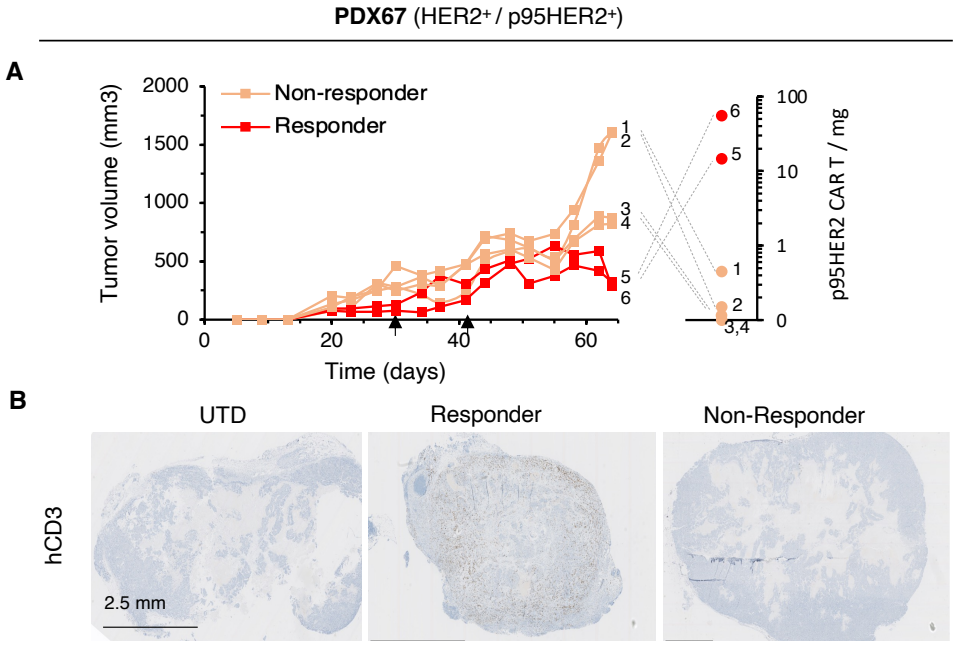

Figure 30: Extended PDX67 figure

(A) Antitumor response correlation with Infiltration of p95HER2 CAR T in PDX67 from previous figure. **(B)** Representative images of anti-human CD3 IHC staining of tumors at endpoint.

5.2. Heterogeneity of p95HER2 expression in BC-PDXs

Despite not being observed in PDX67, one of the main limitations of CAR T cell therapy is antigen heterogeneity. To explore the distribution pattern of p95HER2 within tumors in a bigger cohort, we performed IHC analysis of a HER2-positive BC PDX tumor microarray (TMA) containing samples from 23 different PDX of origin. For comparison, we also performed HER2 staining **(Fig.31A).** 13 samples were positive for p95HER2 and HER2, whereas 7 were only HER2-positive. Moreover, antigen heterogeneity manifested in 5 of the p95HER2-positive PDX, while HER2 staining was homogeneous and more intense in all case. Some of these different scenarios are highlighted in **Fig.31B**. Case1 represents a HER2-positive/p95HER2-negative, while case 4 presents a very high and homogeneous expression of both antigens. However, there are other intermediate scenarios, in which we observe p95HER2 positivity, but less homogeneous and intense than that of HER2. General strategies to increase the potential of T cell redirection and chances of complete tumor eradication in all possible scenarios are needed.

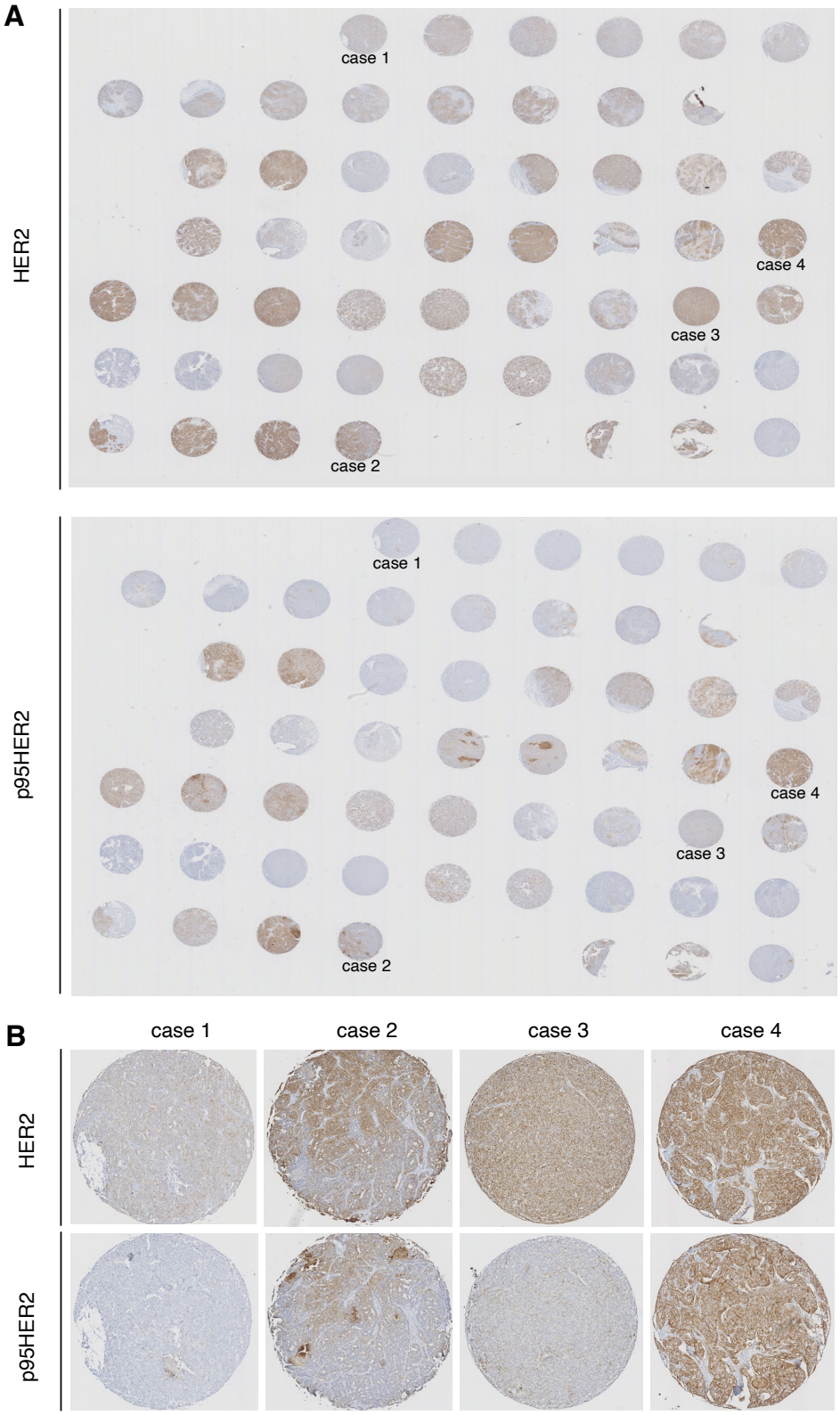

Figure 31: Immunohistochemistry analysis of a HER2-positive BC PDXs TMA

(A) HER2 (upper) and p95HER2 (lower) IHC staining images of a TMA containing 23 cases of BC-PDXs and some control samples. **(B)** Selected cases are shown with higher amplification.

6. Increasing antitumor potential and tackling antigen heterogeneity: rational for armored CAR T cells

To date, no CAR T cell therapy has been approved for the treatment of solid tumors, one of the reasons being lack of effective antitumor response. Due to the results observed with our second-generation p95HER2 CAR T against a PDX model, we aimed to increase its efficacy by adding additional therapeutic components, with the firm compromise of maintaining its safety.

Although there is not exactly a direct correlation between HER2 and p95HER2 expression, p5HER2 tends to be expressed when HER2 is overexpressed at high levels, and therefore, HER2 expression is more abundant, although less tumor-specific, than p95HER2. Therefore, we hypothesized that incorporating HER2 targeting TCEs could increase the efficacy of CAR-redirected lymphocytes against cells expressing p95HER2, by incrementing the potential targeted population within the tumor and minimizing the risk of antigen-escape. Moreover, a potential advantage of secreted bispecific antibody over alternative options, such as the co-expression of a second CAR molecule, is that a bsAb could potentially recruit bystander untransduced T cells and elicit additional cytotoxicity [188].

Engineered bispecific antibodies offer a spectrum of formats. Bispecific T cell engagers, popularly referred to as BiTEs®, represent a compact and versatile form of bispecific antibodies. We selected this structure because of their relatively small size, which allows for efficient secretion by T cells.

These bispecific antibodies were denominated TECH2s, which stands for T cell Engagers against CD3 and HER2. Given that TECH2s based on Herceptin likely recognize cells expressing normal levels of HER2, and that our main goal is to treat HER2 positive tumors in a safe way, we used scFv with attenuated affinities previously described [164]. This rationale is depicted in **Fig.32.**

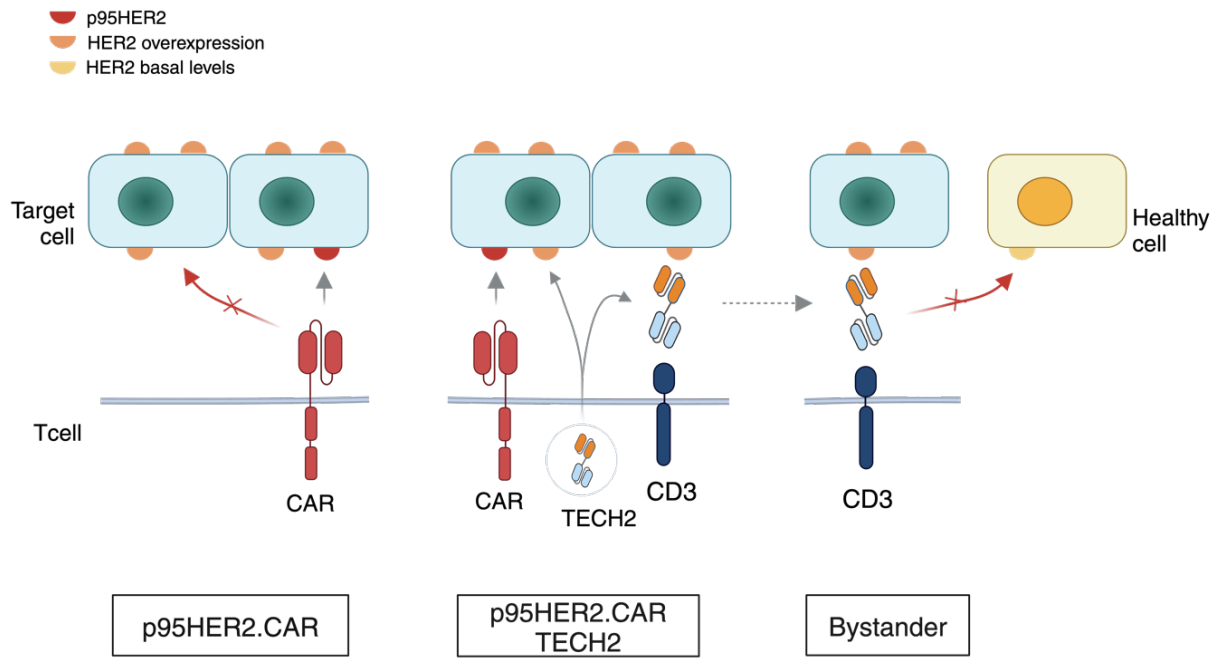

Figure 32: Rational for armoring p95HER2 CAR T cells with HER2xCD2 bispecific T cell engagers

As HER2 expression is more abundant, albeit less tumor-specific than p95HER2, we postulated that incorporating HER2-targeting T cell bispecific antibodies, referred to as TECH2s (T cell Engagers against CD3 and HER2), could enhance the efficacy of p95HER2 CAR-redirected lymphocytes. This approach aims to expand the targeted population within the tumor, counteract antigen escape and recruit additional bystander T cells. To ensure safety, the affinity of TECH2 molecules should guarantee exclusive targeting of HER2-overexpressing cells, without affecting those expressing HER2 at basal levels.

7. Development of HER2-CD3 bispecific engagers: TECH2

7.1. Bispecific T cell engager design: selection of CD3 and HER2 scFvs

We generated TECH2s of different affinities using available public sequences. The Anti-CD3 scFv sequence and the several linkers' sequences were obtained from Blinatumomab®, as it is the only approved BiTE®. The HER2 scFv sequences were obtained from [164]. These affinity-tuned antibodies have been shown to discriminate between cells expressing normal levels and those overexpressing HER2. Consequently, we generated retroviral vectors expressing a TECH2 based on trastuzumab (TECH2Hi) and two variants with decreasing affinity (TECH2Me and TECH2Lo) **(Fig.33).**

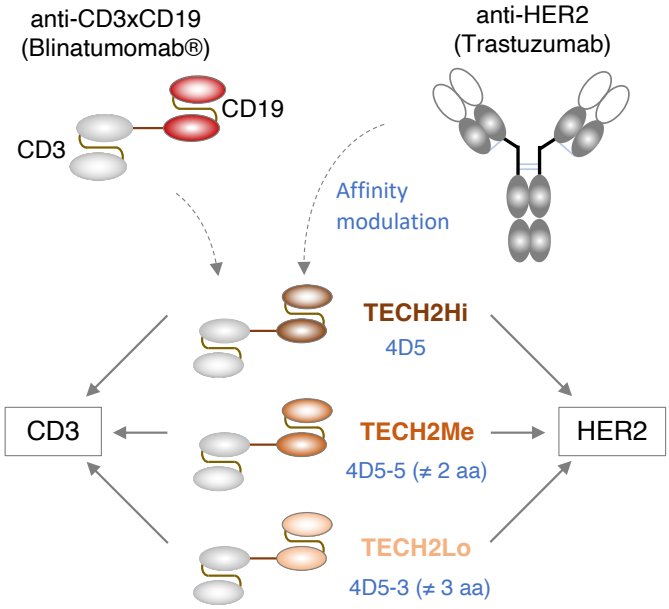

TECH2s (**T** cell **E**ngager **C**D3 x **H**ER**2**)

Figure 33: Schematic showing the generation of the TECH2 with different affinities

The single chain fragment variables containing the VH and VL of antibodies against CD3ε and HER2 were fused using linkers to generate a bispecific T cell engager named TECH2 (T cell Engager anti CD3 and anti-HER2). Anti-HER2 scFvs with different affinities led to three different versions of TECH2s, named TECH2Hi, TECH2ME and TECH2Lo, in decreasing order of affinity towards HER2.

7.2. Characterization of TECH2 cytotoxicity and binding to target antigens

To assess the functionality of these TECH2s, we first sought to evaluate the binding and killing capacities of TECH2s secreted by T cells. We generated bicistronic constructs in which we inserted the TECH2 gene and the eGFP encoding sequence, separated by a T2A **(Fig.34A).** All the vectors transduced with similar efficiencies, assessed by the percentage of eGFP positive cells by FACS analysis **(Fig.34B).** We cultured transduced T cells with control MCF7 cells or cells from a HER2-positive PDX (PDX433) **(Fig.34C).** T cells expressing the TECH2Hi readily killed MCF7 cells, arguing that, as expected, this bispecific antibody targets cell expressing normal levels of HER2. In contrast, T cells expressing TECH2Me had no effect on MCF7 cells but were effective killing cells from the HER2-amplified PDX433, although to a lower extent than TECH2Hi. TECH2Lo had no effect against a PDX expressing high levels of HER2, indicating that the affinity of this bispecific is too low for being used to armor a p95HER2 CAR T.

To confirm these results in an additional *in vitro* model, we used MCF10A cells, which are derived from normal epithelium and express normal levels of HER2 that can be targeted by TECH2Hi but not TECH2Me or Lo**.** In contrast, TECH2Me killed the same cells overexpressing HER2 **(Fig.34D)**. TECH2 Lo was discarded from further testing, as it was unable to target even cells expressing high levels of the antigen.

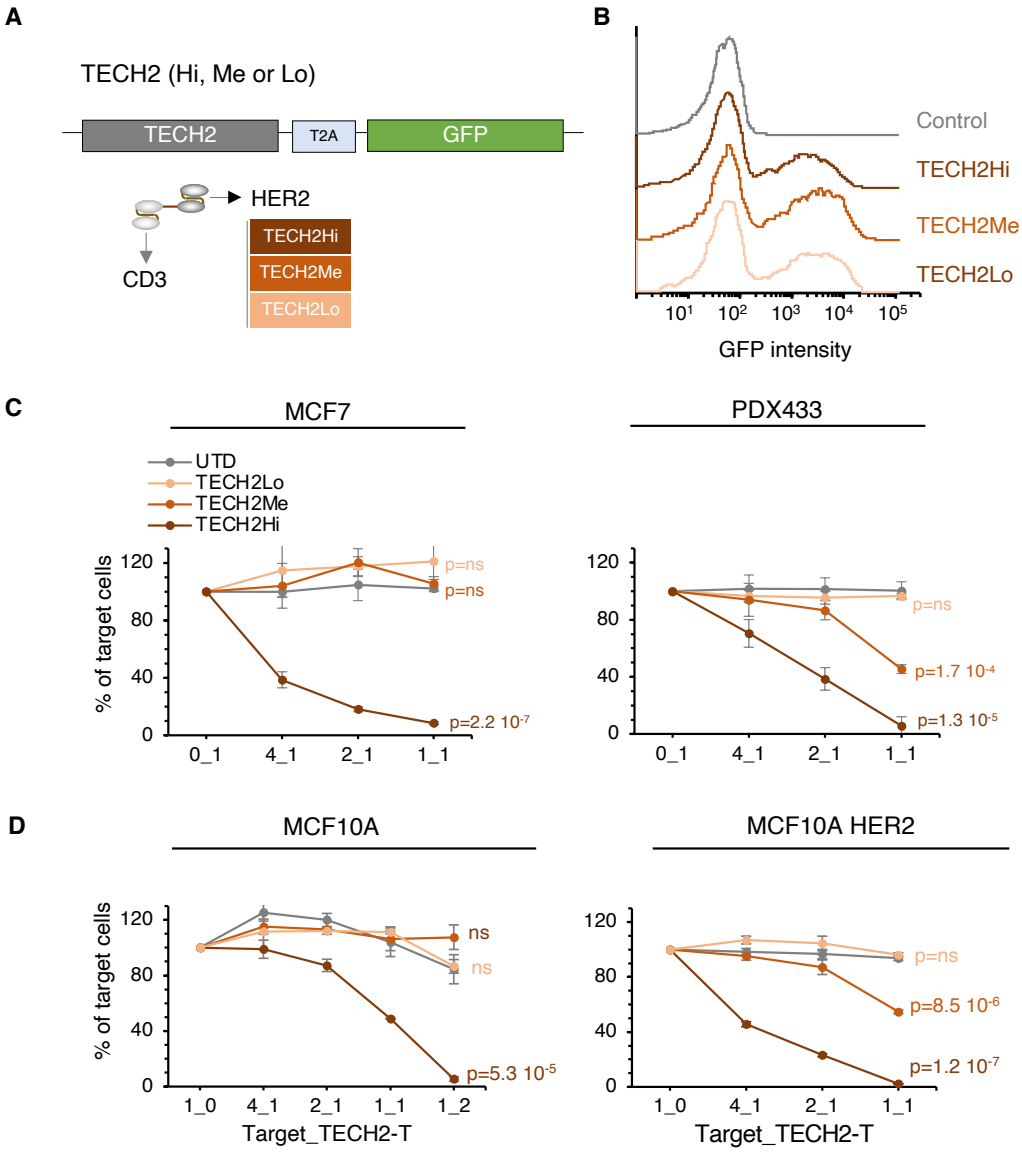

Figure 34: *In vitro* testing of TECH2s with different affinities secreted by T cells

(A) Simplified scheme of bicistronic pMSGV1-based vectors, in which the TECH2 Hi, Lo or Me encoding gene is separated through a T2A from an eGFP gene. **(B)** Transduction efficiency assessed by eGFP expression using flow cytometry. **(C,D)** Parental MCF7 cells or cells from the HER2/p95HER2-positive PDX433 were co-cultured with T cells expressing the different TECH2s at different ratios. Then, viable target cells were quantified by flow cytometry using EpCAM as a marker. Results are expressed as averages of three independent experiments. **(E,F)** Same co-culture experiment was performed using the non-transformed MCF10A cell line and the same cells overexpressing HER2. Statistical two-tailed *t* test was performed, *p* value is shown at last ratio.

Next, binding experiments were performed to demonstrate the functionality of both

binding moieties. To produce larger amounts of TECH2s, HEK293T cells were transduced with TECH2Hi or Me retroviral vectors. After 72 hours, supernatants were harvested, and TECH2 proteins purified by affinity chromatography, diafiltered for further concentration and quantified using a competitive enzyme-linked immunosorbent assay (ELISA) based on 6xHistidine-tag. Concentrations were normalized accordingly, and protein size was checked by western blot **(Fig. 35A).**

Secreted TECH2s bound specifically to target cells expressing the appropriate cognate antigens: TECH2s bound to T cells via their anti-CD3 scFv domains with similar intensity, as the anti-CD3 sequences are identical **(Fig. 35B).** TECH2 Hi bound to both parental MCF7 and MCF10A cells, which express physiological levels of HER2, and to MCF10A overexpressing HER2 with higher intensity **(Fig. 35C).** In contrast, TECH2 Me only bound to MCF10A HER2 cells **(Fig. 35C).** These results demonstrate that TECH2Me discriminates between cells expressing normal levels of HER2 and overexpressing cells. Thus, the addition of TECH2Me to the p95HER2 CAR is expected to increase antitumor efficacy without compromising safety.

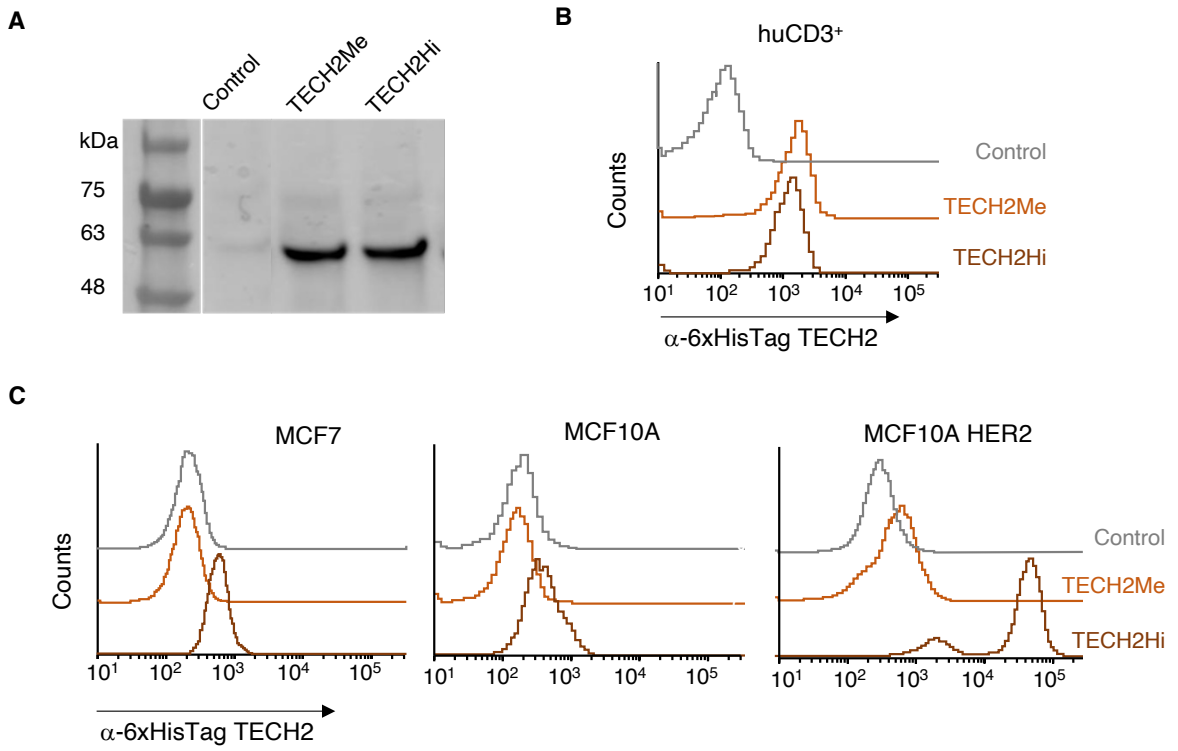

Figure 35: Characterization of the binding affinities of TECH2Hi and TECH2Me

(A) Purified media conditioned by HEK293 transduced with the indicated constructs, tagged with a 6xHis epitope at the C-terminus, were analyzed by Western blot using an anti-His tag antibody. **(B)** Human CD3+ lymphocytes from healthy donors were stained with vehicle (control) or the indicated TECH2s, purified from transduced HEK293 cells, and secondary antibodies. Stained samples were analyzed by flow cytometry and representative histograms from three replicates are shown. **(C)** Same analysis was performed on MCF7, MCF10A and MCF10AHER2 cells.

In addition to its binding capacity, TECH2ME's bystander killing ability, engaging any CD3 positive cell, was demonstrated. Highly pure TECH2ME protein was produced for *in vitro* and *in vivo* assays. MCF7 and PDX433 cells were seeded alone or co-cultured with PBMCs at a 1:1 ratio and increasing concentrations of purified TECH2ME were added to the media **(Fig.36A)**. Results revealed that TECH2ME had no effect on cells expressing basal levels of HER2, regardless PBMCs presence. However, it exhibited potent cytotoxicity against PDX433 cells only in the presence of PBMCs **(Fig.36B).** The observed cytotoxicity correlated with CD3 activation, both in terms of percentage of activated cells **(Fig.36C)** and intensity of activation (MFI) **(Fig.36D),** assessed by flow cytometry using CD25 as a marker. This confirms that TECH2ME alone has no

effect on cells expressing normal HER2 levels, supporting its role as a bispecific T cell engager.

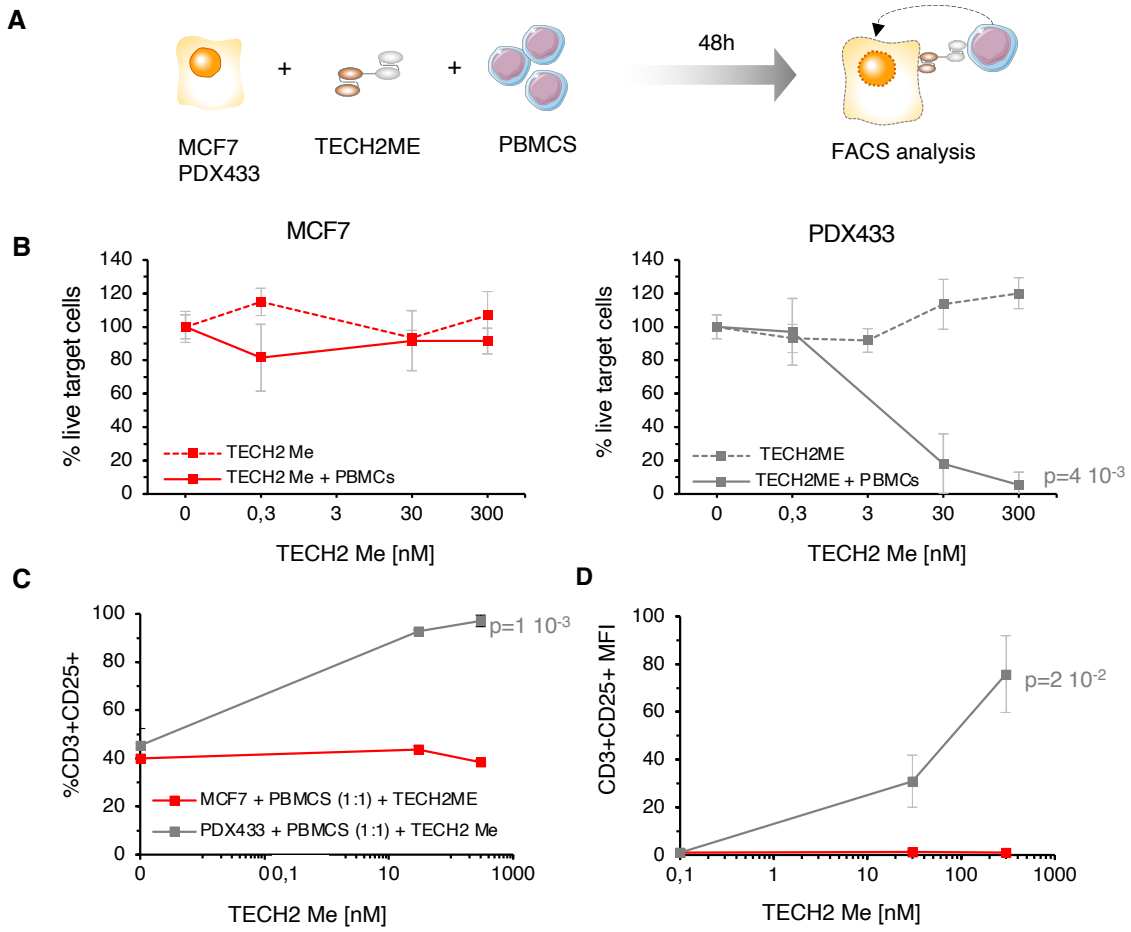

Figure 36: TECH2Me is able to recruit untransduced T cells only against cells overexpressing HER2.

(A) Scheme describing the co-culture experiment. **(B)** Increasing molar concentrations of TECH2Me were added to MCF7 (red) or PDX433 (grey), in the presence (solid line) or absence (dashed line) of PBMCS in a 1:1 target: T cell ratio. **(C-D)** Activation of PBMCS in these co-cultures expressed as percentage of activated cells (C) or Mean Fluorescence Intensity (MFI) (D). Results are represented as averages ± SD (n=3). Statistical two-tailed *t* test was performed, statistically significant *p*-values are shown at last point.

8. Development of p95HER2 CAR T cells secreting TECH2s

8.1. Design of p95HER2.CAR-TECH2 bicistronic vector

Once we characterized the different TECH2 proteins and validated their binding and killing abilities, selecting TECH2Me as the most promising candidate, we proceeded to combine the expression of the p95HER2.CAR and the secretion of TECH2s in the same T cell using a single vector. Similar to TECH2-eGFP constructs, we generated bicistronic vectors by inserting the TECH2Hi or Me encoding DNA sequence after the p95HER2 CAR, separated by a T2A processing site. Both genes are under the control of the constitute LTR retroviral promoter. Therefore, we based transduction efficiency assessment on CAR expression detection by FACS, assuming that both genes would be equally transcribed.

8.2. *In vitro* characterization p95HER2.CAR-TECH2 T cells

We followed the same process as described in the previous section with the newly generated p95HE2.CAR -TECH2 vectors **(Fig.37A).** Briefly, we retrovirally transduced human PMBCS with empty (UTD), p95HER2.CAR-TECH2Hi or Me vectors, determined transduction efficiencies **(Fig.37B)** and co-cultured them with target cells expressing different levels of HER2 and p95HER2 at different ratios. Once again, we observed that p95HER2.CAR-TECH2 Me did not target MCF7 cells, contrary to p95HER2.CAR-TECH2 Hi, but both were able to target PDX 433 **(Fig.37C).** An identical result was observed in co-cultures with parental or HER2 overexpressing MCF10A cells **(Fig. 37D).**

This indicated that, not only as individual elements, p95HER2 CAR and TECH2Me, but the combination of them, did not target cells expressing normal levels of HER2, but were very effective at killing cells overexpressing the two target antigens, HER2 and p95HER2.

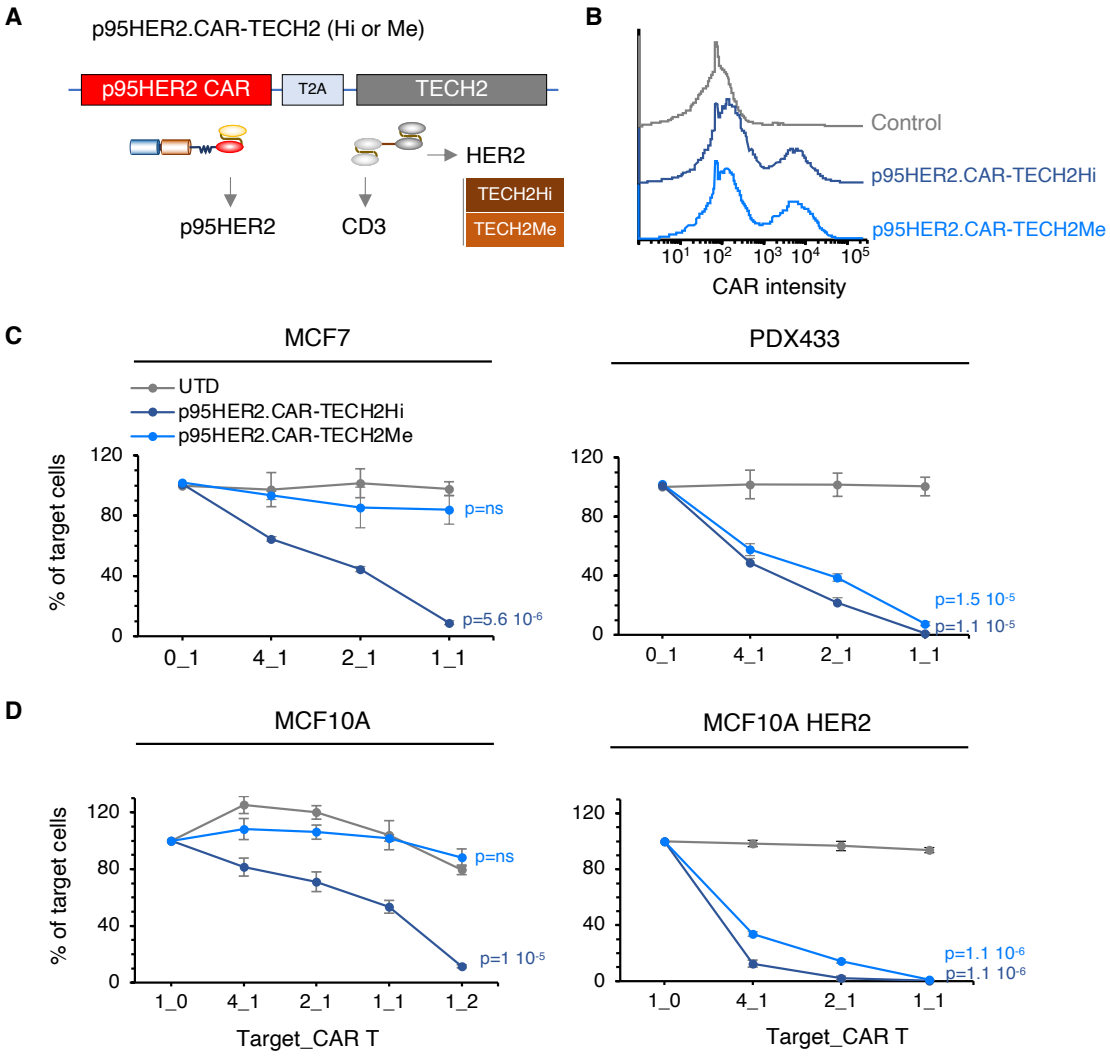

Figure 37: Effects of T cells expressing p95HER2 CARs and TECH2s on different cell lines

(A) Simplified scheme of bicistronic pMSGV1-based vectors, containing the p95HER2 CAR and the TECH2 Hi, Lo or Me encoding genes, separated through a T2A. **(B)** Transduction efficiency assessed by CAR expression using flow cytometry. **(C)** Parental MCF7 cells or cells from the HER2/p95HER2-positive PDX433 were co-cultured with UTD T cells or p95HER2.CAR-TECH2 Hi or Me T cells different ratios. Then, flow cytometry was employed to quantify viable target cells, with EpCAM serving as a marker. Results are expressed as averages of three independent experiments. **(D)** Same co-culture experiment was performed using the non-transformed MCF10A cell line alongside the same cells overexpressing HER2. Results are represented as averages ± SD (n=3). Statistical two-tailed *t* test was performed, statistically significant *p*-values are indicated in the highest ratio.

8.3. Bystander effect of TECH2Me secreted by p95HER2.CAR-TECH2Me T cells

When secreted by T cells, it is conceivable that a portion of the TECH2s remains bound to transduced T cells, while another portion is secreted and could bind to non-transduced T cells. Analysis of the media conditioned by human lymphocytes transduced with the p95HER2.CAR-TECH2Me revealed the accumulation of soluble TECH2Me during expansion **(Fig.38A)**, analyzed using an anti-His ELISA.

To assess if TEHC2s secreted by p95HER2 CAR T cells could activate bystander T cells, p95HER2.CAR-TECH2Me was co-cultured with PDX433 cells, resulting in the activation of both transduced and non-transduced T cells **(Fig.38B).** In contrast, co-culture of p95HER2 CAR T with PDX433 did not activate untransduced T cells. TECH2Hi secreting T cells were used as a control for activation against MCF7 cells, confirming the lack of activity of TECH2Me on cells expressing normal levels of HER2. We did not observe activation of bystander nor p95HER2.CAR-TECH2Me transduced T cells in the presence of MCF7 cells **(Fig.38B).**

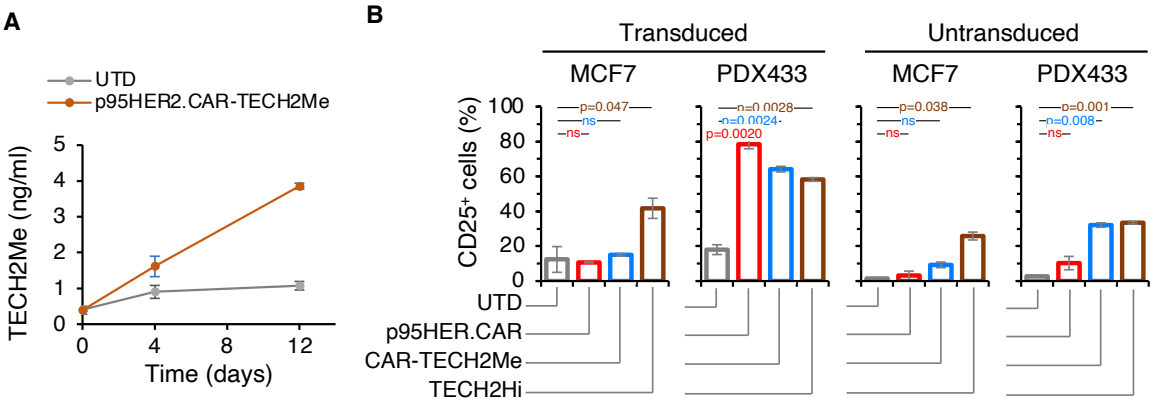

Figure 38: Assessment of TECH2Me bystander effect.

(A) ELISA quantification of unbound TECH2Me secreted by p95HER2.CAR-TECH2Me T cells, cultured at 1x10^{6}cells/ml **(B)** P95HER2.CAR-TECH2Me, p95HER2 CAR or TECH2Hi T cells were co-cultured with PDX433 or MCF7 cells at 1:1 ratio, for the assessment of transduced or untransduced T cell activation (%CD25) by FACS. Results are represented as averages ± SD (n=3). Statistical two-tailed *t* test was performed, statistically significant *p*-values are indicated.

8.4. Safety assessment of p95HER2.CAR-TECH2Me: effect on cells expressing normal levels of HER2, compared to HER2 CAR T cells or p95HER2.CAR-TECH2Hi

8.4.1. *In vitro*: effect on healthy cardiomyocytes & small airway epithelial cells

To further support the safety of our T cell therapy, we analyzed its effect on healthy cardiomyocytes and primary lung cells, specifically small airway epithelial cells (hSAEpC). These cell types are known targets of anti-HER2 therapies, which are often associated with undesired toxicities. Both primary cell cultures expressed HER2, albeit at different levels **(Fig.39A).** TECH2Hi stained human cardiomyocytes **(Fig.39B)** and cells from the small airway epithelium **(Fig.39C),** whereas TECH2Me did not bind to either of them. When testing the killing effect, HER2.CAR T cells consistently targeted both cardiomyocytes and lung cells, as reported in the clinic. In contrast, and indicative of their safety, T cells expressing p95HER2.CAR-TECH2Me showed no detectable effect **(Fig.39D, E).**

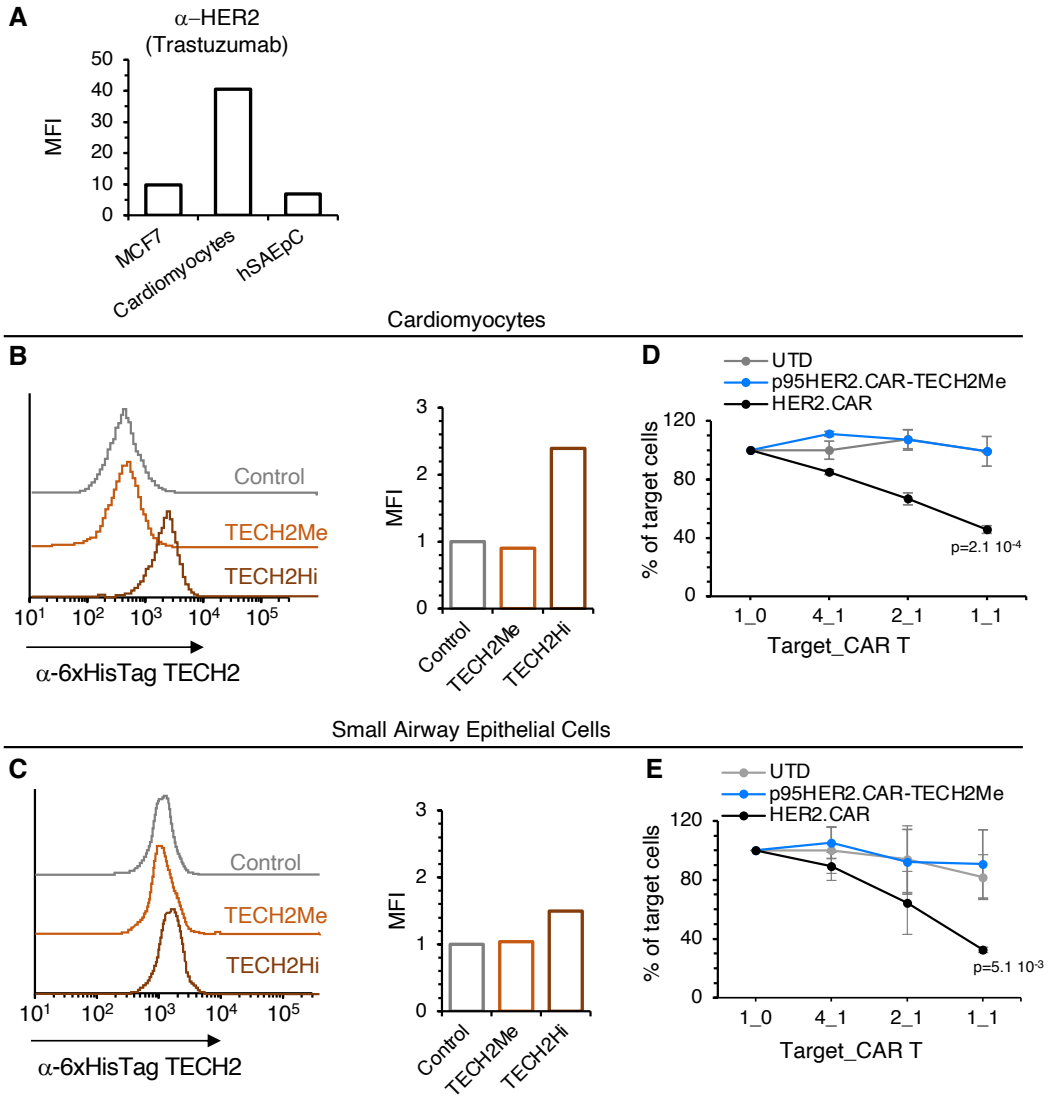

Figure 39: Toxicity assessment on cardiomyocytes and lung cells from primary culture origin

(A) Levels of HER2 quantified by flow cytometry using trastuzumab as an anti-HER2 antibody, presented as Median Fluorescence Intensity (MFI) normalized to the isotype staining of each primary cell culture. **(B-C)** Representative histograms (left) and relative MFI values (right) illustrating binding of the indicated TECH2s to human cardiomyocytes (B) and human small airway epithelial cells (hSAEpC). **(D-E)** Cardiomyocytes and hSAEpC were co-cultured with UTD T cells, p95HER2.CAR-TECH2ME or HER2.CAR T at various ratios. The percentage of viable target cells compared to UTD after 48 hours of co-culture was assessed by flow cytometry using CD3-negative selection. Results represent averages from three replicates. A statistical two-tailed t-test was performed, with the p-value indicated in the highest ratio

8.4.2. *In vivo:* effect on MCF7 tumors

Safety of p95HER2.CAR-TECH2Me was also confirmed *in vivo*, using the previously described MCF7 orthotopic model **(Fig.26)**. T cells expressing TECH2Hi, alone or in combination with p95HER2.CAR, efficiently killed MCF7 cells **(Fig. 40A),** whereas T cells expressing TECH2Me, alone or in combination with p95HER2.CAR, had no effect on MCF7 cells **(Fig.40B)**, despite detecting circulating human lymphocytes in mice blood.

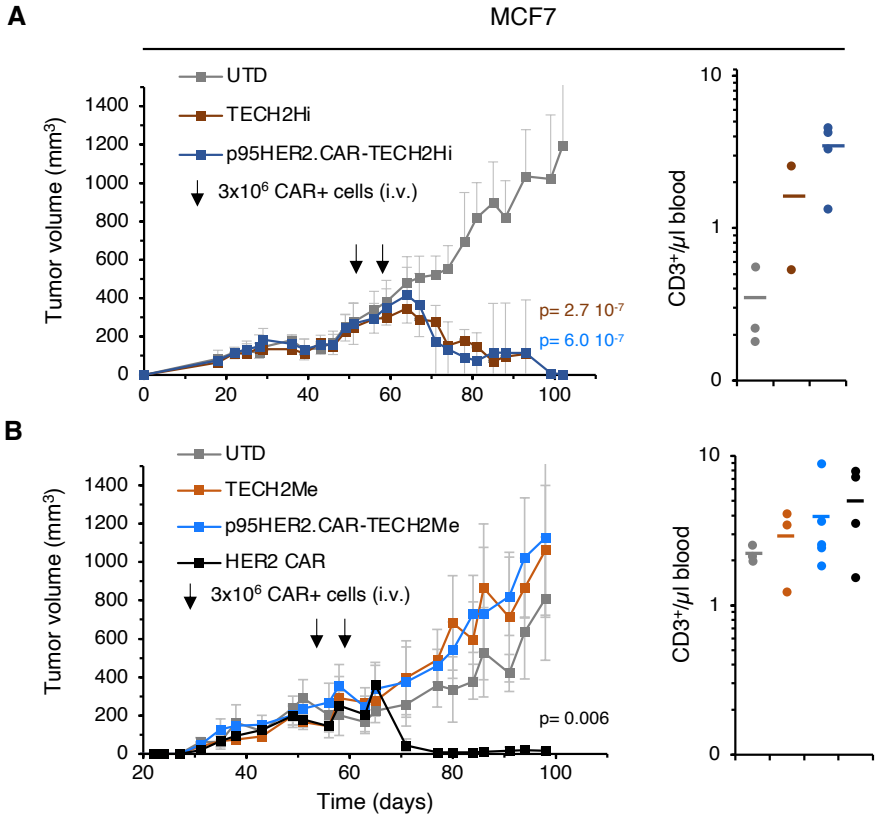

Figure 40: Effect of TECH2s and p95HER2.CAR-TECH2s CAR on MCF7 cells

(A) 3x10^6 T cells transduced with empty vector (UTD), TECH2Hi or p95HER2.TECH2Hi were injected intravenously (arrows) in NSG mice bearing MCF7 breast tumors. Numbers of circulating human CD3+ lymphocytes (right) were analyzed at endpoint and expressed as counts per µl of blood. **(B)** Same experiment and analysis as A but comparing T cells transduced with empty vector (UTD), TECH2Me, p95HER2.TECH2Me and HER2 CAR. A statistical two-tailed t-test was performed in comparison to UTD group, with p-values indicated at the last timepoint when significant.

All *in vitro* and *in vivo* results consistently demonstrated that T cells expressing p95HER2.CAR and/or TECH2Me had no impact on cells expressing normal levels of HER2, including MCF7 BC cells, non-transformed MCF10A breast epithelial cells, cardiomyocytes and normal lung epithelial cells. Consequently, we conclude that this next-generation CAR T is likely to have limited side effects in patients, at least those related with off-tumor HER2 targeting.

9. Antitumoral activity of p95HER2 CAR-TECH2

9.1. Antitumor effect against orthotopic BC PDXs

To further assess efficacy of p95HER2.CAR-TECH2Me *in vivo*, we used different BC HER2- and p95HER2-positive PDXs. IHC analysis of both antigens is shown in **Fig.41A.**

In the first PDX, PDX667, we demonstrated the advantage of dual targeting versus single targeting: we observed partial effects of p95HER2 CAR T cells or TECH2Me T cells, but p95HER2.CAR-TECH2Me resulted in complete responses in all treated mice **(Fig.41B).** Circulating human CD3 levels were also higher in the armored CAR T cell group **(Fig.41B-rigth)** and all the treated mice remained tumor-free for almost 100 days **(Fig.42A).**

PDX67, which is partially resistant to second-generation p95HER2 CAR T cells **(Figs.29, 30),** showed sensitivity, albeit limited, to T cells expressing TECH2Me. Again, p95HER2.CAR-TECH2Me showed overall only partial response **(Fig.41C)**, although two out of four mice achieved complete and durable responses, and the other two initially responded but ultimately relapsed **(Fig.42B).** For unknown reasons, this PDX models seem to be very resistant to T cell redirecting therapies targeting p95HER2 and HER2, although we observed a 50% complete response rate.

In the third PDX, PDX433, we also evidenced the superiority of p95HER2.CAR-TECH2ME over TECH2ME alone **(Fig. 41D),** and we observed complete responses in practically all mice, although in one, the tumor, despite significant response, did not completely disappear at the time of endpoint **(Fig.42C).**

Thus, in the three PDXs tested, p95HER2.CAR-TECH2Me Ts had a remarkable antitumor activity and in most individual cases the responses were complete.

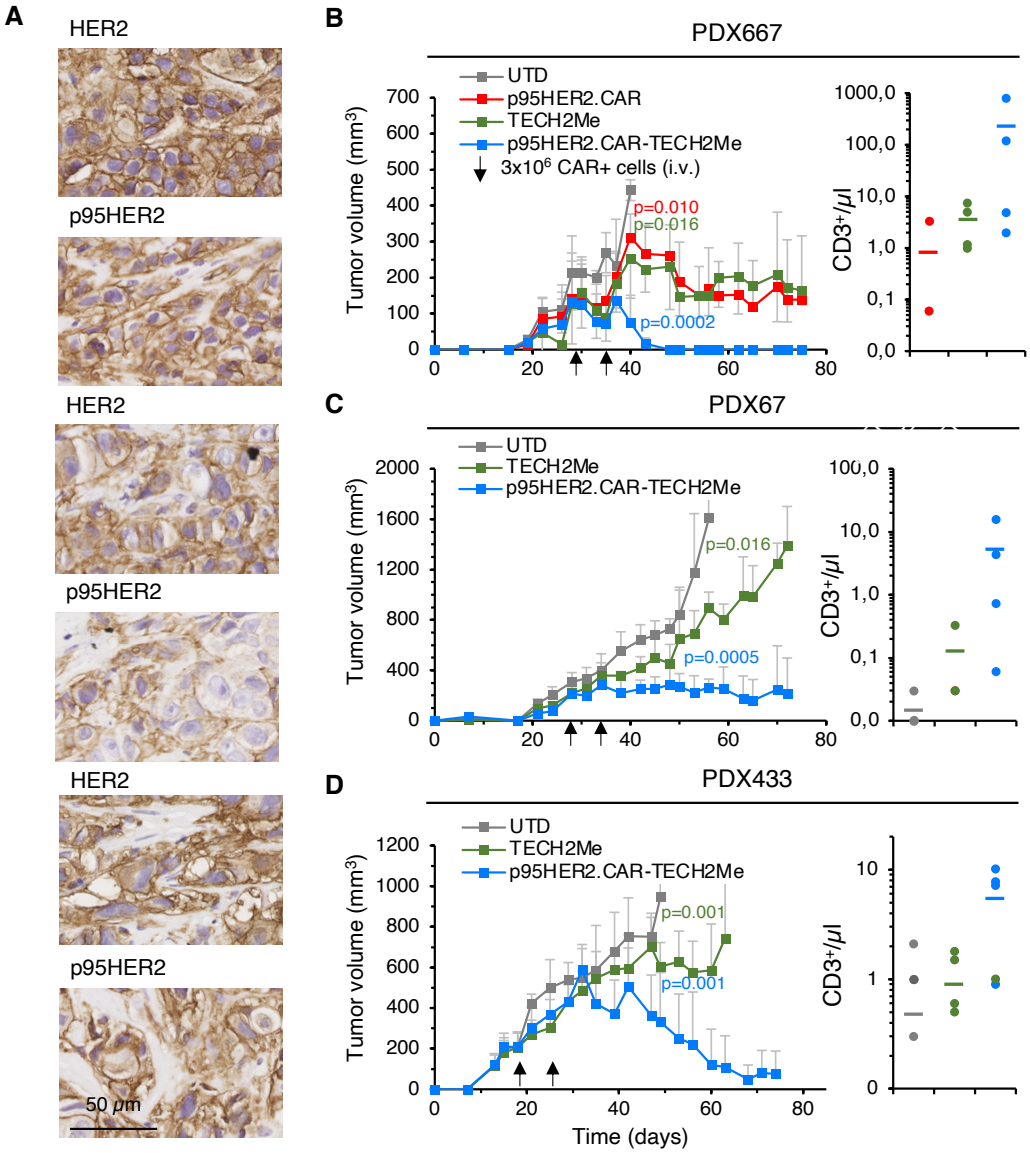

Figure 41: Efficacy of T cells expressing p95HER2 CARs and TECH2s of high and medium affinity.

(A) Immunohistochemical analysis of HER2 and p95HER2 expression on samples from the indicated PDXs. **(B-D)** The indicated PDXs were engrafted into the mammary fat pads of NSG mice. At the time points indicated by the arrows, $3x10^6$ T cells expressing control T cells expressing vector (UTD), or the indicated factors were injected i.v. Tumor volumes are represented as averages ± SD (n=4 per arm). At the end of the experiment, the numbers of human lymphocytes were analyzed and expressed as number of $CD3^+$ cells per µl of blood. A statistical two-tailed t-test was performed in comparison to UTD group, with significant p-values indicated in the graphs. UTD: untransduced T cells; i.v.: intravenous administration Is in the lateral tail vein.

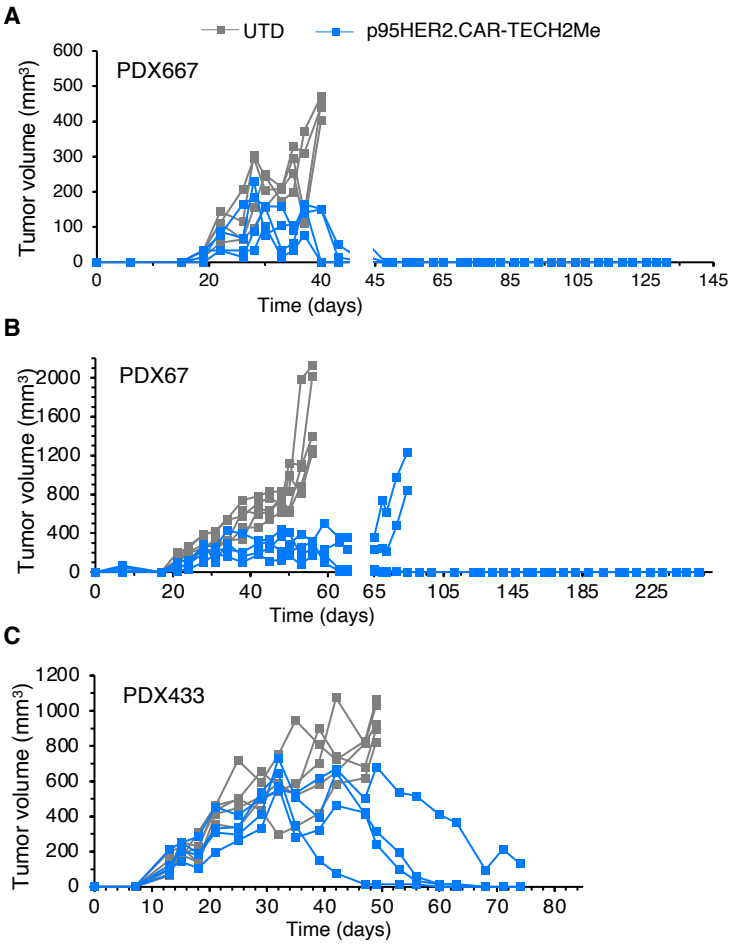

Figure 42: Growth curves of individual tumors shown in Figure 45

(A,B,C) Previous figure (Fig.40) Individual tumor volume curves from UTD (grey) and p95HER2.CAR-TECH2ME (blue) from the indicated PDXs. UTD: untransduced T cells.

9.2. Dual flank experiment: assessment effectivity and safety balance

To further support that, even when p95HER2.CAR-TECH2Me Ts are activated by the presence of HER2-amplified/p95HER2-positive tumor cells, they do not affect cells expressing normal levels of HER2, we engrafted MCF7 and PDX433 cells, in opposite mammary glands of the same mouse. Once both types of tumors reached a readily detectable volume, we treated mice with control T cells transduced with empty vector, T cells expressing p95HER2.CAR-TECH2Me or, as a control, with T cells expressing the HER2.CAR **(Fig.43A)**. As expected, HER2.CAR T cells efficiently killed both types of tumors. In contrast, T cells expressing p95HER2.CAR-TECH2Me did not have any effect on MCF7 tumors **(Fig.43B).**

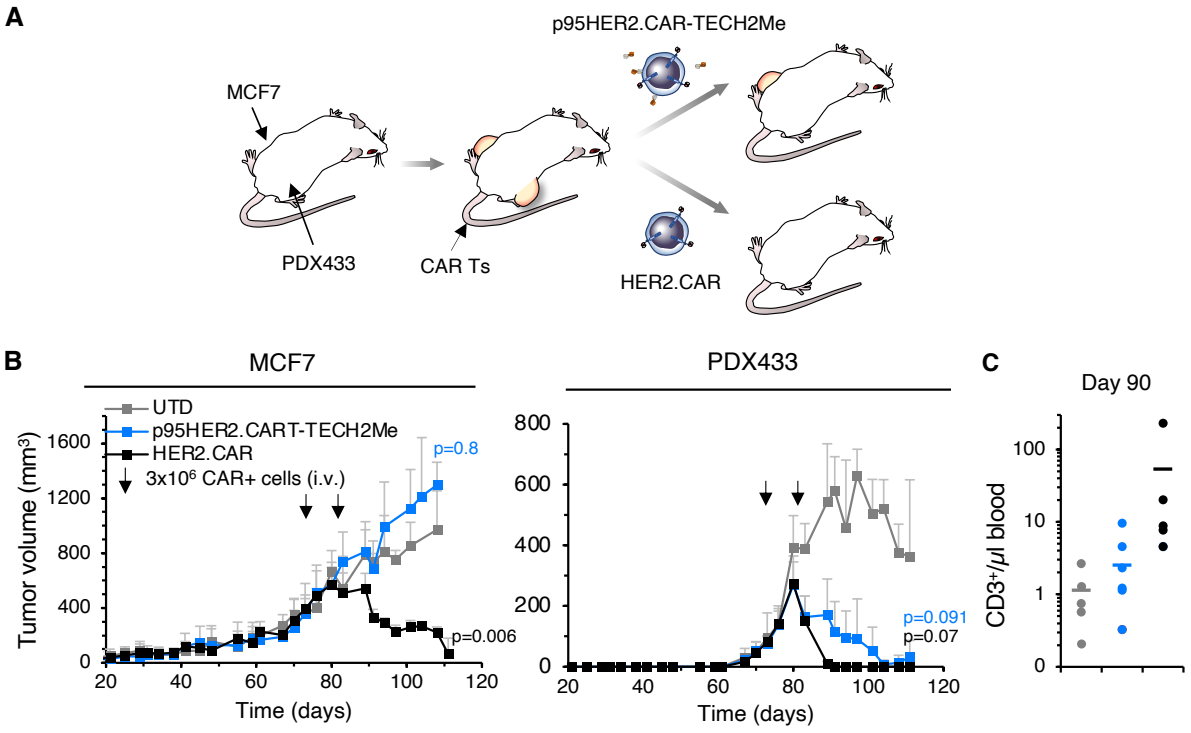

Figure 43: Dual flank experiment demonstrates balance between effectivity and safety of p95HER2.CAR-TECH2Me

(A) Schematic showing the experimental setting: MCF7 or PDX433 cells were engrafted into opposite mammary fat pads of NSG mice. When tumors reached 200-400 mm³, mice were treated with the indicated CAR T cells. Expected outcomes in terms of antitumor activity are drawn. **(B)** Tumor volumes of each flank are represented as averages ± SD (n=5 per arm). Statistical two-tailed *t* test was performed, *p* value at last timepoint is shown. **(C)** At the end of the experiment, the numbers of human lymphocytes were analyzed and expressed as number of $CD3^+$ cells per µl of blood. Average values are represented with horizontal lines. UTD: untransduced T cells; i.v.: intravenous administration Is in the lateral tail vein.

9.3. p95HER2.CAR-TECH2Me effectivity against PDX-derived lung tumors

The p95HER2.CAR-TECH2Me was also far more effective than the second-generation p95HER2.CAR on lung metastases caused by cells from the p95HER2 and HER2-positive PDX433 expressing luciferase (**Fig.44A-C**). Unexpectedly, in these mice we also observed the generation of tumors at the site of injection, in the tail vein **(Fig.44D, E)**, but they were also efficiently targeted by second-generation p95HER2 CAR T or p95HER2.CAR-TECH2Me, further supporting the efficacy of these CAR T cells,

particularly the latter one, on tumors located in different organs.

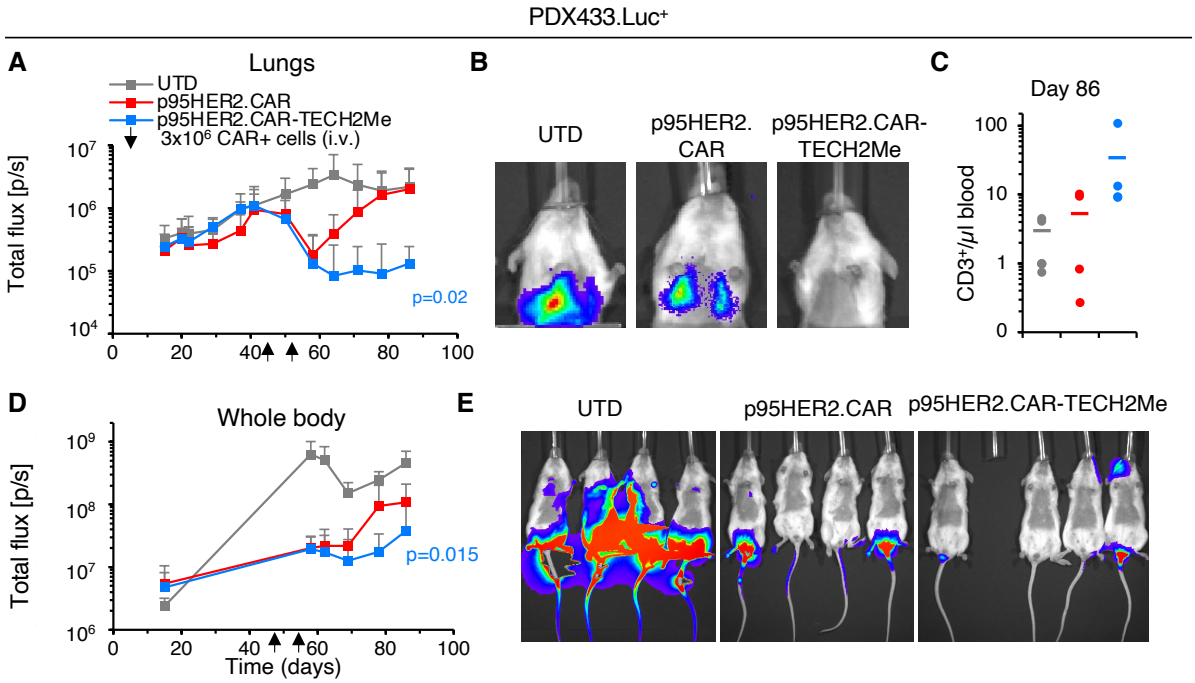

Figure 44: Activity of p95HER2.CAR-TECH2Me against lung and tumors

(A) PDX433 derived cells expressing luciferase were injected in the tail vein of NSG mice. After two weeks, lungs tumors were evident by assessing bioluminescence. Mice were treated with $3x10^6$ UTD, p95HER2 CAR T cells or p95HER2.CAR-TECH2ME T cells at the timepoint indicated by the black arrows. **(B)** Representative images taken at the end of the experiment. **(C)** Circulating human lymphocytes were analyzed and expressed as number of $CD3^+$ cells per μl of blood. **(D-E)** Whole-body bioluminescence from the animals was measured at the indicated time points and images at endpoint are shown. Results are expressed as averages ± SD (n=3-4 per group). Statistical two-tailed *t* test was performed, significant *p* values at last timepoint is shown. UTD: untransduced T cells; i.v.: intravenous administration Is in the lateral tail vein.

9.4. Characterization of p95HER2.CAR-TECH2Me cells generated from a BC patient's PBMCs

Scientific studies of CAR T cells often use cells derived from PBMCs from healthy donors because of their accessibility and consistency. However, we wanted to evaluate the functionality of a CAR T cell derived from a BC patient. Specifically, we obtained PBMCs from a 44-year-old woman who had been diagnosed with luminal B HER2-positive BC and was in partial response to chemotherapy. T cells from this volunteer

patient were transduced and screened in parallel with T cells from a healthy donor.

The patient's T cells transduced less than the healthy donor T cells, both in percentage and intensity **(Fig.45A, B),** which could be simply attributed to donor variability, independently of the health status. In terms of expansion capacity, both proliferated at the same rate in IL-2 supplemented media **(Fig.45C).** Importantly, specificity and potency were equivalent between the two donors in terms of killing capacity against MCF7 and PDX433 cells **(Fig.45D),** although higher T cell activation measured by CD25 expression was observed in the co-culture of healthy donor PBMCS with PDX433 **(Fig.45E).**

According to these results, and despite the lower transduction efficiency, both patient and healthy donor T cells exhibit similar expansion and killing capacities, suggesting the feasibility of producing functional p95HER2.CAR-TECH2Me from pre-treated cancer patients based on *in vitro* assessments.

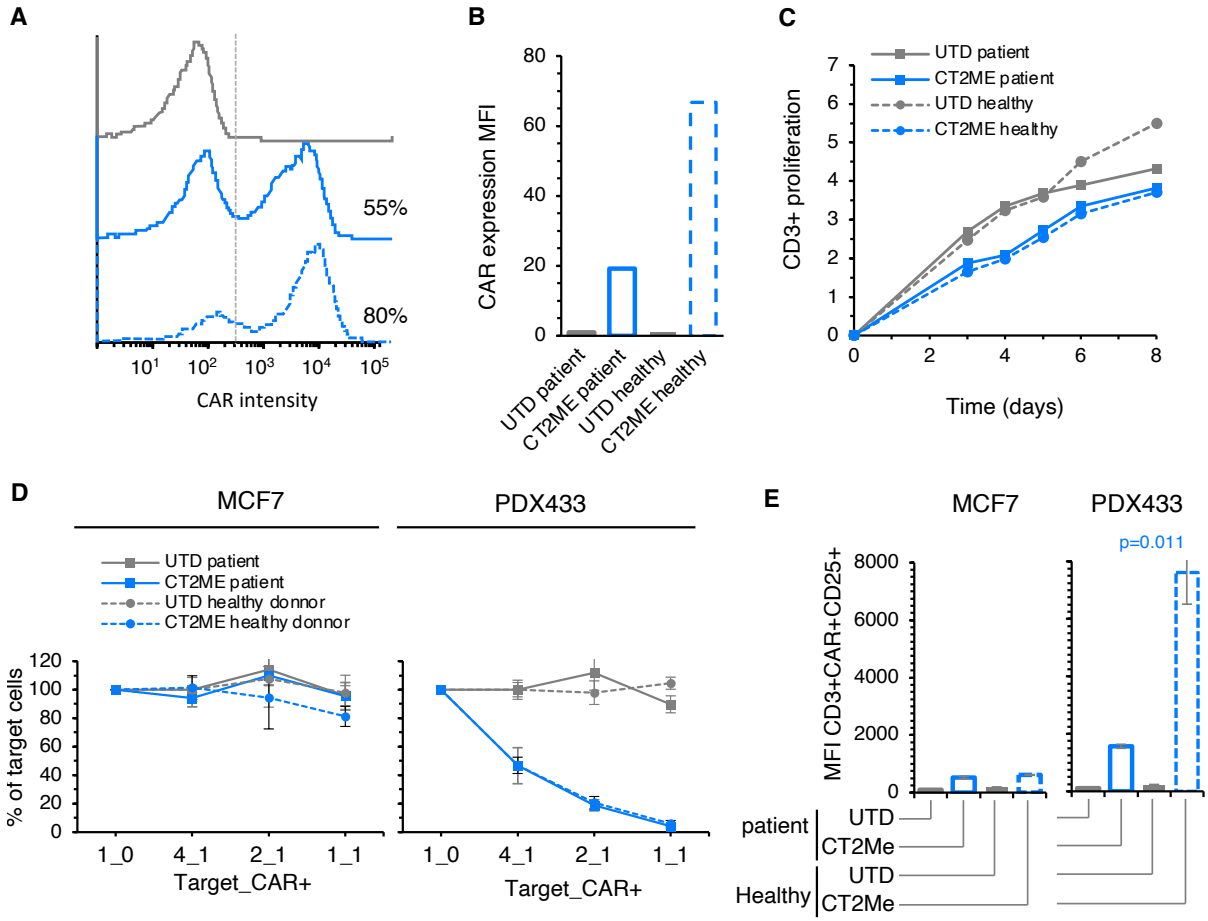

Figure 45: comparative analysis of CAR T cells from a cancer patient and healthy donor. **(A)** Histograms and **(B)** MFI depicting CAR expression levels in patient and healthy donor T cells. **(C)** Proliferation curves of patient and healthy donor T cells under IL-2 supplementation. **(D)** Evaluation of killing capacity and against MCF7 and PDX433 cells. Results are expressed as averages ± SD (n=3). **(E)** T cell activation levels measured by CD3+CD25+ MFI by FACS at 1_1 ratio. Two-tailed t test. Statistics compare healthy versus patient for both UTD and p95HER2.CAR-TECH2Me. Significant p values are shown. CT2Me: p95HER2.CAR-TECH2Me .

10. Antitumor potential of p95HER2.CAR-TECH2Me on HER2-amplified tumors other than BCs

10.1. Evaluation of p95HER2 expression in GC samples

The gene encoding HER2 is amplified in ~15% of esophageal and GCs (source,cBioPortal). Several drugs approved for the treatment of HER2-positive BC, such as, Lapatinib, T-DM1 or the combination trastuzumab/pertuzumab have not shown remarkable efficacy on tumors of the upper gastrointestinal tract [241–243]. Therefore, although trastuzumab-deruxtecan has shown some promising activity, there is a need to develop more effective and safer drugs for these patients.

We were interested in determining the prevalence of p95HER2 among HER2-positive GCs, that could potentially benefit from our therapy. To do so, we performed HER2 and p95HER2 IHC analysis on a HER2-positive GC patient samples TMA **(Fig.46A),** which included samples from 19 patients (cases) collected at Vall D'Hebron Hospital. 7 cases (37%) stained positive for HER2 and, and of the 6 that could be analyzed for p95HER2 expression, 4 were also p95HER2 positive **(Fig.46B)**. Therefore, taking into account the limited sample size, our GC TMA reveals a prevalence of p95HER2 expression among HER2-positive GCs of more than 60%.

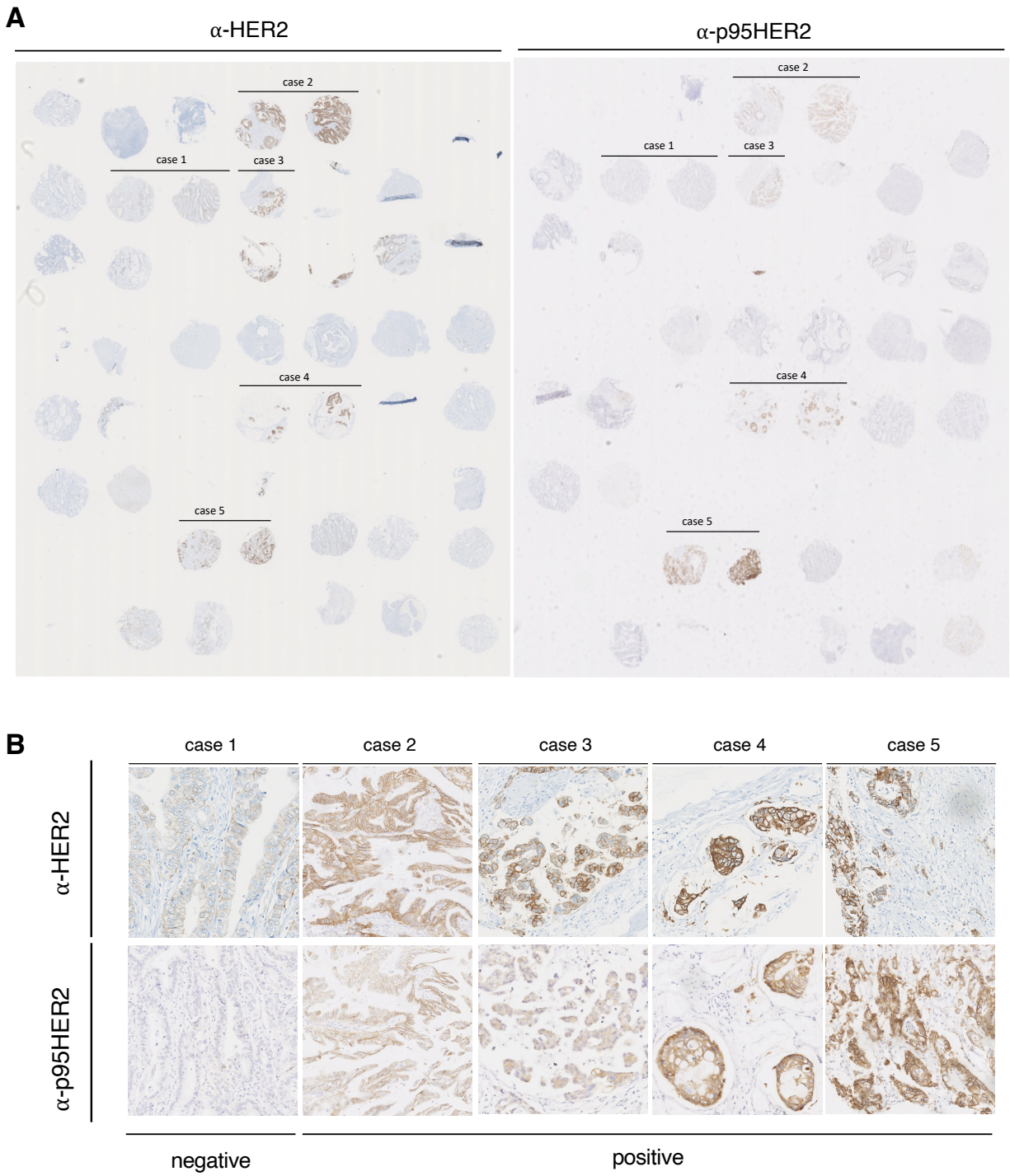

Figure 46: IHC analysis of a HER2-positive GC samples TMA

(A) Images of the HER2 and p95HER2 IHC staining results of the GC TMA, which includes 19 cases, mostly with duplicate samples. **(B)** Selected cases are highlighted in this section with a higher level of amplification, offering a closer view of the IHC staining patterns for HER2 and p95HER2.

10.2. p95HER2 expression in lung, ovarian, gastric, and esophageal cancer cell lines overexpressing HER2

To search for non-breast tumor experimental models in which investigate the effectiveness of p95HER2.CAR-TECH2ME, we quantified the levels of HER2 and p95HER2 in cancer cell lines from different origins. We selected four HER2-amplified cancer cell lines (H2170, lung; SKOV3, ovarian; NCI-N87, gastric; and OE19, gastroesophageal junction) and three non-HER2-amplified cell lines (H1781, lung; COV434, ovarian; MKN45, gastric) as controls.

Total protein levels were assessed through Western Blot analysis using a monoclonal antibody that recognizes the intracellular domain of HER2 **(Fig.47A),** allowing for the detection of both full-length and truncated variants. Band intensities at 185 kDa (HER2) and 100–110 kDa (p95HER2) were quantified and normalized to endogenous beta-tubulin levels **(Fig. 47B).** All cancer cell lines had detectable HER2 protein, with cells expressing elevated full-length HER2 (OE19, NCI-N87, SKOV3, H2170) also showing p95HER2. In cells with low HER2 (MKN45, COV434, H1781), carboxy-terminal fragments of HER2 were undetectable.

Then we proceeded to analyze the surface expression levels of both proteins by FACS using α-HER2 and α-p95HER2 specific antibodies. While surface HER2 aligned with total HER2, p95HER2 did not exhibit an exact linear **(Fig.47C).** Interestingly, p95HER2 and HER2 expression did not follow a linear range **(Fig. 47D),** suggesting that p95HER2 expression is not solely proportional to HER2 overexpression and that unknown mechanisms may contribute to its higher expression in certain cells.

In summary, OE19, NCIN87, SKOV3, and H2170 are considered naturally p95HER2 positive cell lines. Consequently, they serve as valuable experimental models for assessing the effectiveness of our therapy.

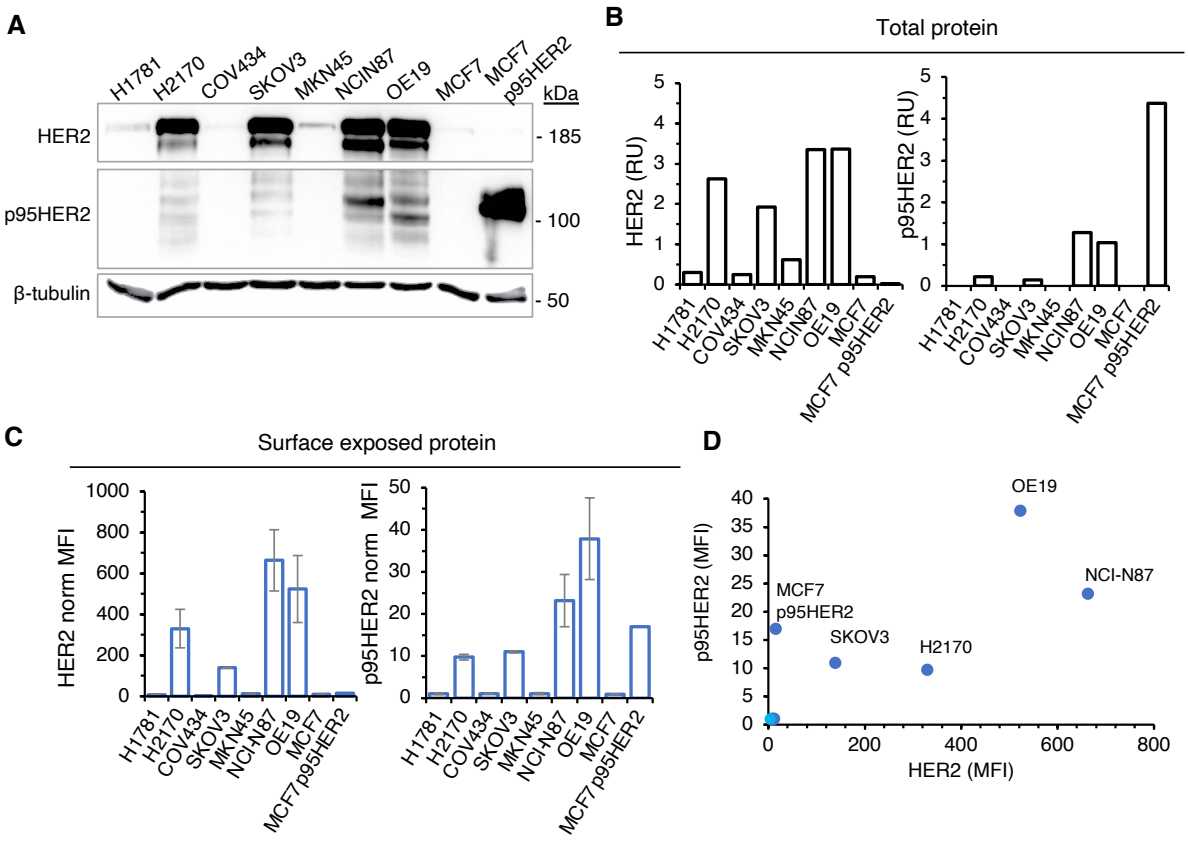

Figure 47: Determination of HER2 and p95HER2 total protein and surface-exposed levels in non-BC cell lines.

(A) Image of western blot analysis stained with an anti-HER2 antibody binding to the intracellular domain in various non-breast human cancer cell lines: H1781 and H2170 (lung); COV434 and SKOV3 (ovarian); MKN45 and NCI-N87 (gastric); and OE19 (gastroesophageal junction). **(B)** Western blot was quantified, normalized to beta-tubulin expression and expressed as relative units (RU). **(C)** HER2 and p95HER2 expression levels were analyzed by flow-cytometry (FACS) in the above-mentioned human cancer cell lines and represented as mean fluoresce intensity (MFI) (isotype subtracted). **(D)** Graph showing the correlation between surface HER2 and surface p95HER2 expression levels by FACS. MCF7 and MCF7 p95HER2 were used as known controls in all assays.

10.3. p95HER2.CAR-TECH2Me cytotoxicity against non-BC cell lines expressing HER2 and p95HER2 *in vitro*

We proceeded to evaluate the antitumor effect of p95HER2.CAR-TECH2Me against the newly identified p95HER2-positive cell lines *in vitro*. Typical co-culture assays results demonstrate that the p95HER2.CAR -TECH2Me is also effective against all of them **(Fig.48).**

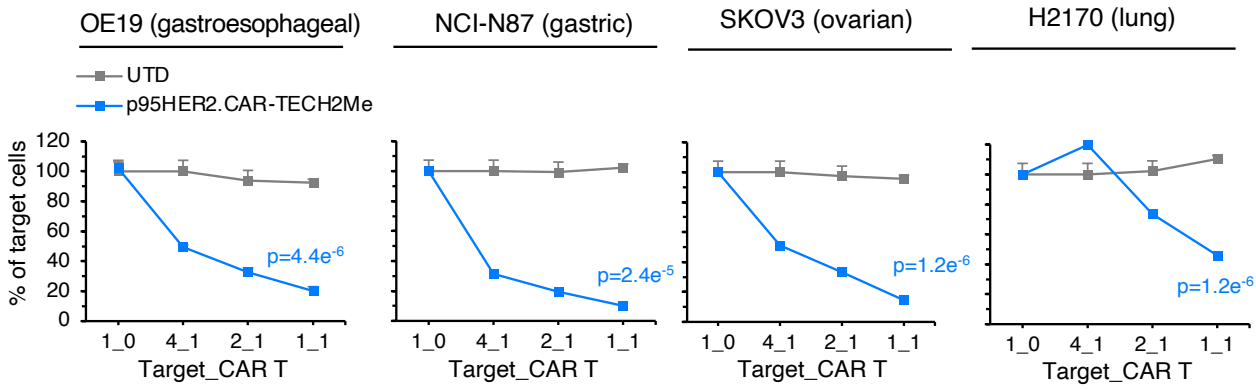

Figure 48: Cytotoxicity of p95HER2.CAR-TECH2Me against four cell lines expressing endogenous levels of p95HER2

The four cell lines identified as p95HER2-positive (OE19, NCI-N87, SKOV3 and H2170) were co-cultured with UTD or p95HER2.CAR-TECH2ME at the indicated ratios. At 48h, viable target cells were assessed by flow cytometry. Representative analyses from one PBMCs healthy donor. N=3 expressed as means ± SD. Two-tailed *t* test was performed and *p* values are shown in the graphs at the last ratio

10.4. p95HER2.CAR-TECH2Me effect against gastric and esophageal cancer cell lines *in vivo*

To test the antitumor potential of p95HER2.CAR-TECH2Me T on these types of cancers *in vivo*, subcutaneous OE19 and NCI-N87 xenografts were used as gastroesophageal and GC models. **Fig.49A, B** show HER2 and p95HER2 positivity of both tumors as determined by IHC staining. p95HER2.CAR-TECH2Me demonstrated remarkable efficacy in both models **(Fig.49C, D),** further supporting the notion that p95HER2.CAR-TECH2Me redirected to cells overexpressing HER2 and p95HER2 may be efficacious independently of the tumor type.

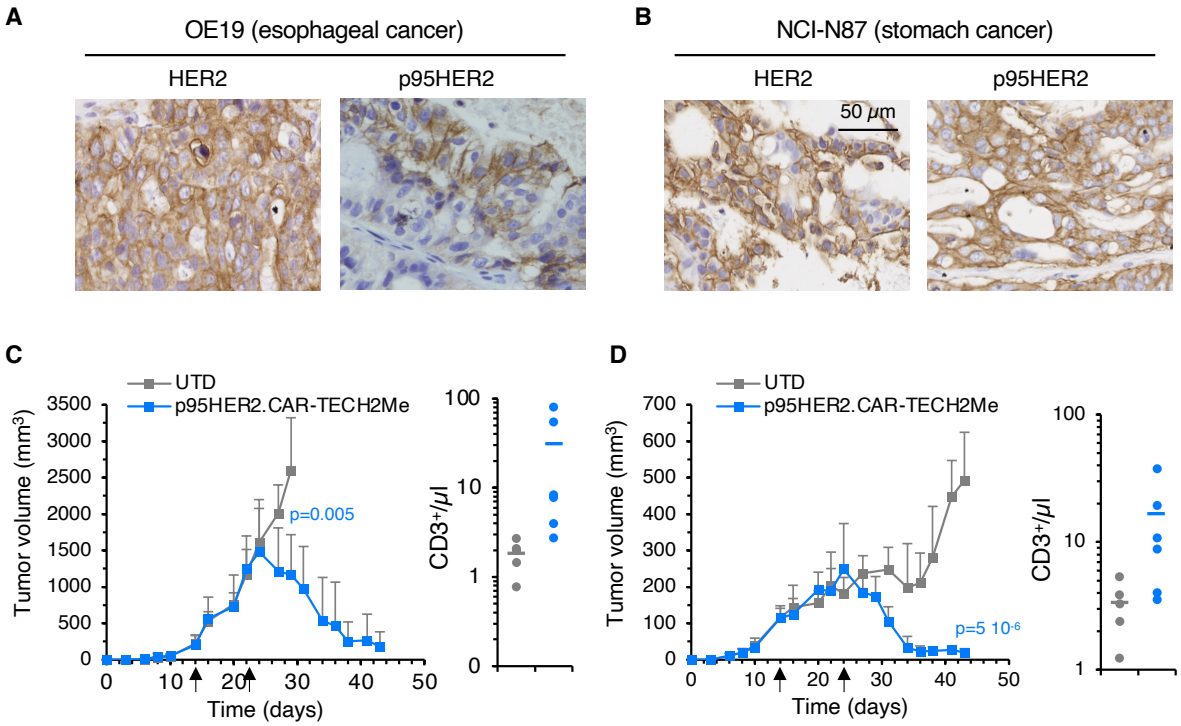

Figure 49: *In vivo* antitumor potential of p95HER2.CAR-TECH2ME against cancers of the upper gastrointestinal tract

(A,B) 5 x 10^5 OE19 (A) or 1 x 10^6 NCI-N87 cells (B) were subcutaneously engrafted into NSG mice. At endpoint, tumors were removed, processed and the levels of HER2 or p95HER2 analyzed by immunohistochemistry with specific antibodies. **(C,D)** When tumors reached around 100 mm3, mice were treated with the indicated CAR T cells. Tumor volumes are represented as averages ± SD (n=5 per arm). Statistical two-tailed t test was performed, p value at last UTD timepoint is shown. At the end of the experiment, the numbers of human lymphocytes were analyzed and expressed as number of CD3+ cells per μl of blood. Average values are represented with horizontal lines

11. Biodistribution of p95HER2.CAR- TECH2Me

CAR T cell therapy differs from the conventional rules of pharmacokinetic studies observed of chemical drugs, as it involves the administration of genetically modified living cells. Unlike chemical drugs that follow predictable metabolic and elimination pathways, CAR T cells expand and persist in the body, eliciting specific immune responses. This unique approach introduces significant challenges in pharmacokinetic assessment, as factors such as proliferation, persistence, and migration of modified cells, along with their interactions with the tissue microenvironment, must be considered. Studying the biodistribution of CAR T cells is of paramount importance and regulatory agencies require a comprehensive evaluation, particularly in cases involving multiple components, as our CAR T therapy, which incorporates both CAR and TECH2ME elements. The complexity arises from the lack of well-defined regulatory guidelines for such dual-component therapies. Our aim was to evaluate the biodistribution of p95HE2.CAR-TECH2ME, by examining both components in different tissues and organs, using specific analytical techniques for each element.

11.1. Half-life of TECH2ME in mouse serum

To assess the antibody's half-life, we injected 325 ng of total TECH2Me in 200 µl PBS intravenously via tail vein injection into NSG immunodeficient mice. At each time point, starting at 15 minutes and ending at 48 hours after dosage, serum samples were obtained from three treated and one untreated, and the remaining TECH2ME levels were analyzed using an anti-His tag ELISA kit, with detection limits ranging from 1ng/ml to 729 ng/ml. The initial concentration drops rapidly, as expected from other BiTEs® with a similar structure and lack of Fc domain. The estimated half-life of TECH2ME is less than 15 minutes **(Fig.50).** After 48 hours, the concentration was around 3ng/ml. As a reference, commonly reported serum concentrations of trastuzumab in the blood serum after clinical administration oscillate between 17,000 to 50,000 ng/ml [244].

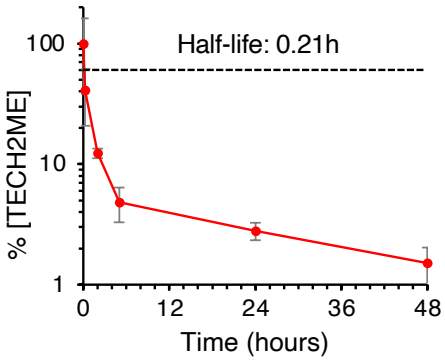

Figure 50: Half-life of TECH2Me

325 ng of purified TECH2Me were injected into NSG mice and serum levels were analyzed by ELISA at the indicated timepoints. Results represent averages of two biological replicates ± SD.

11.2. Biodistribution experimental model and blood analyses

Following the confirmation of its short half-life and the suitability of the kit for detecting serum TECH2ME at very low concentrations, we proceeded to study the distribution of p95HER2.CAR-TECH2Me Ts. We used female and male NSG mice with xenografted with NCI-N87 cells, and three animals of each sex were euthanized per time-point, along with one untreated male and one untreated female.

Despite all previous experiments were performed using a double dose regimen, we decided administer a single dose of $6x10^6$ p95HER2.CAR-TECH2Me Ts to replicate better the clinical scenario, in which p95HER2.CAR-TECH2ME will be given as a single dose in a phase I safety assessment clinical trial. However, although double dose of second-generation p95HER2 CAR T cells showed an advantage over other treatment schedules, p95HER2.CAR-TECH2ME, at least in this model, resulted in complete tumor eradication in all mice **(Fig. 51A),** similar to the double-dose result **(Fig.49)**.

Throughout the experiment, CAR T cells were detectable, displaying an expansion phase that peaked on day 15, coinciding with the complete eradication of all tumors. Following tumor regression, CAR T cell blood levels began to decrease but remained detectable until at least day 30 **(Fig.51B).** In contrast, TECH2 Me was undetectable in the serum fraction at all time points **(Fig.51C).** This finding highlights that the secreted levels of TECH2ME at the intended dose are too low to be detected. Therefore, effects

related to TECH2ME are expected to manifest primarily at the sites where CAR T cells are actively secreting it, rather than in distant sites.

Although not comparable, since TECH2ME is secreted by living cells and not a directly administered antibody, the concentration of TECH2Me is lower than that of other bispecific antibodies targeting HER2 with high affinity in the clinic (i.e., Runimotamab®). This suggests a negligible likelihood of off-tumor side effects associated with TECH2ME and implies that the adverse effects of this therapy will be less pronounced than those observed with other anti-HER2 agents currently in clinical use.

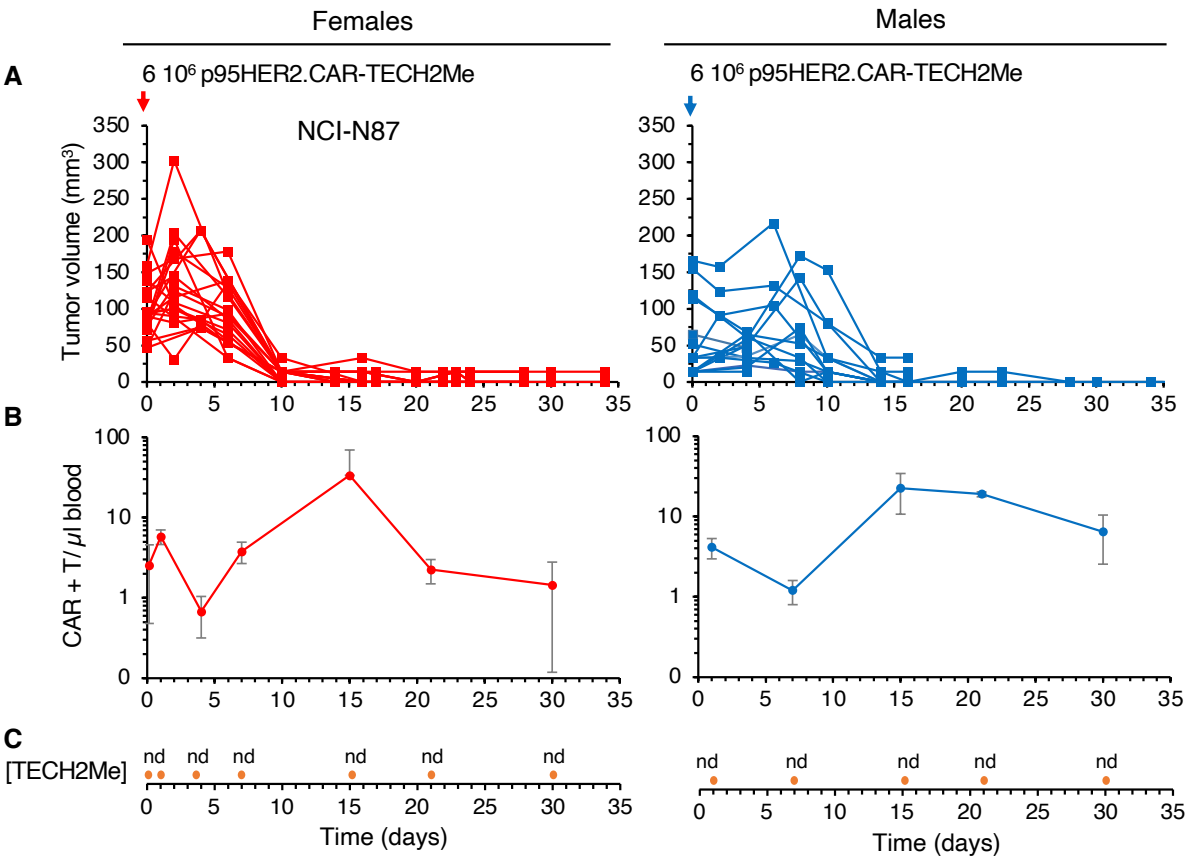

Figure 51: Analysis of tumor volumes and p95HER2.CAR-TECH2Me T cells in blood

(A) NCI-N87 cells were subcutaneously engrafted into female (red) or male (blue) NSG mice as previously described. When tumors reached an average size of ~100 mm3 (day 0), mice were treated intravenously with 6x10⁶ CAR-positive p95HER2.HER2.CAR-TECH2Me T cells and tumor volumes were measured periodically. **(B)** At the indicated time points, blood was withdrawn from mice, and the number circulating p95HER2.HER2.CAR-TECH2Me T cells was analyzed by flow cytometry. Results represent averages of triplicate determinations ± SD. **(C)** A portion of the blood was processed to obtain serum and the concentrations of TECH2Me in sera were analyzed by ELISA. TECH2Me was undetectable in all cases. Nd: not detected

11.3. Analysis of p95HER2.CAR-TECH2Me biodistribution in main organs by flow cytometry

Next, we aimed to detect CAR T cells in different organs using flow cytometry, as this will shape both their antitumoral efficacy and undesired effects. Complete necropsies were conducted on all animals, and the main organs related to metabolism (kidney, liver), immune system (spleen), HER2 targeting derived-toxicities (lung) and CAR T

cells side effects (brain) were processed and freshly analyzed. Tumor infiltration was analyzed when it was detectable and processable. Results are represented as CAR-positive T cell counts per mg of organ **(Fig.52A)** and tumor **(Fig.52B),** categorized by sex.

Based on this data, consistent with the nature of a "living drug" administered into the bloodstream, p95HER2.CAR-TECH2Me T cells exhibited widespread distribution and expansion throughout the body. This holds particular significance for solid tumor treatment, increasing the likelihood of CAR T cells reaching tumor sites, including metastatic locations, and effectively exerting their antitumor effects. Although absolute CAR T cell counts in the tumor were lower compared to the spleen, liver, and lungs, the fold expansion within the tumor proved to be the most relevant, peaking at day 15, the time when tumors achieved complete response **(Fig.51A).** It is reasonable to not observe significant infiltration in the brain because it is a less immunogenic site, and the blood-brain barrier (BBB) further restricts the entry of immune cells into the brain. Additionally, since there are no tumors in this region, a substantial expansion of CAR T cells was not anticipated. As expected, TECH2ME was neither detected in tissues samples showing the highest CAR T cell infiltration, spleen and lung at day 15, in p95HER2.CAR-TECH2ME treated mice (data not shown), analyzed by ELISA.

Notably, various studies, including our own observations, underscore the complexity and limited understanding of CAR T cell biodistribution, with significant infiltration observed in organs such as the spleen, lungs and liver [245].

We have previously shown that p95HE2-CAR-TECH2Me lacks cytotoxic effects on primary cultures of normal small airway epithelial cells. While similar investigations with splenocytes, hepatocytes, and renal cells may be considered desirable, it is crucial to note that the safety profiles of p95HER2.CAR, TECH2Me, and the combined therapy, have been thoroughly validated in preceding sections.

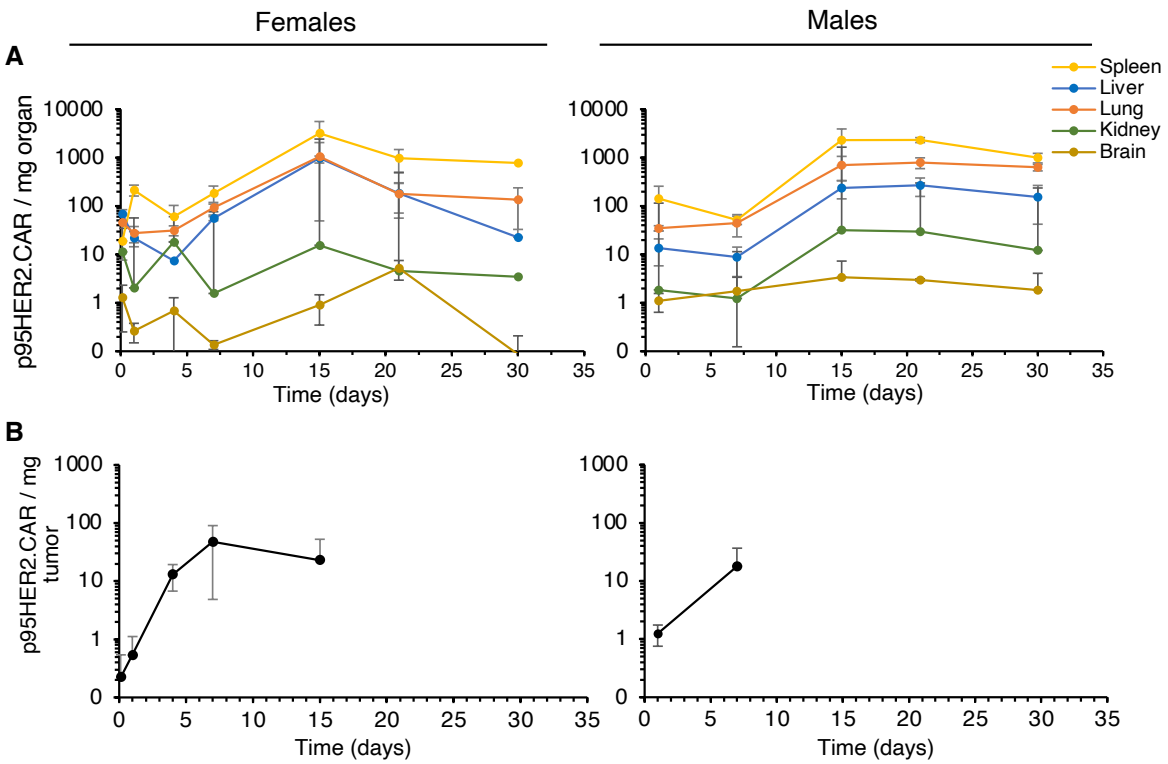

Figure 52: Biodistribution of p95HER2.CAR – TECH2Me in relevant organs

(A) At the indicated time points, three mice were euthanized from the females (left) or male (right) groups. From each animal, spleens, liver, lung, kidney and brain were processed and p95HER2.HER2.CAR-TECH2Me T cell counts analyzed by flow cytometry. **(B)** when tumors were processable, p95HER2.HER2.CAR-TECH2Me T cells were analyzed as in A. Results are expressed as average of three replicates ± SD

11.4. Comparison between females and males

When comparing the results from males and females, despite differences that can be expected due to the technical complexity of the experimental design and organ processing, the overall differences are not significant **(Fig.53).** Therefore, it can be concluded that there were no significant sex differences observed in terms of the antitumor effect and biodistribution of p95HER2 CAR TECH2ME.

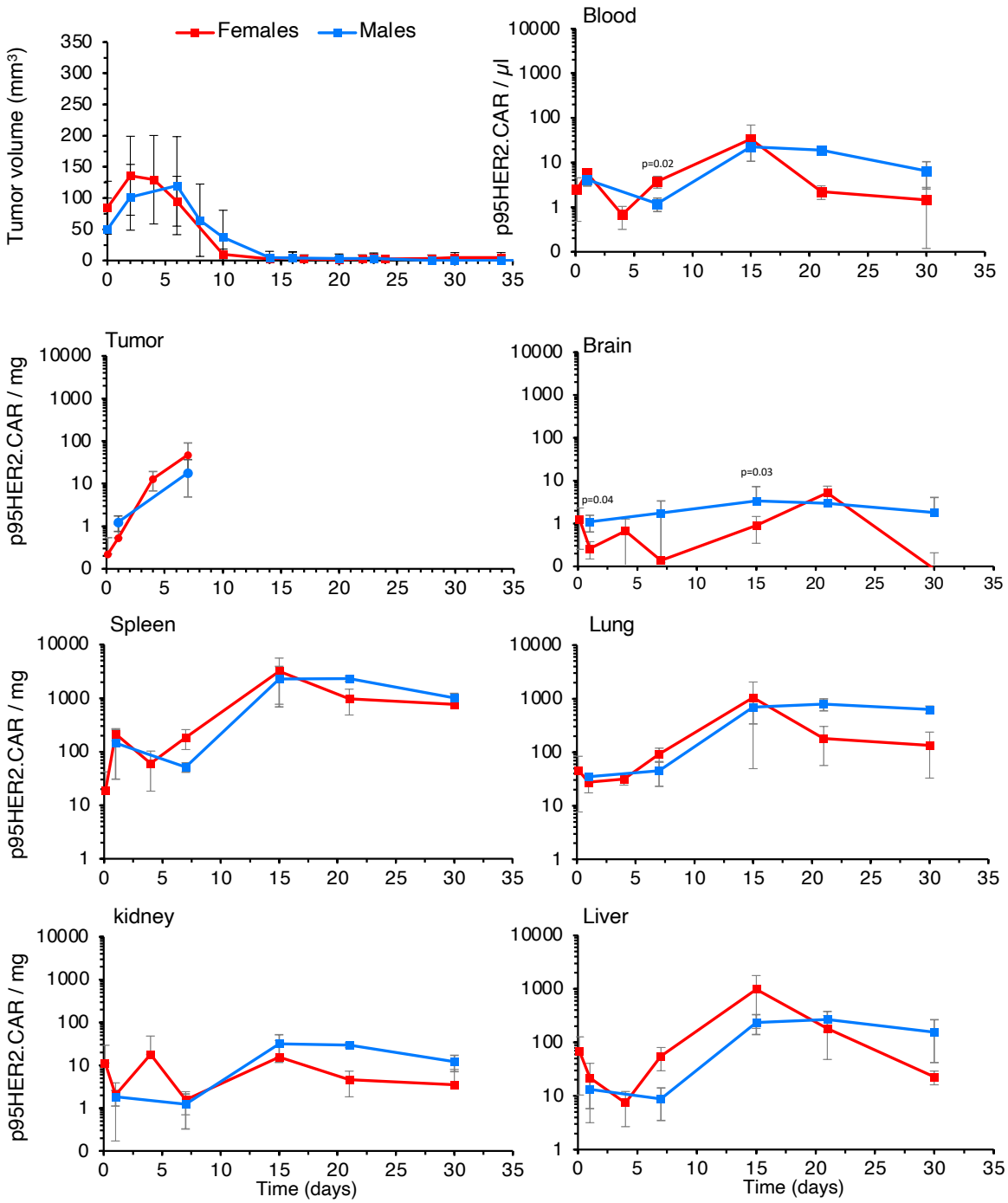

Figure 53: Gender comparison of biodistribution of p95HER2.CAR-TECH2 Me

Comparison between females and males after p95HER2.CAR-TECH2ME administration in antitumor responses, blood levels, tumors infiltration and organ biodistribution of CAR+ cells (brain, spleen, lung, kidney, liver). Results expressed as average of three replicates ± SD

12. GMP manufacturing of p95HER2.CAR-TECH2Me for a phase I clinical trial

A critical step in bringing a CAR T-cell product to the clinic is to optimize scale-up and production under Good Manufacturing Practices (GMP) conditions. There are significant differences between preclinical manufacturing and the GMP-compliant manufacturing processes employing a closed system, such as the CliniMACS Prodigy® platform. This adherence to closed-system procedures minimize the risk of contamination and maintains the sterility required for GMP compliance. Therefore, this transition requires careful consideration and adaptation of methodologies to meet the stringent regulatory requirements, to ensure consistent and high-quality production of CAR T cells, and to demonstrate functional equivalence of the final product. In the concluding section of this thesis, we examine these differences and assess the comparability of the two products.

The scale-up of retrovirus production will not be discussed in this thesis in order to focus fully on CAR T cell production. However, it is important to acknowledge that regulatory compliant retrovirus production is equally important and has been extremely challenging.

12.1. Differences between preclinical and clinical production

Our typical preclinical production process begins with the isolation of peripheral blood mononuclear cells (PBMCs) from whole blood or concentrated buffy coats from healthy donors, using centrifugation with a ficoll gradient, in a conventional biosafety cabinet. Typically, these cells are cryopreserved and thawed two days prior to transduction. During this phase, T cells are activated using magnetic beads coated with anti-CD3/CD28 stimulating antibodies in media supplemented with 10% fetal bovine serum (FBS) and IL-2. It is important to note that no CD4 or CD8 selection was performed in any of the experiments presented in this thesis. After 48 hours of activation, magnetic beads are removed, and the T cells are centrifuged with retrovirus on retronectin-coated plates, a protein used to co-localize T cells and viral particles for increasing

transduction yields. After 2 days, CAR T cells are harvested from plates, transferred to flasks, and allowed to expand for 7-10 days, with periodic replenishment of media containing IL-2, until freezing. Cryopreservation of the finished product (FP) employs serum-free CS10 Cryostor® medium, which contains 10% of dimethyl sulfoxide (DMSO), and regular cryogenic vials.

On the other hand, the clinical-grade manufacturing process initiates with a patients' leukapheresis in an authorized hospital environment under GMP guidelines. After leukapheresis, the collected cells undergo magnetic separation of CD4+ and CD8+ T cells in the controlled environment of a clean room using the CliniMACS Prodigy® system and will remain in this closed system until the end of production.

After isolation of CD4/CD8 T cells, they are activated using a serum-free medium, known as TexMACS®, supplemented with TransAct®, a colloidal polymeric nanomatrix conjugated to humanized CD3 and CD28 agonists. The transduction process then takes place in suspension, facilitated using Vectofusin®, a transduction enhancer that ensures efficient gene delivery to the T cells. Then, transduced T cells are expanded in in TexMACS® medium supplemented with GMP-grade cytokines with medium changes and occasional agitation for 7-10 days. The FP is cryopreserved in CryoMACS® freezing bags in Plasmalyte, a clinically approved solution for perfusion, supplemented at 5% w/v with human serum albumin (HSA) and at 10% DMSO. The main differences between preclinical and clinical-grade production are illustrated in **Fig.54.**

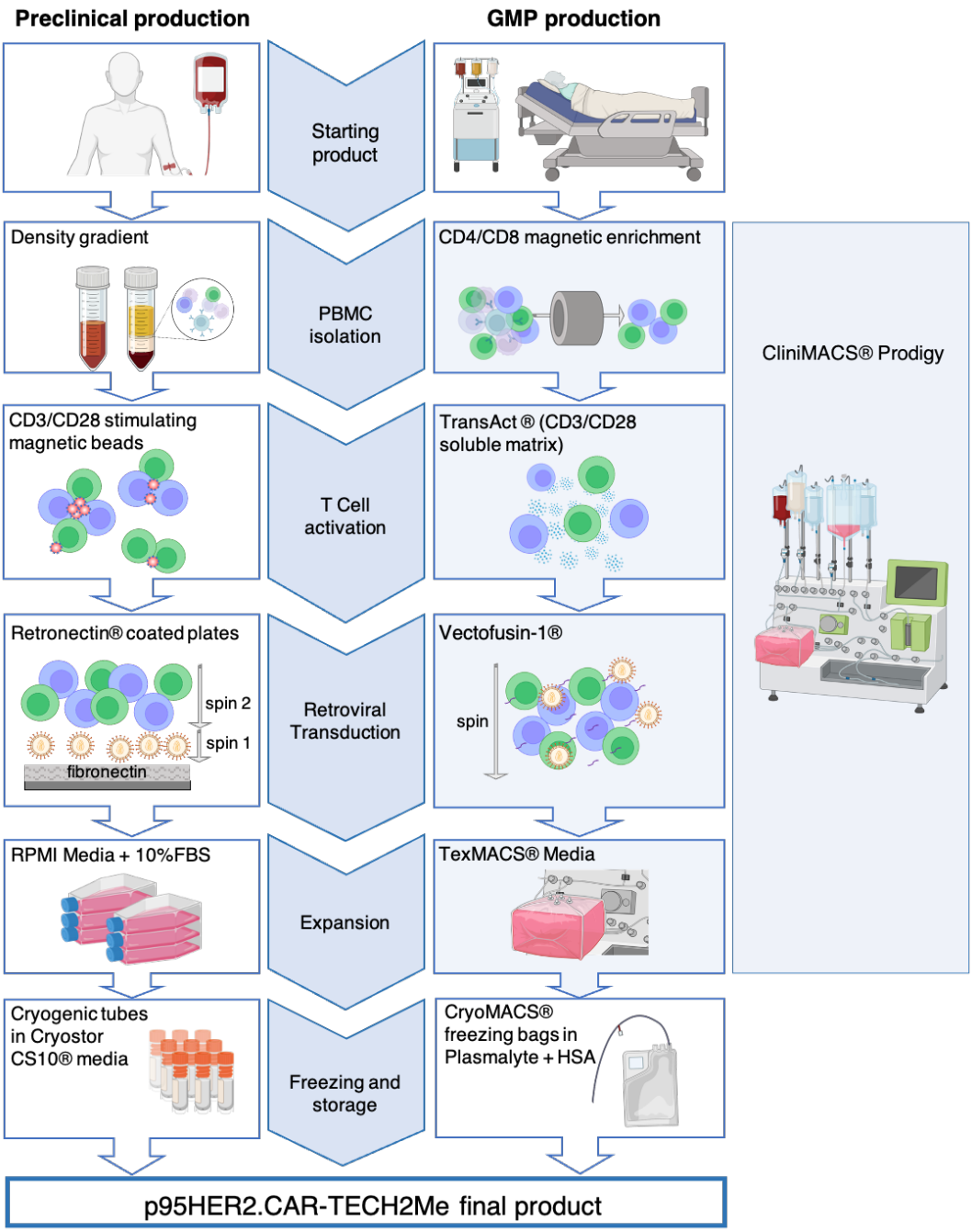

Figure 54: Schematic comparing preclinical and GMP manufacturing of CAR T cells

Preclinical methods entail isolation of PBMCs from healthy donors, activation with anti-CD3/CD28 beads in FBS-containing media, and retroviral transduction on retronectin-coated plates, followed by expansion and cryopreservation in standard cryogenic tubes in Cryostor CS10® media. In contrast, clinical-grade procedures begin with patient leukapheresis, involve CD4+/CD8+ T magnetic cell isolation using CliniMACS Prodigy® system, activation in serum-free TexMACS® medium with TransAct®, suspension transduction with Vectofusin®, and cryopreservation in CryoMACS® bags with Plasmalyte and HSA supplementation. HSA: Human serum albumin

12.2. Side by side comparison of a GMP-produced and a research grade-produced p95HER2.CAR-TECH2Me final product

Taking these differences into account, we aimed to compare the two p95HER2.CAR-TECH2Me products, one produced under our standard preclinical protocol and the other produced under GMP-conditions at the Blood and Tissue Bank of Catalonia (BST). Notably, for this GMP validation we used a leukapheresis from a healthy volunteer as starting material instead of a cancer patient's leukapheresis, and we used the same PBMCs for the preclinical manufacturing to avoid donor-related differences. UTD control was produced from the same donor under preclinical manufacturing conditions only.

Transduction efficiencies (around 70%) **(Fig.55A)** and CD4/CD8 **(Fig.55B)** ratios were comparable between the two manufacturing processes. T cell expansion, measured by CD3-positive T cells population doublings, was also very similar **(Fig.55C)**. Analyzing the phenotype of CD4 and CD8 T cells separately, slight differences were observed in their differentiation state, measured by the markers CCR7 (naive) and CD45RO (memory), with most cells belonging to the central memory (CM) and effector memory (EM) fraction, and a low percentage to terminally differentiated cells (TE) **(Fig.55D).** The more significant difference is observed regarding the TE fraction in CD8 T cells, which is lower in the GMP manufacturing process, potentially favoring antitumor activity of the product.

Then, we analyzed the individual exhaustion markers (Lag3, PD1, and TIM3) in both CD4 and CD8 subsets, as well as the percentage of cells positive for all three markers (3+), representing the highly exhausted fraction **(Fig.55E)**. Few significant differences were observed between the two products, mainly the percentage of CD4 T cells expressing TIM3, which was increased in the GMP product. However, when co-cultured with MCF7 and NCI-N87 cells, these p95HER2.CAR-TECH2Me cells exhibited similar *in vitro* specific cytotoxicity compared to the preclinical product **(Fig.55F).** All together, these results prove the feasibility of GMP-manufacturing of our product, p95HER2.CAR-TECH2ME, exhibiting very similar *in vitro* phenotypic and exhaustion properties, as well as identical potency *in vitro.*

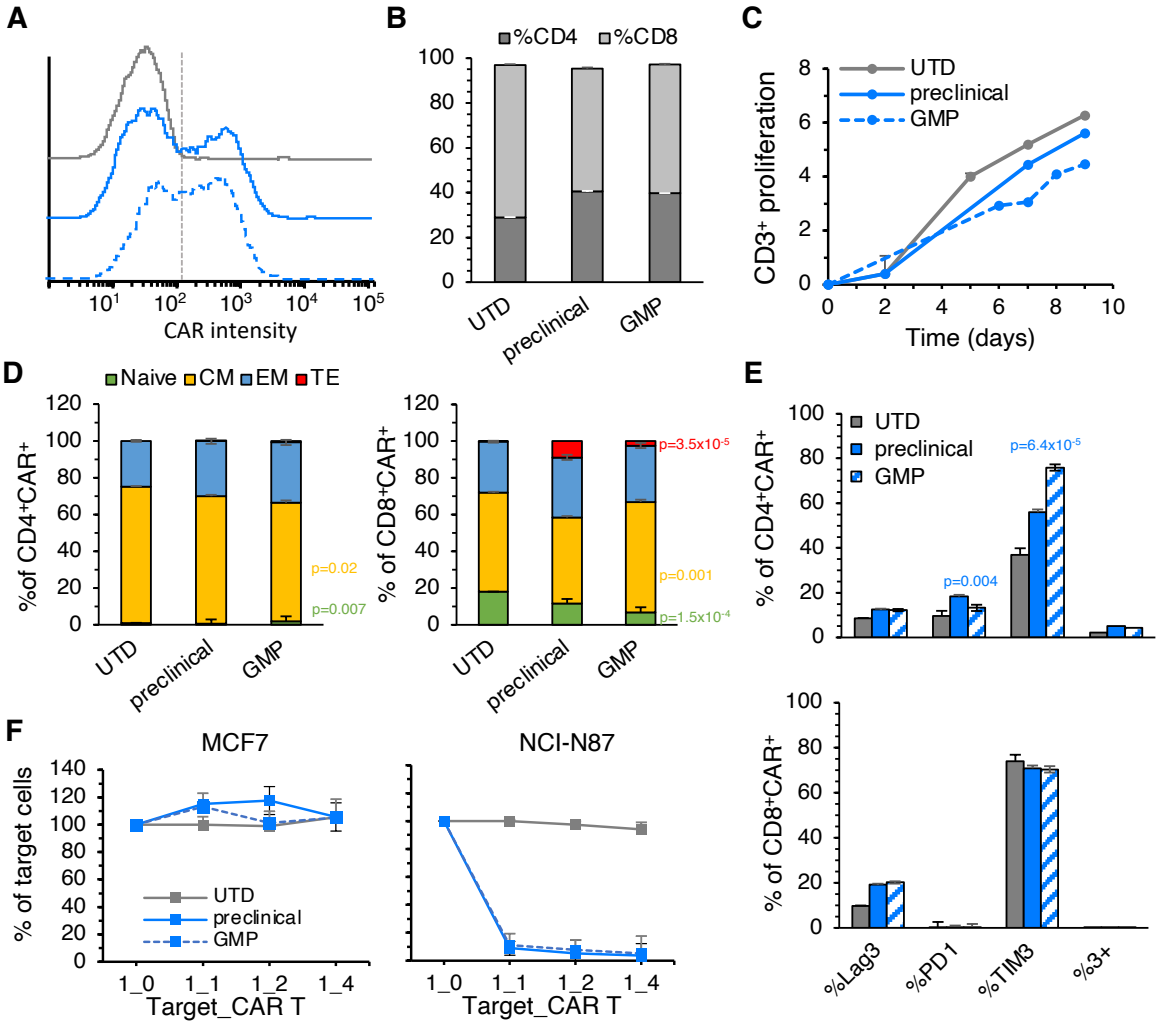

Figure 55: Comparative analysis of preclinical and GMP production of p95HER2 CAR-TECH2Me T cells.

(A) Transduction efficiencies and **(B)** CD4/CD8 ratios were analyzed by flow-cytometry. **(C)** T cells were counted at the indicated time points and expansion assessed by the quantification of CD3+ T cell population doublings. **(D)** Phenotypic analysis by flow cytometry based on CCR7 and CD45RO markers, classified cells as: Naïve (CCR7⁺/CD45RO⁻), Central memory (CM) (CCR7⁺/CD45RO⁺), effector memory (EM) (CCR7⁻/CD45RO⁺), and terminal effector (TE) (CCR7⁻/CD45RO⁻). **(E)** Exhaustion profile through the analysis of marker Lag3, PD1 and TIM3 markers, in CD4+ and CD8+ T cells, along with the percentage of cells positive for all three markers (3+). **(F)** *In vitro* cytotoxicity assays by co-culturing the two products with MCF7 or NCI-N87 cells, at the indicated ratios. T cells from the same donor transduced with an empty vector (UTD) were used as control. Average of three replicates ± SD are represented. Statistical t test analysis was performed comparing between preclinical and GMP product, and p values shown in the graphs when significant.

Collectively, this thesis proves that targeting p95HER2 with a CAR and, in addition,

HER2, with the secretion of reduced affinity BiTE® (TECH2Me), is a safe and efficacious strategy to redirect T cells against p95HER2/HER2-positive tumors. In addition, we have proven clinical-grade manufacturing feasibility and product equivalence, and the next step will be to apply for regulatory approval to test this next-generation CAR T cell in a first-in-human phase I academic clinical trial.

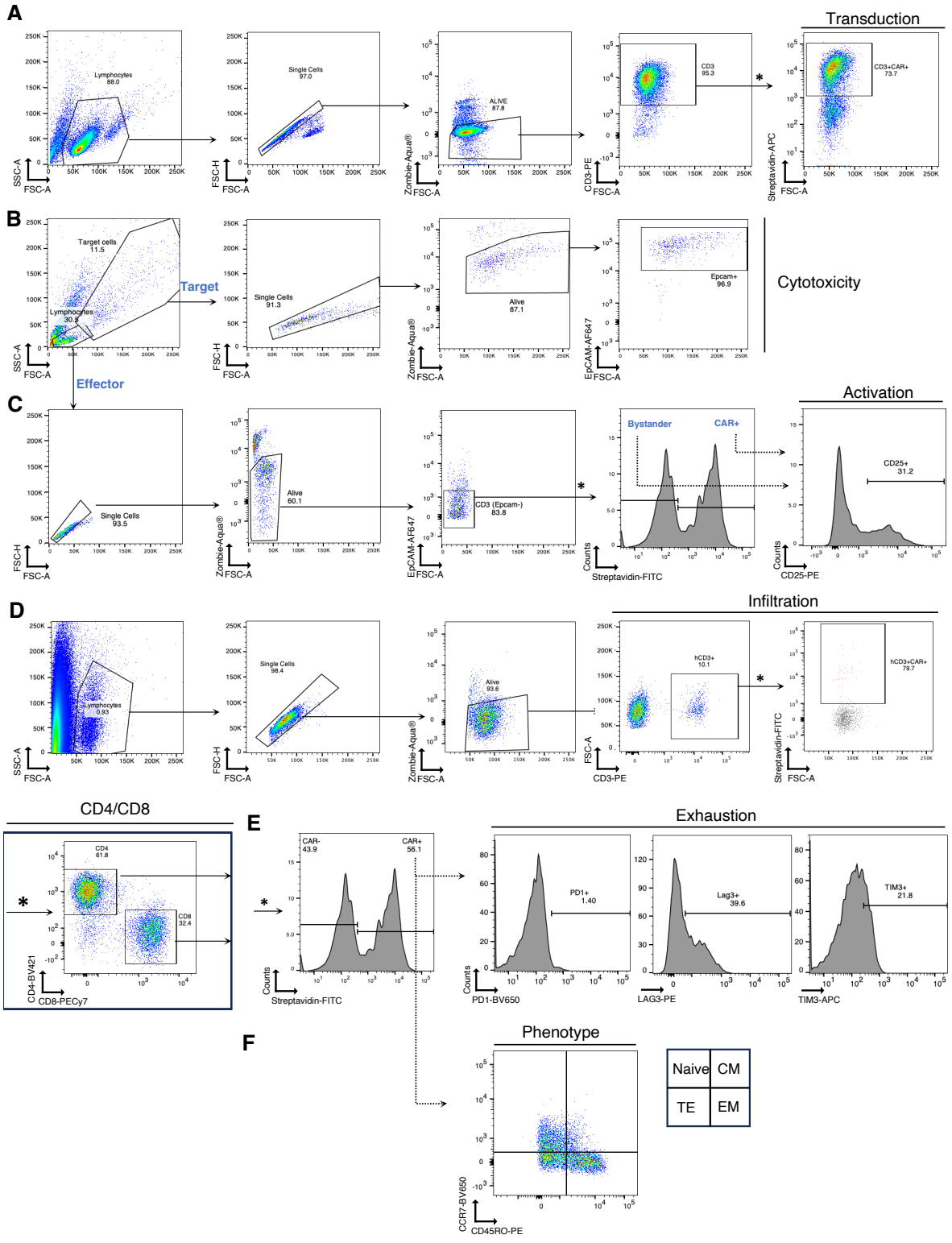
A
Transduction
Lymphocytes
88.0
Single Cells
97.0
ALIVE
87.8
CD3
95.3
CD3+CAR+
73.7
SSC-A
FSC-A
FSC-H
Zombie-Aqua®
CD3-PE
Streptavidin-APC
B
Target cells
11.5
Lymphocytes
30.5
Target
Single Cells
91.3
Alive
87.1
Epcam+
96.9
Cytotoxicity
Effector
EpCAM-AF647
C
Activation
Single Cells
93.5
Alive
60.1
CD3 (Epcam-)
83.8
Bystander
CAR+
CD25+
31.2
Counts
Streptavidin-FITC
CD25-PE
D
Infiltration
Lymphocytes
0.93
Single Cells
98.4
Alive
93.6
hCD3+
10.1
hCD3+CAR+
79.7
CD3-PE
CD4/CD8
CD4
61.8
CD8
32.4
CD4-BV421
CD8-PECy7
E
Exhaustion
CAR-
43.9
CAR+
56.1
PD1+
1.40
Lag3+
39.6
TIM3+
21.8
PD1-BV650
LAG3-PE
TIM3-APC
F
Phenotype
CCR7-BV650
CD45RO-PE
Naive
CM
TE
EM

Figure 56: General examples of gating strategies for FACS analysis

(A) Analysis of CAR expression. **(B)** Analysis of the viability of target cells at the end of a cytotoxicity co-culture assay with CAR T cells at different ratios. **(C)** Analysis of CAR-positive cells of bystander T cell activation within a cytotoxicity co-culture experiment. **(D)** Analysis of infiltrations of human CD3 T cell and human CD3 CAR-positive T cells in blood, tumors and organs. **(E)** Gating strategies to analyze exhaustion markers (PD1, Lag3 and TIM3) and phenotype, though CCR7 and CD45RO markers. Classification of cells in each quadrant is shown. *Sometimes subclassification by CD4 /CD8 T cells is performed

DISCUSSION

The prognosis of patients with HER2-positive tumors, especially breast [19] and esophagogastric tumors [36], has significantly improved over the last two decades due to the development of anti-HER2 targeted therapies. In fact, early-stage HER2-positive BC is currently treated successfully with surgery, combined with neo- and adjuvant chemotherapy and precision therapies. However, in advanced BC the 4-year survival rate drops drastically to less than 40% compared to more than 90% in early BC [246]. Moreover, some non-breast HER2-positive tumors are intrinsically resistant to the anti-HER2 therapies whereas others acquire resistance after an initial response [247, 248]. For example, HER2-positive GC tumors are intrinsically more resistant than HER2-positive BC to current anti-HER2 therapies [249–251].

Another limitation of current anti-HER2 treatments is toxicities, because HER2 is expressed at basal levels in many epithelial and some mesenchymal healthy tissues. Particularly worrying are the cardiac [47] and the lung toxicities [252] observed with several HER2 mAbs and ADCs, such as trastuzumab and T-DXd, as well as HER2 CAR T cells [154]. In this context, there is a need to develop safer and more effective therapeutic options for non-responding patients, and cancer immunotherapy stands out as a promising alternative venue [57].

In this thesis, we developed CAR T cells redirected towards p95HER2, a TSA expressed in a subset of HER2-positive tumors. Additionally, these p95HER2 CAR T cells secrete BiTEs® targeting CD3 and HER2 with modulated affinity (TECH2Me), discriminating between high-expressing HER2 tumor cells and cells with basal levels of HER2. This discussion comprehensively examines the rationale, design, potency, safety and clinical considerations of this therapy, named p95HER2.CAR-TECH2Me, as a potentially safe and effective option for the treatment of a subset of advanced HER2-positive solid tumors. Given the high prevalence of HER2-amplification in all cancers (3.5%) **(Fig.2),** applying these new immunotherapies to any other unresponsive HER2-positive tumors seems a reasonable approach.

1. Opportunities and challenges of immunotherapy in advanced HER2-positive solid tumors

Immune cell infiltration in the TME reflects a pre-existing antitumor immune response and plays a key role in clinical outcomes, providing an actionable target to improve and develop new immunotherapeutic strategies for cancer treatment [128]. BCs were initially considered “cold” or “immunologically silent” tumors and were not considered preferential candidates for immunotherapeutic developments [92]. However, later research demonstrated that HER2-positive BC tumors are indeed immunogenic, thereby holding promise for immunotherapeutic developments [253–255]. Accordingly, higher TIL infiltration has been correlated with better outcomes in HER2-positive BC in diverse treatment settings [256, 257]. Therefore, several immunotherapeutic approaches aimed to increase the T cell infiltrate, such as ICIs, vaccines and T cell redirection strategies [254, 258] are under investigation to overcome resistance to available anti-HER2 treatments, especially in HER2-positive BC [57, 259, 260]. The PD-1/PD-L1 axis is the most studied ICB in HER2-positive tumors, mainly in combination with trastuzumab [260], since it is known to upregulate PD-L1 [261]. In patients with trastuzumab-resistant/PD-L1-positive metastatic HER2-positive, some studies have shown improved response rates with the addition of pembrolizumab (anti–PD-1) to trastuzumab [262, 263]. However, in most of the cases, ICIs have failed to increase efficacy but have enhanced toxicity [264, 265]. Discouraging result have also been observed with therapeutic vaccines in HER2-positive cancer, despite widely studied in clinical trials [259, 266–268]. These failures have increased the interest in the development of other immunotherapies such as HER2 TCBs [269, 270] and HER2 CAR T cells [271], which are favored by their advantage of eliciting T cell cytotoxicity upon direct recognition of surface HER2, bypassing MHC-restriction [57]. Due to the scarcity of TSAs, T cell redirection therapies mainly target TAAs, which are inherently associated with side effects from targeting healthy tissues [154, 272], usually managed through dose reductions that limit the therapeutic effect [231]. Despite the general failure in solid tumors, researchers remain optimistic about enhancing these therapies to achieve outcomes like those observed in hematological malignancies.

Making a direct comparison and determining the optimal approach between CAR T cells and TCBs is challenging, and there is no definitive answer [174, 273]. A precise clinical comparison between CAR T cells and TCBs is restricted to the target antigen CD19 in hematological malignancies, fundamentally the first CD19 CAR T cells Kymriah® and Yescarta® versus the only currently approved CD19 BiTE® Blincyto®. Despite variability of clinical responses depending on the specific clinical context, patient's overall health and immune system status meta-analysis data indicated that CAR T-cell therapy exhibited notably prolonged overall survival (OS) and relapse-free survival (RFS) in comparison to blinatumomab (2-year OS 55% vs 25%; 2-year RFS 40% vs 22%) in patients with relapsed/refractory acute lymphoblastic leukemia [274]. Therefore, CAR T cells seem to exhibit major advantages in achieving complete and durable responses, allowing for long-term immunosurveillance without constant administration [274, 275]. In addition, CAR T cells offer a more suitable platform for further armoring strategies than antibodies, which require biochemically complex antibody engineering technologies [276], to enhance infiltration, potency, persistence or multiple antigens targeting, as presented in this thesis [187, 206, 212, 213, 221, 277–279]. On the other hand, TCBs offer the flexibility to promptly halt administration in case of acute toxicities and are favored in terms of ease of use, immediate availability and costs, at least for pharmaceutical companies specialized in antibody developing technologies [275]. Nevertheless, the potential future availability of universal allogenic CAR T cells [280] and progressive reduction in manufacturing costs, may reduce the total price of this therapy alleviating health system's funding issues [281].

CAR T and TCB approaches may benefit in terms of safety by targeting TSAs, like p95HER2, although they are very scarce. Both, the p95HER2 TCB developed by our group [87] and the here presented second-generation p95HER2 CAR T cells, have demonstrated lack of cytotoxicity on cells expressing normal levels of HER2, making them a safer treatment option compared to a HER2 TCB [87] or HER2 CAR T cells (**Fig.26**). In terms of effectivity, despite differences in the animal models employed (p95HER2-TCB required the used of humanized mice for recruitment of human T cells) results are very similar between the p95HER2 TCB and the second-generation CAR

T, showing high potency against cell line-derived breast, lung and brain tumors **(Figs.21, 22, 27,28),** but only partial efficacy on PDXs **(Fig.29,30)** [87]. The fact that CAR T cells can be more easily armored with additional molecules than TCBs [188, 277, 282] was key to prioritizing the further development of p95HER2 CAR T cells over TCBs. Indeed, this work demonstrates that armoring p95HER2 CAR T cells with BITEs® resulted in enhanced efficacy in PDX models, providing hope for clinical translation

2. Design and generation of second-generation humanized p95HER2 CAR T cells

To date, there are more than 25.000 publications about CAR T cells (Pubmed search in February 2024), more than half published in the last decade with an increasing tendency. Much of this research is focused on finding optimal co-stimulatory domains, different gene integrations strategies and selecting optimal lymphocyte subpopulations, aiming to improve CAR T cell functionality, particularly for the treatment of solid tumors [283, 284]. Due to this unmanageable amount of information and constantly evolving strategies, we decided to prioritize simplicity of designs and transduction methodologies in our first second-generation CAR T cell development, taking already clinically approved CAR T cell therapies as examples. Consequently, we used the whole PBMCs population as a source for CAR production, without selection of CD4/CD8 or more specific populations.

For transduction, we used the same γ–retroviral vector [285] (pMSGV1) for random gene integration as Yescarta® [286], the second approved CAR T for CD19-positive malignancies. Despite recent concerns about reported cases of patients treated with retrovirally transduced CAR T cells developing secondary T cell malignancies, the FDA finally reported only 20 cases (0.02%) of T cells malignancies out of 8,000 patients treated with commercially available CAR T cells, although the true nature and correlation with retroviral or lentiviral insertion remains unknown [287]. In addition, the study by Scholler and colleagues a decade ago provided evidence supporting the long-

term safety and persistence of retrovirally transduced CAR T cells, with no signs of insertional oncogenesis or clonal expansion in 11 subjects followed for up for more than 10 years [288]. In any case, regulatory agencies require concerted efforts for effective 15-year follow-up studies to comprehensively assess any potential long-term genotoxicity risks.

In terms of co-stimulation, 4-1BB co-stimulatory domain is widely considered to produce less potent but more durable responses than CD28-based CAR T cells [219], with approved CAR T cell therapies containing both, even for the same target. To empirically select the best domain for our second-generation p95HER2 CAR T cells, we performed some initial comparative *in vitro* and *in vivo* pilot experiments, not included in this thesis for the sake of simplification and avoidance of redundant data. Results showed that our CD28-based p95HER2 CAR T produced long-term responses and protection from relapse (**Fig. 23**). Together with a higher potency than 4-1BB constructs (not shown), our CD28-based p95HER2 CAR T proved superior performance.

Therefore, in this thesis, we successfully developed and preclinically validated first-in-class second-generation p95HER2 CAR T cells using the scFvs of three anti-human p95HER2 mAbs of murine origin [81], with CD28 co-stimulatory domain **(Figs.12,13).** Intriguingly, the CAR based on the 32H2 mAb, which was the one used to generate the p95HER2 TCB [87], was not expressed on the T cell surface for unknown reasons **(Fig.14)**. Nevertheless, additional monoclonal antibodies allowed us to continue our preclinical development.

Non-humanized CAR T cells have the potential to trigger immunogenic human anti-mouse antibody (HAMA) responses, limiting CAR T cell persistence and causing allergic reactions [237]. To mitigate these concerns, although all the currently approved CAR T cells except the BCMA-targeting CAR T Carvykti® are not humanized [289], we collaborated with experts from Roche Innovation Center in Zurich to humanize the scFv sequences of 14D and 15C antibodies, the ones that were efficiently expressed in the membrane. We used the sequence of the humanized antibody trastuzumab as a reference since it is known that produces little HAMA responses [238]. The

humanization process involved bioinformatic predictions, incorporating aminoacidic changes in the framework regions, with some minor and careful changes in the complementarity determining regions to avoid damaging their antigen-binding properties. This process resulted in 6 humanized versions, three derived from 14D and three from 15C antibodies **(Fig.14)**.

In vitro co-culture assays allowed the selection of the most promising candidates for subsequent *in vivo* testing, based on specific cytotoxicity**,** proliferation and tonic signaling, measured as levels of antigen-unspecific activation [290]**.** Collectively these assays revealed that, H1-15C was very cytotoxic and proliferative **(Fig.17B-right, 18)**, but also showed the highest activation and killing when co-cultured with antigen negative cells **(Fig.17B-left, C),** suggesting an increased tonic signaling profile [218, 290]**.** Conversely, H1-14D displayed comparable activity **(Fig.17A-right)** and proliferation **(Fig.18)** against p95HER2-positive cells but showed lower activation levels and had no effect **(Fig.17A-left)** when co-cultured with antigen-negative cells.

The implications of increased tonic signaling on T cell exhaustion detected *in vitro*, compromising their effectiveness against tumors *in vivo* [291], were corroborated with our results. Our *in vivo* observations demonstrated that H1-14D outperformed H1-15D **(Fig.21),** potentially due to a decreased tonic profile. In contrast, the failure of H2-14 to achieve complete responses *in vivo* **(Fig.22)** can be attributed to the lower potency observed *in vitro* **(Figs.17,18).**

To avoid rejection of CAR T cells and xenografts from human origin we needed to use the highly immunodeficient NSG mouse model [292, 293]. While this model does not recapitulate the immune status of many cancer patients, it is widely recognized as the gold-standard for preclinical *in vivo* assessments of CAR T cells, including those that have received regulatory approval [294]. In addition, these xenograft models, including PDXs, do not entirely resemble the immunosuppressive TME present in solid tumors, since perpetuation of PDX primarily supports the survival of tumor cells without adequately representing other components of the TME. Furthermore, while humanized mouse models offer a means to partially reconstitute the T and B cell compartments, they still lack the representation of key immunosuppressive elements such as myeloid-

derived suppressor cells (MDSCs) and tumor-associated macrophages (TAMs) present in the TME [295]. Alternatively, to mimic the crosstalk between the TME and the different immune populations, CAR T cell therapies may be tested in immunocompetent mouse models. However, these models require the production of murine CAR T cells from the same mouse strain and the development of either spontaneous or syngeneic tumors of murine origin, posing a limitation for the direct extrapolation of findings and molecules to the clinical context in humans.

Despite these limitations, using the standard immunodeficient NSG model, H1-14D derived p95HER2 CAR T cells exhibited high effectiveness against the artificial and homogeneous MCF7p95HER2 cell line, not only against orthotopic breast tumors **(Figs)** but also against lung and brain tumors **(Figs.29, 30)**, which constitute a particularly urgent medical need. The proven ability of our p95HER2 CAR T cells to target solid malignancies in diverse body locations supports our decision of systemic intravenous administration. Nevertheless, other routes of administration have been proposed to target brain malignant lesions more effectively and with less toxic effects, such as intraventricular and intracerebral injections, with no unequivocal consensus [296, 297]

CAR T cells have generally failed in the treatment of solid tumors due to several reasons [209], despite exceptional cases of success, particularly with G2D-based CAR T cells for the treatment of neuroblastoma [200]. Possible factor behind this success is the use of a third-generation CAR T configuration, containing both CD28 and 4-1BB co-stimulatory domains, which, together with manufacturing using IL-5 and IL-7, contributed to an enhanced persistence [298], as well as the use of multiple administrations in some patients. We made a significant effort to avoid therapeutic failure of our product by setting complete responses in PDX *in vivo* as our standard for clinical transition. Unlike cell lines, PDX tumors are considered to reflect the heterogeneity of human cancer and replicate drug sensitivity in patients and predict therapeutic response better compared to cell line models, despite the limitation of properly resembling the immunosuppressive TME [299, 300]. As expected from a second-generation CAR T cell, the effectiveness on a PDX model (PDX67) was

significantly reduced compared to homogeneous cell lines and failed to achieve complete responses (**Fig.29**), similarly to p95HER2-TCB in different PDXs [87].

Antigen heterogeneity or loss were ruled out in this PDX model (PDX67) as a potential resistance mechanism of our CAR T cells [301], due to the notably uniform expression of p95HER2 by IHC at the beginning (**Fig.29**) and in the unresponsive tumors at the study endpoint (data not shown). Nonetheless, when analyzing TMAs containing a larger BC-PDX cohort (samples from 23 different PDX of origin) p95HER2 heterogeneity manifested in 5 out of 13 p95HER2-positive PDX, in contrast to HER2 expression, which was much more intense and homogeneous in all 20 positive cases **(Fig.31).** The mechanism underlying resistance in this PDX is still unknown, and approaches to elucidate it may involve the analyses of expression of immune checkpoints (PD-L1/PD-L2), immunosuppressive molecules (i.e., TGF-beta) within the TME and defects on IFN-γ intrinsic signaling pathway, as well as the and the use of more sophisticated single cell (sc) multi-omic technologies, such as scRNA sequencing or sc spatial proteomics or transcriptomics [302, 303]. However, mechanisms of resistance may differ across cancer types and between patients and it is difficult to prioritize how to address them when clinical evidence with p95HER2 CAR T cells is missing. Acknowledging all resistance mechanisms cannot be addressed at once, we opted to focus on finding a potentially widely applicable enhancement for treating p95HER2/HER2-positive tumors with CAR T cells, rather than delving into the reasons for treatment failure. Nevertheless, future work will try to elucidate potential biomarkers of response and delve into these resistance mechanisms.

3. Improving the therapeutic potential: next generation p95HER2 CAR T cells

Among all the innovative strategies in the field of next generation CAR T cells, we chose to armor our p95HER2 CAR T cells with the secretion of BITEs® targeting a second TAA, HER2, with decreased affinity [164]. This dual strategy, inspired by the pioneering work of Dr. Marcela Maus' laboratory [188], aims to synergize two different

effector molecules, a CAR and a BiTE®, boost the immune response by recruiting bystander T cells, and bypass or prevent the likely occurrence of heterogeneity in the expression of p95HER2 and the possibility of antigen-downmodulation [187, 189]. According to the result of second-generation p95HER2 CAR T cells on PDX67, the first two mechanisms seem to be more relevant, although all of them may play a role in different scenarios. Bryan Choi and colleagues engineered CAR T cells designed to target the glioblastoma TSA EGFRvIII, which was known to be downmodulated in patients upon CAR T cell targeting [304] secrete a BiTE® targeting wild type (wt) EGFR, a TAA like HER2 [188]. They employed constitutive system for the secretion of the BiTE® targeting wtEGFR, and demonstrated the absence of toxicities in EGFR-basal healthy tissues due to the low concentration and local secretion of the BiTE®, which tended to accumulate in the tumor [188]. However, this assumption may not be adequate to ensure safety in human subjects.

A common approach to mitigate toxicities is the incorporation of genetic suicide systems or safety switches [305, 306], which prompt CAR T cell death upon activation or drug administration. Alternatively, labeling CAR T cells with surface proteins, such as CD20 and truncated EGFR, allows for targeting and killing with the administration of approved mAbs rituximab [307] or cetuximab respectively [308]. Nevertheless, integrating these systems in our designs would require a third genetic modification and complex validation. Therefore, we opted to enhance potency while maintaining safety through the constitutive secretion of BiTEs® with reduced affinity towards HER2 [164, 236]. This modification ensures that recognition is limited to cells expressing high levels of HER2, such as HER2-positive tumors, sparing the rest of healthy tissues, which express basal levels. This safety strategy, instead of relying solely on tumor accumulation, was further supported by our biodistribution experiments, which revealed infiltration of p95HER2.CAR-TECH2Me into other organs and tissues, surpassing even the extent observed in tumors (**Fig.52**).

4. Design and antitumor potential of p95HER2.CAR-TECH2ME

HER2 mAb with reduced affinities have been preclinically tested for developing HER2 CAR T cells [164] and TCBs [165, 166], undergoing thorough safety assessment on several healthy primary cultures expressing basal levels of HER2 and confirming that decreasing the affinity of HER2 scFv could increase the therapeutic index while maintaining a potent antitumor effect [309]. We selected three HER2 scFv versions previously described [164, 236] and the linkers and CD3 scFv sequences from Blinatumomab® [188] to generate a bispecific CD3xHER2 BiTE® named them TECH2. We selected this format since it is small and easy to secrete. The variant with highest affinity (TECH2Hi) contains the same HER2 scFv as trastuzumab (4-D5), and the two affinity-reduced versions TECH2Me (4D5-5) and TECH2Lo (4D5-3), using HER2 scFvs with relatively 500 or 2000-fold decrease affinities respectively [164].

We confirmed this decreasing binding affinity towards HER2 in several *in vitro* cytotoxicity co-cultures and binding experiments with cells expressing variable levels of HER2 (**Figs. 34, 35**). The intermediate affinity TECH2Me variant demonstrated a compelling balance of efficacy and safety. Furthermore, purified TECH2Me added to a 1:1 ratio co-culture of PBMCs and target cells induced potent activation of untransduced PBMCs only when target cells overexpressed HER2 (PDX433) **(Fig.36)**, highlighting its potential to boost potency of conventional second-generation p95HER2 CAR T cells.

Next, to armor CAR T cells with these TECH2s, instead of dual vector transduction strategy, which will increase the risk of insertional mutagenesis and thus genotoxicity, we generated bicistronic retroviral vectors the nucleotide sequences encoding for the two genes of interest, under the control of the constitutive LTR retroviral promoter, separated though a T2A sequence, which translates into a self-cleavable peptide (**Fig.37**). Despite the large size of this insert (3 Kilobases), retroviral vectors transduced T cells efficiently.

Finally, we met our self-established efficacy criteria for clinical transition:

p95HER2.CAR-TECHMe achieved complete responses in two PDX models, PDX667 and PDX433, surpassing the effectiveness of p95HER2 CAR T and/or TECH2ME alone **(Fig.41B, D and Fig.42A, C).** These two PDX models exhibit high and uniform p95HER2 expression, supporting the idea that combining two effector molecules may have an additive effect in enhancing the immune response, even when antigen heterogeneity is not a limitation. Notably, since NSG mice are highly immunodeficient, the engaging activity of the TECH2Me is restricted to the administered cells, either by binding to CAR-positive secreting cells or to bystander untransduced co-administered CD3-positive cells. Therefore, enhancing antitumor potency in a more relevant immunocompetent model may involve the recruitment of endogenous T cells, although immunosuppressive cells in the TME may simultaneously counteract this effect.

On the other hand, in PDX67, complete responses were observed following p95HER2.CAR-TECH2Me treatment in two mice, with partial response in two others, demonstrating superior effect to that of T cells secreting TECH2ME **(Fig.41D)** and that of second-generation p95HER2 CAR T cells in this same PDX model **(Fig.29C and Fig.30),** although not in a side-by-side comparison. This finding suggests that this PDX model may be particularly resistant to T cell redirection therapies, probably due to the expression of potent immunosuppressive factors or ligands, since intensity of response correlates with tumor infiltration, at least in the case of second-generation p95HER2 CAR T cells. This potential immunosuppression is not completely overcome by armoring the second-generation CAR T with additional TECH2ME. Therefore, this result underscores the importance of identifying biomarkers of response and anticipating scenarios where a given product may not be effective. Testing the effectiveness of p95HER2.CAR-TECH2Me in a wider array or PDX models will further help in this assessment and will also help to establish a threshold of p95HER2 expression for effective targeting.

In addition, we demonstrated that p95HER2 is naturally expressed in HER2-positive cell lines beyond BC, such as lung (H2170), gastric (NCI-N87), esophageal (OE-19) and ovarian (SKOV3) cells, both by FACS and WB analyses **(Figs.47)**, and that all of

them demonstrated *in vitro* susceptibility to p95HER2.CAR-TECH2Me treatment **(Fig.48)**. While experiments with GC and other tumor types-PDXs are pending, positive *in vivo* results with xenografts derived from NCI-N87 and OE19 cell lines are shown in **Fig.49.** All together our findings support that p95HER2-CAR-TECH2ME holds promise for efficacy against diverse tumors, not just BC but also those in the upper gastrointestinal region with lower treatment success rates and high clinical demand.

Lastly, while most studies base their preclinical development in the use of CAR T cells from healthy donors, quality of the patient-derived starting material is highly variable due to disease burden and prior treatment differences [210], leading sometimes to manufacturing challenges in clinical translation [209]. For this reason, we also generated and assessed the phenotype and effectiveness of CAR T cells derived from a patient with a HER2-positive Luminal B BC, who had already undergone neoadjuvant chemotherapy plus dual trastuzumab-pertuzumab blockade. We validated *in vitro* functionality, employing a healthy donor for a side-by-side comparison, demonstrating the viability of generating potent p95HER2.CAR-TECH2Me T cells from a pretreated cancer patient (**Fig.45)**. Future work will involve evaluating these CAR T cells against in vivo, ideally against their matching PDX.

5. Safety profile of p95HER2.CAR-TECH2 Me

We have previously mentioned the challenges of using xenograft models in immunodeficient mice to study immunotherapies for proper effectivity assessment, since they do not enable proper understanding of the interactions between the TME and the tumors [293, 310]. However, these limitations also apply to the proper safety evaluation. Humanization by transplantation of human CD34-positive hematopoietic stem cells or human PBMCs in NSG mice [292] or SGM3-NSG mice, which constitutively secrete human hematopoietic cytokines to allow superior engraftment of myeloid lineages [311], will render a more complete immune system while allowing PDX engraftment, and therefore will better recapitulate toxicities observed in patients

related to an exacerbated immune response, like cytokine release syndrome (CRS)[312, 313].

However, even if using fully immunocompetent mouse model that better recapitulate the interaction of our therapy with the TME and the whole immune system [310, 314, 315], the most relevant issue will persist, which arises from the differences between all mouse and human epitopes targeted with p95HE2.CAR-TECH2Me. HER2 Abs based on trastuzumab, as is the case of TECH2ME, do not recognize mouse nor rat ERBB2 [316], and preclinical safety studies have usually been performed in non-human primates, using cynomolgus monkey as the relevant species [317, 318]. Anti-p95HER2 mAbs used to generate the scFv of the CAR T cells described in this thesis were generated using the human ERBB2 sequence as antigen [81], and therefore do not recognize the corresponding murine epitope, which differs only in one amino acid (**Fig.12**). Again, non-human primates will be the relevant species for testing p95HER2 targeting antibodies or CAR T cells. Blinatumomab®-derived CD3 scFv reacts only with human or chimpanzee antigens [319], but not with other primate species. This leaves chimpanzees to be the only non-human species sharing all three antigen targets sequences with humans, and experimentation with this superior primate species is banned in the EU for ethical reasons.

This limitation could be potentially overcome in two ways: generating a surrogate p95HER2-CAR.TECH2Me that recognizes all the murine epitopes or using mice genetically modified to express HER2 human protein instead of the murine ERBB2. The first option is technically complex, since it requires the generation of three new antibodies with reactivity for murine p95HER2, HER2 and CD3, which will likely not have equivalent binding affinity to the human targeting ones. On the other hand, some HER2 transgenic mice have been developed but with HER2 expression limited to certain organs, such as the mammary glands [320]. Moreover, the fact that they are not widely used for preclinical testing of the armamentarium of anti-HER2 agents evidence that they were not good mice models. To our knowledge, HER2 transgenic models expressing HER2 across all tissues have not been developed so far, which reveals the complexity of this strategy. Such a model would be tremendously useful to

study all trastuzumab based anti-HER2 therapies which do not cross-react with murine ERBB2 [316]. A surrogate mouse anti-CD3 cross-reacting molecule or crossing these mice with a human CD3 transgenic mouse model [321] will be additionally necessary for complete assessment of all the components. Moreover, both strategies oversee the potential differences in expression levels and patterns between mouse and human ERBB2 [322, 323].

Acknowledging that there may be models that potentially better recapitulate toxic effects, most CAR T cells and TCBs taken to the clinic have relied on NSG mice engrafted with healthy human tissues. We used the MCF7 tumor cell, which expresses HER2 levels similar to those expressed in healthy tissues, as our safety preclinical assessment model. Neither the p95HER2 CAR T **(Fig.26)** nor p95HER2.CAR-TECH2Me **(Fig.40)** showed activity against these tumors in contrast to HER2 CAR T cells, which as expected completely eradicated them. In an experiment that better simulates a real patients' scenario, we implanted a HER2/p95HER2-positive PDX433 culture in one flank, simulating the tumor, and MCF7 cells in the other flank, mimicking a healthy tissue (**Fig.43**). Despite the successful eradication of the PDX433 flank, and thus assuming the presence of antigen-activated CAR T cells, no antitumor effect was observed on the MCF7 flank. Notwithstanding these limitations and the unavailability of an ideal *in vivo* model [324], we believe that the lack of targeting of MCF7 tumors reveals a favorable safety profile of p95HER2.CAR-TECH2Me over HER2 CAR T cells previously tested in the clinic, which was further complemented by numerous *in vitro* studies throughout this thesis.

Co-culture cytotoxicity and binding experiments on cells expressing low levels of HER2 evidenced the specificity of both constituting moieties, p95HER2 CAR and TECH2Me, for HER2-overexpressing cells. Second-generation p95HER2 CAR T showed no killing, activation nor proliferation when co-cultured with MCF7 cells **(Figs.17, 18)**. Similarly, TECH2Me alone demonstrated no binding to MCF7, MCF10A, primary lung cells and cardiomyocytes **(Figs.34, 39),** while TECH2Hi illustrated the risks and toxicities associated with current anti-HER2 therapies by binding all of them. Consistently, p95HER2.CAR-TECH2Me did not display any cytotoxicity or killing on

these 4 cell lines and primary cultures **(Fig.36, 38)**

In addition, as we aim to target p95HER2 for the first time in the clinical setting, we decided to perform an MPA to assess potential off targets of H1-14D scFv among 6.000 membrane proteins, covering 94% of the human membrane proteome. This platform has been widely used in other CAR T or antibodies preclinical safety assessments [325–327] and offers several advantages over other techniques, such as healthy tissues IHC screens, as the method uses live unfixed cells and flow cytometry, which provides higher sensitivity and ensures that all detected membrane proteins maintain their native conformations and appropriate post-translational modifications [328]. Results provided by the company suggested two potential off targets: UBXN8 and IL2RB **(Fig.24),** which needed further validated in-house. Our results demonstrated that H1-14 scFv could not recognize these proteins even when artificially overexpressed, and the corresponding CAR T did not show any killing activity when co-cultured with them **(Fig.25)**. Given that T cells express IL2RB on their surface as part of the IL-2 receptor, we would have observed killing of CAR T cells if IL2RB was indeed an off-target. However, this was not the case, as evidenced by normal viability and proliferation levels compared to UTD controls. Similarly, other authors were also unable to validate a potential off target provided by the MPA [329] and have recently started a phase I clinical trial (NCT04422912). Therefore, we concluded that this MPA revealed two false positives, an error rate (0.033%) that could be expected from any analytical technique, and that p95HER2 CAR T cells based on H1-14D scFv do not bind to full-length HER2 nor any other detectable off-target, supporting the safety profile observed in our *in vitro* and *in vivo* experiments

Taking all these results into consideration, despite the absence of optimal animal models, in this thesis we provided extensive preclinical evidence that supports the consideration of p95HER2.CAR-TECH2Me as potentially safe or at least safer than high affinity HER2 CAR T cells.

6. Biodistribution studies

Understanding the biodistribution of drugs, including adoptive cellular products like CAR T cells, is crucial for predicting both therapeutic and adverse effects [330][331]. However, given that CAR T cells are living cells, predicting their interactions within the body can pose challenges [245]. CAR T cells are expected to widely distribute within the tissues, exert their antitumor effects, undergo programmed cell death, and be eliminated through natural T cell catabolic pathways [332] whereas a small subset of cells may persist for a long time as memory T cells [245, 333]. Techniques for evaluating the biodistribution of CAR T cells encompass live imaging modalities, such as positron emission tomography (PET) [334], bioluminescence or fluorescence imaging[335] , as well as ex vivo qPCR [245], flow cytometry (ref), IHC and in situ hybridization analyses [336]. All of them have advantages and drawbacks [337], and specific regulatory guidelines on proper procedures are missing [245, 338]. We conducted a comprehensive biodistribution assessment of both cellular (CAR T) and protein (TECH2Me) components by flow cytometry on disaggregated tissue homogenates and ELISA respectively, in selected organs and tissues (blood, spleen, liver, lungs, kidney, brain and tumors), considering expected relevant distribution [245].

Our results revealed that p95HER2.CAR-TECH2ME infiltrated tumors with the fastest rate upon administration **(Fig.52).** However, higher absolute T cell infiltration levels were found in spleen, lung and liver, peaking at day 15, and to lower extent in kidney (**Fig.52)** and peripheral blood (**Fig.51)**. Minimal accumulation in brain was expected from the absence of tumors because the CNS is an immunosuppressive site [339]. Our results correlate with Michael R. Weist's findings using PET imaging of intravenously administered CD19 CAR T cells, which only accumulated in tumors in a very small percentage of CAR T in contrast to a high initial lung entrapment followed by high accumulation also in liver and spleen over 7 days follow-up [334]. Other studies have also revealed spleen, lung and liver as preferential accumulation sites, followed by kidney, heart, and bone marrow, with additional detectable levels of CAR T cells in a range of other tissues including fat, stomach, epididymis, muscle, testis, and duodenum [245, 330]. Altogether, our results and other group's findings confirm the

expected wide-spread distribution of CAR T cells within the body, reinforcing our strategy of decreasing HER2 targeting affinity rather than relying in tumor accumulation [188].

In addition, we verified the anticipated short half-life of TECH2ME, which has been escribed for other BITEs® due to the lacking Fc stabilization [161], in an experiment injecting the highest possible dose of purified TEC2H2Me **(Fig.50)**. As expected, we could not detect TECH2ME from p95HER2.CAR-TECH2ME treated mice by ELISA in serum at any timepoint (**Fig.51**) and neither in tissue samples showing the highest CAR T cell infiltration: spleen and lung at day 15 (data not shown). Therefore, TECH2ME levels must be below the kit's lower detection limit of 1ng/ml. This feature, together with its short half-life, potentially limits the activity of TECH2ME to the proximity of secreting T cells or the secretory T cells themselves, thereby minimizing, albeit unlikely, on-target off-tumor potential effects.

We believe that these results, together with the extensive safety assessment of our product, provide a good overview of p95HER2.CAR-TECH2Me biodistribution. However, future work may involve qPCR analysis of CAR genomic DNA in all other organs using frozen specimens, since this technique presents higher sensitivity. PET imaging using T cell tracers is also ongoing, which possess the advantage of longitudinal and real-time imaging of mice, without the need of euthanizing them at each time-point [334].

7. Potential future improvements for our therapy

From the selection of a candidate until the treatment of the first patient, advancements in the CAR T cell field continue to evolve, potentially leading to the emergence of new strategies to enhance your product. We are confident that our findings are sufficiently promising to warrant entry into a phase I clinical trial, which will offer valuable insights regarding safety and preliminary efficacy of p95HER2.CAR-TECH2Me, which may help in refining the therapy, if necessary. Nonetheless, we already contemplate potential future enhancements to our therapy.

We are aware that our therapy will not be useful for HER2-low patients due to low affinity-targeting of HER2, in contrast to the novel ADCs, such as T-DXd [55], but may constitute an alternative strategy when they fail in the HER2-high subpopulation. Therefore, the first evident way of improving our therapy would be through the inducible gene switches [306], in this case, for controlled secretion of TECH2Hi, exclusively upon encounter of p95HER2 in the tumor, increasing the antitumor potential without risk of on-target off-tumor toxicities. However, these systems require complex synthetic biology approaches and need to be tightly controlled to avoid even minimal leakiness, potentially leading to toxicities. Future work in our laboratory includes the testing of some of these strategies, such as using p95HER2 synthetic receptors named SynNotch receptors, which, akin to CARs, feature an extracellular scFv-based antigen binding domain but differ in their transmembrane and intracellular domains [340, 341]. In essence, SynNotch receptors encompass a cytosolic domain that undergoes cleavage upon antigen binding, releasing a protein capable of triggering the expression of specific target genes, which in our case would be a TECH2Hi.

Second, we could combine p95HER2.CAR-TECH2Me with additional molecules or treatments, either by further armoring the CAR T s or in co-administration modality. Taking into account the main limitations of CAR T cells in solid tumors, which include difficult trafficking and penetration into the tumor and the low CAR T cell expansion and persistence due to immunosuppressive and hypoxic TME [342], we could increase tumor infiltration adding the ECM degrading enzyme heparinase [279] or chemokines **(ref),** combat the immunosuppressive TME with ICIs [223]**,** anti-VEGF [343]**,** TGF-β inhibitors [277, 344]**,** or increase T cell persistence through the secretion of cytokines (ref).

Lastly, targeted integration of the CAR using CRISPR/Cas9 gene editing techniques to the TCR locus (TRAC) may improve the antitumor capacity of our product by generating CAR T cells with better phenotype and exhaustion profile [198]. Also, eliminating the TCR is one of the requisites to deliver allogenic T cells, and is already being tested in the clinic for the treatment of hematological malignancies (NCT04557436, NCT05377827). This would be very useful from a manufacturing

perspective but also if heavily pretreated HER2-positive patients included in a potential clinical trial have insufficient or dysfunctional T cells which do not to pass potency assays, consisting in co-culture *in vitro* assays with p95HER2-expressing cells.

8. Bringing p95HER2.CAR-TECH2Me to the clinic

8.1. Transition to clinical grade manufacturing

Clinical-grade upscaling of CAR T cell products and other advanced therapy medicinal products (ATMPs), poses a significant challenge due to the strict regulatory requirement of GMP-compliant manufacturing process. To minimize issues with this transition, often underestimated by preclinical researchers, it is recommended to establish a preclinical manufacturing process as close as possible to the clinical manufacturing from the beginning of development [209]

The manufacturer has to show that the product is consistently manufactured in a pre-defined quality and that the product is safe and efficacious in patients [345]. In this thesis, we present a comparative analysis of two products generated through either a preclinical process or a GMP-manufacturing at the Blood and Tissue Banc of Catalonia (BST) facility, involving a semi-automatic closed system, the cliniMACS Prodigy® from Miltenyi [346], which has been already used for the manufacturing of CAR T cells in clinical trials, like ARI001 at Hospital Clinic in Barcelona (Spain) [347]. We analyzed killing, expansion kinetics and phenotype induced by the two manufacturing processes, although we used a healthy donor instead of patient's leukapheresis, since it constituted a validation production for regulatory approval application, rather than an actual clinical trial manufacturing process. This allowed for a focused comparison on manufacturing protocol differences, which demonstrated a remarkable equivalence in terms of transduction efficiency, CD4/CD8 ratios, tonic signaling (activation, exhaustion, and phenotype) and cytotoxic activity **(Fig.55).** In terms of expansion, proliferation rates were also comparable, and cells expanded 1000-fold up to 10^9 total cells. Considering the effective preclinical dose, 6 million CAR-positive cells per

mouse, and calculating the human equivalent dose according to body weight, we will need to reach doses in the range of 10^{10} CAR-positive cells. We are currently investigating the recent bigger culture chamber of cliniMACS Prodigy® that could presumably allow reaching these high doses (≥ 1.5×10^{10}) [348].

Lastly, another important aspect of clinical manufacturing of CAR T cells is expansion times. Apart from increasing the turnaround times of treatment, prolonged expansion of CAR T cells (≥ 10 days) may decrease stem and memory T cells in favor of more differentiated and exhausted populations, diminishing their antitumor activity [349]. Interestingly, a recent study has demonstrated that CAR T cells can be manufactured using a next-generation platform in less than 2 days, while retaining T-cell stemness and enhancing clinical activity even at lower doses (NCT03960840) [350]. Taking this into account, we will try to reduce expansion times to less than 10 days.

8.2. Management of adverse effects in CAR T and bispecific antibody therapy

Off-target and on-target/off-tumor adverse effects associated with p95HER2.CAR-TECH2Me are not expected based on our preclinical safety results, although clinical experience is needed to corroborate these findings. In addition, allergic reactions against any of the exogenous protein components (p95HER2CAR, TECH2) have been minimized by humanizing the p95HER2 scFv **(Fig.15),** using a HER2 scFv derived from trastuzumab, which is already humanized and the CD3 scFv from Blinatumomab, which is known to produce little immunogenic with the development of neutralizing antibodies in less than 1% of the patients treated [351]

However, it is important to acknowledge the potential occurrence of other prevalent toxicities inherent to CAR T cell therapies and bispecific antibodies, irrespective of the targeted antigen, such as cytokine release syndrome (CRS) and immune effector cell-associated neurotoxicity syndrome (ICANS) [167, 168]. CRS is the most prevalent adverse event, reported across all CAR T cell clinical trials, and is produced by an exacerbated systemic inflammation from immune cell activation [313, 352], involving IL-6- and IL-1-producing myeloid cells [312, 353]. Neurological symptoms are not fully

understood, and symptoms may include confusion, difficulty speaking, seizures, and loss of consciousness. Since NSG mice harbor defects in monocytes and macrophages [354], they do not allow for proper assessment of these AEs, although there are some *in vitro* assays [355] and mouse models, such as humanized mice [353] and SCID-beige mice [312], which are capable of reconstituting better the myeloid cell compartment responsible for these risks. Although consider using these models to preclinically assess CRS, we assume that these toxicities are expected and that there are clinical protocols already established to mitigate them, such as continuous and intensive monitoring of patients for weeks after infusion and therapeutic immunosuppressive interventions, with corticosteroids and IL-6 receptor antagonists like tocilizumab, which have made these reactions generally manageable [167, 356]. In this regard, we are confident that a clinical trial conducted at Vall D'Hebron Hospital, which is one of the reference centers in Spain for ACTs according to the Spanish Health Ministry, together with a careful dose escalation design, will ensure the best possible assistance to treated patients.

8.3. Initiation of an academic first-in-human, phase I clinical trial

Trial design

We have designed an interventional open label, non-randomized, dose-escalation, phase I clinical trial to evaluate the safety and tolerability of the administration of p95HER2-CAR-TECH2 Me cells in our target patients and to identify the maximum tolerated dose and recommended phase-2 dose. Nevertheless, we will also aim to evaluate preliminary clinical activity of the p95HER2-CAR-TECH2Me cells and survival as secondary objectives. We will make efforts to obtain the maximum clinical and biological information out of this, independently of the outcome, obtaining and analyzing pre- and post-treatment blood and tumor samples, to explore the relative subsets of p95HER2.CAR-TECH2Me cells, changes in serum cytokine and chemokine levels, *in vivo* expansion and persistence, relative trafficking to tumor and explore potential predictive/prognostic biomarkers, that will help to understand the mechanisms of response to CAR T cells to better redesign our construct.

Patient eligibility

Eligible patients are those with locally advanced, recurrent, or metastatic solid tumors with positive expression for HER2 and p95HER2 that have progressed after at least one available standard therapy or for whom standard therapy does not exist, have proven to be ineffective or intolerable, or is considered inappropriate. For this phase I clinical trial, we will consider p95HER2 positivity by IHC following the same criteria as for validated HER2 IHC analysis, like HercepTest [357], considering all 1^+, 2^+ and 3^+ as p95HER2-positive tumors. A total of 15 patients may be enrolled over 36-48 months for all cohorts. We believe that limiting this therapy to a single cancer type, such as BC, will be a lost opportunity for other cancers to also benefit from this therapy. A recent opinion note by André Fabrice and colleagues supports our believe, claiming that in the era of molecular biomarkers, classifying metastatic cancers according to their organ of origin and conducting clinical trials sequentially for each cancer type, is an obsolete approach that is hampering access to potentially life-saving drugs [358] Therefore, assessment of the prevalence of p95HER2 in any cancer type is important for proper patient recruitment. In this thesis we demonstrated that p95HER2 expression correlates with HER2 overexpression (**Figs.31, 47**), although a threshold upon which this alternative initiation of translation occurs is not established nor other possible mechanisms promoting this to happen well understood. The correlation between ERBB2 copy numbers and p95HER2 positivity occurrence is also being analyzed at the moment. So far, this TSA is known to be expressed in at least one third of HER2-positive BCs [81], and also in lung [89], endometrial [90] and gastric HER2-overexpressing tumors **(Fig.46).** Preliminary results reveal positivity of p95HER2 expression in a wide variety of other HER2-positive cancers samples by IHC such as ovary, rectum, pancreas, ampulla of vater, esophagus, salivary gland and bladder tumors (data not shown).

In summary, this thesis provides extensive preclinical evidence on the safety and antitumor activity of p95HER2.CAR-TECH2ME, a next generation CAR T cell therapy product, to support its consideration for subsequent clinical testing. As of the date of the submission of this thesis, our laboratory and clinicians in charge of conducting this clinical trial are finishing the IMPD documents for clinical trial approval request. If granted, the phase I clinical trial will start at Vall D'Hebron Hospital and Hospital del Mar Hospital at later stages. Since it will constitute the first time p95HER2 is being targeted in the clinic, lessons learnt from this potential phase I clinical trial would be of great value to the scientific community.

CONCLUSIONS

1. Second-generation humanized p95HER2 CAR T cells are effective against breast cancer cell lines grown orthotopically or in metastatic sites, such as the brain and the lungs.
2. Second-generation humanized p95HER2 CAR T cells are not as effective on PDXs *in vivo.*
3. We successfully armored second-generation humanized p95HER2 CAR T cells with additional BiTEs® targeting CD3 and HER2, named TECH2.
4. Contrary to therapies targeting HER2 with high affinity, p95HER2 CAR T, TECH2Me and, consequently, p95HER2.CAR-TECH2Me, have no effect on cells expressing normal levels of HER2 *in vitro*.
5. Similarly, p95HER2 CAR T and p95HER2.CAR-TECH2Me have no effect against MCF7 tumors *in vivo*, which express levels of HER2 comparable to healthy tissues, in contrast to high affinity HER2 CAR T cells or p95HER2.CAR-TECH2Hi.
6. Next generation p95HER2.CAR-TECH2Me demonstrated an increased effectiveness, evidenced by complete responses on two PDX models *in vivo*
7. Clinical grade manufacturing of p95HER2.CAR-TECH2Me under GMP conditions yields a product comparable to our preclinically produced cellular therapy product.
8. p95HER2.CAR-TECH2Me T cells represent a good balance between safety and efficacy, warranting application for a phase I clinical trial approval to the AEMPS.

Bibliography

1. Yarden Y, Sliwkowski MX (2001) Untangling the ErbB signalling network. Nat Rev Mol Cell Biol 2:127–137

2. Zhang X, Gureasko J, Shen K, Cole PA, Kuriyan J (2006) An Allosteric Mechanism for Activation of the Kinase Domain of Epidermal Growth Factor Receptor. Cell 125:1137–1149

3. Olayioye MA (2001) Intracellular signaling pathways of ErbB2/HER-2 and family members. Breast Cancer Res 3:385

4. Arteaga CL, Engelman JA (2014) ERBB Receptors: From Oncogene Discovery to Basic Science to Mechanism-Based Cancer Therapeutics. Cancer Cell 25:282–303

5. Cho H-S, Mason K, Ramyar KX, Stanley AM, Gabelli SB, Denney DW, Leahy DJ (2003) Structure of the extracellular region of HER2 alone and in complex with the Herceptin Fab. Nature 421:756–760

6. Baselga J, Swain SM (2009) Novel anticancer targets: revisiting ERBB2 and discovering ERBB3. Nat Rev Cancer 9:463–475

7. Iqbal N, Iqbal N (2014) Human Epidermal Growth Factor Receptor 2 (HER2) in Cancers: Overexpression and Therapeutic Implications. Mol Biol Int 2014:852748

8. Marchiò C, Annaratone L, Marques A, Casorzo L, Berrino E, Sapino A (2021) Evolving concepts in HER2 evaluation in breast cancer: Heterogeneity, HER2-low carcinomas and beyond. Semin Cancer Biol 72:123–135

9. Slamon DJ, Clark GM, Wong SG, Levin WJ, Ullrich A, McGuire WL (1987) Human Breast Cancer: Correlation of Relapse and Survival with Amplification of the HER-2/neu Oncogene. Science 235:177–182

10. Hanahan D (2022) Hallmarks of Cancer: New Dimensions. Cancer Discov 12:31–46

11. Olayioye MA, Neve RM, Lane HA, Hynes NE (2000) The ErbB signaling network: receptor heterodimerization in development and cancer. EMBO J 19:3159–3167

12. Yarden Y, Pines G (2012) The ERBB network: at last, cancer therapy meets systems biology. Nat Rev Cancer 12:553–563

13. Yan M, Schwaederle M, Arguello D, Millis SZ, Gatalica Z, Kurzrock R (2015) HER2 expression status in diverse cancers: review of results from 37,992 patients. Cancer Metastasis Rev 34:157–164

14. Oh D-Y, Bang Y-J (2020) HER2-targeted therapies — a role beyond breast cancer. Nat Rev Clin Oncol 17:33–48

15. Yan M, Parker BA, Schwab R, Kurzrock R (2014) HER2 aberrations in cancer: Implications for therapy. Cancer Treat Rev 40:770–780

16. Amisha F, Malik P, Saluja P, Gautam N, Patel TH, Roy AM, Singh SRK, Malapati SJ (2023) A Comprehensive Review on the Role of Human Epidermal Growth Factor Receptor 2 (HER2) as a Biomarker in Extra-Mammary and Extra-Gastric Cancers. Onco 3:96–124

17. Arya N, Saha S (2021) Multi-modal advanced deep learning architectures for breast cancer survival prediction. Knowl-Based Syst 221:106965

18. Perou CM, Sørlie T, Eisen MB, et al (2000) Molecular portraits of human breast tumours. Nature 406:747–752

19. Harbeck N, Penault-Llorca F, Cortes J, Gnant M, Houssami N, Poortmans P, Ruddy K, Tsang J, Cardoso F (2019) Breast cancer. Nat Rev Dis Prim 5:66

20. Kennecke H, Yerushalmi R, Woods R, Cheang MCU, Voduc D, Speers CH, Nielsen TO, Gelmon K (2010) Metastatic Behavior of Breast Cancer Subtypes. J Clin Oncol 28:3271–3277

21. Cortesi L, Rugo HS, Jackisch C (2021) An Overview of PARP Inhibitors for the Treatment of Breast Cancer. Target Oncol 16:255–282

22. Bianchini G, Angelis CD, Licata L, Gianni L (2022) Treatment landscape of triple-negative breast cancer — expanded options, evolving needs. Nat Rev Clin Oncol 19:91–113

23. Dri A, Arpino G, Bianchini G, et al (2024) Breaking barriers in triple negative breast cancer (TNBC) – Unleashing the power of antibody-drug conjugates (ADCs). Cancer Treat Rev 123:102672

24. Won K-A, Spruck C (2020) Triple-negative breast cancer therapy: Current and future perspectives (Review). Int J Oncol 57:1245–1261

25. Baselga J, Bradbury I, Eidtmann H, et al (2012) Lapatinib with trastuzumab for HER2-positive early breast cancer (NeoALTTO): a randomised, open-label, multicentre, phase 3 trial. Lancet 379:633–640

26. Banerji U, Herpen CML van, Saura C, et al (2019) Trastuzumab duocarmazine in locally advanced and metastatic solid tumours and HER2-expressing breast cancer: a phase 1 dose-escalation and dose-expansion study. Lancet Oncol 20:1124–1135

27. Modi S, Jacot W, Yamashita T, et al (2022) Trastuzumab Deruxtecan in Previously Treated HER2-Low Advanced Breast Cancer. N Engl J Med 387:9–20

28. Tarantino P, Hamilton E, Tolaney SM, et al (2020) HER2-Low Breast Cancer: Pathological and Clinical Landscape. J Clin Oncol 38:1951–1962

29. Goldhirsch A, Wood WC, Coates AS, Gelber RD, Thürlimann B, Senn H-J, members P (2011) Strategies for subtypes—dealing with the diversity of breast cancer: highlights of the St Gallen International Expert Consensus on the Primary Therapy of Early Breast Cancer 2011. Ann Oncol 22:1736–1747

30. Cardoso F, Senkus E, Costa A, et al (2018) 4th ESO–ESMO International Consensus Guidelines for Advanced Breast Cancer (ABC 4) † † These guidelines were

developed by the European School of Oncology (ESO) and the European Society for Medical Oncology (ESMO). Ann Oncol 29:1634–1657

31. Verde NL, Collovà E, Blasi L, et al (2021) Overall Survival in Metastatic Breast Cancer Patients in the Third Millennium: Results of the COSMO Study∗. Clin Breast Cancer 21:e489–e496

32. Gobbini E, Ezzalfani M, Dieras V, et al (2018) Time trends of overall survival among metastatic breast cancer patients in the real-life ESME cohort. Eur J Cancer 96:17–24

33. Buonomo OC, Caredda E, Portarena I, Vanni G, Orlandi A, Bagni C, Petrella G, Palombi L, Orsaria P (2017) New insights into the metastatic behavior after breast cancer surgery, according to well-established clinicopathological variables and molecular subtypes. PLoS ONE 12:e0184680

34. Li B, Zhang F, Niu Q, Liu J, Yu Y, Wang P, Zhang S, Zhang H, Wang Z (2023) A molecular classification of gastric cancer associated with distinct clinical outcomes and validated by an XGBoost-based prediction model. Mol Ther - Nucleic Acids 31:224–240

35. Smyth EC, Nilsson M, Grabsch HI, Grieken NC van, Lordick F (2020) Gastric cancer. Lancet 396:635–648

36. Gravalos C, Jimeno A (2008) HER2 in gastric cancer: a new prognostic factor and a novel therapeutic target. Ann Oncol 19:1523–1529

37. Slamon DJ, Leyland-Jones B, Shak S, et al (2001) Use of chemotherapy plus a monoclonal antibody against HER2 for metastatic breast cancer that overexpresses HER2. N Engl J Med 344:783–92

38. Loibl S, Poortmans P, Morrow M, Denkert C, Curigliano G (2021) Breast cancer. Lancet 397:1750–1769

39. Klapper LN, Waterman H, Sela M, Yarden Y (2000) Tumor-inhibitory antibodies to HER-2/ErbB-2 may act by recruiting c-Cbl and enhancing ubiquitination of HER-2. Cancer Res 60:3384–8

40. Petricevic B, Laengle J, Singer J, Sachet M, Fazekas J, Steger G, Bartsch R, Jensen-Jarolim E, Bergmann M (2013) Trastuzumab mediates antibody-dependent cell-mediated cytotoxicity and phagocytosis to the same extent in both adjuvant and metastatic HER2/neu breast cancer patients. J Transl Med 11:307

41. Boross P, Leusen JHW (2012) Boosting antibody therapy with complement. Blood 119:5945–5947

42. Tsao L-C, Crosby EJ, Trotter TN, et al (2022) Trastuzumab/Pertuzumab combination therapy stimulates anti-tumor responses through complement-dependent cytotoxicity and phagocytosis. JCI Insight 7:e155636

43. Sakai K, Yokote H, Murakami-Murofushi K, Tamura T, Saijo N, Nishio K (2007) Pertuzumab, a novel HER dimerization inhibitor, inhibits the growth of human lung cancer cells mediated by the HER3 signaling pathway. Cancer Sci 98:1498–1503

44. Swain SM, Baselga J, Kim S-B, et al (2015) Pertuzumab, Trastuzumab, and Docetaxel in HER2-Positive Metastatic Breast Cancer. N Engl J Med 372:724–734

45. Minckwitz G von, Procter M, Azambuja E de, et al (2017) Adjuvant Pertuzumab and Trastuzumab in Early HER2-Positive Breast Cancer. N Engl J Med 377:122–131

46. Martínez-Sáez O, Prat A (2021) Current and Future Management of HER2-Positive Metastatic Breast Cancer. JCO Oncol Pr 17:594–604

47. Yu AF, Dang CT, Jorgensen J, Moskowitz CS, DeFusco P, Oligino E, Oeffinger KC, Liu JE, Steingart RM (2023) Rationale and design of a cardiac safety study for reduced cardiotoxicity surveillance during HER2-targeted therapy. Cardio-Oncol 9:13

48. Phillips GDL, Li G, Dugger DL, et al (2008) Targeting HER2-Positive Breast Cancer with Trastuzumab-DM1, an Antibody–Cytotoxic Drug Conjugate. Cancer Res 68:9280–9290

49. Ferraro E, Drago JZ, Modi S (2021) Implementing antibody-drug conjugates (ADCs) in HER2-positive breast cancer: state of the art and future directions. Breast Cancer Res 23:84

50. Verma S, Miles D, Gianni L, et al (2012) Trastuzumab Emtansine for HER2-Positive Advanced Breast Cancer. N Engl J Med 367:1783–1791

51. Williamson M, Press DJ, Hansen SA, Tomar A, Jhuti GS, Revil C, Gururaj K (2024) Population-level impact of adjuvant trastuzumab emtansine on the incidence of metastatic breast cancer: an epidemiological prediction model of women with HER2-positive early breast cancer and residual disease following neoadjuvant therapy. Breast Cancer 31:84–95

52. Modi S, Saura C, Yamashita T, et al (2019) Trastuzumab Deruxtecan in Previously Treated HER2-Positive Breast Cancer. N Engl J Med 382:610–621

53. Modi S, Jacot W, Yamashita T, et al (2022) Trastuzumab Deruxtecan in Previously Treated HER2-Low Advanced Breast Cancer. N Engl J Med 387:9–20

54. Li BT, Smit EF, Goto Y, et al (2021) Trastuzumab Deruxtecan in HER2-Mutant Non–Small-Cell Lung Cancer. N Engl J Med 386:241–251

55. Bartsch R, Berghoff AS, Furtner J, et al (2022) Trastuzumab deruxtecan in HER2-positive breast cancer with brain metastases: a single-arm, phase 2 trial. Nat Med 28:1840–1847

56. Tarantino P, Ricciuti B, Pradhan SM, Tolaney SM (2023) Optimizing the safety of antibody–drug conjugates for patients with solid tumours. Nat Rev Clin Oncol 20:558–576

57. Duro-Sánchez S, Alonso MR, Arribas J (2023) Immunotherapies against HER2-Positive Breast Cancer. Cancers 15:1069

58. Morikawa A, Peereboom DM, Thorsheim HR, et al (2015) Capecitabine and lapatinib uptake in surgically resected brain metastases from metastatic breast cancer patients: a prospective study. Neuro-Oncol 17:289–295

59. Fernandez-Martinez A, Krop IE, Hillman DW, et al (2020) Survival, Pathologic Response, and Genomics in CALGB 40601 (Alliance), a Neoadjuvant Phase III Trial of Paclitaxel-Trastuzumab With or Without Lapatinib in HER2-Positive Breast Cancer. J Clin Oncol 38:4184–4193

60. Yuan Y, Liu X, Cai Y, Li W (2022) Lapatinib and lapatinib plus trastuzumab therapy versus trastuzumab therapy for HER2 positive breast cancer patients: an updated systematic review and meta-analysis. Syst Rev 11:264

61. Pivot X, Manikhas A, Żurawski B, et al (2015) CEREBEL (EGF111438): A Phase III, Randomized, Open-Label Study of Lapatinib Plus Capecitabine Versus Trastuzumab Plus Capecitabine in Patients With Human Epidermal Growth Factor Receptor 2–Positive Metastatic Breast Cancer. J Clin Oncol 33:1564–1573

62. Gelmon KA, Boyle FM, Kaufman B, et al (2015) Lapatinib or Trastuzumab Plus Taxane Therapy for Human Epidermal Growth Factor Receptor 2–Positive Advanced Breast Cancer: Final Results of NCIC CTG MA.31. J Clin Oncol 33:1574–1583

63. Burstein HJ, Sun Y, Dirix LY, et al (2010) Neratinib, an Irreversible ErbB Receptor Tyrosine Kinase Inhibitor, in Patients With Advanced ErbB2-Positive Breast Cancer. J Clin Oncol 28:1301–1307

64. Martin M, Holmes FA, Ejlertsen B, et al (2017) Neratinib after trastuzumab-based adjuvant therapy in HER2-positive breast cancer (ExteNET): 5-year analysis of a randomised, double-blind, placebo-controlled, phase 3 trial. Lancet Oncol 18:1688–1700

65. Dhillon S (2019) Neratinib in Early-Stage Breast Cancer: A Profile of Its Use in the EU. Clin Drug Investig 39:221–229

66. Saura C, Oliveira M, Feng Y-H, et al (2020) Neratinib Plus Capecitabine Versus Lapatinib Plus Capecitabine in HER2-Positive Metastatic Breast Cancer Previously Treated With ≥ 2 HER2-Directed Regimens: Phase III NALA Trial. J Clin Oncol 38:3138–3149

67. Kulukian A, Lee P, Taylor J, Rosler R, Vries P de, Watson D, Forero-Torres A, Peterson S (2020) Preclinical Activity of HER2-Selective Tyrosine Kinase Inhibitor Tucatinib as a Single Agent or in Combination with Trastuzumab or Docetaxel in Solid Tumor Models. Mol Cancer Ther 19:976–987

68. Murthy RK, Loi S, Okines A, et al (2019) Tucatinib, Trastuzumab, and Capecitabine for HER2-Positive Metastatic Breast Cancer. N Engl J Med 382:597–609

69. Schlam I, Swain SM (2021) HER2-positive breast cancer and tyrosine kinase inhibitors: the time is now. npj Breast Cancer 7:56

70. Sunder SS, Sharma UC, Pokharel S (2023) Adverse effects of tyrosine kinase inhibitors in cancer therapy: pathophysiology, mechanisms and clinical management. Signal Transduct Target Ther 8:262

71. Yang J, Ju J, Guo L, et al (2022) Prediction of HER2-positive breast cancer recurrence and metastasis risk from histopathological images and clinical information via multimodal deep learning. Comput Struct Biotechnol J 20:333–342

72. Gámez-Chiachio M, Sarrió D, Moreno-Bueno G (2022) Novel Therapies and Strategies to Overcome Resistance to Anti-HER2-Targeted Drugs. Cancers 14:4543

73. Arribas J, Parra-Palau JL, Pedersen K (2010) HER2 Fragmentation and Breast Cancer Stratification. Clin Cancer Res 16:4071–4073

74. Díaz-Rodríguez E, Gandullo-Sánchez L, Ocaña A, Pandiella A (2021) Novel ADCs and Strategies to Overcome Resistance to Anti-HER2 ADCs. Cancers 14:154

75. Arribas J, Baselga J, Pedersen K, Parra-Palau JL (2011) p95HER2 and Breast Cancer. Cancer Res 71:1515–1519

76. Yuan C-X, Lasut AL, Wynn R, Neff NT, Hollis GF, Ramaker ML, Rupar MJ, Liu P, Meade R (2003) Purification of Her-2 extracellular domain and identification of its cleavage site. Protein Expr Purif 29:217–222

77. Anido J, Scaltriti M, Serra JJB, Josefat BS, Todo FR, Baselga J, Arribas J (2006) Biosynthesis of tumorigenic HER2 C-terminal fragments by alternative initiation of translation. EMBO J 25:3234–3244

78. García-Castillo J, Pedersen K, Angelini P-D, Bech-Serra JJ, Colomé N, Cunningham MP, Parra-Palau JL, Canals F, Baselga J, Arribas J (2009) HER2 Carboxyl-terminal Fragments Regulate Cell Migration and Cortactin Phosphorylation*. J Biol Chem 284:25302–25313

79. Pedersen K, Angelini P-D, Laos S, et al (2009) A Naturally Occurring HER2 Carboxy-Terminal Fragment Promotes Mammary Tumor Growth and Metastasis. Mol Cell Biol 29:3319–3331

80. Chumsri S, Sperinde J, Liu H, et al (2018) High p95HER2/HER2 Ratio Associated With Poor Outcome in Trastuzumab-Treated HER2-Positive Metastatic Breast Cancer NCCTG N0337 and NCCTG 98-32-52 (Alliance). Clin Cancer Res 24:clincanres.1864.2017

81. Parra-Palau JL, Pedersen K, Peg V, et al (2010) A Major Role of p95/611-CTF, a Carboxy-Terminal Fragment of HER2, in the Down-modulation of the Estrogen Receptor in HER2-Positive Breast Cancers. Cancer Res 70:8537–8546

82. Scaltriti M, Rojo F, Ocaña A, et al (2007) Expression of p95HER2, a truncated form of the HER2 receptor, and response to anti-HER2 therapies in breast cancer. J Natl Cancer Inst 99:628–38

83. Loibl S, Bruey J, Minckwitz GV, et al (2011) Validation of p95 as a predictive marker for trastuzumab-based therapy in primary HER2-positive breast cancer: A translational investigation from the neoadjuvant GeparQuattro study. J Clin Oncol 29:530–530

84. Parra-Palau JL, Morancho B, Peg V, et al (2014) Effect of p95HER2/611CTF on the Response to Trastuzumab and Chemotherapy. JNCI: J Natl Cancer Inst.

85. Sperinde J, Huang W, Vehtari A, et al (2018) p95HER2 Methionine 611 Carboxy-Terminal Fragment Is Predictive of Trastuzumab Adjuvant Treatment Benefit in the FinHer Trial. Clin Cancer Res 24:3046–3052

86. Guix M, Aura C, Jimenez J, et al (2009) Lapatinib is active in patients with HER2-amplified breast tumors expressing p95HER2. Cancer Res 69:708

87. Ruiz IR, Vicario R, Morancho B, et al (2018) p95HER2–T cell bispecific antibody for breast cancer treatment. Sci Transl Med.

88. Sperinde J, Jin X, Banerjee J, et al (2010) Quantitation of p95HER2 in Paraffin Sections by Using a p95-Specific Antibody and Correlation with Outcome in a Cohort of Trastuzumab-Treated Breast Cancer Patients. Clin Cancer Res 16:4226–4235

89. Cappuzzo F, Cho YG, Sacconi A, et al (2012) p95HER2 Truncated Form in Resected Non-small Cell Lung Cancer. J Thorac Oncol 7:520–527

90. Growdon WB, Groeneweg J, Byron V, et al (2015) HER2 over-expressing high grade endometrial cancer expresses high levels of p95HER2 variant. Gynecol Oncol 137:160–166

91. Smet CD, Lurquin C, Plaen ED, Brasseur F, Zarour H, Backer OD, Coulie PG, Boon T (1997) Genes coding for melanoma antigens recognised by cytolytic T lymphocytes. Eye 11:243–248

92. Alexandrov LB, Nik-Zainal S, Wedge DC, et al (2013) Signatures of mutational processes in human cancer. Nature 500:415–421

93. Chen DS, Mellman I (2017) Elements of cancer immunity and the cancer–immune set point. Nature 541:321–330

94. Schumacher TN, Schreiber RD (2015) Neoantigens in cancer immunotherapy. Science 348:69–74

95. Mellman I, Steinman RM (2001) Dendritic Cells Specialized and Regulated Antigen Processing Machines. Cell 106:255–258

96. Speiser DE, Chijioke O, Schaeuble K, Münz C (2023) CD4+ T cells in cancer. Nat Cancer 4:317–329

97. Chen DS, Mellman I (2013) Oncology Meets Immunology: The Cancer-Immunity Cycle. Immunity 39:1–10

98. Galon J, Bruni D (2020) Tumor Immunology and Tumor Evolution: Intertwined Histories. Immunity 52:55–81

99. Smith-Garvin JE, Koretzky GA, Jordan MS (2009) T Cell Activation. Immunology 27:591–619

100. Onnis A, Baldari CT (2019) Orchestration of Immunological Synapse Assembly by Vesicular Trafficking. Front Cell Dev Biol 7:110

101. Dustin ML (2014) The Immunological Synapse. Cancer Immunol Res 2:1023–1033

102. Rudd CE (2023) CD8+ T cell killing of MHC class I–deficient tumors. Nat Cancer 4:1214–1216

103. Chen L, Flies DB (2013) Molecular mechanisms of T cell co-stimulation and co-inhibition. Nat Rev Immunol 13:227–242

104. Schnell A, Bod L, Madi A, Kuchroo VK (2020) The yin and yang of co-inhibitory receptors: toward anti-tumor immunity without autoimmunity. Cell Res 30:285–299

105. Curtsinger JM, Mescher MF (2010) Inflammatory cytokines as a third signal for T cell activation. Curr Opin Immunol 22:333–340

106. Schroder K, Hertzog PJ, Ravasi T, Hume DA (2004) Interferon-γ: an overview of signals, mechanisms and functions. J Leukoc Biol 75:163–189

107. Golstein P, Griffiths GM (2018) An early history of T cell-mediated cytotoxicity. Nat Rev Immunol 18:527–535

108. O'Donnell JS, Teng MWL, Smyth MJ (2019) Cancer immunoediting and resistance to T cell-based immunotherapy. Nat Rev Clin Oncol 16:151–167

109. Dunn GP, Bruce AT, Ikeda H, Old LJ, Schreiber RD (2002) Cancer immunoediting: from immunosurveillance to tumor escape. Nat Immunol 3:991–998

110. Smyth MJ, Dunn GP, Schreiber RD (2006) Cancer Immunosurveillance and Immunoediting: The Roles of Immunity in Suppressing Tumor Development and Shaping Tumor Immunogenicity. Adv Immunol 90:1–50

111. Labani-Motlagh A, Ashja-Mahdavi M, Loskog A (2020) The Tumor Microenvironment: A Milieu Hindering and Obstructing Antitumor Immune Responses. Front Immunol 11:940

112. Hinshaw DC, Shevde LA (2019) The Tumor Microenvironment Innately Modulates Cancer Progression. Cancer Res 79:4557–4566

113. Beatty GL, Gladney WL (2015) Immune Escape Mechanisms as a Guide for Cancer Immunotherapy. Clin Cancer Res 21:687–692

114. Spranger S, Gajewski TF (2017) Mechanisms of Tumor Cell—Intrinsic Immune Evasion. Annu Rev Cancer Biol 2:1–16

115. Bates JP, Derakhshandeh R, Jones L, Webb TJ (2018) Mechanisms of immune evasion in breast cancer. BMC Cancer 18:556

116. Shiravand Y, Khodadadi F, Kashani SMA, Hosseini-Fard SR, Hosseini S, Sadeghirad H, Ladwa R, O'Byrne K, Kulasinghe A (2022) Immune Checkpoint Inhibitors in Cancer Therapy. Curr Oncol 29:3044–3060

117. Dhatchinamoorthy K, Colbert JD, Rock KL (2021) Cancer Immune Evasion Through Loss of MHC Class I Antigen Presentation. Front Immunol 12:636568

118. Sade-Feldman M, Jiao YJ, Chen JH, et al (2017) Resistance to checkpoint blockade therapy through inactivation of antigen presentation. Nat Commun 8:1136

119. Martínez-Sabadell A, Morancho B, Ruiz IR, et al (2022) The target antigen determines the mechanism of acquired resistance to T cell-based therapies. Cell Rep 41:111430

120. Mocikat R, Braumüller H, Gumy A, et al (2003) Natural Killer Cells Activated by MHC Class ILow Targets Prime Dendritic Cells to Induce Protective CD8 T Cell Responses. Immunity 19:561–569

121. Choi S, Schwartz RH (2011) Impairment of Immunological Synapse Formation in Adaptively Tolerant T Cells. J Immunol 187:805–816

122. Shin DS, Zaretsky JM, Escuin-Ordinas H, et al (2017) Primary Resistance to PD-1 Blockade Mediated by JAK1/2 Mutations. Cancer Discov 7:188–201

123. Freeman AJ, Vervoort SJ, Michie J, Ramsbottom KM, Silke J, Kearney CJ, Oliaro J (2021) HOIP limits anti-tumor immunity by protecting against combined TNF and IFN-gamma-induced apoptosis. EMBO Rep 22:e53391

124. Kearney CJ, Lalaoui N, Freeman AJ, Ramsbottom KM, Silke J, Oliaro J (2017) PD-L1 and IAPs co-operate to protect tumors from cytotoxic lymphocyte-derived TNF. Cell Death Differ 24:1705–1716

125. Falcomatà C, Bärthel S, Schneider G, Rad R, Schmidt-Supprian M, Saur D (2023) Context-Specific Determinants of the Immunosuppressive Tumor Microenvironment in Pancreatic Cancer. Cancer Discov 13:OF1–OF20

126. Zhang S, Fang W, Zhou S, et al (2023) Single cell transcriptomic analyses implicate an immunosuppressive tumor microenvironment in pancreatic cancer liver metastasis. Nat Commun 14:5123

127. Egen JG, Ouyang W, Wu LC (2020) Human Anti-tumor Immunity: Insights from Immunotherapy Clinical Trials. Immunity 52:36–54

128. Zhang Y, Zhang Z (2020) The history and advances in cancer immunotherapy: understanding the characteristics of tumor-infiltrating immune cells and their therapeutic implications. Cell Mol Immunol 17:807–821

129. Saxena M, Burg SH van der, Melief CJM, Bhardwaj N (2021) Therapeutic cancer vaccines. Nat Rev Cancer 21:360–378

130. Andtbacka RHI, Kaufman HL, Collichio F, et al (2015) Talimogene Laherparepvec Improves Durable Response Rate in Patients With Advanced Melanoma. J Clin Oncol 33:2780–2788

131. Rosenberg SA, Mulé JJ, Spiess PJ, Reichert CM, Schwarz SL (1985) Regression of established pulmonary metastases and subcutaneous tumor mediated by the systemic administration of high-dose recombinant interleukin 2. J Exp Med 161:1169–1188

132. Leukemia ICSG on CM, Tura S, Baccarani M, Zuffa E, Russo D, Fanin R, Zaccaria A, Fiacchini M (1994) Interferon Alfa-2a as Compared with Conventional Chemotherapy for the Treatment of Chronic Myeloid Leukemia. N Engl J Med 330:820–825

133. Kirkwood JM, Strawderman MH, Ernstoff MS, Smith TJ, Borden EC, Blum RH (1996) Interferon alfa-2b adjuvant therapy of high-risk resected cutaneous melanoma: the Eastern Cooperative Oncology Group Trial EST 1684. J Clin Oncol 14:7–17

134. Berraondo P, Sanmamed MF, Ochoa MC, Etxeberria I, Aznar MA, Pérez-Gracia JL, Rodríguez-Ruiz ME, Ponz-Sarvise M, Castañón E, Melero I (2019) Cytokines in clinical cancer immunotherapy. Br J Cancer 120:6–15

135. Conlon KC, Miljkovic MD, Waldmann TA (2019) Cytokines in the Treatment of Cancer. J Interf Cytokine Res 39:6–21

136. Choi Y, Shi Y, Haymaker CL, Naing A, Ciliberto G, Hajjar J (2020) T-cell agonists in cancer immunotherapy. J Immunother Cancer 8:e000966

137. Melero I, Tanos T, Bustamante M, et al (2023) A first-in-human study of the fibroblast activation protein–targeted, 4-1BB agonist RO7122290 in patients with advanced solid tumors. Sci Transl Med 15:eabp9229

138. Claus C, Ferrara C, Xu W, et al (2019) Tumor-targeted 4-1BB agonists for combination with T cell bispecific antibodies as off-the-shelf therapy. Sci Transl Med.

139. Darvin P, Toor SM, Nair VS, Elkord E (2018) Immune checkpoint inhibitors: recent progress and potential biomarkers. Exp Mol Med 50:1–11

140. Abdou Y, Goudarzi A, Yu JX, Upadhaya S, Vincent B, Carey LA (2022) Immunotherapy in triple negative breast cancer: beyond checkpoint inhibitors. npj Breast Cancer 8:121

141. Marin-Acevedo JA, Kimbrough EO, Lou Y (2021) Next generation of immune checkpoint inhibitors and beyond. J Hematol Oncol 14:45

142. Cristescu R, Mogg R, Ayers M, et al (2018) Pan-tumor genomic biomarkers for PD-1 checkpoint blockade–based immunotherapy. Science.

143. Dhasmana A, Dhasmana S, Haque S, Cobos E, Yallapu MM, Chauhan SC (2023) Next-generation immune checkpoint inhibitors as promising functional molecules in cancer therapeutics. Cancer Metastasis Rev 42:597–600

144. Rosenberg SA, Packard BS, Aebersold PM, et al (1988) Use of Tumor-Infiltrating Lymphocytes and Interleukin-2 in the Immunotherapy of Patients with Metastatic Melanoma. N Engl J Med 319:1676–1680

145. Wang S, Sun J, Chen K, et al (2021) Perspectives of tumor-infiltrating lymphocyte treatment in solid tumors. BMC Med 19:140

146. Rosenberg SA, Yang JC, Sherry RM, et al (2011) Durable Complete Responses in Heavily Pretreated Patients with Metastatic Melanoma Using T-Cell Transfer Immunotherapy. Clin Cancer Res 17:4550–4557

147. Stevanović S, Helman SR, Wunderlich JR, et al (2019) A Phase II Study of Tumor-infiltrating Lymphocyte Therapy for Human Papillomavirus–associated Epithelial Cancers. Clin Cancer Res 25:1486–1493

148. Creelan BC, Wang C, Teer JK, et al (2021) Tumor-infiltrating lymphocyte treatment for anti-PD-1-resistant metastatic lung cancer: a phase 1 trial. Nat Med 27:1410–1418

149. Eric T, F. RP, Yong-Chen L, et al (2016) T-Cell Transfer Therapy Targeting Mutant KRAS in Cancer. N Engl J Med 375:2255–2262

150. Zacharakis N, Chinnasamy H, Black M, et al (2018) Immune recognition of somatic mutations leading to complete durable regression in metastatic breast cancer. Nat Med 24:724–730

151. Morgan RA, Dudley ME, Wunderlich JR, et al (2006) Cancer Regression in Patients After Transfer of Genetically Engineered Lymphocytes. Science 314:126–129

152. Morgan RA, Chinnasamy N, Abate-Daga D, et al (2013) Cancer Regression and Neurological Toxicity Following Anti-MAGE-A3 TCR Gene Therapy. J Immunother 36:133–151

153. Parkhurst MR, Yang JC, Langan RC, et al (2011) T Cells Targeting Carcinoembryonic Antigen Can Mediate Regression of Metastatic Colorectal Cancer but Induce Severe Transient Colitis. Mol Ther 19:620–626

154. Morgan RA, Yang JC, Kitano M, Dudley ME, Laurencot CM, Rosenberg SA (2010) Case Report of a Serious Adverse Event Following the Administration of T Cells Transduced With a Chimeric Antigen Receptor Recognizing ERBB2. Mol Ther 18:843–851

155. Kunert A, Straetemans T, Govers C, Lamers C, Mathijssen R, Sleijfer S, Debets R (2013) TCR-Engineered T Cells Meet New Challenges to Treat Solid Tumors: Choice of Antigen, T Cell Fitness, and Sensitization of Tumor Milieu. Front Immunol 4:363

156. Jones HF, Molvi Z, Klatt MG, Dao T, Scheinberg DA (2021) Empirical and Rational Design of T Cell Receptor-Based Immunotherapies. Front Immunol 11:585385

157. Edeline J, Houot R, Marabelle A, Alcantara M (2021) CAR-T cells and BiTEs in solid tumors: challenges and perspectives. J Hematol Oncol 14:65

158. Inoue M, Mimura K, Izawa S, et al (2012) Expression of MHC Class I on breast cancer cells correlates inversely with HER2 expression. OncoImmunology 1:1104–1110

159. Roda-Navarro P, Álvarez-Vallina L (2020) Understanding the Spatial Topology of Artificial Immunological Synapses Assembled in T Cell-Redirecting Strategies: A Major Issue in Cancer Immunotherapy. Front Cell Dev Biol 7:370

160. Benmebarek M-R, Karches CH, Cadilha BL, Lesch S, Endres S, Kobold S (2019) Killing Mechanisms of Chimeric Antigen Receptor (CAR) T Cells. Int J Mol Sci 20:1283

161. Einsele H, Borghaei H, Orlowski RZ, Subklewe M, Roboz GJ, Zugmaier G, Kufer P, Iskander K, Kantarjian HM (2020) The BiTE (bispecific T-cell engager) platform: Development and future potential of a targeted immuno-oncology therapy across tumor types. Cancer 126:3192–3201

162. Kebenko M, Goebeler M-E, Wolf M, et al (2018) A multicenter phase 1 study of solitomab (MT110, AMG 110), a bispecific EpCAM/CD3 T-cell engager (BiTE®) antibody construct, in patients with refractory solid tumors. OncoImmunology 7:e1450710

163. Thistlethwaite FC, Gilham DE, Guest RD, et al (2017) The clinical efficacy of first-generation carcinoembryonic antigen (CEACAM5)-specific CAR T cells is limited by poor persistence and transient pre-conditioning-dependent respiratory toxicity. Cancer Immunol, Immunother 66:1425–1436

164. Liu X, Jiang S, Fang C, et al (2015) Affinity-Tuned ErbB2 or EGFR Chimeric Antigen Receptor T Cells Exhibit an Increased Therapeutic Index against Tumors in Mice. Cancer Res 75:3596–3607

165. Slaga D, Ellerman D, Lombana TN, et al (2018) Avidity-based binding to HER2 results in selective killing of HER2-overexpressing cells by anti-HER2/CD3. Sci Transl Med.

166. Staflin K, Zafra CLZ de, Schutt LK, et al (2020) Target arm affinities determine preclinical efficacy and safety of anti-HER2/CD3 bispecific antibody. JCI Insight 5:e133757

167. Maus MV, Alexander S, Bishop MR, et al (2020) Society for Immunotherapy of Cancer (SITC) clinical practice guideline on immune effector cell-related adverse events. J Immunother Cancer 8:e001511

168. Santomasso B, Bachier C, Westin J, Rezvani K, Shpall EJ (2019) The Other Side of CAR T-Cell Therapy: Cytokine Release Syndrome, Neurologic Toxicity, and Financial Burden. Am Soc Clin Oncol Educ Book 39:433–444

169. Tiller KE, Tessier PM (2014) Advances in Antibody Design. Annu Rev Biomed Eng 17:1–26

170. Staerz UD, Kanagawa O, Bevan MJ (1985) Hybrid antibodies can target sites for attack by T cells. Nature 314:628–31

171. Baeuerle PA, Reinhardt C (2009) Bispecific T-Cell Engaging Antibodies for Cancer Therapy. Cancer Res 69:4941–4944

172. Tapia-Galisteo A, Álvarez-Vallina L, Sanz L (2023) Bi- and trispecific immune cell engagers for immunotherapy of hematological malignancies. J Hematol Oncol 16:83

173. Wilkinson I, Anderson S, Fry J, Julien LA, Neville D, Qureshi O, Watts G, Hale G (2021) Fc-engineered antibodies with immune effector functions completely abolished. PLoS ONE 16:e0260954

174. Goebeler M-E, Bargou RC (2020) T cell-engaging therapies — BiTEs and beyond. Nat Rev Clin Oncol 17:418–434

175. Li H, Saw PE, Song E (2020) Challenges and strategies for next-generation bispecific antibody-based antitumor therapeutics. Cell Mol Immunol 17:451–461

176. Allen C, Zeidan AM, Bewersdorf JP (2021) BiTEs, DARTS, BiKEs and TriKEs—Are Antibody Based Therapies Changing the Future Treatment of AML? Life 11:465

177. Hagop K, Anthony S, Nicola G, et al (2017) Blinatumomab versus Chemotherapy for Advanced Acute Lymphoblastic Leukemia. N Engl J Med 376:836–847

178. Moreau P, Garfall AL, Donk NWCJ van de, et al (2022) Teclistamab in Relapsed or Refractory Multiple Myeloma. N Engl J Med 387:495–505

179. Nathan P, Hassel JC, Rutkowski P, et al (2021) Overall Survival Benefit with Tebentafusp in Metastatic Uveal Melanoma. N Engl J Med 385:1196–1206

180. Elgundi Z, Reslan M, Cruz E, Sifniotis V, Kayser V (2017) The state-of-play and future of antibody therapeutics. Adv Drug Deliv Rev 122:2–19

181. Goebeler M-E, Knop S, Viardot A, et al (2016) Bispecific T-Cell Engager (BiTE) Antibody Construct Blinatumomab for the Treatment of Patients With Relapsed/Refractory Non-Hodgkin Lymphoma: Final Results From a Phase I Study. J Clin Oncol 34:1104–1111

182. Heidbuechel JPW, Engeland CE (2021) Oncolytic viruses encoding bispecific T cell engagers: a blueprint for emerging immunovirotherapies. J Hematol Oncol 14:63

183. Speck T, Heidbuechel JP, Veinalde R, Jaeger D, Kalle C von, Ball CR, Ungerechts G, Engeland CE (2018) Targeted BiTE expression by an oncolytic vector augments therapeutic efficacy against solid tumors. Clin Cancer Res 24:clincanres.2651.2017

184. Compte M, Blanco B, Serrano F, Cuesta ÁM, Sanz L, Bernad A, Holliger P, Álvarez-Vallina L (2007) Inhibition of tumor growth in vivo by in situ secretion of bispecific anti-CEA × anti-CD3 diabodies from lentivirally transduced human lymphocytes. Cancer Gene Ther 14:380–388

185. Bonifant CL, Szoor A, Torres D, et al (2016) CD123-Engager T Cells as a Novel Immunotherapeutic for Acute Myeloid Leukemia. Mol Ther 24:1615–1626

186. Díez-Alonso L, Falgas A, Arroyo-Ródenas J, et al (2024) Engineered T cells secreting anti-BCMA T cell engagers control multiple myeloma and promote immune memory in vivo. Sci Transl Med 16:eadg7962

187. Yin Y, Rodriguez JL, Li N, et al (2022) Locally secreted BiTEs complement CAR T cells by enhancing killing of antigen heterogeneous solid tumors. Mol Ther 30:2537–2553

188. Choi BD, Yu X, Castano AP, et al (2019) CAR-T cells secreting BiTEs circumvent antigen escape without detectable toxicity. Nat Biotechnol 37:1049–1058

189. Blanco B, Ramírez-Fernández Á, Bueno C, et al (2022) Overcoming CAR-Mediated CD19 Downmodulation and Leukemia Relapse with T Lymphocytes Secreting Anti-CD19 T-cell EngagersT Cells Secreting Anti-CD19 T-cell Engagers Prevent Relapse. Cancer Immunol Res 10:498–511

190. Lum LG, Sen M (2001) Activated T-Cell and Bispecific Antibody Immunotherapy for High-Risk Breast Cancer. Acta Haematol 105:130–136

191. Swain SM, Shastry M, Hamilton E (2023) Targeting HER2-positive breast cancer: advances and future directions. Nat Rev Drug Discov 22:101–126

192. Cattaruzza F, Nazeer A, To M, et al (2023) Precision-activated T-cell engagers targeting HER2 or EGFR and CD3 mitigate on-target, off-tumor toxicity for immunotherapy in solid tumors. Nat Cancer 4:485–501

193. Dumbrava EE, Calvo E, Garralda E, et al (2023) 1075TiP A phase I/Ib open-label, first-in-human, single agent, dose escalation and expansion study of a HER2-targeted T cell engager (SAR443216) in patients with relapsed/refractory HER2-expressing solid tumors. Ann Oncol 34:S647

194. Whalen KA, Rakhra K, Mehta NK, Steinle A, Michaelson JS, Baeuerle PA (2023) Engaging natural killer cells for cancer therapy via NKG2D, CD16A and other receptors. mAbs 15:2208697

195. Sadelain M, Brentjens R, Rivière I (2013) The Basic Principles of Chimeric Antigen Receptor Design. Cancer Discov 3:388–398

196. Rivière I, Sadelain M (2017) Chimeric Antigen Receptors: A Cell and Gene Therapy Perspective. Mol Ther 25:1117–1124

197. Wei W, Chen Z-N, Wang K (2023) CRISPR/Cas9: A Powerful Strategy to Improve CAR-T Cell Persistence. Int J Mol Sci 24:12317

198. Eyquem J, Mansilla-Soto J, Giavridis T, Stegen SJC van der, Hamieh M, Cunanan KM, Odak A, Gönen M, Sadelain M (2017) Targeting a CAR to the TRAC locus with CRISPR/Cas9 enhances tumour rejection. Nature 543:113–117

199. Qasim W, Zhan H, Samarasinghe S, et al (2017) Molecular remission of infant B-ALL after infusion of universal TALEN gene-edited CAR T cells. Sci Transl Med.

200. Bufalo FD, Angelis BD, Caruana I, et al (2023) GD2-CART01 for Relapsed or Refractory High-Risk Neuroblastoma. N Engl J Med 388:1284–1295

201. Eshhar Z, Waks T, Gross G, Schindler DG (1993) Specific activation and targeting of cytotoxic lymphocytes through chimeric single chains consisting of antibody-binding domains and the gamma or zeta subunits of the immunoglobulin and T-cell receptors. Proc Natl Acad Sci 90:720–724

202. Stancovski I, Schindler DG, Waks T, Yarden Y, Sela M, Eshhar Z (1993) Targeting of T lymphocytes to Neu/HER2-expressing cells using chimeric single chain Fv receptors. J Immunol 151:6577–6582

203. Abken H (2021) Building on Synthetic Immunology and T Cell Engineering: A Brief Journey Through the History of Chimeric Antigen Receptors. Hum Gene Ther 32:1011–1028

204. Kawalekar OU, O'Connor RS, Fraietta JA, et al (2016) Distinct Signaling of Coreceptors Regulates Specific Metabolism Pathways and Impacts Memory Development in CAR T Cells. Immunity 44:380–390

205. Salter AI, Ivey RG, Kennedy JJ, et al (2018) Phosphoproteomic analysis of chimeric antigen receptor signaling reveals kinetic and quantitative differences that affect cell function. Sci Signal.

206. Tokarew N, Ogonek J, Endres S, Bergwelt-Baildon M von, Kobold S (2019) Teaching an old dog new tricks: next-generation CAR T cells. Br J Cancer 120:26–37

207. Maus MV, June CH (2016) Making Better Chimeric Antigen Receptors for Adoptive T-cell Therapy. Clin Cancer Res 22:1875–1884

208. Sterner RC, Sterner RM (2021) CAR-T cell therapy: current limitations and potential strategies. Blood Cancer J 11:69

209. Hartmann J, Schüßler-Lenz M, Bondanza A, Buchholz CJ (2017) Clinical development of CAR T cells—challenges and opportunities in translating innovative treatment concepts. EMBO Mol Med 9:1183–1197

210. Mehta PH, Fiorenza S, Koldej RM, Jaworowski A, Ritchie DS, Quinn KM (2021) T Cell Fitness and Autologous CAR T Cell Therapy in Haematologic Malignancy. Front Immunol 12:780442

211. Michels A, Ho N, Buchholz CJ (2022) Precision medicine: In vivo CAR therapy as a showcase for receptor-targeted vector platforms. Mol Ther 30:2401–2415

212. Hong M, Clubb JD, Chen YY (2020) Engineering CAR-T Cells for Next-Generation Cancer Therapy. Cancer Cell 38:473–488

213. Milone MC, Xu J, Chen S-J, Collins MA, Zhou J, Powell DJ, Melenhorst JJ (2021) Engineering-enhanced CAR T cells for improved cancer therapy. Nat Cancer 2:780–793

214. Zhao Z, Condomines M, van der Stegen SJC, Perna F, Kloss CC, Gunset G, Plotkin J, Sadelain M (2015) Structural Design of Engineered Costimulation Determines Tumor Rejection Kinetics and Persistence of CAR T Cells. Cancer Cell 28:415–428

215. Feucht J, Sun J, Eyquem J, Ho Y-J, Zhao Z, Leibold J, Dobrin A, Cabriolu A, Hamieh M, Sadelain M (2019) Calibration of CAR activation potential directs alternative T cell fates and therapeutic potency. Nat Med 25:82–88

216. Acuto O, Michel F (2003) CD28-mediated co-stimulation: a quantitative support for TCR signalling. Nat Rev Immunol 3:939–951

217. Wherry EJ, Kurachi M (2015) Molecular and cellular insights into T cell exhaustion. Nat Rev Immunol 15:486–499

218. Ajina A, Maher J (2017) Strategies to Address Chimeric Antigen Receptor Tonic Signaling. Mol Cancer Ther 17:1795–1815

219. Guedan S, Posey AD, Shaw C, et al (2018) Enhancing CAR T cell persistence through ICOS and 4-1BB costimulation. JCI Insight 3:e96976

220. Torikai H, Reik A, Liu P-Q, et al (2012) A foundation for universal T-cell based immunotherapy: T cells engineered to express a CD19-specific chimeric-antigen-receptor and eliminate expression of endogenous TCR. Blood 119:5697–5705

221. Adachi K, Kano Y, Nagai T, Okuyama N, Sakoda Y, Tamada K (2018) IL-7 and CCL19 expression in CAR-T cells improves immune cell infiltration and CAR-T cell survival in the tumor. Nat Biotechnol 36:346–351

222. Pegram HJ, Lee JC, Hayman EG, Imperato GH, Tedder TF, Sadelain M, Brentjens RJ (2012) Tumor-targeted T cells modified to secrete IL-12 eradicate systemic tumors without need for prior conditioning. Blood 119:4133–4141

223. Adusumilli PS, Zauderer MG, Rivière I, et al (2021) A Phase I Trial of Regional Mesothelin-Targeted CAR T-cell Therapy in Patients with Malignant Pleural Disease, in Combination with the Anti–PD-1 Agent PembrolizumabRegional CAR T-Cell Therapy for Mesothelioma. Cancer Discov 11:2748–2763

224. Rotolo R, Leuci V, Donini C, Cykowska A, Gammaitoni L, Medico G, Valabrega G, Aglietta M, Sangiolo D (2019) CAR-Based Strategies beyond T Lymphocytes: Integrative Opportunities for Cancer Adoptive Immunotherapy. Int J Mol Sci 20:2839

225. Pan K, Farrukh H, Chittepu VCSR, Xu H, Pan C, Zhu Z (2022) CAR race to cancer immunotherapy: from CAR T, CAR NK to CAR macrophage therapy. J Exp Clin Cancer Res 41:119

226. Klichinsky M, Ruella M, Shestova O, et al (2020) Human chimeric antigen receptor macrophages for cancer immunotherapy. Nat Biotechnol 38:947–953

227. Szőőr Á, Tóth G, Zsebik B, Szabó V, Eshhar Z, Abken H, Vereb G (2020) Trastuzumab derived HER2-specific CARs for the treatment of trastuzumab-resistant breast cancer: CAR T cells penetrate and eradicate tumors that are not accessible to antibodies. Cancer Lett 484:1–8

228. Hegde M, Mukherjee M, Grada Z, et al (2016) Tandem CAR T cells targeting HER2 and IL13Rα2 mitigate tumor antigen escape. J Clin Investig 126:3036–3052

229. Grada Z, Hegde M, Byrd T, et al (2013) TanCAR: A Novel Bispecific Chimeric Antigen Receptor for Cancer Immunotherapy. Mol Ther - Nucleic Acids 2:e105

230. Ahmed N, Brawley V, Hegde M, et al (2017) HER2-Specific Chimeric Antigen Receptor–Modified Virus-Specific T Cells for Progressive Glioblastoma: A Phase 1 Dose-Escalation Trial. JAMA Oncol 3:1094

231. Ahmed N, Brawley VS, Hegde M, et al (2015) Human Epidermal Growth Factor Receptor 2 (HER2) -Specific Chimeric Antigen Receptor-Modified T Cells for the Immunotherapy of HER2-Positive Sarcoma. J Clin Oncol : Off J Am Soc Clin Oncol 33:1688–96

232. Feng K, Liu Y, Guo Y, Qiu J, Wu Z, Dai H, Yang Q, Wang Y, Han W (2018) Phase I study of chimeric antigen receptor modified T cells in treating HER2-positive advanced biliary tract cancers and pancreatic cancers. Protein Cell 9:838–847

233. Arenas EJ, Martínez-Sabadell A, Ruiz IR, Alonso MR, Escorihuela M, Luque A, Fajardo CA, Gros A, Klein C, Arribas J (2021) Acquired cancer cell resistance to T cell bispecific antibodies and CAR T targeting HER2 through JAK2 down-modulation. Nat Commun 12:1237

234. Boulch M, Cazaux M, Cuffel A, et al (2023) Tumor-intrinsic sensitivity to the pro-apoptotic effects of IFN-γ is a major determinant of CD4+ CAR T-cell antitumor activity. Nat Cancer 4:968–983

235. Parra-Palau JL, Pedersen K, Peg V, et al (2010) A major role of p95/611-CTF, a carboxy-terminal fragment of HER2, in the down-modulation of the estrogen receptor in HER2-positive breast cancers. Cancer Research 70:8537–8546

236. Carter P, Presta L, Gorman CM, Ridgway JB, Henner D, Wong WL, Rowland AM, Kotts C, Carver ME, Shepard HM (1992) Humanization of an anti-p185HER2 antibody for human cancer therapy. Proc Natl Acad Sci 89:4285–4289

237. Maus MV, Haas AR, Beatty GL, Albelda SM, Levine BL, Liu X, Zhao Y, Kalos M, June CH (2013) T cells expressing chimeric antigen receptors can cause anaphylaxis in humans. Cancer Immunol Res 1:26–31

238. Swain SM, Tan AR, Gianni L, et al (2023) Incidence and severity of anaphylaxis and hypersensitivity in trials of intravenous pertuzumab plus trastuzumab or the fixed-dose combination of pertuzumab and trastuzumab for subcutaneous injection for HER2-positive breast cancer. Eur J Cancer 178:70–81

239. Madsen L, Kriegenburg F, Vala A, Best D, Prag S, Hofmann K, Seeger M, Adams IR, Hartmann-Petersen R (2011) The Tissue-Specific Rep8/UBXD6 Tethers p97 to the Endoplasmic Reticulum Membrane for Degradation of Misfolded Proteins. PLoS ONE 6:e25061

240. Byrne AT, Alférez DG, Amant F, et al (2017) Interrogating open issues in cancer precision medicine with patient-derived xenografts. Nat Rev Cancer 17:254–268

241. Satoh T, Xu R-H, Chung HC, et al (2014) Lapatinib plus paclitaxel versus paclitaxel alone in the second-line treatment of HER2-amplified advanced gastric cancer in Asian populations: TyTAN--a randomized, phase III study. J Clin Oncol : Off J Am Soc Clin Oncol 32:2039–49

242. Thuss-Patience PC, Shah MA, Ohtsu A, et al (2016) Trastuzumab emtansine versus taxane use for previously treated HER2-positive locally advanced or metastatic gastric or gastro-oesophageal junction adenocarcinoma (GATSBY): an international randomised, open-label, adaptive, phase 2/3 study. Lancet Oncol 18:640–653

243. Tabernero J, Hoff PM, Shen L, et al (2018) Pertuzumab plus trastuzumab and chemotherapy for HER2-positive metastatic gastric or gastro-oesophageal junction cancer (JACOB): final analysis of a double-blind, randomised, placebo-controlled phase 3 study. Lancet Oncol 19:1372–1384

244. Stemmler H-J, Schmitt M, Willems A, Bernhard H, Harbeck N, Heinemann V (2007) Ratio of trastuzumab levels in serum and cerebrospinal fluid is altered in HER2-positive breast cancer patients with brain metastases and impairment of blood–brain barrier. Anti-Cancer Drugs 18:23–28

245. Ying Z, He T, Wang X, et al (2021) Distribution of chimeric antigen receptor-modified T cells against CD19 in B-cell malignancies. BMC Cancer 21:198

246. Howlader N, Cronin KA, Kurian AW, Andridge R (2018) Differences in Breast Cancer Survival by Molecular Subtypes in the United States. Cancer Epidemiology Prev Biomark 27:cebp.0627.2017

247. Martínez-Sáez O, Prat A (2021) Current and Future Management of HER2-Positive Metastatic Breast Cancer. Jco Oncol Pract 17:594–604

248. Vasan N, Baselga J, Hyman DM (2019) A view on drug resistance in cancer. Nature 575:299–309

249. Satoh T, Xu R-H, Chung HC, et al (2014) Lapatinib Plus Paclitaxel Versus Paclitaxel Alone in the Second-Line Treatment of HER2-Amplified Advanced Gastric Cancer in Asian Populations: TyTAN—A Randomized, Phase III Study. J Clin Oncol 32:2039–2049

250. Thuss-Patience PC, Shah MA, Ohtsu A, et al (2017) Trastuzumab emtansine versus taxane use for previously treated HER2-positive locally advanced or metastatic gastric or gastro-oesophageal junction adenocarcinoma (GATSBY): an international randomised, open-label, adaptive, phase 2/3 study. Lancet Oncol 18:640–653

251. Tabernero J, Hoff PM, Shen L, et al (2018) Pertuzumab plus trastuzumab and chemotherapy for HER2-positive metastatic gastric or gastro-oesophageal junction cancer (JACOB): final analysis of a double-blind, randomised, placebo-controlled phase 3 study. Lancet Oncol 19:1372–1384

252. Tarantino P, Modi S, Tolaney SM, Cortés J, Hamilton EP, Kim S-B, Toi M, Andrè F, Curigliano G (2021) Interstitial Lung Disease Induced by Anti-ERBB2 Antibody-Drug Conjugates. JAMA Oncol 7:1873–1881

253. Swoboda A, Nanda R (2018) Optimizing Breast Cancer Management. Cancer Treat Res 173:155–165

254. Olza MO de, Rodrigo BN, Zimmermann S, Coukos G (2020) Turning up the heat on non-immunoreactive tumours: opportunities for clinical development. Lancet Oncol 21:e419–e430

255. Pusztai L, Karn T, Safonov A, Abu-Khalaf MM, Bianchini G (2016) New Strategies in Breast Cancer: Immunotherapy. Clin Cancer Res 22:2105–2110

256. Luen SJ, Salgado R, Fox S, et al (2017) Tumour-infiltrating lymphocytes in advanced HER2-positive breast cancer treated with pertuzumab or placebo in addition to trastuzumab and docetaxel: a retrospective analysis of the CLEOPATRA study. Lancet Oncol 18:52–62

257. Savas P, Salgado R, Denkert C, Sotiriou C, Darcy PK, Smyth MJ, Loi S (2016) Clinical relevance of host immunity in breast cancer: from TILs to the clinic. Nat Rev Clin Oncol 13:228–241

258. Waldman AD, Fritz JM, Lenardo MJ (2020) A guide to cancer immunotherapy: from T cell basic science to clinical practice. Nat Rev Immunol 20:651–668

259. Costa RLB, Czerniecki BJ (2020) Clinical development of immunotherapies for HER2+ breast cancer: a review of HER2-directed monoclonal antibodies and beyond. npj Breast Cancer 6:10

260. Debien V, Caluwé AD, Wang X, Piccart-Gebhart M, Tuohy VK, Romano E, Buisseret L (2023) Immunotherapy in breast cancer: an overview of current strategies and perspectives. npj Breast Cancer 9:7

261. Chaganty BKR, Qiu S, Gest A, Lu Y, Ivan C, Calin GA, Weiner LM, Fan Z (2018) Trastuzumab upregulates PD-L1 as a potential mechanism of trastuzumab resistance through engagement of immune effector cells and stimulation of IFNγ secretion. Cancer Lett 430:47–56

262. Loi S, Giobbie-Hurder A, Gombos A, et al (2019) Pembrolizumab plus trastuzumab in trastuzumab-resistant, advanced, HER2-positive breast cancer (PANACEA): a single-arm, multicentre, phase 1b–2 trial. Lancet Oncol 20:371–382

263. Janjigian YY, Kawazoe A, Bai Y, et al (2023) Pembrolizumab plus trastuzumab and chemotherapy for HER2-positive gastric or gastro-oesophageal junction adenocarcinoma: interim analyses from the phase 3 KEYNOTE-811 randomised placebo-controlled trial. Lancet 402:2197–2208

264. Emens LA, Esteva FJ, Beresford M, et al (2020) Trastuzumab emtansine plus atezolizumab versus trastuzumab emtansine plus placebo in previously treated, HER2-positive advanced breast cancer (KATE2): a phase 2, multicentre, randomised, double-blind trial. Lancet Oncol 21:1283–1295

265. Galsky MD, Conte GD, Foti S, et al (2022) Primary analysis from DS8201-A-U105: A phase 1b, two-part, open-label study of trastuzumab deruxtecan (T-DXd) with nivolumab (nivo) in patients (pts) with HER2-expressing urothelial carcinoma (UC). J Clin Oncol 40:438–438

266. Mittendorf EA, Clifton GT, Holmes JP, Schneble E, Echo D van, Ponniah S, Peoples GE (2014) Final report of the phase I/II clinical trial of the E75 (nelipepimut-S) vaccine with booster inoculations to prevent disease recurrence in high-risk breast cancer patients. Ann Oncol 25:1735–1742

267. Clifton GT, Hale D, Vreeland TJ, et al (2020) Results of a Randomized Phase IIb Trial of Nelipepimut-S + Trastuzumab versus Trastuzumab to Prevent Recurrences in Patients with High-Risk HER2 Low-Expressing Breast Cancer. Clin Cancer Res 26:2515–2523

268. You Z, Zhou W, Weng J, Feng H, Liang P, Li Y, Shi F (2021) Application of HER2 peptide vaccines in patients with breast cancer: a systematic review and meta-analysis. Cancer Cell Int 21:489

269. Zhang J, Ji D, Cai L, et al (2021) First-in-human HER2-targeted Bispecific Antibody KN026 for the Treatment of Patients with HER2-positive Metastatic Breast Cancer: Results from a Phase I Study. Clin Cancer Res 28:618–628

270. Xu J, Ying J, Liu R, et al (2023) KN026 (anti-HER2 bispecific antibody) in patients with previously treated, advanced HER2-expressing gastric or gastroesophageal junction cancer. Eur J Cancer 178:1–12

271. Budi HS, Ahmad FN, Achmad H, Ansari MJ, Mikhailova MV, Suksatan W, Chupradit S, Shomali N, Marofi F (2022) Human epidermal growth factor receptor 2 (HER2)-specific chimeric antigen receptor (CAR) for tumor immunotherapy; recent progress. Stem Cell Res Ther 13:40

272. Kiewe P, Hasmüller S, Kahlert S, et al (2006) Phase I Trial of the Trifunctional Anti-HER2 × Anti-CD3 Antibody Ertumaxomab in Metastatic Breast Cancer. Clin Cancer Res 12:3085–3091

273. Slaney CY, Wang P, Darcy PK, Kershaw MH (2018) CARs versus BiTEs: A Comparison between T Cell–Redirection Strategies for Cancer Treatment. Cancer Discov 8:924–934

274. Zhai Y, Hong J, Wang J, et al (2023) Comparison of blinatumomab and CAR T-cell therapy in relapsed/refractory acute lymphoblastic leukemia: a systematic review and meta-analysis. Expert Rev Hematol ahead-of-print:1–10

275. Strohl WR, Naso M (2019) Bispecific T-Cell Redirection versus Chimeric Antigen Receptor (CAR)-T Cells as Approaches to Kill Cancer Cells. Antibodies 8:41

276. Klein C, Schaefer W, Regula JT, Dumontet C, Brinkmann U, Bacac M, Umaña P (2019) Engineering therapeutic bispecific antibodies using CrossMab technology. Methods 154:21–31

277. Chen X, Yang S, Li S, et al (2021) Secretion of bispecific protein of anti-PD-1 fused with TGF-β trap enhances antitumor efficacy of CAR-T cell therapy. Mol Ther - Oncolytics 21:144–157

278. Roselli E, Faramand R, Davila ML (2021) Insight into next-generation CAR therapeutics: designing CAR T cells to improve clinical outcomes. J Clin Investig 131:e142030

279. Caruana I, Savoldo B, Hoyos V, Weber G, Liu H, Kim ES, Ittmann MM, Marchetti D, Dotti G (2015) Heparanase promotes tumor infiltration and antitumor activity of CAR-redirected T lymphocytes. Nat Med 21:524–529

280. Benjamin R, Jain N, Maus MV, et al (2022) UCART19, a first-in-class allogeneic anti-CD19 chimeric antigen receptor T-cell therapy for adults with relapsed or refractory B-cell acute lymphoblastic leukaemia (CALM): a phase 1, dose-escalation trial. Lancet Haematol 9:e833–e843

281. Mikhael J, Fowler J, Shah N (2022) Chimeric Antigen Receptor T-Cell Therapies: Barriers and Solutions to Access. JCO Oncol Pr 18:800–807

282. Altvater B, Kailayangiri S, Spurny C, et al (2023) CAR T cells as micropharmacies against solid cancers: Combining effector T-cell mediated cell death with vascular targeting in a one-step engineering process. Cancer Gene Ther 30:1355–1368

283. Rafiq S, Hackett CS, Brentjens RJ (2020) Engineering strategies to overcome the current roadblocks in CAR T cell therapy. Nat Rev Clin Oncol 17:147–167

284. Sorkhabi AD, Khosroshahi LM, Sarkesh A, Mardi A, Aghebati-Maleki A, Aghebati-Maleki L, Baradaran B (2023) The current landscape of CAR T-cell therapy for solid tumors: Mechanisms, research progress, challenges, and counterstrategies. Front Immunol 14:1113882

285. Mo F, Mamonkin M (2019) Chimeric Antigen Receptor T Cells, Development and Production. Methods Mol Biol 2086:119–130

286. Kochenderfer JN, Feldman SA, Zhao Y, Xu H, Black MA, Morgan RA, Wilson WH, Rosenberg SA (2009) Construction and Preclinical Evaluation of an Anti-CD19 Chimeric Antigen Receptor. J Immunother 32:689–702

287. Levine BL, Pasquini MC, Connolly JE, et al (2024) Unanswered questions following reports of secondary malignancies after CAR-T cell therapy. Nat Med 30:338–341

288. Scholler J, Brady TL, Binder-Scholl G, et al (2012) Decade-Long Safety and Function of Retroviral-Modified Chimeric Antigen Receptor T Cells. Sci Transl Med 4:132ra53

289. Khan AN, Chowdhury A, Karulkar A, Jaiswal AK, Banik A, Asija S, Purwar R (2022) Immunogenicity of CAR-T Cell Therapeutics: Evidence, Mechanism and Mitigation. Front Immunol 13:886546

290. Calderon H, Mamonkin M, Guedan S (2019) Chimeric Antigen Receptor T Cells, Development and Production. Methods Mol Biol 2086:223–236

291. Long AH, Haso WM, Shern JF, et al (2015) 4-1BB costimulation ameliorates T cell exhaustion induced by tonic signaling of chimeric antigen receptors. Nat Med 21:581–590

292. Day C-P, Merlino G, Van Dyke T (2015) Preclinical Mouse Cancer Models: A Maze of Opportunities and Challenges. Cell 163:39–53

293. Shultz LD, Goodwin N, Ishikawa F, Hosur V, Lyons BL, Greiner DL (2014) Human Cancer Growth and Therapy in Immunodeficient Mouse Models. Cold Spring Harb Protoc 2014:pdb.top073585

294. Rodriguez-Garcia A, Watanabe K, Guedan S (2019) Chimeric Antigen Receptor T Cells, Development and Production. Methods Mol Biol 2086:251–271

295. Coughlan AM, Harmon C, Whelan S, et al (2016) Myeloid Engraftment in Humanized Mice: Impact of Granulocyte-Colony Stimulating Factor Treatment and Transgenic Mouse Strain. Stem Cells Dev 25:530–541

296. Baldo GD, Bufalo FD, Pinacchio C, Carai A, Quintarelli C, Angelis BD, Merli P, Cacchione A, Locatelli F, Mastronuzzi A (2023) The peculiar challenge of bringing CAR-T cells into the brain: Perspectives in the clinical application to the treatment of pediatric central nervous system tumors. Front Immunol 14:1142597

297. E. BC, Darya A, Renate S, et al (2016) Regression of Glioblastoma after Chimeric Antigen Receptor T-Cell Therapy. N Engl J Med 375:2561–2569

298. Quintarelli C, Orlando D, Boffa I, et al (2018) Choice of costimulatory domains and of cytokines determines CAR T-cell activity in neuroblastoma. OncoImmunology 7:e1433518

299. Hidalgo M, Amant F, Biankin AV, et al (2014) Patient-derived xenograft models: an emerging platform for translational cancer research. Cancer Discov 4:998–1013

300. DeRose YS, Wang G, Lin Y-C, et al (2011) Tumor grafts derived from women with breast cancer authentically reflect tumor pathology, growth, metastasis and disease outcomes. Nat Med 17:1514–1520

301. Shah NN, Fry TJ (2019) Mechanisms of resistance to CAR T cell therapy. Nat Rev Clin Oncol 16:372–385

302. Massimino M, Martorana F, Stella S, Vitale SR, Tomarchio C, Manzella L, Vigneri P (2023) Single-Cell Analysis in the Omics Era: Technologies and Applications in Cancer. Genes 14:1330

303. Arora R, Cao C, Kumar M, et al (2023) Spatial transcriptomics reveals distinct and conserved tumor core and edge architectures that predict survival and targeted therapy response. Nat Commun 14:5029

304. O'Rourke DM, Nasrallah MP, Desai A, et al (2017) A single dose of peripherally infused EGFRvIII-directed CAR T cells mediates antigen loss and induces adaptive resistance in patients with recurrent glioblastoma. Sci Transl Med.

305. Sahillioglu AC, Schumacher TN (2022) Safety switches for adoptive cell therapy. Curr Opin Immunol 74:190–198

306. Stasi AD, Tey S-K, Dotti G, et al (2011) Inducible apoptosis as a safety switch for adoptive cell therapy. N Engl J Med 365:1673–83

307. Serafini M, Manganini M, Borleri G, Bonamino M, Imberti L, Biondi A, Golay J, Rambaldi A, Introna M (2004) Characterization of CD20-Transduced T Lymphocytes as an Alternative Suicide Gene Therapy Approach for the Treatment of Graft-Versus-Host Disease. Hum Gene Ther 15:63–76

308. Wang X, Chang W-C, Wong CW, Colcher D, Sherman M, Ostberg JR, Forman SJ, Riddell SR, Jensen MC (2011) A transgene-encoded cell surface polypeptide for selection, in vivo tracking, and ablation of engineered cells. Blood 118:1255–1263

309. Chmielewski M, Hombach A, Heuser C, Adams GP, Abken H (2004) T Cell Activation by Antibody-Like Immunoreceptors: Increase in Affinity of the Single-Chain Fragment Domain above Threshold Does Not Increase T Cell Activation against Antigen-Positive Target Cells but Decreases Selectivity. J Immunol 173:7647–7653

310. Chuntova P, Hou Y, Naka R, et al (2021) Novel EGFRvIII-CAR transgenic mice for rigorous preclinical studies in syngeneic mice. Neuro-Oncol 24:259–272

311. Wunderlich M, Chou F-S, Mizukawa B, Link KA, Mulloy JC (2009) A New Immunodeficient Mouse Strain, NOD/SCID IL2Rγ–/– SGM3, Promotes Enhanced Human Hematopoietic Cell Xenografts with a Robust T Cell Component. Blood 114:3524

312. Giavridis T, Stegen SJC van der, Eyquem J, Hamieh M, Piersigilli A, Sadelain M (2018) CAR T cell–induced cytokine release syndrome is mediated by macrophages and abated by IL-1 blockade. Nat Med 24:731–738

313. Cosenza M, Sacchi S, Pozzi S (2021) Cytokine Release Syndrome Associated with T-Cell-Based Therapies for Hematological Malignancies: Pathophysiology, Clinical Presentation, and Treatment. Int J Mol Sci 22:7652

314. Taha Z, Crupi MJF, Alluqmani N, et al (2023) Syngeneic mouse model of human HER2+ metastatic breast cancer for the evaluation of trastuzumab emtansine combined with oncolytic rhabdovirus. Front Immunol 14:1181014

315. Stöcklin E, Botteri F, Groner B (1993) An activated allele of the c-erbB-2 oncogene impairs kidney and lung function and causes early death of transgenic mice. J cell Biol 122:199–208

316. Phillips GL, Guo J, Kiefer JR, Proctor W, Yadav DB, Dybdal N, Shen B-Q (2022) Trastuzumab does not bind rat or mouse ErbB2/neu: implications for selection of non-clinical safety models for trastuzumab-based therapeutics. Breast Cancer Res Treat 191:303–317

317. Poon KA, Flagella K, Beyer J, Tibbitts J, Kaur S, Saad O, Yi J-H, Girish S, Dybdal N, Reynolds T (2013) Preclinical safety profile of trastuzumab emtansine (T-DM1): Mechanism of action of its cytotoxic component retained with improved tolerability. Toxicol Appl Pharmacol 273:298–313

318. Kumagai K, Aida T, Tsuchiya Y, Kishino Y, Kai K, Mori K (2020) Interstitial pneumonitis related to trastuzumab deruxtecan, a human epidermal growth factor receptor 2-targeting Ab–drug conjugate, in monkeys. Cancer Sci 111:4636–4645

319. Schlereth B, Quadt C, Dreier T, et al (2006) T-cell activation and B-cell depletion in chimpanzees treated with a bispecific anti-CD19/anti-CD3 single-chain antibody construct. Cancer Immunol, Immunother 55:503–514

320. Fry EA, Taneja P, Inoue K (2016) Clinical applications of mouse models for breast cancer engaging HER2/neu. Integr Cancer Sci Ther 3:593–603

321. Crespo J, Koh YT, Hu N, Moore PA, Bonvini E, Glasebrook AL, Martin AP, Benschop RJ (2021) A humanized CD3ε-knock-in mouse model for pre-clinical testing of anti-human CD3 therapy. PLoS ONE 16:e0245917

322. Moreno P, Fexova S, George N, et al (2021) Expression Atlas update: gene and protein expression in multiple species. Nucleic Acids Res 50:gkab1030-

323. Noguchi S, Arakawa T, Fukuda S, et al (2017) FANTOM5 CAGE profiles of human and mouse samples. Sci Data 4:170112

324. Lebrec H, Maier CC, Maki K, Ponce R, Shenton J, Green S (2021) Nonclinical safety assessment of engineered T cell therapies. Regul Toxicol Pharmacol 127:105064

325. Tan Y, Cai H, Li C, et al (2021) A novel full-human CD22-CAR T cell therapy with potent activity against CD22low B-ALL. Blood Cancer J 11:71

326. Fan S, Wang T, You F, et al (2023) B7-H3 chimeric antigen receptor-modified T cell shows potential for targeted treatment of acute myeloid leukaemia. Eur J Méd Res 28:129

327. Faber ML, Oldham RAA, Thakur A, et al (2023) Novel anti-CD30/CD3 bispecific antibodies activate human T cells and mediate potent anti-tumor activity. Front Immunol 14:1225610

328. Huston-Paterson DJ, Banik SSR, Doranz BJ (2016) Screening the Membrane Protein: A High-Throughput Platform for Identifying Membrane Protein Antibody Targets. Genet Eng Biotechnol N 36:18–19

329. Lee J, Lundgren DK, Mao X, et al (2020) Antigen-specific B-cell depletion for precision therapy of mucosal pemphigus vulgaris. J Clin Investig 130:6317–6324

330. Qi T, McGrath K, Ranganathan R, Dotti G, Cao Y (2022) Cellular kinetics: A clinical and computational review of CAR-T cell pharmacology. Adv Drug Deliv Rev 188:114421

331. Norelli M, Casucci M, Bonini C, Bondanza A (2016) Clinical pharmacology of CAR-T cells: Linking cellular pharmacodynamics to pharmacokinetics and antitumor effects. Biochim Biophys Acta (BBA) - Rev Cancer 1865:90–100

332. Krammer PH, Arnold R, Lavrik IN (2007) Life and death in peripheral T cells. Nat Rev Immunol 7:532–542

333. Porter DL, Hwang W-T, Frey NV, et al (2015) Chimeric antigen receptor T cells persist and induce sustained remissions in relapsed refractory chronic lymphocytic leukemia. Sci Transl Med 7:303ra139

334. Weist MR, Starr R, Aguilar B, et al (2018) PET of Adoptively Transferred Chimeric Antigen Receptor T Cells with 89Zr-Oxine. J Nucl Med 59:1531–1537

335. Pfeifer R, Henze J, Wittich K, et al (2022) A multimodal imaging workflow for monitoring CAR T cell therapy against solid tumor from whole-body to single-cell level. Theranostics 12:4834–4850

336. Pimentel H, Jarnagin H, Zong H, Todorov C, Anderson CM, Zhang B, Bunker C, Ma X-J (2019) Preclinical CAR-T cell target safety, biodistribution, and tumor infiltration analysis using in situ hybridization technology. J Clin Oncol 37:112–112

337. Wen H, Huang Y, Hou T, Wang J, Huo Y (2021) Determination of the biodistribution of chimeric antigen receptor-modified T cells against CD19 in NSG mice. Methods Cell Biol 167:15–37

338. Kamiyama Y, Naritomi Y, Moriya Y, et al (2021) Biodistribution studies for cell therapy products: Current status and issues. Regen Ther 18:202–216

339. Huang Z, Dewanjee S, Chakraborty P, Jha NK, Dey A, Gangopadhyay M, Chen X-Y, Wang J, Jha SK (2023) CAR T cells: engineered immune cells to treat brain cancers and beyond. Mol Cancer 22:22

340. Zhu I, Liu R, Garcia JM, Hyrenius-Wittsten A, Piraner DI, Alavi J, Israni DV, Liu B, Khalil AS, Roybal KT (2022) Modular design of synthetic receptors for programmed gene regulation in cell therapies. Cell 185:1431-1443.e16

341. Choe JH, Watchmaker PB, Simic MS, et al (2021) SynNotch-CAR T cells overcome challenges of specificity, heterogeneity, and persistence in treating glioblastoma. Sci Transl Med.

342. Tormoen GW, Crittenden MR, Gough MJ (2018) Role of the immunosuppressive microenvironment in immunotherapy. Adv Radiat Oncol 3:520–526

343. Dong X, Ren J, Amoozgar Z, Lee S, Datta M, Roberge S, Duquette M, Fukumura D, Jain RK (2023) Anti-VEGF therapy improves EGFR-vIII-CAR-T cell delivery and efficacy in syngeneic glioblastoma models in mice. J Immunother Cancer 11:e005583

344. Li Y, Wu H, Chen G, et al (2020) Arming Anti-EGFRvIII CAR-T With TGFβ Trap Improves Antitumor Efficacy in Glioma Mouse Models. Front Oncol 10:1117

345. (CAT) C for AT, Secretariat CS, Schneider CK, et al (2010) Challenges with advanced therapy medicinal products and how to meet them. Nat Rev Drug Discov 9:195–201

346. Mock U, Nickolay L, Cheung GW-K, Zhan H, Peggs K, Johnston IC, Kaiser A, Pule M, Thrasher A, Qasim W (2015) Automated Lentiviral Transduction of T Cells with Cars Using the Clinimacs Prodigy. Blood 126:2043

347. Castella M, Caballero-Baños M, Ortiz-Maldonado V, et al (2020) Point-Of-Care CAR T-Cell Production (ARI-0001) Using a Closed Semi-automatic Bioreactor: Experience From an Academic Phase I Clinical Trial. Front Immunol 11:482

348. Francis N, Braun M, Neagle S, et al (2023) Development of an automated manufacturing process for large-scale production of autologous T cell therapies. Mol Ther - Methods Clin Dev 31:101114

349. Ghassemi S, Nunez-Cruz S, O'Connor RS, et al (2018) Reducing Ex Vivo Culture Improves the Antileukemic Activity of Chimeric Antigen Receptor (CAR) T Cells. Cancer Immunol Res 6:1100–1109

350. Dickinson MJ, Barba P, Jager U, et al (2023) A Novel Autologous CAR-T Therapy, YTB323, with Preserved T-Cell Stemness Shows Enhanced CAR T-Cell Efficacy in Preclinical and Early Clinical Development. Cancer Discov 13:1982–1997

351. Zhu M, Wu B, Brandl C, Johnson J, Wolf A, Chow A, Doshi S (2016) Blinatumomab, a Bispecific T-cell Engager (BiTE®) for CD-19 Targeted Cancer Immunotherapy: Clinical Pharmacology and Its Implications. Clin Pharmacokinet 55:1271–1288

352. Leclercq G, Servera LA, Danilin S, et al (2022) Dissecting the mechanism of cytokine release induced by T-cell engagers highlights the contribution of neutrophils. OncoImmunology 11:2039432

353. Norelli M, Camisa B, Barbiera G, et al (2018) Monocyte-derived IL-1 and IL-6 are differentially required for cytokine-release syndrome and neurotoxicity due to CAR T cells. Nat Med 24:739–748

354. Shultz LD, Schweitzer PA, Christianson SW, Gott B, Schweitzer IB, Tennent B, McKenna S, Mobraaten L, Rajan TV, Greiner DL (1995) Multiple defects in innate and adaptive immunologic function in NOD/LtSz-scid mice. J Immunol (Baltim, Md : 1950) 154:180–91

355. Nouri Y, Weinkove R, Perret R (2023) An In Vitro Model to Assess CRS Potential of CAR T Cells Using a Tumor Cell Line and Autologous Monocytes. Curr Protoc 3:e864

356. Acharya UH, Dhawale T, Yun S, Jacobson CA, Chavez JC, Ramos JD, Appelbaum J, Maloney DG (2019) Management of cytokine release syndrome and neurotoxicity in chimeric antigen receptor (CAR) T cell therapy. Expert Rev Hematol 12:195–205

357. Jacobs TW, Gown AM, Yaziji H, Barnes MJ, Schnitt SJ (1999) Specificity of HercepTest in Determining HER-2 / neu Status of Breast Cancers Using the United States Food and Drug Administration–Approved Scoring System. J Clin Oncol 17:1983–1983

358. André F, Rassy E, Marabelle A, Michiels S, Besse B (2024) Forget lung, breast or prostate cancer: why tumour naming needs to change. Nature 626:26–29